UNIVERSITY OF CALIFORNIA,
IRVINE

Studies of Halogenated Lipids and Progress Toward the Synthesis of Crotogoudin

DISSERTATION

submitted in partial satisfaction of the requirements
for the degree of

DOCTOR OF PHILOSOPHY

in Chemistry

by

Dmitriy Igorovich Uchenik

Dissertation Committee:
Professor Christopher D. Vanderwal, Chair
Professor Elizabeth R. Jarvo
Professor Kenneth J. Shea

2017

DEDICATION

To my family.
To my friends.

TABLE OF CONTENTS

LIST OF SCHEMES

LIST OF FIGURES

LIST OF TABLES

LIST OF EQUATIONS

Page

LIST OF ABBREVIATIONS

Å	Ångstrom
λ	wavelength
µ	micro
$[\alpha]_D^{20} = (c,)$	specific rotation at λ of sodium D line
°C	degrees Celsius
Ac	acetyl
Bn	benzyl
bp	boiling point
br	broad
ca.	circa
cat.	catalytic
calcd	calculated
CCl_4	carbon tetrachloride
$ClSO_3H$	chlorosulfonic acid
$CHCl_3$	chloroform
CI	chemical ionization
cm^{-1}	wavenumbers
d	doublet
DCM	methylene chloride
$(DHQD)_2PHAL$	hydroquinidine 1,4-phthalazinediyl diether
DMAP	4-dimethylaminopyridine
DMF	dimethylformamide
DMP	Dess–Martin periodinane
DMSO	dimethylsulfoxide
dr	diastereomeric ratio
EDCI	*N*-(3-dimethylaminopropyl)-(N)′-ethylcarbodiimide
ee	enantiomeric excess
e.g.	for example (Latin)
EI	electron impact ionization
equiv	equivalent
ESI	electrospray ionization
Et	ethyl
EtOAc	ethyl acetate
EtOH	ethanol
Et_3N	triethylamine
g	gram(s)
h	hour(s)
HCl	hydrochloric acid
HRMS	high-resolution mass spectrometry
Hz	Hertz
$IC_{\%}$	(percent) maximal inhibitory concentration
i.e.	that is (Latin)
IEDDA	invers electron demand Diels–Alder reaction
IMDA	intra molecular Diels–Alder reaction
IPA	2-propanol
i-Pr	isopropyl
IR	infrared
J	coupling constant
K	kelvin

kcal	kilocalorie
K_2CO_3	potassium carbonate
KH_2PO_4	potassium phosphate, monobasic
KHMDS	potassium hexamethyldisilizane
KOtBu	potassium *tert*-butoxide
LDA	lithium diisopropylamide
LHMDS	lithium hexamethyldisilizane
lit.	literature value
m	multiplet
M	molar (molecular ion when appropriate)
m/z	mass to charge ratio
*m*CPBA	*meta*-chloroperoxybenzoic acid
Me	methylene chloride
MeOH	methanol
$MgSO_4$	magnesium sulfate
MHz	megahertz
min	minute(s)
mol	mole(s)
mp	melting point
Ms	methanesulfonyl
MTBE	methyl *tert*-butyl ether
n	nano
Na_2SO_3	sodium sulfite
$Na_2S_2O_3$	sodium thiosulfate
Na_2SO_4	sodium sulfate
$NaBH_4$	sodium borohydride
$NaHCO_3$	sodium bicarbonate
NaHMDS	sodium hexamethyldisilizane
n-BuLi	*n*-butyl lithium
n-BuOH	*n*-butyl alcohol
NCS	*n*-chlorosuccinamide
NH_4Cl	ammonium chloride
NMR	nuclear magnetic resonance
PCC	pyridinium chlorochromate
Ph	phenyl
PhMe	toluene
ppm	parts per million
Py	pyridine
q	quartet
rt	room temperature (20–25 °C)
s	singlet
t	triplet
t-$BuNH_2$	*tert*-butyl amine
t-BuOH	*tert*-butyl alcohol
TBAF	tetrabutylammonium fluoride
TBAI	tetrabutylammonium iodide
TBDPS	*tert*-butlydiphenylsilyl
TBS	*tert*-butyldimethylsilyl
t-BuOK	potassium *tert*-butoxide
TES	triethylsilyl
TEEDA	*N*,*N*,*N*′,*N*′-tetraethylethylenediamine
Tf	trifluoromethanesulfonyl
TFA	trifluoroacetoxy
TFAA	trifluoroacetic anhydride

THF	tetrahydrofuran
TLC	thin-layer chromatography
TMS	trimethylsilyl
TMDS	tetramethyldisilazane
TOF	time-of-flight
Ts	*p*-toluenesulfonyl

ACKNOWLEDGMENTS

I would like to thank my graduate advisor Professor Chris Vanderwal for inviting me to join his group and providing an excellent learning environment. Your enthusiasm for synthetic chemistry is addictive. Joining a total synthesis group with no synthetic experience can be daunting, but you put stock in my enthusiasm, which made getting up to speed fun. Some students are lucky enough to have a smooth time during their graduate career, but I was lucky enough to have an advisor who is as understanding out of lab as he is supportive in lab, and that's made all the difference.

Thank you, Professor Elizabeth Jarvo and Professor Kenneth Shea for your invaluable guidance over the years. Liz, you weren't on my candidacy exam committee, but our discussions went a long way to supporting a proposal based on organometallic chemistry.

My thanks to Dr. D. Karl Bedke and Amgen Inc. for the opportunity to work with you as a graduate student intern. Karl you helped me set up my first reaction in the Vanderwal lab while you were writing your thesis and it was a pleasure to get to work with you again. Learning about the operations of a medicinal chemistry department first hand, running chemical reactions with the support of an industrial chemistry department, and getting to do all of that in San Francisco was an excellent opportunity.

The Vanderwal lab is unique place to work. I'm immensely grateful to everyone who's been in the group during my time here. The combination of supportive attitude and scathing comments make the group an amazing place to spend six days a week. I cannot do justice to all the people I've had the pleasure of working with over the last seven years, but some deserve specific recognition: Without Dr. Peter Mai, chapter three of this dissertation would likely look quite different. We did not get a chance to work on crotogoudin together for very long, but I am grateful to you for setting the stage for my work. Dr. Sam Tartakoff and Dr. Jon Lam, you mentored me when I first joined the group, taught me to read chemical literature with a critical eye, and were equally available for lunch as for discussions of reactions that would never work. Sam you put up with me as your bay mate for three years during which time you reviewed every document I produced, repeatedly, and came back to edit my thesis. For the first part, you likely deserve hazard pay, for the second, I hold you personally responsible for any writing ability I may have developed. Professor Won-jin Chung, I'm still a bit hazy on when you actually joined the group, but I'll always remember the late night pizza and beer after long days of work. Your quiet, unwavering persistence, attention to detail, and love of a good Starcraft match are things I carry with me (But only after distilling them).

My mom Galina and my dad Igor left their homes and their friends in Ukraine, moved to the United States, and struggled for years to establish themselves here, all to give me the *chance* at a better life. You've supported me, encouraged me to never fear a bit of hard work, and above all taught me to never stop learning. I would not be here without you.

CURRICULUM VITAE

Dmitriy Uchenik

2722 Verano Place, Irvine, California, 92617
duchenik@uci.edu Mobile: (818) 919-2450

Education:

Ph.D. Candidate, Organic Synthesis January 2017
University of California, Irvine

- Mentor: Christopher D. Vanderwal
- G.P.A.: 4.0

B.S., Biochemistry March 2010
University of California, San Diego

- Mentor: Yitzhak Tor
- G.P.A.: 3.25
- Chemistry Department Honors

Employment Experience:

Graduate Student Research Associate February 2011 – December 2017
University of California, Irvine Advisor: Professor Christopher D. Vanderwal

- Designed and carried out an efficient synthetic route toward the core of the cytotoxic natural product crotogoudin.
- Discovered a hitherto unexplained copper-mediated hydrosilylation that is dependent on the presence of molecular oxygen.
- Demonstrated an expanded scope of reactivity for Mn(III) generated enolic radicals which contradicts canonical teaching.
- Currently pursuing the completion of crotogoudin.

Graduate Student Intern June 2013 – September 2013
Amgen Inc. Advisor: Advisor: Dr. D. Karl Bedke, Ph.D.

- Explored directing group effects on diastereoselectivity in vicinal dichlorination.
- Pursued development of a broadly applicable method for catalytic asymmetric vicinal dichlorination.

Laboratory Assistant 1 April 2010 – July 2010
Center of Excellence for Advanced Materials Advisor: Advisor: Dr. Haim Weizman, Ph.D.

- Delivered custom monomeric substrates for research on novel self-healing polymers.
- Performed chemical transformations on scales of up to 200g, delivered up to 20g batches.
- Optimized synthesis to reduce cost and simplify purification.
- Trained lead engineering researcher to perform necessary transformation and purifications.

Undergraduate Research Associate June 2008 – July 2010
University of California, San Diego Advisor: Advisor: Professor Yitzhak Tor

- Designed and synthesized two fluorescent reporters tuned to biological pH ranges.
- Synthesized nucleosides sensitive to pH in the major groove of the DNA double helix.

Publications:

Sinkeldam, R. W.; Marcus, P.; Uchenik, D.; Tor, Y. *ChemPhysChem* **2011**, *12*, 2260.

Honors:

- Outstanding Contributions to the Chemistry Department Teaching Program by a TA - Lower Division, June 2015
- Graduated with UCSD Chemistry/Biochemistry Department Honors
- Provost's Honors: Spring, Fall 2008; Winter, Fall 2009

Relevant Skills:

Teaching Assistant, Organic Chemistry, UCI 2010 – Present, Intermittent

- Organic Chemistry Discussions: Three quarters with five sections per quarter.
- Organic Chemistry Labs: Seven quarters with two labs per quarter.
- General Chemistry Labs: Three quarters with two labs per quarter.

Organic Chemistry Teaching Assistant, UCSD Spring 2010

- Teaching Assistant for 3rd quarter honors organic chemistry.
- Employed immediately after obtaining bachelor's degree

Computer Skills

- 10+ years experience working with Microsoft Windows, Word, Excel, and Powerpoint
- Six years experience with PerkinElmer ChemDraw software.
- Six years experience with Bruker Topspin software.
- Four years experience with Ubuntu Linux.
- One year experience with Linux Mint
- Amateur, experience with Quantum Mechanical Molecular Modeling using Gaussian 09 and Spartan. Contribution acknowledge in:
  - Calvo, E.; Barasoain, I.; Matesanz, R.; Pera, B.; Camafeita, E.; Pineda, O.; Hamel, E.; Vanderwal, C. D.; Andreu, J. M.; López, J. A.; Díaz, J. F. Biochemistry 2012, 51 (1), 329.
- Amateur experience with general /bash scripting.
- Amateur experience with LaTeX 2_ε programing.
- Beginner proficiency with Python programing.

ABSTRACT OF THE DISSERTATION

Studies of Halogenated Lipids and
Progress Toward the Synthesis of Crotogoudin

By

Dmitriy Igorovich Uchenik

Doctor of Philosophy in Chemistry

University of California, Irvine, 2017

Professor Christopher D. Vanderwal, Chair

This dissertation describes three separate projects which range from work toward the development of new chemical methods to the synthesis of natural products. Chapter one introduces the intricacies involved in bimolecular elimination reactions and reports my efforts to elucidate the source of the highly diastereoselective dehydrohalogenation of β-dichloro sulfates. Our group has previously found that exposure of β,β,-dichloro sulfates to LDA provided exclusively the (*E*)-vinyl sulfate while the same elimination conducted with *t*-BuOK gave a 1:5 ratio of (*E*)- to (*Z*)- alkene diastereomers. Experiments exploring the effects of base strength, different countercations, and substrate substitution were carried out to attempt to elucidate the source of this surprising diastereocontrol. Early elimination experiments performed on 2,2-dichlorohexyl sulfate supported an initial hypothesis of diastereocontrol based on competing cation chelation, but further experimentation demonstrated that the trend did not extend to other β-chloro sulfates.

Chapter two describes synthetic explorations toward the synthesis of the sponge derived natural product mollenyne A. Synthetic efforts focused on the synthesis of the dibromochlorohydrin stereo-triad demonstrated the challenge associated with the regioselective synthesis of a trisubstituted (*E*)-alkenyl bromide. Failing to install the

alkenyl bromide *via* hydrometalation, a ring-closing metathesis strategy was proposed to set the alkene geometry. While a 1,1-disubstituted alkenyl bromide was synthesized, we were unable to achieve the desired metathesis.

Chapter 3 focuses on my efforts toward the total synthesis of the *seco*-atisane diterpene crotogoudin. A variety of methods for the installation of bicyclo-[2.2.2]-octanes are discussed in the context of various natural product syntheses and the two previous syntheses of crotogoudin by the Carreira and Liu groups are presented. Work toward improving the synthetic approach designed by Dr. Peter Mai led to the discovery of an unprecedented, oxygen-dependent copper catalyzed conjugate reduction. An expansion of Snyder's manganese(III) mediated free radical enolate cyclization is presented as a novel method for forming bicyclo-[2.2.2]-octanes.

Chapter 1:

Stereochemical Dichotomy in Dehydrohalogenation of Lipids

1.1 Introduction

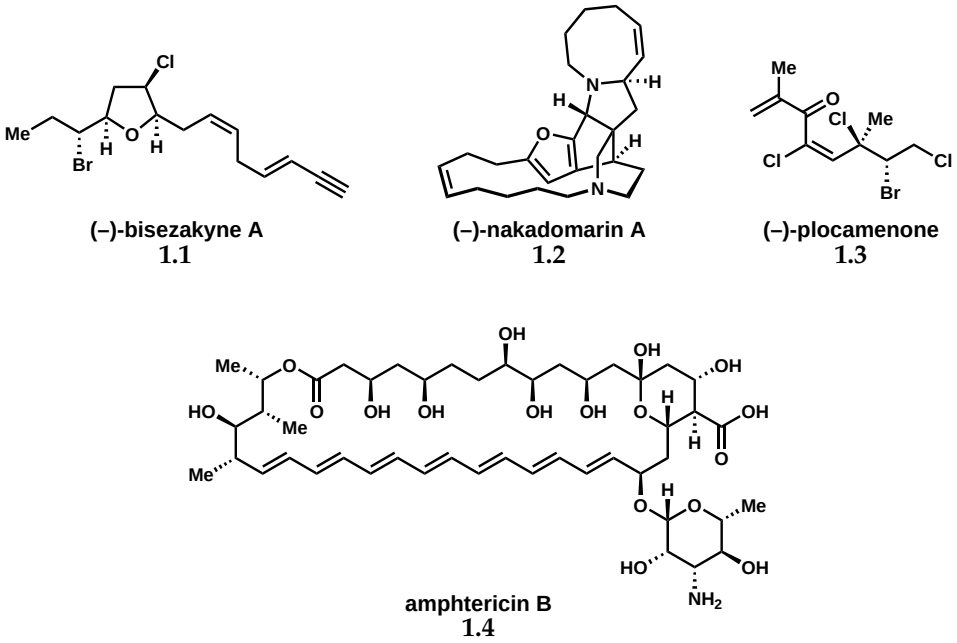

Figure 1.1: Select bioactive natural products with complex alkene geometry.

Stereochemically defined alkenes appear ubiquitously in natural products such as (–)-bisezakyne A (**1.1**),[1] (–)-nakadomarin A (**1.2**),[2–15] and (–)-plocamenone (**1.3**)[16] as well as marketed pharmaceuticals such as amphotericin B (**1.4**).[17–23] Moreover alkenes are versatile functional groups, allowing fragmentation of long hydrocarbon chains and supporting a wide array of functional group transformations including selective oxidation to epoxides as well as various alcohols, amines, halides, carbonyls, and carboxylic acids. Alkenes can be used as potent electrophiles in organometalic chemistry including the Heck reaction and rhodium catalyzed hydroformylation and hydroacylation. While many of these reactions have been rendered enantioselective using chiral ligands, the diastereomer of the product necessarily depends on the diastereomer of the alkene starting material. Despite the utility of stereochemically defined olefins, there is no general method for the diastereoselective synthesis of olefins.

1.2 Mechanism of Base Promoted Vicinal Elimination Reactions

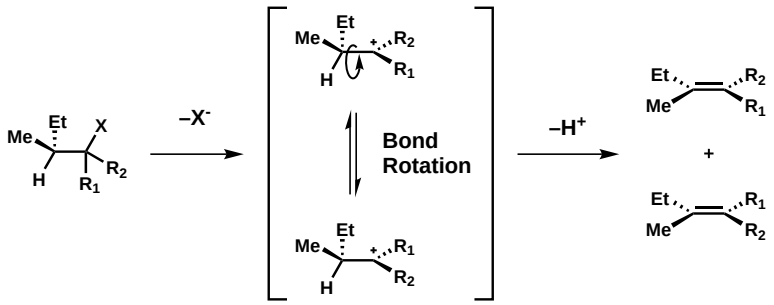

1.5

Scheme 1.1: Mechanism of E1 elimination.

Elimination reactions are related by the loss of two electronically commuted substituents and the formation of a new double bond. Three basic mechanisms for this transformation have been demonstrated and studied for over seventy years: E1, E2, and $E1_{cB}$. While all of these reactions lead to alkene products, the stereochemistry and product distribution is directly related to the mechanism of the reaction. The reaction mechanism is, in turn, characterized by the corresponding rate determining step.

The rate of E1 reactions is dependent on the dissociation of the leaving group as a preliminary step to deprotonation (**Scheme 1.1**). As a result, E1 reactions are accelerated by increasing the stability of carbocation **1.5**. Facile rotation around the C_α–C_β single bond combined with the planarity of the C_β carbocation results in the predominant formation of the most thermodynamically stable olefin and loss of stereochemical information. While these factors are important to consider and are of use in later discussion, the formation of a carbocation is precluded under basic conditions, and a further discussion of E1 elimination dynamics is not pertinent here.

Conversely, $E1_{cB}$ reactions proceed through a carbanion intermediate (**Scheme 1.2**). As a result, deprotonation at C_α is of paramount importance. While the classical example of an $E1_{cB}$ reaction utilizes the electron withdrawing power of carbonyls to stabilize the carbanion formed as an enolate, anions formed from aryl and diaryl methanes as well as

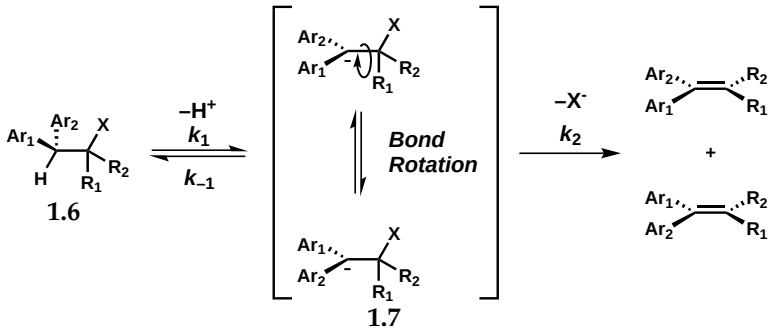

Scheme 1.2: Mechanism of $E1_{cB}$ elimination.

other species demonstrate a strong tendency toward this step-wise reaction pathway.[24] $E1_{cB}$ reactions can follow three different reaction pathways.[25] If the pKa of the substrate **1.6** is approximately equal to that of the base used, the rate of deprotonation k_1 will be close to k_{-1}. In these reversible $E1_{cBR}$ reactions the rate of the reaction is first order in both substrate and base. If the rate of protonation of **1.7** (k_{-1}) is small compared to k_1, the deprotonation step can be considered irreversible; however, k_1 is dependent on the concentration of both the substrate and the base and the overall reaction is still second order.

The truly unimolecular $E1_{cB}$ reaction, $E1_{cB\ anion}$ can be observed if both k_{-1} and k_2 are small compared to k_1. If the proton at C_α is acidic while C_β carries a poor leaving group, the anion **1.7** can be assumed to be formed stoichiometrically, making the reaction rate independent of the base concentration.

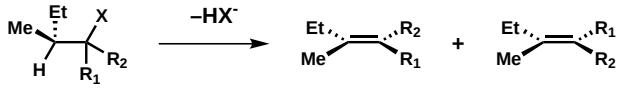

Scheme 1.3: Mechanism of E2 elimination

While E2 reactions are classically presented as a deprotonation with a synchronous expulsion of the leaving group, studies have shown that E2 reactions, while concerted, can be highly asynchronous, spanning a range of reaction pathways, nearly to the extremes of E1 and $E1_{cB}$ (**Figure 1.2**). The concerted nature of the E2 elimination requires

orbital overlap between the C_α–H bond and C_β–leaving group bond. The geometry around the C_α–C_β bond is thus restricted such that the leaving group and proton must be either *anti*- or *syn*-periplanar.[26] Since the synperiplanar conformation requires all functional groups to be eclipsed, the antiperiplanar conformation, which staggers the substituents, is usually preferred. Despite this, experimental and computational evidence has demonstrated that ion pairing of the leaving group to the base-associated cation can result in *syn*- elimination being preferred by as much as 8 kcal/mol.[27,28]

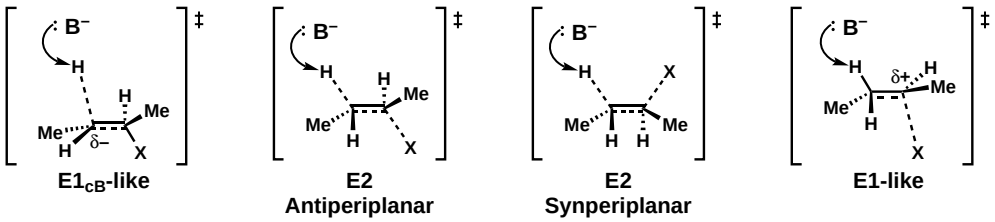

Figure 1.2: Possible E2 transition states.

1.2.1 Variability in the E2 Mechanism

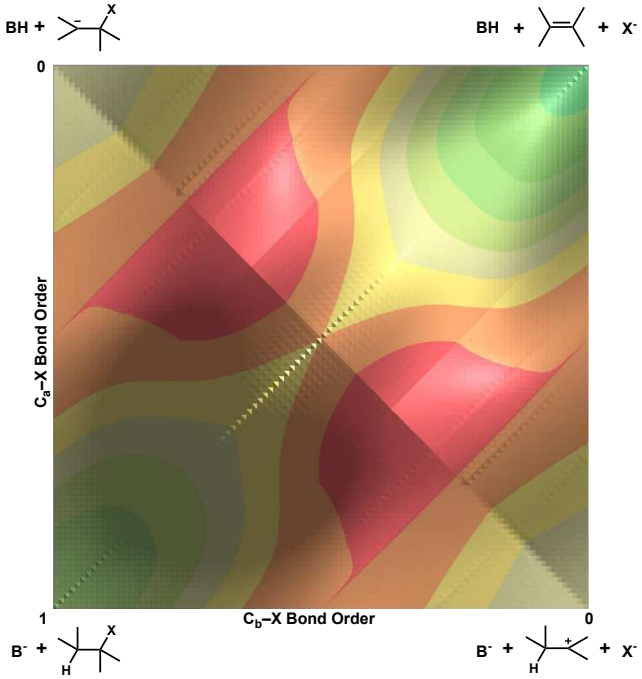

Figure 1.3: Idealized More O'Ferrall plot of an E2 reaction. Enthalpy increases green to yellow to red.

The variety of possible E2 reactions is best represented with the More O'Ferrall plot, **Figure 1.3**. The bottom left corner of the graph represents the starting material, while the top right represents the resultant alkene. Moving horizontally along the X-axis from the starting materials represents leaving group dissociation, while moving vertically along the Y-axis represents deprotonation. The Z-axis, which lies perpendicular to the plane of the page, represents the overall energy of the system ΔG. An E1 reaction progresses linearly along the X-axis demonstrating formation of the carbocation, then linearly toward product, showing loss of the C_α proton. An $E1_{cB}$ reaction must first proceed linearly up the Y-axis to form a carbanion, then toward the loss of the leaving group at C_β.

With these reaction coordinate axes established, a diagonal line connecting the starting material to the products represents the archetypal E2 elimination in which the dissociation of the leaving group and deprotonation are both concerted and synchronous. Thus, in the hypothetical three dimensional reaction coordinate diagram shown, the saddle point, which represents the transition state, is made to lie at the center of the graph; however, since the deprotonation and loss of the leaving group may be asynchronous, the transition state of an E2 reaction can range anywhere along the X,Y plane, from E2 to $E1_{cB}$. Increasing the acidity at C_α favors deprotonation, shifting the saddle point of the graph toward the top left corner of the graph, while increasing substitution at C_β favors carbocation formation, shifting the saddle point toward the bottom right corner. In keeping with the Hammond Postulate, increasing the stability of starting materials results in a later transition state, represented by migration of the saddle point toward the products in the top right. Similarly, increasing the stability of products results in an earlier transition state, represented by the migration of the saddle point toward the starting materials.[29]

1.2.2 Consequences of Base Species on E2 Eliminations

The complex nature of the E2 reaction is dependent not only on the structure of the substrate, but also on the polarity of the solvent, as well as the strength, aggregation sate, and countercation of the base used. As has been well established by the Collum group, the nature of a base in solution is only remotely related to the identity of the base itself.[30–32] Base clusters as well as free anions may be active base species in elimination reactions, though it is generally accepted that the free anion is the most basic species.

(1.1) $$RB^- + M^+ \rightleftharpoons (RB^-M^+) \rightleftharpoons (RB^-M^+)_2 \rightleftharpoons (RB^-M^+)_n$$

Excluding various solvation states, **Equation 1.1** describes the solution phase equilibrium of the generic base B, where RB^- + M^+ and (RB^-M^+) represent dissociated and associated ion pairs, respectively, while $(RB^-M^+)_2$ and $(RB^-M^+)_n$ represent dimeric and higher order complexes of the base. This equilibrium is perturbed by the identity of the cation species as well as the substituents on the base. Exner and Steiner have demonstrated that ion pairing constants (first equilibrium, **Equation 1.1**) for lithium, sodium, potassium, and cesium *tert*-butoxides in DMSO are 10^8, 10^6, 270, and 200 M^{-1}.[33] These results suggest that potassium would favor dissociated ions; however, Saunders has shown that a 0.1M solution of sodium *tert*-butoxide in *tert*-butyl alcohol is only 6% more conductive than pure *tert*-butyl alcohol.[34]

It is expected that as solvent polarity decreases, the ion association and aggregation should be more evident. As the base aggregates, the negative charge is dispersed to more nearby atoms, reducing the basicity, and increasing the size of the base, while limited access to the inside of the aggregate significantly decreases the effective concentration of the base. The Zavada group has demonstrated (**Table 1.1**) that as solvent polarity decreases, the amount of 1-decene produced is increased and the reaction temperature

Table 1.1: E2 elimination reactions as a function of solvent polarity.

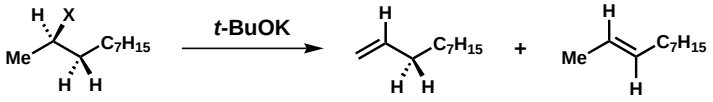

	DMSO, 20 °C		*t*-BuOH, 100 °C		PhH, 120 °C	
L.G.	%1-decene	trans:cis[a]	%1-decene	trans:cis[a]	%1-decene	trans:cis[a]
I	32.1	5.7	68.2	1.8	66.1	1.5
Br	48.0	5.3	79.4	1.3	79.9	0.8
Cl	59.4	5.1	84.5	1.1	86.0	0.7

[a] Ratio trans:cis 2-decene

must be raised.[35] Increased temperature not only favors base dissociation entropically, but accelerates eliminations performed by the associated and aggregated base species. As the aggregated base is large, it is expected that the approach to the less substituted C_α is preferred.

Table 1.2: E2 elimination reactions as a function of base concentration.

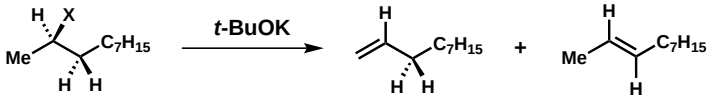

	0.25 M *t*-BuOK		0.50 M *t*-BuOK		1.00 M *t*-BuOK	
L.G.	% 1-decene	trans:cis[a]	% 1-decene	trans:cis[a]	% 1-decene	trans:cis[a]
I	37.5	5.44	39.5	5.30	42.2	4.90
Br	54.0	4.61	55.6	4.09	58.8	3.72
Cl	69.5	3.48	10.5	3.15	12.8	2.36
OTs	84.1	1.30	84.5	1.18	85.7	1.10

[a] Ratio trans:cis 2-decene

Base aggregation can be mitigated by the addition of additives to help solvate the cation. Zavada reports that the addition of dicyclohexyl-18-crown-6 ether to potassium *tert*-butoxide in DMF, *tert*-butyl alcohol, and benzene increased the conductivity of the solution 2, 10, and 34 fold, respectively.[36] While these results suggest that chelating additives overcome the aggregation observed in apolar solvents, the conductivity of potassium *tert*-butoxide in *tert*-butyl alcohol in the presence of crown ether is lower than

that of potassium *tert*-butoxide in DMF, meaning that despite the solubilizing effects of the crown ether, potassium *tert*-butoxide in *tert*-butyl alcohol maintains a significant degree of ionic association. Base aggregation can also be mitigated by decreasing base concentration. As the dissociated base species is, by necessity, solvated, decreasing the base concentration favors the dissociation side of the equilibrium. Zavada has shown (**Table 1.2**) that regardless of leaving group, increasing the base concentration results in a minor increases the amount of 1-alkene produced while decreasing the trans:cis 2-alkene ratio.[37]

Table 1.3: E2 elimination reactions as a function of base strength.

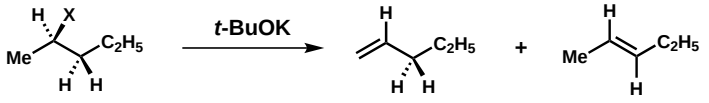

Base[a]	pKa	% 1-butene
Potassium *p*-nitrobenzoate	8.9	5.8
Potassium benzoate	11.0	7.2
Potassium *p*-nitrophenoxide	11.0	7.5
Potassium *o*-nitrophenoxide	11.0	7.5
Potassium acetate	11.6	7.4
Potassium *p*-aminobenzoate	12.7	8.0
Potassium 2,6-di-tert-butylphenoxide	15.0	19.2
Potassium phenoxide	16.4	11.4
Sodium 2,2,2-trifluoroethoxide	21.6	14.3
Sodium methoxide	27.0	17.0
Sodium ethoxide	27.4	17.1
Sodium *n*-propoxide	28.0	18.5
Potassium *tert*-butoxide	29.2	20.7

[a] All reactions performed on 2-iodobutane in DMSO at 50 °C

Following on the studies on base dissociation equilibria, the Bartsch group demonstrated a direct correlation between base strength and the percent of 1-butene observed in elimination reactions of 2-iodobutane (**Table 1.3**).[38] The increasing amount of 1-butene obtained when increasingly strong bases were used suggests that the reaction is shifting toward $E1_{cB}$ reactivity. As the base strength increases, the deprotonation of the substrate becomes more prevalent and the transition state of the E2

elimination shifts toward the $E1_{cB}$ corner of the reaction coordinate, exhibiting an increased anionic character in the transition state (**Figure 1.2**).

1.2.3 Consequences of Leaving Group on E2 Elimination Reactions

Table 1.4: E2 elimination reactions as a function of leaving group.

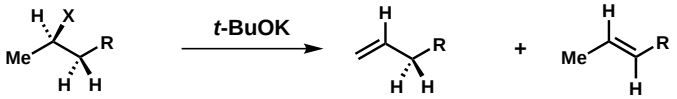

trans+cis

					X = I		X = Br		X = Cl		X = F		X = OTs	
Entry	R	Base	Solvent	Temp. (°C)	%1-alkene	trans:cis	%1-alkene	trans:cis	%1-alkene	trans:cis	%1-alkene	trans:cis	%1-alkene	trans:cis
1	C_3H_{13}	NaOMe	MeOH	100	19	3.6	28	3.0	33	2.9	70	2.3	39	1.7
2	C_2H_5	NaOEt	EtOH	78	20	4.1	25	3.8	35	3.5	82	2.6		
3	CH_3	Et_3COK	THF	25	25	4.1	34	3.1	49	2.7				
4	CH_3	Et_3COK	Et_3COH	50	49	1.5	71	1.3	80	1.1				
5	CH_3	Et_3COK	DMSO	25	21	3.8	33	3.9	44	4.2				
6	CH_3	*t*-BuOK	PhMe	50	36	1.7	52	1.4	67	1.0				
7	C_7H_{15}	*t*-BuOK	PhH	130	66	1.5	80	0.8	86	0.7	94	0.5	88	0.7
8	C_7H_{15}	*t*-BuOK (18-Crown-6)	PhH	20	47	3.2	62	2.7	71	2.8	95	1.4	82	1.7
9	CH_3	*t*-BuOK	t-BuOH	50	33	2.2	54	1.4	67	1.3			62	0.6
10	C_3H_{13}	*t*-BuOK	t-BuOH	100	69	1.8	80	1.4	88	1.1	97	1.2	80	0.4
11	C_7H_{15}	*t*-BuOK	t-BuOH	100	68	1.8	79	1.3	85	1.1	92	0.8	77	0.4
12	C_7H_{15}	*t*-BuOK (18-Crown-6)	t-BuOH	100	42	5.4	53	5.1	65	3.6	91	2.9	75	2.2
13	CH_3	*t*-BuOK	THF	25	20	3.6	34	3.3	49	2.9				
14	C_7H_{15}	*t*-BuOK	THF	50	40	5.3	56	4.0	70	3.2				
15	CH_3	*t*-BuOK	DMSO	25	20	3.5	32	3.8	41	4.1				
16	C_3H_{13}	*t*-BuOK	DMSO	25	35	5.2	47	4.9	59	4.9			73	2.9
17	C_7H_{15}	*t*-BuOK	DMSO	20	32	5.7	48	5.3	59	5.1	97	3.0	75	3.2
18	C_7H_{15}	*t*-BuOK (18-Crown-6)	DMSO	20	31	5.5	47	5.7	59	5.3	97	3.0	79	6.0

In E1 eliminations, the gradual rehybridization of C_β from sp^3 to sp^2 as a leaving group leaves results in increasing interaction between the C_α and C_β alkyl groups, which results in an increasing preference for the formation of trans-alkenes. **Table 1.4**[35,37,39–44] shows that as the electronegativity of the leaving group decreases (F>Cl>Br>I), the trans:cis ratio of 2-alkene increases suggesting that improving leaving group ability results in the E2 reaction approaching an E1-like transitions state. Additionally, the fact that as leaving group ability improves, the amount of 1-alkene formed *decreases* is an indicator of decreasing $E1_{cB}$ character in the E2 reaction, which is consistent with a shift

of the transition state toward the bottom right of **Figure 1.3**. While this simplified model is sufficient to predict many elimination trends, it notably breaks down for enantioenriched substrates as the stereochemistry of the elimination comes into play.

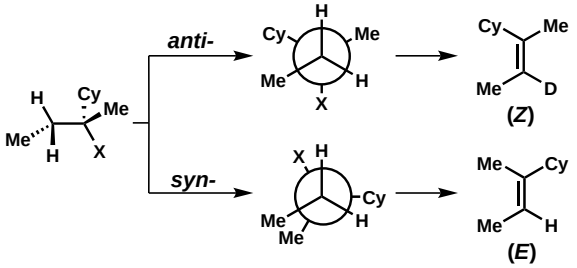

Scheme 1.4: Determining elimination stereochemistry from tertiary alkenes.

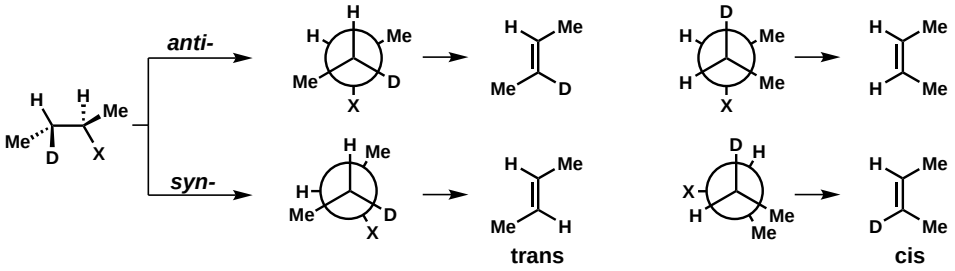

Scheme 1.5: Determining elimination stereochemistry from secondary alkenes.

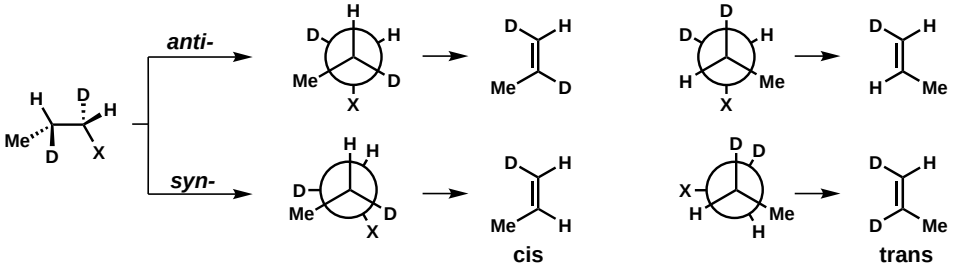

Scheme 1.6: Determining elimination stereochemistry from primary alkenes.

Elimination stereochemistry can be determined by analysis of the alkene diastereomers produced from a single diastereomer of starting material. The (*E*):(*Z*) ratio of tertiary alkenes are directly related to the elimination stereochemistry (**Scheme 1.4**);

however if the alkene product is secondary, an isotopic label must be stereoselectively introduced in order to effect the same analysis (**Scheme 1.5**). The kinetic isotopic effects introduced by the label must be accounted for as the dedeutero-elimination faces a primary kinetic isotope effect, while the dehydro-elimination faces a secondary kinetic isotope effect. These adjustments become more complicated in trying to determine the stereochemical pathways leading to elimination of primary alkyl halides as two isotope labels must be introduced stereoselectively (**Scheme 1.6**), to say nothing of attempting to determine stereochemistry of eliminations forming 1-alkenes from 2-halo-alkanes. The difficulty involved in generating a stereochemically defined methyl group bearing a proton, deuterium, and tritium atom means that the stereochemistry in this case remains largely unexplored.

Table 1.5: Stereochemistry of E2 dehydrohalogenation reactions

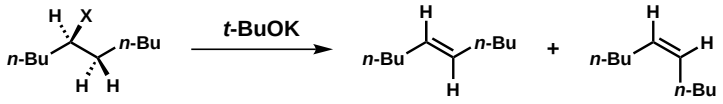

trans cis

		$(trans:cis)^{syn}$	$(trans:cis)^{anti}$	$(syn:anti)^{trans}$	$(syn:anti)^{cis}$
in Benzene	Br	6.7	0.56	0.5	0.04
	Cl	7.1	0.48	1.9	0.13
	F	21.5	0.74	7.3	0.25
in DMSO	Br	2.2	6.5	0.03	0.09
	Cl	2.5	6.7	0.06	0.16
	F	2.5	5.1	0.12	0.24

Demonstrated as early as 1962,[45] computational and experimental evidence has demonstrated the *syn*-elimination pathway to be preferred in dehydrofluorination and competitive in dehydrochlorination reactions performed in low polarity solvents **Table 1.5**.[27,28] The fact that low polarity solvents, and thus chelating conditions, are required for *syn*-eliminations to be preferred strongly indicates that leaving group chelation is key to the elimination mechanism.

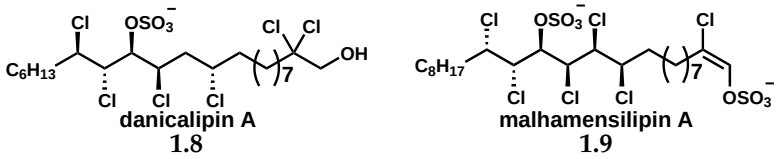

Scheme 1.7: The importance of diastereoselective dehydrochlorination.

1.3 Dehydrohalogenation of β-chlorosulfates

The diastereoselective installation of alkenes remains a problematic synthetic transformation. While diastereoselective eliminations are known, they largely rely on the steric bulk of the substituents to favor alkene geometry.[46,47] Despite these challenges, comparing danicalipin (**1.8**) and malhamensilipin (**1.9**) the Vanderwal group hypothesized that the β,β-dichlorohydrin of **1.8** may be a biosynthetic precursor to the (*E*)-vinylsulfate of **1.9** *via* an E2 elimination reaction. Pursuing this hypothesis, Dr. Grant Shibuya demonstrated that exposing β,β-dichlorosulfate (**1.10**) to LDA led to the to exclusive formation of the (*E*)-vinyl sulfate (**1.11**), while using *t*-BuOK resulted in predominantly the (*Z*)-vinyl sulfate (**1.12**). This discovery allowed the Vanderwal group to complete the first enantioselective synthesis of **1.9**, but the source of the elimination selectivity had not been elucidated.[48]

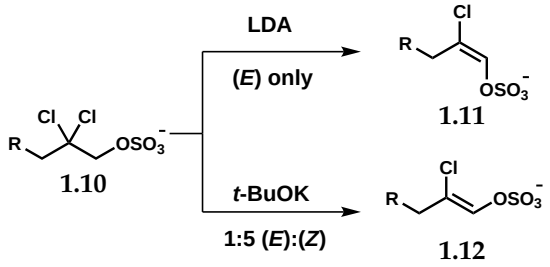

Scheme 1.8: Dr. Grant Shibuya's observed elimination selectivity

The ability to synthesize alkenes with high diastereoselectivity as well as the potential for exploration into new reactions of vinyl sulfates motivated us to continue studying the reaction in the hope of discovering broadly applicable lessons in acyclic stereocontrol and reactivity. We had optimistically hypothesized that the observed

diastereoselectivity in dehydrochlorination of β,β-dichloro sulfates was influenced by competing chelation effects between the leaving group and a metal cation.

1.3.1 Hypothesis Based on Computational Models

Ab initio studies of the ground state energies of 2,2-dichlorobutyl sulfate (**1.10**) performed in implicit tetrahydrofuran using Spartan '08, suggest that the cation associated with the sulfate prior to the elimination significantly biases the ground state conformation (**Figure 1.4**). Calculations carried out with the B3LYP[49–52] functional using the 6-31G*[53–58] basis set and the SM8[59] model for implicit solvent show a bias in the ground state conformation of **1.10** that appears to be caused by an association between the sodium and one of the chlorine atoms (**Figure 1.4A**). This effect was observed in the ground state for all conformational isomers that were modeled. Despite the fact that prior to energy minimization the sodium cation was placed between the three partially negative oxygen atoms of the sulfate after ground state energy minimization, the chlorine–sodium distance was found to be 2.72Å while the sodium–oxygen distance was found to be 2.24Å. When a conformation search was performed in the absence of an associated cation, the ground state conformation appeared to favor dipole minimization (**Figure 1.4B**), placing the sulfate gauche to the ethyl group. Though far from conclusive, this data may help to shape a theory for cation chelation model for the observed diastereoselective elimination.

The chelation effect observed in our *ab initio* studies would predispose dichloride **1.10** to forming **1.11** *via* an *anti*-elimination. If such a chelating effect is operative in the real system, formation of **1.12** would require freeing of the sulfate to rotate into the dipole minimized conformation such as that found in the low energy conformer in **Figure 1.4B**. A strongly chelating cation such as lithium or sodium may be able to coordinate the bound sulfate, displacing the originally present sodium cation, and freeing the sulfate to rotate into a dipole minimized conformation. This dipole minimized conformer may now readily undergo elimination to give trans-olefin **1.11**.

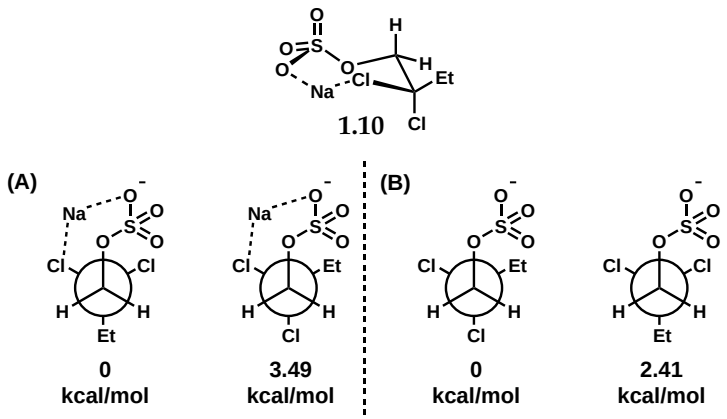

Figure 1.4: Ground state energies of neutral and anionic β,β-dichloro sulfate.
(A) Conformers including sodium countercation.
(B) Conformers of the free anion.

Meanwhile, the less strongly chelating potassium cation would, hypothetically, compete less with sodium for sulfate coordination, causing the potassium bases to yield selectivity for trans-isomer **1.12**.

1.3.2 Elimination Results

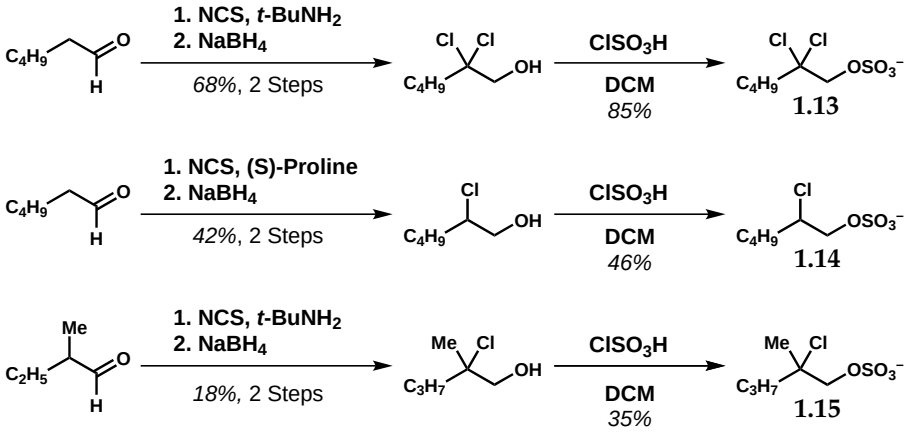

Scheme 1.9: Synthesis of β-chloro sulfates.

In order to probe the mechanism of stereoselectivity in dehydrohalogenation, substrates were designed to include steric and electronic differences compared to the original substrate **1.13** (**Scheme 1.9**). The effect of the geminal dichloride was tested by performing eliminations on monochloride **1.14** and steric considerations were examined using the 2-chloro-2-methyl substrate **1.15**. Commercially available lithium, sodium, and

potassium hexamethyldisilazide (LHMDS, NaHMDS, KHMDS) bases were chosen for the elimination reactions in order to determine if cation effects were significant. The use of lithium diisopropylamide (LDA) and potassium tert-butoxide (KOtBu) allowed us to further investigate whether the strength of the base was a factor in stereoselectivity as diisopropylamine has a pKa of ~40, while hexamethyldisilazane and tert-butyl alcohol have pKa's of 30 and 29.4, respectively (pKa's in DMSO).

Table 1.6: Selectivity in dehydrochlorination of β-chloro sulfates.

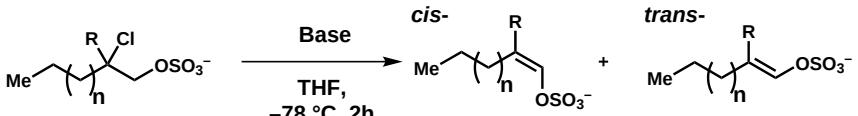

1.13 R = Cl n = 2 **1.16** R = Cl n = 2 **1.17** R = Cl n = 2
1.14 R = H n = 2 **1.18** R = H n = 2 **1.19** R = H n = 2
1.15 R = CH_3 n = 1 **1.20** R = CH_3 n = 1 **1.21** R = CH_3 n = 1

Entry	R	Base	*cis* : *trans*[a]	Conversion
1	Cl	LDA	1.0 : 0	5%
2	Cl	LHMDS	6.7 : 1.0	4%
3	Cl	NaHMDS	1.0 : 1.2	74%
4	Cl	KHMDS	1.0 : 2.8	54%
5	Cl	*t*-BuOK	1.0 : 3.0	39%
6	H	LDA	1.0 : 6.4	29%
7	H	LHMDS	1.0 : 1.5	53%
8	H	NaHMDS	1.0 : 3.0	34%
9	H	KHMDS	1.0 : 2.8	56%
10	H	*t*-BuOK	1.5 : 1.0	87%
11	CH_3	LDA		~0.5%
12	CH_3	LHMDS		~0.5%
13	CH_3	NaHMDS	1.0 : 1.5	32%
14	CH_3	KHMDS	1.0 : 1.6	29%
15	CH_3	KOtBu	1.0 : 1.8	68%

[a]For Entries 1–5, the (*E*) isomer is *cis*- and the (*Z*) isomer is *trans*-. For all others, the (*E*) isomer is *trans*- and the (*Z*) isomer is *cis*-.

Substrates **1.13**, **1.14**, and **1.15** were synthesized in three steps in 58%, 19%, and 6% overall yield, respectively. Since the sulfate-forming reaction was quenched with sodium bicarbonate, sodium is assumed to be the countercation of the sulfate anion, though no attempts to determine the nature of this cation have been made. The averaged results of duplicate elimination experiments on **1.13**, **1.14**, and **1.15** are summarized in **Table 1.6**.

While no pervasive trends were observed based on cation or base strength, examination of the individual substrates may suggest that different selectivity mechanisms are operative. Though LDA, LHMDS, and NaHMDS were found to favor formation of cis-chlorovinyl sulfate **1.16** (entries 1-4), neither hexamethyldisilazide was as selective as LDA. KOtBu and KHMDS were both found to form the *trans*-chlorovinyl sulfate isomer **1.17** preferentially. The fact that both potassium bases gave preference for **1.17**, while bases carrying lithium and sodium cations gave selectivity for **1.16**, lends support to our hypothesis that a cation effect is responsible for the observed selectivity in eliminations of substrates such as **1.13**.

Table 1.7: Preliminary dehydrochlorination with varying sulfate countercation.

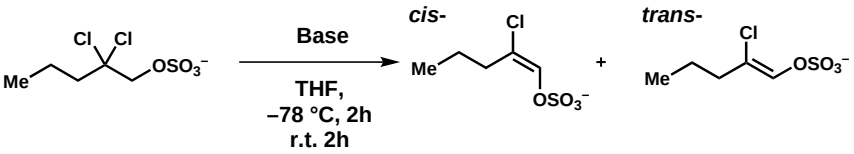

Entry	Cation	Base	*cis* : *trans*	Conversion
16	Li	LDA	*cis* only	5.5%
17	Li	LHMDS	2.5 : 1	0.3%
18	Li	NaHMDS	8.9 : 1	0.8%
19	Li	KHMDS	4.4 : 1	1.9%
20	Li	*t*-BuOK	*trans* only	1.7%
1	Na	LDA	1.0 : 0	5%
2	Na	LHMDS	6.7 : 1.0	4%
3	Na	NaHMDS	1.2 : 1.0	74%
4	Na	KHMDS	1.0 : 2.8	54%
5	Na	*t*-BuOK	1.0 : 3.0	39%
21	K	LDA	*cis* only	0.1%
22	K	LHMDS	7.2 : 1	50%
23	K	NaHMDS	1 : 1.4	3%
24	K	KHMDS	1 : 3.5	58%
25	K	*t*-BuOK	1 : 3.6	45%

The scope of cation chelation effects appears to be limited to β,β-dichlorosulfates because the elimination of sulfate **1.14** gave the trans-isomer **1.19** selectively in all cases (entries 6-9) except in elimination effected by KOtBu (entry 10), which showed selectivity for **1.18**. While this may be evidence of a pKa dependent process for this

substrate, exploration of tert-butoxide bases bearing lithium or sodium cations did not corroborate this idea. Additionally, eliminations carried out on **1.15** gave a slight preference to **1.21** over **1.20** (entries 13-15) regardless of cation or base, suggesting that the addition of a methyl group was sufficient to override any cation chelation or pKa mediated selectivity and give simply the less sterically hindered olefin. Furthermore, preliminary elimination experiments on substrates varying the cation associated to sulfate **1.13** (**Table 1.7**) gave results that varied from entries 1-5, but did not reinforce the hypothesized chelation control.

1.4 Experimental Procedures

General Information

^{1}H NMR were obtained at 298 K at 500 MHz using a CRYO500 probe or at 600 MHz using an AVANCE600 probe, as indicated. ^{13}C spectra were obtained at 298 K at 125 MHz using a CRYO500 probe. All chemical shifts are referenced to the residual protonated solvent signal as an internal standard ($CDCl_3$ is referenced to 7.26 ppm for ^{1}H and 77.16 ppm for ^{13}C. CD_3OD is referenced to 3.31 ppm for ^{1}H and 49 ppm for ^{13}C) and reported in parts per million (ppm). Coupling constants are reported in hertz (Hz) and peak multiplicities are listed as follows: s, singlet; d, doublet; t, triplet; q, quartet; m, multiplet. Extended multiplicity is reported by combinations of these abbreviations (dt, doublet of triplets). IR Spectra were recorded on a Perkin Elmer RXI FT-IR spectrometer and are reported in wave numbers (cm^{-1}). High-resolution mass spectra were referenced to an internal standard.

General Experimental

Unless otherwise noted, all reactions were run under an atmosphere of argon in flame dried flasks equipped with Teflon-coated magnetic stir bars. Anhydrous solvents were dried by filtration through activated alumina. Amine bases were distilled over CaH_2 prior to use. All reagents were prepared by known literature procedures or used as obtained from commercial sources, unless otherwise described. Reactions were monitored by thin-layer chromatography (TLC) on 0.25 mm precoated Dynamic Adsorbents, F254 or EMD 60 F254 glass plates using UV light for visualization and *para*-anisaldehyde for development. Syringes used were plastic Airtight syringes unless otherwise noted.

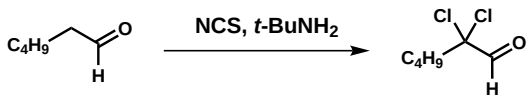

Preparation of 2,2-dichlorohexanal: To neat hexanal (1.2 mL, 9.76 mmol) at 0 °C was added *t*-$BuNH_2$ (1.1 mL, 10.47 mmol). After the reaction mixture was stirred at 0 °C for 15 min, 10 mL of CCl_4 were added, resulting in a cloudy, colorless solution. $MgSO_4$ was added and the suspension was stirred for 30 seconds. The drying agent was removed by vacuum filtration and rinsed with approximately 10 mL of DCM. The previous step was repeated until the filtrate appeared clear. *N*-Chlorosuccinimide (NCS) (4.03 g, 30.18 mmol) was added and the reaction mixture was stirred shielded from light for six hours at room temperature. Precipitated succinimide was removed by vacuum filtration and rinsed with DCM. The filtrate was concentrated *in vacuo* to a volume of approximately 20 mL, 10 mL of 6 M aqueous HCl were added, and the biphasic mixture was stirred vigorously for 6 h. The organic layer was removed and the aqueous layer was extracted with 2 x 15 mL of hexanes. The combined organic layers were washed with approximately 15 mL of water and 15 mL of brine, dried with Na_2SO_4 and concentrated *in vacuo* to give a slightly yellow oil, with some solids present. The crude mixture was carried on to the next step without further purification. (See General Experimental – Reduction of α-chloro alcohols to β-chloro alcohols) ^{1}H NMR (500 MHz, $CDCl_3$) δ 9.25 (s, 1H), 2.29–2.26 (m, 2H), 1.61 (tt, 8.3, *J* = 7.3, 2H), 1.45–1.37 (qt, *J* = 7.5, 7.4, 2H), 0.95 (t, *J* = 7.4, 3H).

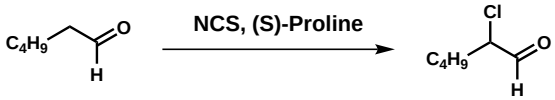

2-Chlorohexanal: Hexanal (1.3 mL, 10.58 mmol) was added to a solution of (*L*)-Proline (0.127 g, 1.10 mmol) in 21 mL of dry DCM. After stirring for 5 min at room temperature, the reaction mixture was cooled to 0 °C and NCS (1.414 g, 10.59 mmol) was added. The reaction mixture was stirred for 10 min at 0 °C, warmed to room temperature, and stirred for an additional 1 h. The resulting suspension was concentrated *in vacuo*, pentane was added, insoluble materials were filtered off, and the filtrate was again concentrated *in vacuo* to yield a clear oil. Crude material was carried on to the next step

without further purification. (See General Experimental – Reduction of α-chloro alcohols to β-chloro alcohols.) ^{1}H NMR (500 MHz, $CDCl_3$) δ 9.49 (d, *J* = 2.5, 1H), 4.15 (ddd, *J* = 8.2, 5.5, 2.4, 1H), 2.02–1.96 (m, 1H), 1.86–1.80 (m, 1H), 1.54–1.48 (m, 2H), 1.47–1.21 (m, 2H), 0.99 (t, *J* = 7.3, 3H).

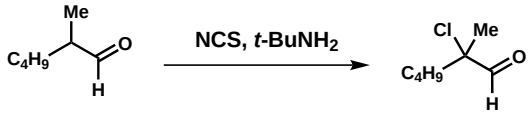

2-Chloro-2-methylpentanal: To neat 2-methylpentanal (5 mL, 40.34 mmol) at room temperature was added *t*-$BuNH_2$ (4.25 mL, 40.44 mmol). The reaction mixture was stirred for 20 min at room temperature and 50 mL of CCl_4 were added resulting in a cloudy solution. After stirring for 5 min at room temperature, $MgSO_4$ was added and the suspension was stirred 5 min further. The drying agent was filtered off and rinsed with approximately 25 mL of DCM. The previous two steps were repeated until no cloudiness was observed in the filtrate. NCS (8.25 g, 61.78 mmol) was added and the reaction mixture was stirred for 48 h and concentrated *in vacuo*. The crude mixture was distilled under vacuum at 60 °C (1.530 g, 28%). Bulb to bulb distillation was carried out without observing a boiling point of the substrate. ^{1}H NMR (500 MHz, $CDCl_3$) δ 9.43 (s, 1H), 1.92 (ddd, *J* = 16.8, 11.7, 5.1, 1H), 1.81 (ddd, *J* = 16.5, 11.5, 4.9, 1H), 1.58 (s, 3H), 1.52–1.40 (m, 2H), 0.96 (t, *J* = 7.4, 3H).

General Experimental — Reduction of α-chloro alcohols to β-chloro alcohols.

$NaBH_4$ (9.99 mmol, 1 equiv.) was added as single portion to a 0 °C solution of crude α-chloro alcohol (≤ 9.76 mmol, 1 equiv.) in 15 mL of EtOH. The cloudy white suspension was stirred, open to air, at 0 °C for 5 min, warmed to room temperature, and stirred for 1 h further. The suspension was poured into 15 mL of 6M HCl with an equal volume of ice and stirred gently. After gas emission had subsided, the aqueous and organic layers were separated and the aqueous layer was extracted with 3 x 30 mL of pentane. The

combined organic layers were washed with approximately 30 mL of brine, dried with Na_2SO_4, filtered, and concentrated *in vacuo*.

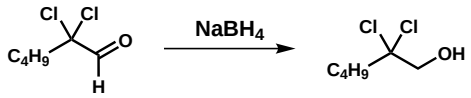

2,2-Dichlorohexan-1-ol: 2,2-dichlorohexanal (1.6 g, crude) was reduced according to the general experimental method and purified by column chromatography (5% EtOAc in hexanes) to give the product as a clear oil (1.131 g, 68% from hexanal): ^{1}H NMR (500 MHz, $CDCl_3$) δ 3.91(s, 2H), 2.36, (br s, 1H), 2.23–2.20 (m, 2H), 1.65–1.59 (m, 2H), 1.39, (qt, *J* = 7.5, 7.4, 2H),0.95 (t, *J* = 7.4, 3H); ^{13}C NMR (125 MHz, $CDCl_3$) δ 94.8, 72.2, 43.5, 27.1, 22.4, 14.0; IR (thin film) 3529, 2933, 1456, 1381, 1069, 740, 708 cm^{-1}; HRMS (CI/DCM) *m / z* calcd for $C_5H_8Cl_2$ (M-CH_3OH)$^+$ 138.0003, found 138.0000.

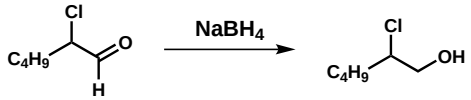

2-Chlorohexan-1-ol: 2-chlorohexanal (1.4 g, crude) was reduced according to the general experimental method and purified by vacuum distillation to give the product as a clear oil (0.600 g, 42% from hexanal): bp = 120 °C at 197 Torr; ^{1}H NMR (500 MHz, $CDCl_3$) δ 4.03 (appar. tdd, J =8.6, 4.6, 3.7, 1H), 3.80 (dd, *J* = 12, 3.6, 1H), 3.67, (dd, *J* = 12.1, 7.1 1H), 2.01 (br s, 1H) 1.81–1.24 (m, 6H), 0.92 (t, *J* = 7.3, 3H); ^{13}C NMR (125 MHz, $CDCl_3$) δ 67.2, 65.6, 34.1, 28.6, 22.4, 14.0; IR (thin film) 3318, 2958, 1466, 1077, 736, 683 cm^{-1}; HRMS (CI/DCM) *m / z* calcd for $C_6H_{14}ClO$ (M+H)$^+$ 137.0733, found 137.0731.

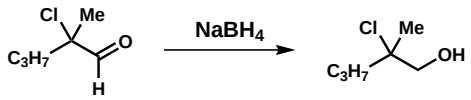

2-Chloro-2-methylpentan-1-ol: 2-chloro-2-methylpentanal (1.530 g, 11.37 mmol) was reduced according to the general experimental method to give a clear oil which was used without purification (1.052 g, 68%, 18% from 2-methylpentanal): ^{1}H NMR (500 MHz, $CDCl_3$) δ 3.63 (d, *J* = 11.8, 1H), 3.58 (d, *J* = 11.8, 1H), 1.99 (br s, 1H), 1.84–1.77

(m, 1H), 1.74–1.68 (m, 1H), 1.52 (s, 3H), 0.95 (t, J = 7.4, 3H); ^{13}C NMR (125 MHz, $CDCl_3$) δ 76.3, 71.3, 42.9, 26.2, 17.9, 14.4; IR (thin film) 3357, 2934, 1466, 1380, 1042, 743 cm^{-1}; HRMS (CI/DCM) m / z calcd for $C_6H_{14}ClO$ $(M+H)^+$ 137.0733, found 137.0727.

General Experimental — Sulfate Formation

To a solution of β-chloro alcohol (3.1 mmol, 1 equiv) in dry DCM (16 mL, 0.2 M) was added $ClSO_3H$ (0.21 mL, 1 equiv.), dropwise, by glass syringe. The reaction mixture became progressively more golden-yellow throughout the addition. After stirring for ten minutes at room temperature, the reaction mixture was slowly poured into 20 mL of saturated aqueous $NaHCO_3$ (6 mL / mmol of starting material) with an added 8 g of solid $NaHCO_3$ (2.5 g / mmol starting material). Solvent was removed *in vacuo* and the resultant solids were loaded onto a silica gel column. Unreacted material was removed by eluting with 50 mL hexanes and 100 mL of 50:50 EtOAc:hexanes. Sulfated materials were eluted from the column using 100 mL of 5% MeOH in DCM followed by 200 mL of 20% MeOH in DCM. Solvent was removed *in vacuo* and the resultant solids were filtered through a column of Celite, eluting with dry THF. Concentration *in vacuo* gave the product as a white solid.

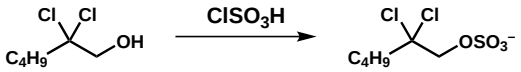

2,2-Dichlorohexyl sulfate (1.13): 2,2-dichlorohexan-1-ol (0.457 g, 2.67 mmol) was subjected to the general reaction conditions above to give the product with no further purification (0.622 g, 85%): mp: decomposed at 125 °C; ^{1}H NMR (600 MHz, CD_3OD) δ 4.31 (s, 2H) 2.26–2.22 (m, 2H), 1.62 (tt, J = 8, 7.5, 2H), 1.39 (qt, J = 7.5, 7.4, 2H), 0.95 (t, J = 7.63, 3H); ^{13}C NMR (125 MHz, CD_3OD) δ 91.1, 75.3, 44.6, 27.7, 23.0, 14.1; IR (KBr pellet) 2963, 2346, 1632, 1243, 1079, 817 cm^{-1}; HRMS (ESI/MeOH) m / z calcd for $C_6H_{11}{}^{35}Cl^{37}ClO_4S^-$ (M^-) 250.9726, found 250.9726.

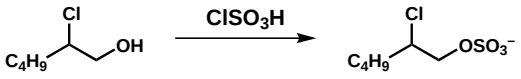

2-Chlorohexyl sulfate (1.14): 2-chlorohexan-1-ol (0.600 g, 4.39 mmol) was subjected to the reaction conditions above and purified by flash chromatography (DCM – 10% MeOH in DCM) to give the product as a white solid (0.483 g, 46%): mp: decomposed at 154 °C; ^{1}H NMR (600 MHz, CD_3OD) δ 4.16–4.11 (m, 2H), 4.04 (dd, *J* = 8.36, 3.0, 1H), 1.98–1.92 (m, 1H), 1.69–1.62 (m, 1H), 1.60–1.51 (m, 1H), 1.46–1.33 (m, 3H), 0.94 (t, *J* = 7.18, 3H); ^{13}C NMR (125 MHz, CD_3OD) δ 72.0, 60.7, 35.3, 29.2, 23.3, 14.3; IR (KBr pellet) 2935, 1625, 1236, 1080, 830, 810 cm^{-1}; HRMS (ESI/MeOH) *m* / *z* calcd for $C_6H_{12}ClO_4S^-$ (M^-) 215.0145, found 215.0137.

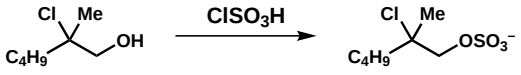

2-Chloro-2-methylpentyl sulfate (1.15): 2-chloro-2-methylpentan-1-ol (0.430 g, 3.14 mmol) was subjected to the reaction conditions above to give the product with no further purification (0.261 g, 35%): mp: decomposed at 112 °C; ^{1}H NMR (600 MHz, CD_3OD) δ 4.05 (d, *J* = 9.9, 1H), 3.99 (d, *J* = 9.8, 1H), 1.81–1.72 (m, 2H), 1.55 (s, 3H; and m, 2H), 0.94 (t, *J* = 7.6, 3H); ^{13}C NMR (125 MHz, CD_3OD) δ 74.9, 71.0, 43.8, 27.8, 18.4, 14.4; IR (KBr pellet) 2963, 1630, 1260, 1078, 823, 645 cm^{-1}; HRMS (ESI/MeOH) *m* / *z* calcd for $C_6H_{12}ClO_4S^-$ (M^-) 215.0145, found 215.0137.

General Experimental — Elimination Reactions

Elimination reactions were run under an atmosphere of nitrogen in flame dried or oven dried dram vials equipped with stir bars. For the first set of data, 0.02 g of each substrate was loaded into each vial, while repeated experiments used 0.01 g of each substrate. In the case that multiple bases were being examined simultaneously, bases were added sequentially, to individual vials, in the order of: LDA, *t*-BuOK, LHMDS, KHMDS,

NaHMDS with, approximately, five minute intervals between each addition. Reaction times refer to the time that passed after the addition of the last base.

β-chloro sulfate, 0.1 M in dry THF, was cooled to –78 °C and base (1 M in THF) was added via glass syringe. Reaction mixture was stirred at –78 °C for 2 h, warmed to room temperature and stirred for 2 h further. 0.5 mL of saturated aqueous $NaHCO_3$ were added per 0.01 g of starting material. The stir bar was removed from the reaction mixture and rinsed with a small amount of methanol. Solvents were removed *in vacuo*, *n*-BuOH or dry THF was added and the suspension was thoroughly stirred. The suspension was filtered through a plug of cotton to remove insoluble materials and solvent was removed *in vacuo* to give the crude reaction mixture as a white solid. Conversion was determined by comparison of the integration of the starting material and C1-H resonance and that of the combined product isomers. Analysis of E:Z selectivity was performed by ^{1}H NMR integration of the peaks bellow. Resonances of the aliphatic chain were not diagnostic. Spectra in the supplemental are of *t*-BuOK elimination products and are representative of both isomers.

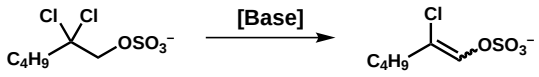

Cis-2-chlorohex-1-en-1-yl sulfate (1.16): ^{1}H NMR (600 MHz, CD_3OD) δ 6.74(s, 1H, C1-H). **Trans-2-chlorohex-1-en-1-yl sulfate (1.17)**: ^{1}H NMR (600 MHz, CD_3OD) δ 6.82(s, 1H, C1-H).

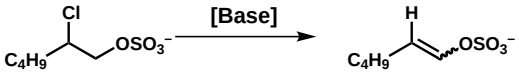

Cis-hex-1-en-1-yl sulfate (1.18): ^{1}H NMR (600 MHz, CD_3OD) δ 6.52(d, J = 12.6, 1H, C1-H), 5.26 (dt, J = 12.3, 7.6, 1H, C2-H). **Trans-hex-1-en-1-yl sulfate (1.19)**: ^{1}H NMR (600 MHz, CD_3OD) δ 6.49 (d, J = 6.1, 1H, C1-H), 4.73 (dt, J = 7.1, 6.6, 1H, C2-H).

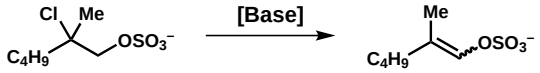

Cis-2-methylpent-1-en-1-yl sulfate (1.20): ^{1}H NMR (600 MHz, CD_3OD) δ 6.35 (s, 1H, C1-H), 1.63 (s, 3H, C2-CH3). **Trans-2-methylpent-1-en-1-yl sulfate (1.21**): ^{1}H NMR (600 MHz, CD_3OD) δ 6.35 (s, 1H, C1-H), 1.59 (s, 3H, C2-CH3).

Ab initio calculation procedures:

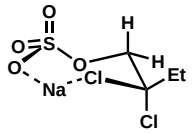

Calculations were done in Wavefunction Inc.'s Spartan'08, version 1.1.2, build 131. Calculations were performed with the Semi Empirical level of theory using the PM3 model or using the B3LYP level of theory with the 6-31G* basis set and SM8 solvent model. The following procedure was used to find the ground state conformation of sodium 2,2,-dichlorobutyl sulfate (**1.10**): The molecule was built and relaxed. Subsequently, a conformation search was performed using the Semi Empirical method. Analysis of all 216 combinations of 60 ° rotations of three bonds gave 11 low energy conformers, many of which were redundant or varied only slightly in energy. The first two different low energy conformers were then minimized using B3LYP 6-31G* in implicit THF. The same procedure was followed for the anion of **1.10**. Coordinates are included beginning on the next page.

Atomic Coordinates:

Sodium Cation: E (B3LYP, 6-31G*, implicit THF) = –101770.12

Sodium 2,2-dichlorobutyl sulfate:

Table 1.8: Low Energy Conformer: E (B3LYP, 6-31G*, implicit THF) = –1216401.31

C	−2.832177	−0.644064	−0.594875
H	−2.640118	−0.908943	−1.641878
H	−3.561577	0.171012	−0.599600
C	−1.514845	−0.097668	−0.055512
C	−0.345381	−1.086623	−0.057846
H	−0.650466	−1.978285	0.496804
H	−0.124508	−1.360026	−1.094749
O	0.801786	−0.528541	0.574969
S	2.341320	−0.441297	−0.267083
Cl	−1.732954	0.550277	1.680668
Cl	−1.037602	1.396461	−1.053597
C	−3.394706	−1.855614	0.157514
H	−2.740725	−2.729559	0.092105
H	−4.352040	−2.130402	−0.295506
H	−3.577737	−1.633044	1.213198
O	3.178506	−1.423427	0.425338
O	2.657080	0.986887	0.071864
O	2.021495	−0.692826	−1.676410
Na	0.737244	1.677616	0.992808

Table 1.9: High energy Conformer: E (B3LYP, 6-31G*, implicit THF) = –1216397.82

C	−1.177821	0.384685	−1.340774
H	−1.020856	−0.451141	−2.032427
H	−0.232959	0.941508	−1.340090
C	−1.330555	−0.248256	0.038010
C	−0.140970	−1.114515	0.500605
H	−0.408313	−1.656396	1.410286
H	0.079112	−1.831067	−0.296566
O	0.995170	−0.305715	0.789596
S	2.422602	−0.327984	−0.225174
Cl	−2.807502	−1.278498	0.133604
Cl	−1.543872	1.134838	1.319226
C	−2.321397	1.266954	−1.837041
H	−3.261147	0.711599	−1.904042
H	−2.078057	1.634532	−2.838691
H	−2.482112	2.135707	−1.190630
O	1.943345	−0.720569	−1.554902
O	3.346379	−1.238043	0.455005
O	2.750148	1.128725	−0.067697
Na	1.080177	1.883649	1.197527

2,2-dichlorobutyl sulfate:

Table 1.10: Low Energy Conformer: E (B3LYP, 6-31G*, implicit THF) = –1114595.38

C	1.213680	−1.376599	0.446839
H	0.409276	−1.795720	−0.166449
H	0.875272	−1.444373	1.488381
C	1.254709	0.114678	0.112048
C	−0.076455	0.833245	0.364479
H	−0.296694	0.746122	1.435655
H	0.022332	1.895913	0.112353
O	−1.088581	0.213410	−0.406575
S	−2.670517	0.408755	0.227671
Cl	1.745761	0.359717	−1.631660
Cl	2.484692	0.969505	1.166736
C	2.506913	−2.166361	0.259874
H	2.334748	−3.211652	0.537542
H	3.313370	−1.779348	0.890387
H	2.844031	−2.145862	−0.780883
O	−3.454619	−0.299628	−0.798100
O	−2.854127	1.875984	0.280455
O	−2.609073	−0.248309	1.552984

Table 1.11: High energy Conformer: E (B3LYP, 6-31G*, implicit THF) = –1114592.96

C	−2.586966	−0.691056	−0.831169
H	−2.465706	−0.443729	−1.892485
H	−3.562916	−0.302728	−0.525079
C	−1.516113	0.109715	−0.073723
C	−0.095266	−0.312512	−0.435473
H	0.032403	−1.363479	−0.149121
H	0.004741	−0.236743	−1.528288
O	0.869960	0.488204	0.211946
S	2.479592	−0.018205	−0.083169
Cl	−1.772769	−0.068517	1.728489
Cl	−1.749270	1.878367	−0.491817
C	−2.543423	−2.210603	−0.644516
H	−1.628125	−2.653781	−1.049284
H	−3.388532	−2.657859	−1.178247
H	−2.625443	−2.493093	0.409594
O	2.517134	−1.410171	0.419528
O	3.222616	0.968583	0.718691
O	2.632149	0.104342	−1.550692

Bibliography

(1) Shin, I.; Lee, D.; Kim, H. *Org. Lett.* **2016**, *18*, 4420–4423.

(2) Nagata, T.; Nakagawa, M.; Nishida, A. *J. Am. Chem. Soc.* **2003**, *125*, 7484–7485.

(3) Nagata, T.; Nakagawa, M.; Nishida, A. *J. Am. Chem. Soc.* **2003**, *125*, 13618–13618.

(4) Ono, K.; Nakagawa, M.; Nishida, A. *Angew. Chem. Int. Ed.* **2004**, *43*, 2020–2023.

(5) Nakagawa, M.; Nagata, T.; Ono, K.; Nishida, A. *J. Synth. Org. Chem. Jpn.* **2005**, *63*, 200–210.

(6) Young, I. S.; Kerr, M. A. *J. Am. Chem. Soc.* **2007**, *129*, 1465–1469.

(7) Jakubec, P.; Cockfield, D. M.; Dixon, D. J. *J. Am. Chem. Soc.* **2009**, *131*, 16632–16633.

(8) Martin, D.; Vanderwal, C. *Angew. Chem. Int. Ed.* **2010**, *49*, 2830–2832.

(9) Nilson, M. G.; Funk, R. L. *Org. Lett.* **2010**, *12*, 4912–4915.

(10) Kyle, A. F.; Jakubec, P.; Cockfield, D. M.; Cleator, E.; Skidmore, J.; Dixon, D. J. *Chem. Commun.* **2011**, *47*, 10037–10039.

(11) Cheng, B.; Wu, F.; Yang, X.; Zhou, Y.; Wan, X.; Zhai, H. *Chem. Eur. J.* **2011**, *17*, 12569–12572.

(12) Jakubec, P.; Kyle, A. F.; Calleja, J.; Dixon, D. J. *Tetrahedron Lett.* **2011**, *52*, 6094–6097.

(13) Wang, C.; Yu, M.; Kyle, A. F.; Jakubec, P.; Dixon, D. J.; Schrock, R. R.; Hoveyda, A. H. *Chem. Eur. J.* **2013**, *19*, 2726–2740.

(14) Bonazzi, S.; Cheng, B.; Wzorek, J. S.; Evans, D. A. *J. Am. Chem. Soc.* **2013**, *135*, 9338–9341.

(15) Clark, J. S.; Xu, C. *Angew. Chem. Int. Ed.* **2016**, *55*, 4332–4335.

(16) Bucher, C.; Deans, R. M.; Burns, N. Z. *J. Am. Chem. Soc.* **2015**, *137*, 12784–12787.

(17) Nicolaou, K. C.; Daines, R. A.; Chakraborty, T. K.; Ogawa, Y. *J. Am. Chem. Soc.* **1987**, *109*, 2821–2822.

(18) Nicolaou, K. C.; Daines, R. A.; Uenishi, J.; Li, W. S.; Papahatjis, D. P.; Chakraborty, T. K. *J. Am. Chem. Soc.* **1988**, *110*, 4672–4685.

(19) Nicolaou, K. C.; Daines, R. A.; Chakraborty, T. K.; Ogawa, Y. *J. Am. Chem. Soc.* **1988**, *110*, 4685–4696.

(20) Nicolaou, K. C.; Daines, R. A.; Ogawa, Y.; Chakraborty, T. K. *J. Am. Chem. Soc.* **1988**, *110*, 4696–4705.

(21) Cereghetti, D. M.; Carreira, E. M. *Synthesis* **2006**, *2006*, 0914–0942.

(22) Volmer, A. A.; Szpilman, A. M.; Carreira, E. M. *Nat. Prod. Rep.* **2010**, *27*, 1329–1349.

(23) Endo, M. M.; Cioffi, A. G.; Burke, M. D. *Synlett* **2016**, *27*, 337–354.

(24) Alunni, S.; De Angelis, F.; Ottavi, L.; Papavasileiou, M.; Tarantelli, F. *J. Am. Chem. Soc.* **2005**, *127*, 15151–15160.

(25) Bunnett, J. F. *Angew. Chem. Int. Ed. Engl.* **1962**, *1*, 225–235.

(26) Klyne, W.; Prelog, V. *Experientia* **1960**, *16*, 521–523.

(27) Saunders, W. H. *J. Org. Chem.* **2000**, *65*, 681–684.

(28) Borchardt, J. K.; Swanson, J. C.; Saunders, W. H. *J. Am. Chem. Soc.* **1974**, *96*, 3918–3920.

(29) Hammond, G. S. *J. Am. Chem. Soc.* **1955**, *77*, 334–338.

(30) Hoepker, A. C.; Collum, D. B. *J. Org. Chem.* **2011**, *76*, 7985–7993.

(31) De Vries, T. S.; Goswami, A.; Liou, L. R.; Gruver, J. M.; Jayne, E.; Collum, D. B. *J. Am. Chem. Soc.* **2009**, *131*, 13142–13154.

(32) Collum, D.; McNeil, A.; Ramirez, A. *Angew. Chem. Int. Ed.* **2007**, *46*, 3002–3017.

(33) Exner, J. H.; Steiner, E. C. *J. Am. Chem. Soc.* **1974**, *96*, 1782–1787.

(34) Saunders, W. H.; Bushman, D. G.; Cockerill, A. F. *J. Am. Chem. Soc.* **1968**, *90*, 1775–1779.

(35) Pánková, M.; Závada, J. *Collect. Czech. Chem. Commun.* **1977**, *42*, 1981–1991.

(36) Bartsch, R. A.; Zavada, J. *Chem. Rev.* **1980**, *80*, 453–494.

(37) Závada, J.; Pánková, M.; Bartsch, R. A.; Cho, B. R. *Collect. Czech. Chem. Commun.* **1981**, *46*, 850–855.

(38) Bartsch, R. A.; Pruss, G. M.; Bushaw, B. A.; Wiegers, K. E. *J. Am. Chem. Soc.* **1973**, *95*, 3405–3407.

(39) Brown, H. C.; Klimisch, R. L. *J. Am. Chem. Soc.* **1965**, *87*, 5517–5518.

(40) Saunders, W. H.; Fahrenholtz, S. R.; Caress, E. A.; Lowe, J. P.; Schreiber, M. *J. Am. Chem. Soc.* **1965**, *87*, 3401–3406.

(41) Bartsch, R. A.; Bunnett, J. F. *J. Am. Chem. Soc.* **1968**, *90*, 408–417.

(42) Griffith, D. L.; Meges, D. L.; Brown, H. C. *Chem. Commun. Lond.* **1968**, 90–91.

(43) Bartsch, R. A.; Bunnett, J. F. *J. Am. Chem. Soc.* **1969**, *91*, 1376–1382.

(44) Bartsch, R. A.; Bunnett, J. F. *J. Am. Chem. Soc.* **1969**, *91*, 1382–1385.

(45) Ingold, C. *Proc. Chem. Soc.* **1962**, 265–274.

(46) Jenn, T.; Heissler, D. *Tetrahedron* **1998**, *54*, 97–106.

(47) Maeda, K.; Shinokubo, H.; Oshima, K. *J. Org. Chem.* **1996**, *61*, 6770–6771.

(48) Bedke, D. K.; Shibuya, G. M.; Pereira, A. R.; Gerwick, W. H.; Vanderwal, C. D. *J. Am. Chem. Soc.* **2010**, *132*, 2542–2543.

(49) Vosko, S. H.; Wilk, L.; Nusair, M. *Can. J. Phys.* **1980**, *58*, 1200–1211.

(50) Lee, C.; Yang, W.; Parr, R. G. *Phys. Rev. B* **1988**, *37*, 785–789.

(51) Becke, A. D. *J. Chem. Phys.* **1993**, *98*, 5648–5652.

(52) Stephens, P. J.; Devlin, F. J.; Chabalowski, C. F.; Frisch, M. J. *J. Phys. Chem.* **1994**, *98*, 11623–11627.

(53) Ditchfield, R.; Hehre, W. J.; Pople, J. A. *J. Chem. Phys.* **1971**, *54*, 724–728.

(54) Hehre, W. J.; Ditchfield, R.; Pople, J. A. *J. Chem. Phys.* **1972**, *56*, 2257–2261.

(55) Hariharan, P. C.; Pople, J. A. *Theoret. Chim. Acta* **1973**, *28*, 213–222.

(56) Hariharan, P. C.; Pople, J. A. *Mol. Phys.* **1974**, *27*, 209–214.

(57) Gordon, M. S. *Chemical Physics Letters* **1980**, *76*, 163–168.

(58) Francl, M. M.; Pietro, W. J.; Hehre, W. J.; Binkley, J. S.; Gordon, M. S.; DeFrees, D. J.; Pople, J. A. *J. Chem. Phys.* **1982**, *77*, 3654–3665.

(59) Marenich, A. V.; Olson, R. M.; Kelly, C. P.; Cramer, C. J.; Truhlar, D. G. *J. Chem. Theory Comput.* **2007**, *3*, 2011–2033.

Chapter 2:

Progress Toward the Synthesis of Mollenyne A

2.1 Halogenated lipids from *Spirastrella mollis*

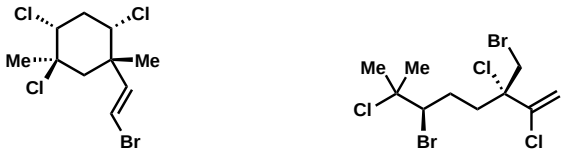

telfairine
2.1

halomon
2.2

Figure 2.1: Select potently bioactive, polyhalogenated algal natural products.

Both algae and sponges make a wide variety of halogenated secondary metabolites for use in chemical defense, as regulatory hormones, and signaling molecules.[1,2] Telfairine (**2.1**) was found to have an LD_{100} of 10 ppm against mosquito larvae.[3,4] Halogenated monoterpenes, such as halomon (**2.2**), have demonstrated potent, diverse cytotoxicity against a variety of human tumor cell lines including brain, renal, and colon cancers, fueling continued interest in the synthesis of polyhalogenated natural products.[5,6] However, while algal natural products containing various halogen atoms are well precedented, and there have been many halogenated natural products isolated from sponges, few sponge derived natural products carry both chlorine and bromine atoms, making mollenyne A (**2.3**) a rare addition to the, otherwise, extensive list.[2]

The long chain chlorodibromohydrin mollenyne A **2.3** was isolated in 2011 by the Molinski group from the sponge *Spirastrella mollis*.[7] The structure of mollenyne A (**Figure 2.2**) was assigned by COSY and HMBC NMR experiments after a positive hit against HCT-116 human colon caner cells. The position of the halogen atoms was determined by careful analysis of C13 shifts and comparison against known synthetic compounds. The stereochemistry of the bromochlorohydrin was determined by *J*-based configurational analysis and reinforced by synthetic derivatization.[8] Four years later, in a survey of different specimens of *Spirastrella mollis*, the Molinski group found that the

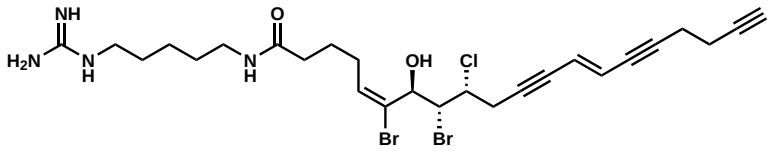

mollenyne A
2.3

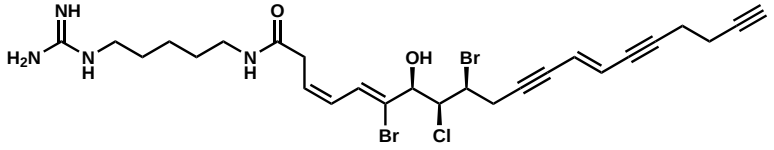

mollenyne B
2.4

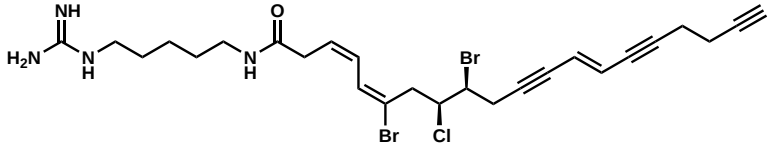

mollenyne C
2.5

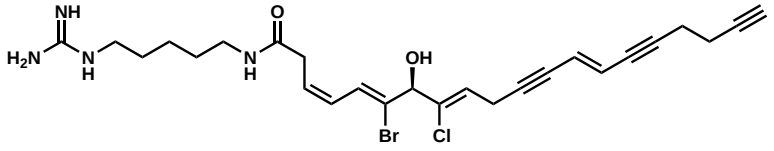

mollenyne D
2.6

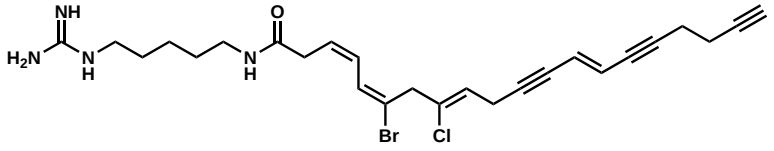

mollenyne E
2.7

Figure 2.2: Mollenynes A-E isolated from *Spirastrella mollis* by the Molinski group.

mollenyne content of the sponge varies by location. While mollenyne A **2.3** was the major bromo-chlorinated analog isolated from sponges obtained near Plana Cays, sponges obtained from Hogsty Reef lacked mollenyne A entirely and contained mollenynes B-E instead.[9] Mollenynes B-E (**2.4**, **2.5**, **2.6**, **2.7**) all share the same long chain carbon framework and guanidinylated amide of mollenyne A; however, mollenyne A has a unique chlorodibromohydrin core, with mollenynes B-E having opposite regio-

and stereochemistry of the vicinal bromochloride. The Molinski group has proposed that the opposite regio- and stereochemistry of mollenyne B and C results from a thermal dyotropic shift, as precedented by the thermal rearrangement of caespitol to isocaespitol[10–12] and that mollenynes D and E are the result of a dehydrobromination of mollenynes B and C, respectively.

2.2 Retrosynthetic Analysis

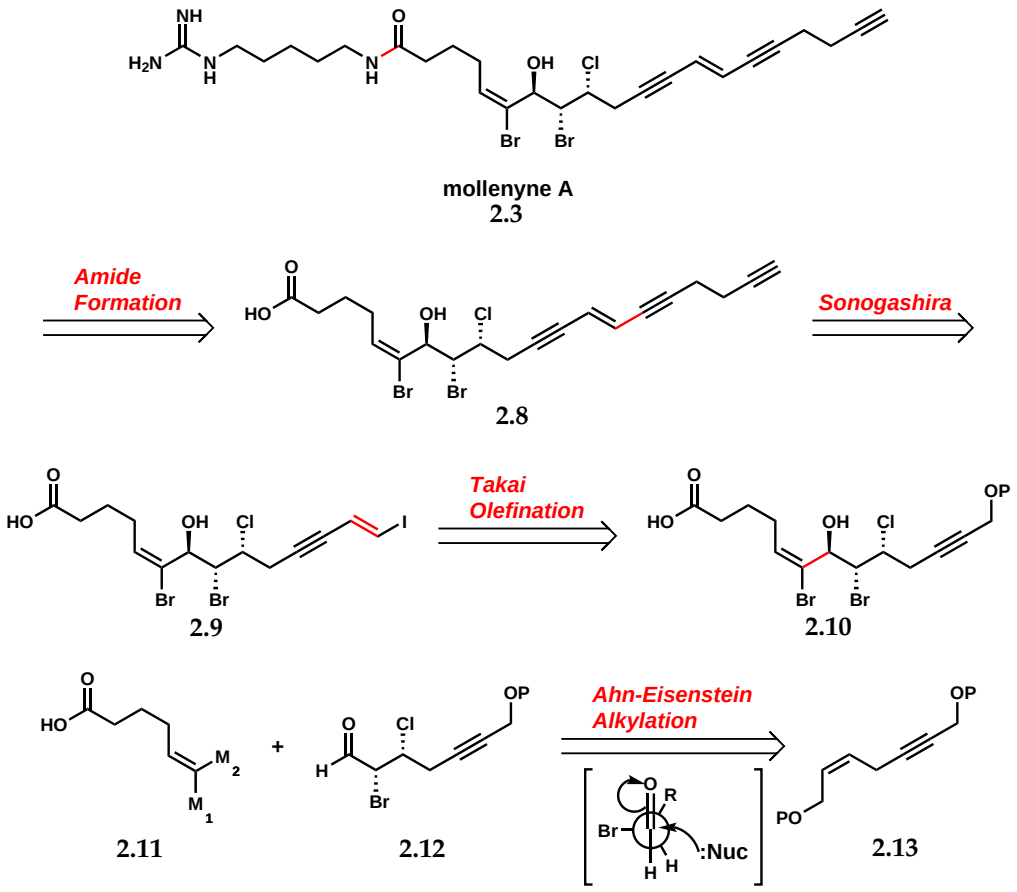

Scheme 2.1: Retrosynthetic analysis of mollenyne A.

Our interest in synthesizing mollenyne A stemmed from a history in the synthesis of halogenated lipids such as danicalipin (**1.4**) and malhamensilipin (**1.5**). The acyclic stereocontrol necessary to prepare the bromochlorohydrin core and the regio- and diastereoselective installation of the (*E*)-alkenyl bromide posed interesting synthetic challenges, while mollenyne A's 1.3 μg/mL IC_{50} against solid human colon cancer

HCT-116 cells made the molecule of medicinal interest as well. Disconnection of the homoagmatine amide to give free acid **2.8** followed by the disconnection of the skipped hexadiyne moiety by a Sonogashira cross coupling reaction led to the core of mollenyne A **2.9** (**Scheme 2.1**). Though mollenyne A contains no cyclic components, the proposed "core" **2.9** contains all of the stereocenters of mollenyne A, as well as functional groups required for elaboration to the complete natural product. The alkenyl iodide **2.9** was envisioned to come from a Takai olefination of the aldehyde derived from protected alcohol **2.10**, which would be synthesized in a convergent manner by Ahn–Eisenstein controlled addition of geminal *bis*-metallated alkene **2.11** into halogenated aldehyde **2.12**. The *cis*- stereochemistry of the vicinal bromochloride **2.12** would in turn come from the *cis*-alkene skipped enyne **2.13**.

2.3 Synthesis of Vicinal Bromo-Chloride Fragment

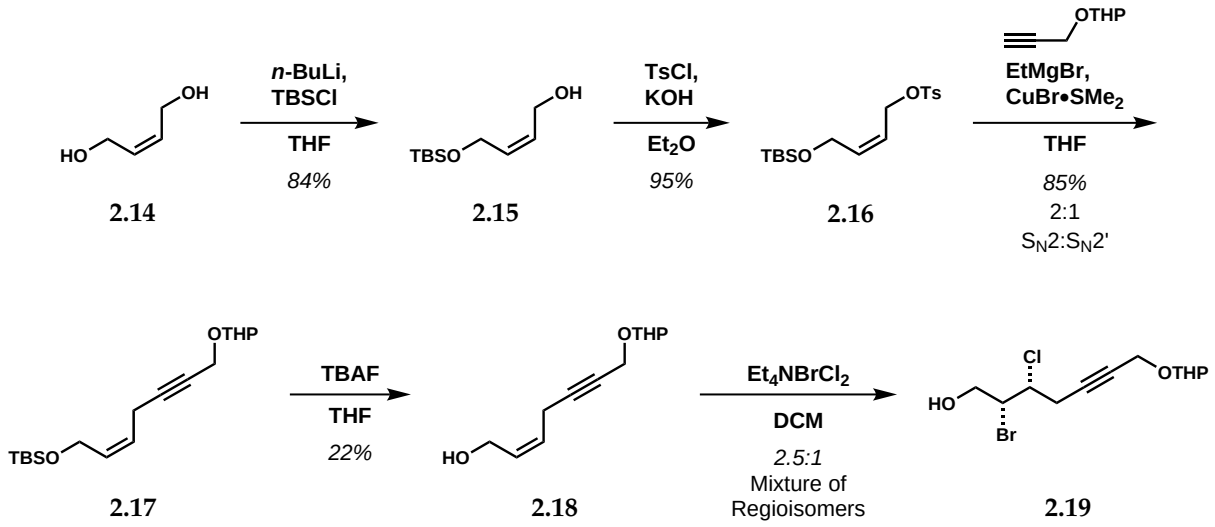

Scheme 2.2: Synthesis of the vicinal bromo-chloride fragment.

In a forward sense (**Scheme 2.2**), *cis*-butenediol **2.14** was monoprotected as the TBS ether in 72% yield, with a 10 mol% contaminant of the doubly protected allylic diol. Following activation of alcohol **2.15** as tosylate **2.16**, S_N2 displacement was found to give a 2:1 selectivity for S_N2:S_N2' in the formation of **2.17**. The crude mixture of products was exposed to TBAF to remove the silyl protecting group, yielding alcohol **2.18**. Though the

linear **2.18** could be separated from the branched S_N2' product (not shown) chromatographically, a more selective displacement is desirable both for the sake of yield and throughput. Bromochlorination of **2.18** using tetraethylammonium bromodichloride[13] gave **2.19** as a 2.5:1 inseparable mixture of regioisomeric bromochlorides.

2.4 Pursuing a *bis*-Metallated Nucleophile

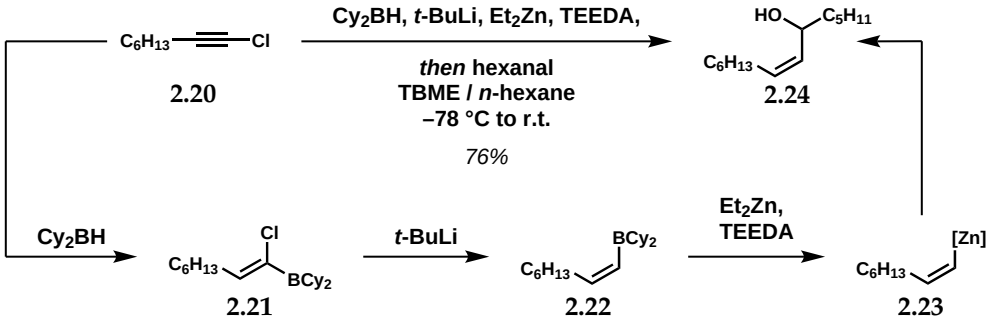

Scheme 2.3: Reproduction of the Walsh borotropic shift / transmetallation approach to (*Z*)-allylic alcohols.

The selectivity of our approach to the halogenated aldehyde **2.13** was wanting; however, the greater challenge of generating geminal *bis*-metallated alkene **2.11** had yet to be approached. Our original inspiration came from work by the Walsh group in the synthesis of (*Z*)-allylic alcohols by the vinylation of the corresponding aldehyde.[14–18] Reproducing work done by the Walsh group (**Scheme 2.3**), hydroboration of alkyne **2.20** to the geminally halo-metallated **2.21** was followed by a borotropic shift using *tert*-butyllithium as a hydride source to effect the displacement of chlorine to give (*Z*) alkene **2.22**.

Transmetallation of the alkylboron with diethylzinc and addition of hexanal resulted in formation of **2.24** in 76% yield. Unfortunately, though the analogous borotropic shift was reported using silyllithium nucleophiles in place of hydride,[19] attempts to apply this chemistry to the Walsh reaction were unsuccessful (**Scheme 2.4**)

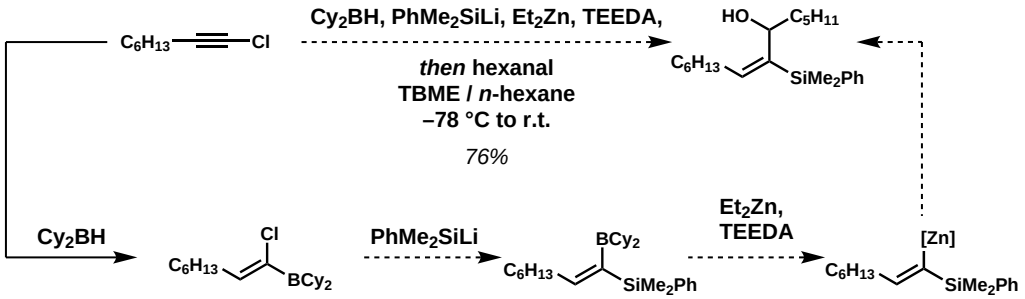

Scheme 2.4: Desired application of Walsh chemistry

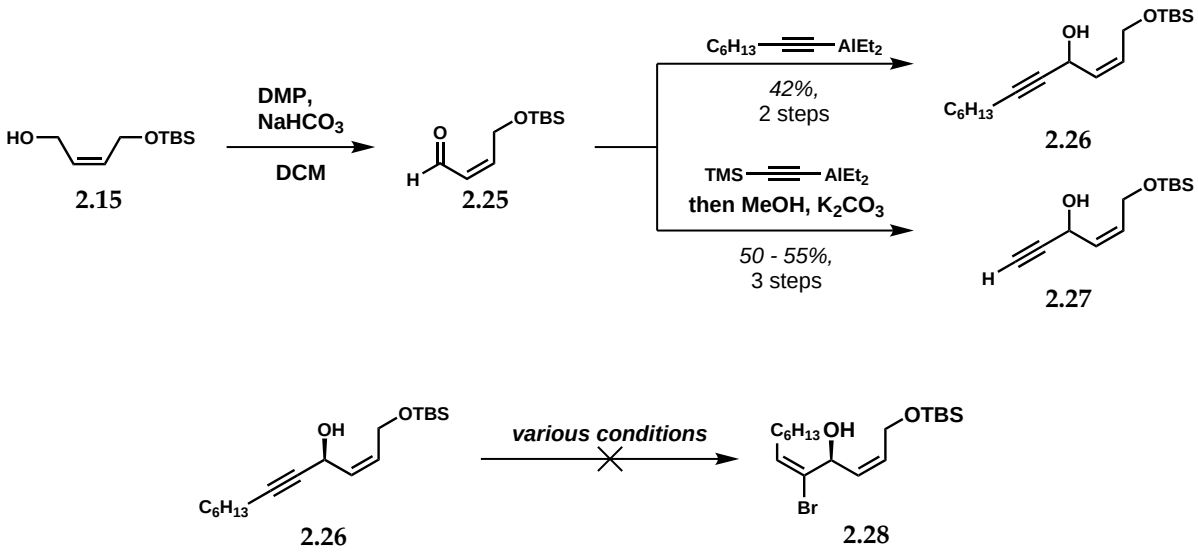

Scheme 2.5: Synthesis of model alkynes for hydrobromination experiments.

As an alternative to the complicated Walsh chemistry, I explored hydrometallation of alkynes as a method of working around the challenging geminal *bis*-metallated alkene **2.11**. To that end, alkynes **2.26** and **2.27** were synthesized from protected *cis*-butenediol **2.15** in 42% and 55% yield using established transformations. Attempts at palladium catalyzed hydrostannylation of internal alkyne **2.26** gave complete control for the undesired regioisomer. Hydrobromination with *in situ* generated HBr or with tetraethylammonium protodibromide resulted in rearrangement of the labile allylic-propargylic alcohol prior to or in lieu of any bromination reactions. Attempts at other hydrometallation reactions such as hydrozirconation gave extensive side reactions with none of the desired alkenyl bromide **2.28** observed.

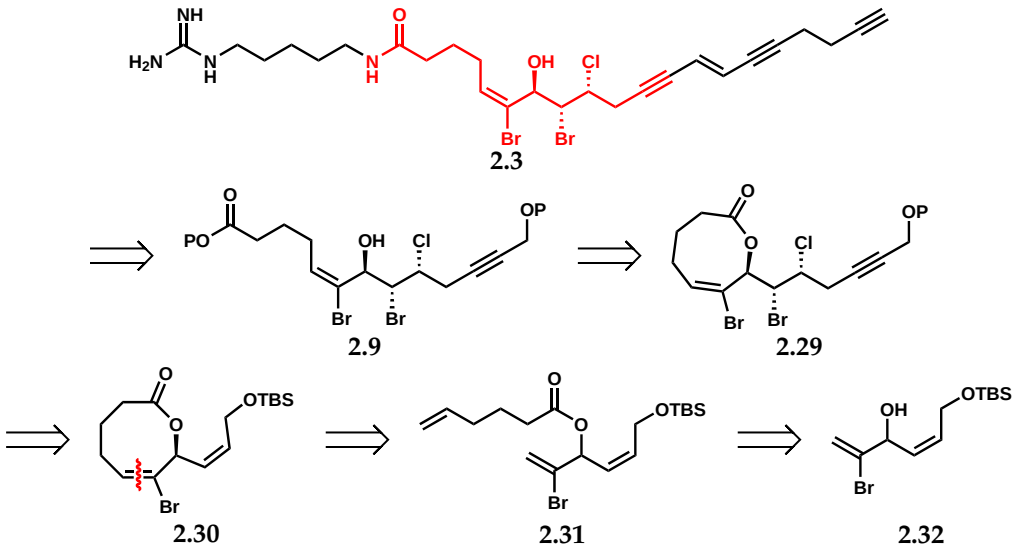

Scheme 2.6: Revised retrosynthetic analysis of mollenyne A.

2.5 A Ring Closing Metathesis Approach

Continuing to face difficulties with the installation of the internal alkenyl bromide **2.28** by hydrometallation of **2.26**, I decided to explore functionalization of the unsubstituted terminal alkyne **2.27**. As **2.27** lacks the substitution which would bear the acid moiety of mollenyne A **2.3**, a new retrosynthetic analysis was needed. Maintaining our previously proposed amide, Sonogashira, and Takai olefination disconnections to get to the core structure **2.10**, I proposed that **2.9** would be obtained by hydrolysis of the eight-membered lactone **2.29**. Though the lactone moiety would render the allylic alcohol more labile, it would obviate the need for protecting group interconversions during the oxidation of the propargylic alcohol leading up to Takai olefination. Dibromochloro lactone **2.29** was proposed to come from the bromochlorination of diene lactone **2.30**. Unlike bromochlorination of the allylic alcohol **2.18**, the halogenation of **2.30** was expected to be highly selective due the electron poor nature of the alkenyl bromide as well as the inductive electron withdrawing power of the lactone biasing the intermediate bromonium ion to open away from the lactone. The diastereoselective installation of alkenyl bromide **2.30** was to come from the innate (Z)-selectivity of ring

closing metathesis of ester **2.31** which would, in turn come from the doubly allylic alcohol alkenyl bromide **2.32**.

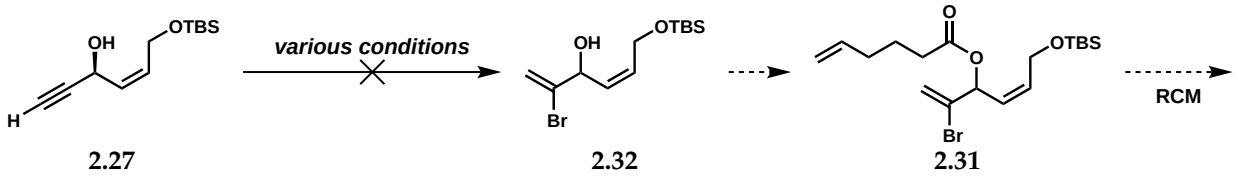

2.27 **2.32** **2.31**

Scheme 2.7: Hydrobromination approach to **2.27**.

Faced again with the problem of installing an alkenyl bromide, I hoped that the innate bias of the unsubstituted alkyne **2.27** would allow for improved regiocontrol compared to that observed on the internal alkyne **2.26** (**Scheme 2.7**); however, once again, hydrobromination reactions with HBr or Lewis acidic reagents rearranged the allylic propargylic alcohol. Attempts to hydrometallate including nickel catalyzed hydroalumination,[20] rhodium catalyzed hydrostannylation,[21] palladium catalyzed hydrostannylation,[22–24] and hydrozirconation[25] all failed to provide the desired alkenyl bromide **2.32**. Looking back to vinylation chemistry, a plausible approach was found in the addition of 1-(trialkylsilyl)-1-lithioethene to aldehydes. 1-(triisopropylsilyl)-1-bromoethylene **2.33** was synthesized in three steps from dibromomethane as reported by Yamamoto.[26] Lithium halogen exchange of **2.33** followed by addition of aldehyde **2.25** gave dienol **2.34** in 76% yield. While the formation of allylic alcohol **2.34** was efficient, the alkenyl TIPS group was found to be unreactive to mild halogenating conditions despite attempts to activate the silane with fluoride.

Before attempting to reproduce the chemistry in **Scheme 2.8** using an alkenyl TMS substituent, my attention was drawn to the Sampson group's work in the lithiation of vinyl bromide (**2.35**) and use of the resultant 1-bromo-1-lithioethene (**2.36**) as a nucleophile.[27] Though some geminal lithiated halides are slow to form carbenes, the

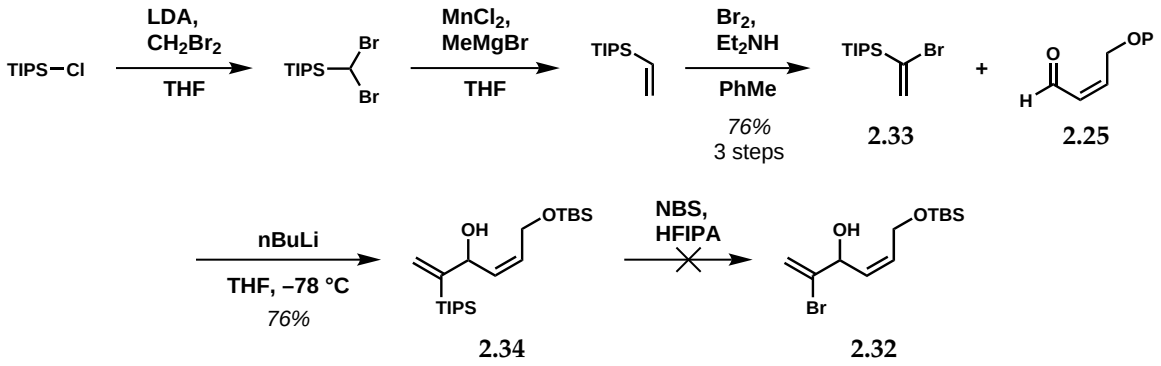

Scheme 2.8: Direct alkenylation with 1-TIPS-1-bromoethylene.

sensitivity of **2.36** was suggested by the elaborate reactor employed by Novikov and Sampson (**Figure 2.3**).

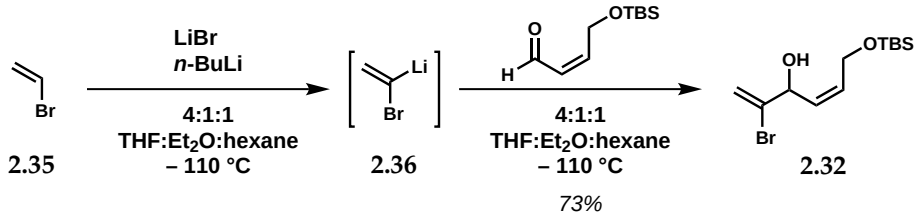

Scheme 2.9: Direct alkenylation with 1-bromo-1-lithioethene.

Indeed, initial attempts at using standard laboratory glassware for the formation of **2.36** gave largely recovered starting material, as well as propargyl alcohol **2.27**, and a limited yield of the desired alkenyl bromide **2.32**. The formation of **2.27** under these conditions suggested that the reaction temperature was rising during the deprotonation of vinyl bromide **2.35**. Motivated by my first observation of the desired alkenyl bromide **2.32**, I continued working to improve the formation of **2.36**. The purported rise in reaction temperature was attributed to the warming of pre-cooled *n*-butyllithium solution during transfer as well as poor agitation of the viscous reaction mixture. Relatively simple improvements to the reaction set up, namely using a cannula immersed in the reaction's cooling bath to transfer *n*-butyllithium and employing a mechanical stirring resulted in a 73% yield of **2.32**.

With **2.32** in hand, the synthesis called for the installation of 5-hexenoic acid (**2.38**) which, though commercially available, is unreasonably expensive. Employing a known

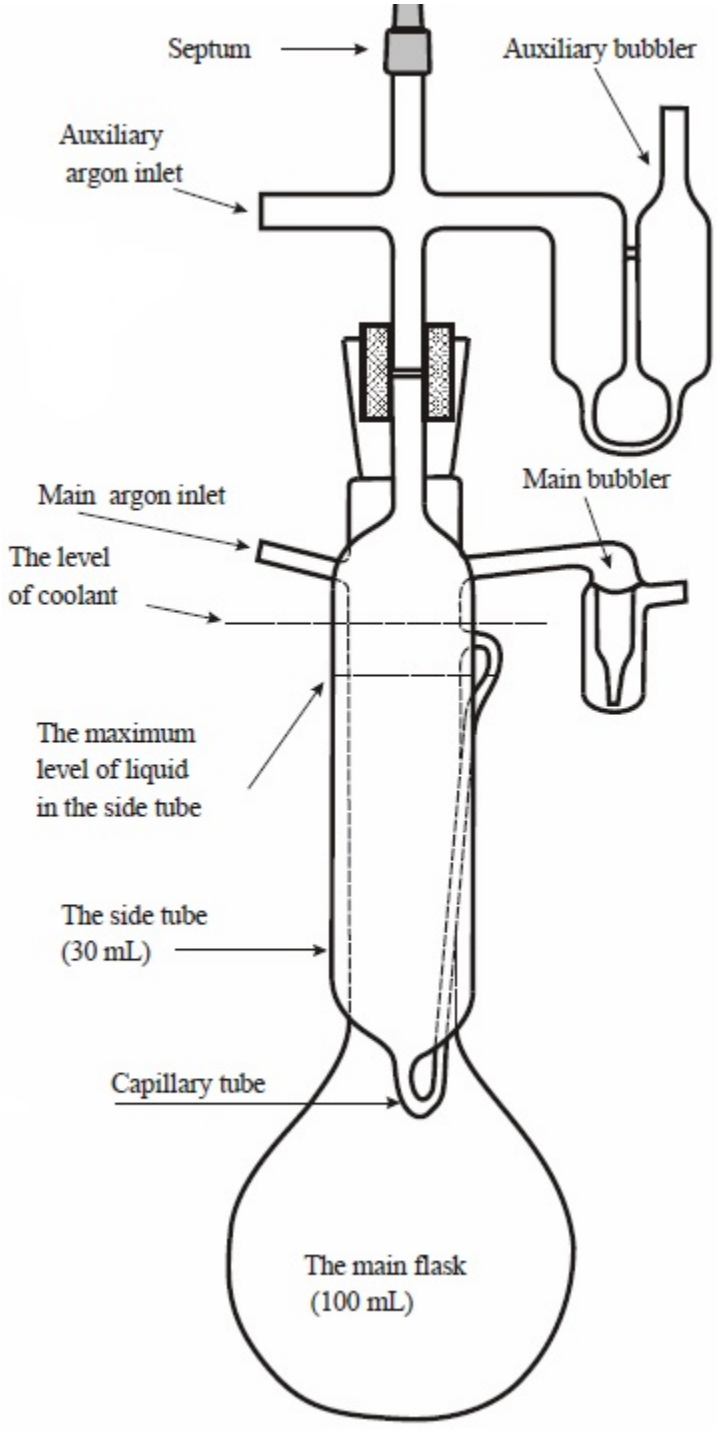

Figure 2.3: Novikov and Sampson's reactor for the synthesis and use of 1-bromo-1-lithioethene.

iron and copper mediated oxidation of inexpensive cyclohexanone **2.37** gave the desired acid **2.38** in 36% yield after distillation.[28] Though not widely reported, this ostensibly radical fragmentation is effective on cyclopentanones as well as cycloheptanones.

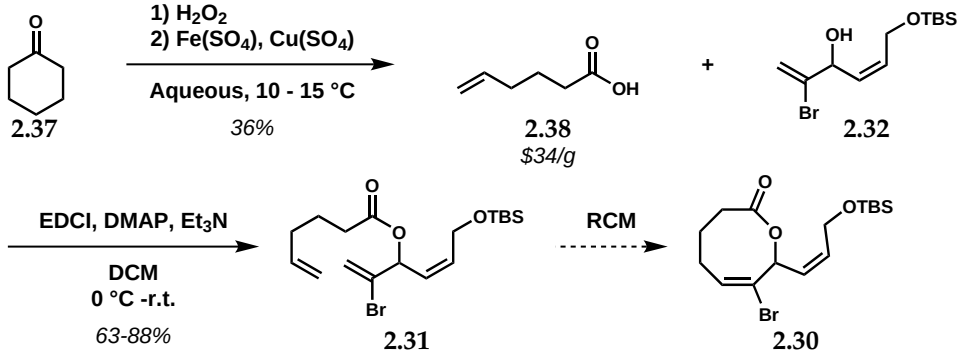

Scheme 2.10: Ring closing metathesis with 1,1-disubstituted alkenyl bromide.

Formation of the acid was followed by EDCI mediated coupling with *bis*-allylic alcohol **2.32** which gave the desired ester **2.31** in up to 88% yield. Despite reports of using ring-closing metathesis to construct eight membered lactones,[29] heating diene **2.31** in the presence of various ruthenium metathesis catalysts including Grubbs 1st and 2nd generation catalysts, Hoveyda-Grubbs 2nd generation catalyst, and *iso*-propyl Stewart-Grubbs 2nd generation catalyst in dichloromethane or toluene at a variety of temperatures failed to give the desired lactone **2.30**. Lewis-basic functional groups such as esters are known to recruit the Lewis-acidic ruthenium metathesis catalysts resulting in reduction of the reaction rate or outright failure of the reaction.[30–32] To combat this effect, ester **2.31** was complexed with titanium(IV) *iso*-propoxide prior to ruthenium catalyst addition and the catalyst screen was repeated, but to no avail.

Table 2.1: The Dorta group's discovery of

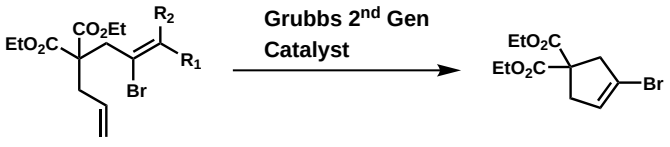

Entry	R1	R2	Result
1	H	H	Catalyst decomp.
2	Me	H	70% Yield
3	Ph	H	98% Yield
4	H	Ph	0% Yield

While ruthenium catalyzed ring-closing metathesis has been applied to diverse molecules, the metathesis of alkenyl halides remains challenging. The Dorta group found that while attempting to perform a ring-closing metathesis cyclization of unsubstituted alkenyl bromide (**Table 2.1**, entry 1) resulted in decomposition of the ruthenium catalyst, the counterintuitive installation of a methyl group *cis*- to the bromide (**Table 2.1**, entry 2) allowed the desired cyclization to proceed and substitution with a phenyl group further increased the reaction yield (entry 3). The diastereomer of the alkenyl halide was vital as the *trans*-alkene (**Table 2.1**, entry 4) prevented the desired cyclization, albeit with no catalyst decomposition observed.[33] Most interestingly, the Dorta group also found that in the absence of the primary alkene of **2.39** no catalyst decomposition was observed, suggesting that alkenyl bromides only decompose the ruthenium catalyst in an intramolecular reaction.

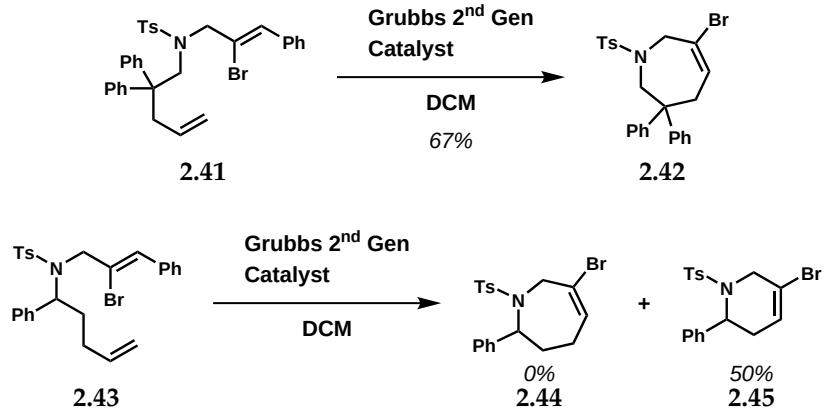

Scheme 2.11: Importance of the Thorpe–Ingold effect in ring-closing metathesis.

Furthermore, the Dorta group observed that the formation of medium-sized rings was highly sensitive to Thorpe–Ingold effect.[33] While geminal diphenyl **2.41** gave the seven-membered enamine **2.42** in 67% yield, the analogous monophenyl compound **2.43** failed to give the desired seven-membered enamine **2.44**, but instead was found to slowly produce the six-membered enamine **2.45**. The formation of the latter was likely the result of slow ruthenium mediated isomerization of the terminal olefin of **2.43** to the internal

olefin, which, while slower in ruthenium insertion, would provide a faster ring-closing metathesis. These results demonstrate that in the absence of geminal substitution biasing the conformation of the linear molecule, cyclization to form medium-sized rings is slow.

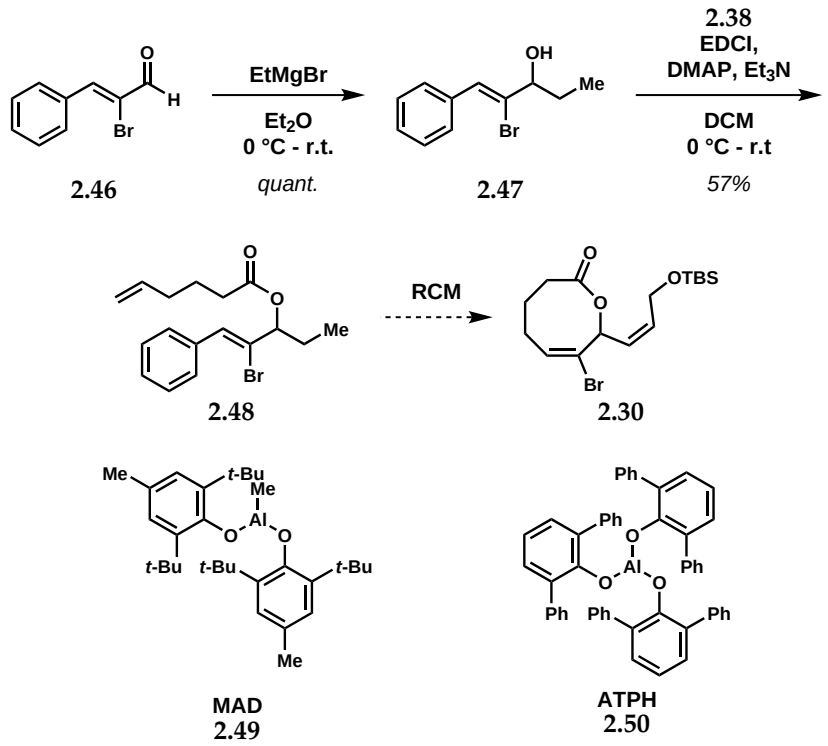

Scheme 2.12: Attempts at ring-closing metathesis of protected alkenyl bromide.

Attempting to harness Dorta's insights, model allylic alcohol **2.47** was synthesized in quantitative yield by addition of ethyl Grignard to commercially available α-bromocinnamaldehyde (**2.46**, **Scheme 2.12**). Esterification with **2.38** gave styrene **2.48** in 57% yield. Initial attempts at ring closing metathesis were unsuccessful, as Dorta's work had suggested. Unfortunately even utilizing large Lewis acids such as MAD (**2.49**) and ATPH (**2.50** which have been demonstrated to improve reactions forming medium-sized rings,[34–36] no cyclization was observed. Finally, while techniques had

been developed for employing ring-closing metathesis for the formation of lactones and medium-sized rings, the synthesis of medium-sized ring lactone alkenyl halides remained outside the scope of ruthenium catalyzed reactions.

2.6 Conclusion

In summary, while its potent anti-cancer activity makes mollenyne A (**2.3**) an attractive synthetic target, the seemingly simple core of the molecule defied my synthetic efforts. Our strategy relied on diastereoselective addition of a geminally substituted nucleophile to an α-bromo-β-chloro aldehyde (**2.12**) in order to furnish the desired bromochlorohydrin stereo-triad (**2.10**). Unfortunately, from the outset poor regioselectivity in my allylic tosylate displacement limited the amount of material available for experimentation with bromochlorination conditions. Hoping that the highly convergent nature of our synthesis would mitigate this issue,I began working on the necessary nucleophile fragment only to find that methods for installing ((*E*))-trisubstituted alkenyl halides provided similarly undesired regiochemistry, placing the desired bromide distal to the alcohol or forming the undesired ((*Z*))-alkenyl bromide. A 1,1-disubstituted alkenyl bromide (**2.32**) was finally synthesized; however, various ring-closing metathesis strategies failed to provide any metathesis reactivity. The success of 1-bromo-1-lithioethene addition to **2.25** remains promising. Application of the Sampson group's methodology to a substituted alkenyl bromide may provide an alkylated derivative of **2.32** which could be subjected to the regio- and enantioselective bromochlorination recently developed by the Burns group to provide the desired bromochlorohydrin in a concise manner.[37–39]

2.7 Experimental Procedures

General Information

For General information please see Chapter 1.4.

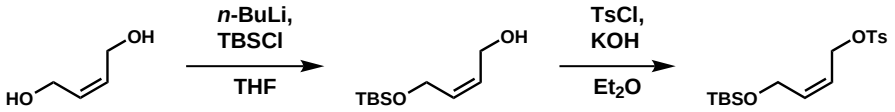

((*Z*))-4-((*tert*-Butyldimethylsilyl)oxy)but-2-en-1-yl 4-methylbenzenesulfonate (2.16): Allylic alcohol **2.15** (1.042 g, 4.42 mmol, synthesized in 84% yield as reported by the Giese group)[40] was diluted with 8.5 mL of dry diethyl ether and cooled to 0 °C. 4-Toluenesulfonyl chloride (0.894 g, 4.69 mmol) was added and the reaction mixture was stirred for five minutes at 0 °C. Potassium hydroxide (1.25 g, 22.3 mmol) was finely ground with a mortar and pestle and added to the reaction mixture in a single portion. Once the reaction was complete by TLC (ca. 5 h), the white, cloudy suspension was quenched by pouring the suspension into 6 mL of a mixture of ice and water. 10 mL of DCM were added, the layers were separated, and the aqueous phase was extracted 2 x 10 mL DCM. The combined organic layers were washed with brine and dried over Na_2SO_4. The resulting suspension was filtered through Celite and concentrated in vacuo to give the title compound. ^{1}H NMR showed complete conversion with a small amount of 4-toluenesulfonyl chloride as a contaminant. Comparison to recovered mass gave a calculated yield of 95 % by average molecular weight and the material was taken on to the next step without further purification. ^{1}H NMR (500 MHz, $CDCl_3$) δ 7.80 (d, *J* = 8.2, 2H), 7.34 (d, *J* = 8.1, 2H), 5.73 – 5.69 (m, 1H), 5.51 – 5.46 (m, 1H), 4.67 (d,*J* = 6.7, 2H), 4.15 (d, *J* = 5.6, 2H), 2.45 (s, 3H), 0.86 (s, 9H), 0.02 (s, 6H); ^{13}C NMR (125 MHz, $CDCl_3$) δ 144.9, 135.5, 133.4, 128.1, 122.4, 66.3, 59.8, 26.0, 21.8, 18.4, –5.2; IR (thin film) 2955, 2928, 2857, 1362, 1254, 1177 cm^{-1}; HRMS (CI/DCM) *m* / *z* calcd for $C_{17}H_{28}O_4SiNa$ $(M+Na)^+$ 379.1375, found 379.1382.

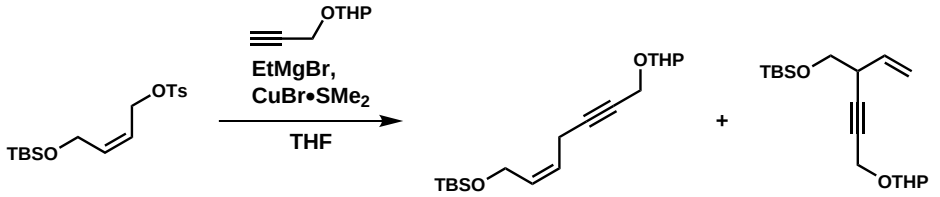

((*Z*))-*tert*-Butyldimethyl((7-((tetrahydro-2H-pyran-2-yl)oxy)hept-2-en-5-yn-1-yl)oxy)silane (2.17): Commercially available 2-(prop-2-yn-1-yloxy)tetrahydro-2H-pyran (0.85 mL, 6.1 mmol) was diluted with 11 mL dry THF and cooled to 0 °C. 2 mL of Ethylmagnesium bromide (3M in THF) were added dropwise, while stirring. The yellow reaction mixture was stirred for one hour at 0 °C, heated to 50 °C for thirty minutes, and cooled back down to 0 °C. Copper bromide dimethyl sulfide complex (0.117 g, 0.570 mmol) was added forming a yellow suspension which was stirred for 10 min at 0 °C. **2.16** (1.578 g, 4.421 mmol) was added as a solution in 8 mL of dry THF and the suspension was allowed to warm slowly to room temperature over 12 h. The yellow suspension was then poured onto 20 mL of a mixture of ice, water, and 100 mL of hexanes forming an emulsion which was allowed to settle over 20 min. The aqueous layer was separated and extracted with 2 x 100 mL hexanes, allowing the emulsion to settle each time. The yellow organic layer was dried over Na_2SO_4 and filtered through Celite, leaving a small amount of yellow residue and yielding a clear filtrate which was concentrated *in vacuo* to give the title compound as a mixture of S_N2 and S_N2' products contaminated with 2-(prop-2-yn-1-yloxy)tetrahydro-2H-pyran. This mixture was carried on to the next step without further purification. ^{1}H NMR analytical peaks listed (600 MHz, $CDCl_3$) δ 5.60 – 5.58 (m, 1H), 5.50 – 5.46 (m, 1H), 4.79 (t, *J* = 3.29, 1H), 4.31 – 4.17 (multiplet of overlapping –CH2–OR), 3.86 – 3.82 (m, 2H), 3.55 – 3.51 (m, 2H), 3.01 (appar. d, *J* = 7.2, 2H), 1.86 –1.81 (m, 1H), 1.77 – 1.71 (m, 1H), 1.65 – 1.52 (m, 4 H), 0.90 (s, 9H), 0.07 (s, 6H).

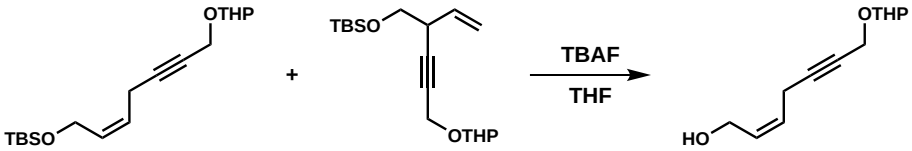

((*Z*))-7-((Tetrahydro-2H-pyran-2-yl)oxy)hept-2-en-5-yn-1-ol (2.18): TBS protected alcohol **2.17** (0.9592 g of a mixture of products) was diluted with 6 mL of wet THF and the reaction mixture was cooled to 0 °C. 3.6 mL of 1M tetrabutylammonium fluoride were added at 0 °C, and the brown reaction mixture was allowed to warm to room temperature over 1 h. 10 mL each of DCM and water were added, the layers were separated and the aqueous phase was extracted 2 x 15 mL DCM. The combined organic layers were washed with 10 mL of H_2O, 10 mL of brine, dried over Na_2SO_4, filtered through Celite and concentrated in vacuo. ^{1}H NMR showed an incomplete reaction; however, resubmitting the crude material to the reaction conditions for 10 minutes resulted in an increased intensity of undesired spots by TLC, and the reaction was quickly worked up again as above. Purification of the crude material by column chromatograph (20% EtOAc in hexanes) gave the title compound as a 33 : 1 mixture of S_N2 to S_N2' materials (0.142 g, 15% over 2 steps). ^{1}H NMR (500 MHz, $CDCl_3$) δ 5.72–5.68 (m, 1H), 5.62–5.57 (m, 1H), 4.79 (t, *J* = 3.4, 1H), 4.29 (dt, *J* = 15.3, 2.2, 1H), 4.23 (br d, *J* = 5.2, 2H), 4.19 (dt, *J* = 15.3, 2.1, 1H), 3.83 (ddd, *J* = 9.5, 2.8, 2.1, 1H), 3.55 – 3.51 (m, 1H), 3.03 (appar. dd, *J* = 6.9, 1.4H), 1.86 – 1.78 (m, 1H), 1.73, (tt, *J* = 13.4, 3.4H), 1.65–1.51 (m, 4H), 1.44 (brs, 1H); ^{13}C NMR (125 MHz, $CDCl_3$) δ 130.6, 127.0, 97.0, 84.2, 76.5, 62.1, 58.5, 54.8, 30.4, 25.5, 19.2, 17.6; IR (thin film) 3402, 2941, 2928, 2868, 2854, 1452 cm^{-1}; HRMS (CI/DCM) *m* / *z* calcd for $C_{12}H_{18}O_3Na$ $(M+Na)^+$ 233.1154, found 233.1155.

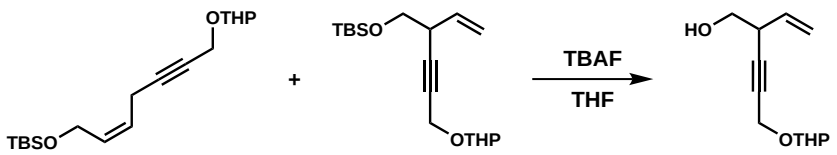

5-((Tetrahydro-2H-pyran-2-yl)oxy)-2-vinylpent-3-yn-1-ol: This material was synthesized as a byproduct of making the above compound **2.18**. It was identified by ^{1}H

NMR and isolated during purification of **2.18**. ^{1}H NMR (500 MHz, $CDCl_3$) δ 5.79 (ddd, *J* = 16.7, 10.2, 6.3, 1H), 5.42 (dd, *J* = 17.0, 1.3, 1H), 5.25 (d, *J* = 10.2, 1H), 4.84 (t, *J* = 2.8, 1H), 4.37 (dd, *J* = 15.5, 1.8, 1H), 4.31 (dd, *J* = 15.5, 1.6, 1H), 3.88 (appar. ddd, *J* = 11.8, 9.3, 2.9, 1H), 3.71 – 3.62 (m, 2H), 3.58 – 3.54 (m, 1H), 1.95 (dd, *J* = 15.4, 7.3, 1H), 1.89 – 1.81 (m, 1H), 1.76 (tt, *J* = 13.2, 3.2, 1H), 1.67 – 1.55 (m, 5H); ^{13}C NMR (125 MHz, $CDCl_3$) δ 134.1, 118.1, 97.2, 83.9, 81.0, 65.4, 62.2, 54.8, 39.5, 30.5, 25.5, 19.2; IR (thin film) 3418, 2941, 2870, 1639, 1440, 1388 cm^{-1}; HRMS (CI/DCM) *m / z* calcd for $C_{12}H_{18}O_3Na$ $(M+Na)^+$ 233.1154, found 233.1155.

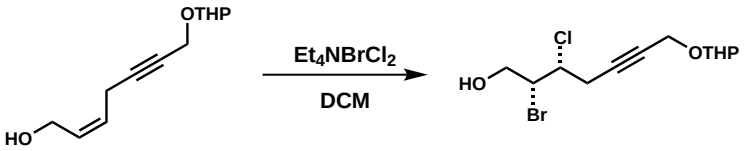

(2R,3R)-2-bromo-3-chloro-7-((tetrahydro-2H-pyran-2-yl)oxy)hept-5-yn-1-ol (2.19): Allylic alcohol **2.18** (0.010 g, 0.062 mmol) was diluted with 1 mL dry DCM and cooled to –75 °C. A solution of Et_4NBrCl_2 (0.033 g, 0.117 mmol, synthesized by Grant Shibuya as reported by the Ikeda group)[41] in 2.1 mL of dry DCM was added dropwise and the yellow-orange solution was allowed to stir at –78 °C 5 h. Excess halogenating reagent was quenched by addition of 1 mL of saturated aqueous $Na_2S_2O_3$. The colorless reaction mixture was diluted with 1 ml of water and the layers were separated. The aqueous phase was extracted 3 x 3 mL DCM, the combined aqueous phases were washed with 5 mL water, 5 mL brine, and dried with Na_2SO_4. The resultant suspension was filtered through cotton and concentrated to give **2.51** as an inseparable mixture of halogen regioisomers. The proton NMR is largely illegible as the introduction of two new chiral centers to a molecule already bearing the chiral, racemic THP protecting group results in the formation of multiple diastereomers. Despite extending the D1 delay time to 2 seconds, quaternary carbons were not found in the ^{13}C NMR; however, the purity of the compound is demonstrable. ^{13}C NMR (125 MHz, $CDCl_3$) δ 97.1, 97.0, 81.8, 79.5, 65.8, 65.8, 64.9, 63.4, 63.4, 62.3, 62.2, 58.5, 57.6, 57.6, 54.6, 54.5, 51.0, 30.4, 30.4, 29.8, 27.7, 27.1,

25.5, 19.2, 19.2; HRMS (ESI/MeOH) *m* / *z* calcd for $C_{12}H_{18}O_2BrClNa$ $(M+Na)^+$ 347.0026, found 347.0030.

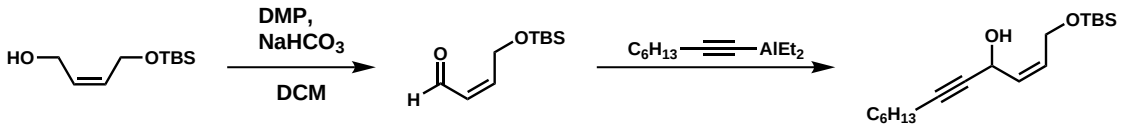

((*Z*))-4-((*tert*-butyldimethylsilyl)oxy)but-2-enal (2.25): Monoprotected diol **2.15** (2.091 g, 10.33 mmol) was diluted with 50 mL DCM saturated with water. $NaHCO_3$ (2.687 g, 31.98 mmol) was added, followed by Dess–Martin periodinane (6.664 g, 15.71 mmol) and the reaction mixture was stirred at room temperature until the starting material could not be detected by TLC (usually about 2 h.) at which point 12 mL of saturated, aqueous $NaHCO_3$ was added followed by 12 mL of saturated, aqueous $Na_2S_2O_3$. The resultant white, cloudy suspension was stirred for 10 min at room temperature and subsequently diluted with 20 mL each of pentane and water to yield a clear biphasic solution with a small amount of undissolved solids at the interface. The resulting layers were separated, the aqueous layer was extracted 3 x 30 mL pentane, the combined organic layers were dried over Na_2SO_4, filtered through Celite, concentrated *in vacuo*, and used without further purification. In some cases, solids were found after concentration, at which point, the material was resuspended in pentane, dried over Na_2SO_4, filtered through Celite, concentrated in vacuo again. This was found to be sufficient to remove any remaining periodic acid residue. Title compound was found to decompose over 24 h when stored as a solution in $CDCl_3$ at room temperature; however, no significant isomerization of the alkene was observed. Furthermore, in subsequent experiments, the aldehyde was found to be stable on silica gel and was sometimes reisolated, though never reused. Title compound was also formed using a Swern protocol, but the oxidation with Dess-Martin periodinane was much cleaner and was thus preferred despite the associated cost of the oxidizing reagent. ^1H NMR (400 MHz,

$CDCl_3$) δ 10.16 (d, *J* = 6.8, 1H), 6.57 (dt, *J* = 11.6, 5.1, 1H), 5.99 (ddt, *J* = 11.4, 7.0, 2.1, 1H), 4.68 (dd, *J* = 5.1, 2.0, 3H), 0.92 (s, 13H), 0.10 (s, 7).

((*Z*))-1-((*tert*-butyldimethylsilyl)oxy)dodec-2-en-5-yn-4-ol (2.26): Commercially available 1-octyne (1.5 mL, 10.168 mmol) was diluted with 50 mL of dry toluene and cooled to –78 °C. *n*-BuLi (4.8 mL, 11.184 mmol) was added dropwise over ten minutes and the reaction mixture was allowed to stir for 30 min (Note: Addition of *n*-BuLi to a more concentrated solution of 1-octyne results in rapid formation of a clear and colorless gelatinous substance which halts magnetic stirring). Reaction mixture was warmed to 0 °C and diethylaluminum chloride (11.4 mL, 11.4 mmol) was added resulting in a white suspension. The white suspension was stirred at 0 °C for 2.5 h and **2.25** was added *via* cannula. Flask containing aldehyde **2.25** was washed 2 x 3 mL dry toluene, the rinsings were cannulated into the reaction mixture, and the reaction mixture was stirred 4 h at 0 °C before being quenched by the addition of 40 mL of water. The aqueous phase was separated, acidified with 1M HCl to help break the aluminum emulsion, and washed 3 x 50 mL pentane. The combined organic phases were washed with 50 mL water, 50 mL brine, dried with Na_2SO_4, and concentrated *in vacuo*. Purification of the crude material by column chromatography (5–10% EtOAc in hexanes) gave **2.26** as a clear oil (0.6394 g, 42% Yield). ^{1}H NMR (600 MHz, $CDCl_3$) δ 5.67–5.63 (m, 2H), 5.16–5.15 (m, 1H), 4.31 (qd, *J* = 13.2, 3.6, 2H), 2.39 (d, *J* = 5.0, 1H), 2.20 (dt, *J* = 7.2, 1.8, 2H), 1.50 (ddd, *J* = 14.9, 7.4, 7.4, 2H), 1.36 (ddd, *J* = 15.0, 7.4, 7.4, 2H), 1.32–1.25 (m, 4H), 0.91 (s, 9H), 0.89 (t, *J* = 7.1, 3H), 0.09 (s, 6H); ^{13}C NMR (125 MHz, $CDCl_3$) δ 131.4, 131.3, 86.1, 80.0, 59.8, 58.9, 31.5, 28.7, 28.7, 26.0, 25.8, 22.7, 18.9, 14.2, -3.4.s

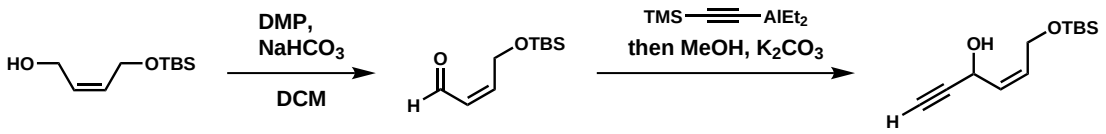

((*Z*))-6-((*tert*-butyldimethylsilyl)oxy)hex-4-en-1-yn-3-ol (2.27): Commercially available

TMS-acetylene (1.5 mL, 10.6 mmol) was diluted with 42 mL of dry toluene, cooled to –78 °C, and *n*-BuLi (4.7 mL, 11.609 mmol) was added dropwise over 10 min. The reaction mixture was stirred at –78 °C 30 min, warmed to 0 °C, diethylaluminum chloride (11.7 mL, 11.7 mmol) was added, and the resultant white suspension was stirred at 0 °C for 1 h. **2.25** (synthesized as above $\leq$ 5.039 mmol) was added as a solution in 6 mL of toluene, the aldehyde flask was washed 2 x 6 mL toluene, and the rinsings were added to the reaction mixture. The resultant reaction mixture was stirred for 2 h at 0 °C before being quenched by the addition of 40 mL of water. The aqueous phase was separated, acidified with 1M HCl to help break the aluminum emulsion, and washed 3 x 50 mL pentane. The combined organic phases were washed with 50 mL water, 50 mL brine, dried with Na_2SO_4, and concentrated *in vacuo* to give a TMS protected terminal alkyne. ^{1}H NMR (600 MHz, $CDCl_3$) δ 5.63 (dd, *J* = 5.1, 3.6, 2H), 5.11 (d, *J* = 6.1, 1H), 4.29 (qd, *J* = 13.8, 3.7, 2H), 0.89 (s, 9H), 0.14 (s, 9H), 0.07 (s, 6H).

The crude material was then resuspended in 32 mL of MeOH, cooled to 0 °C and K_2CO_3 was added. The reaction mixture stirred until no starting material was present by TLC. MeOH was removed *in vacuo* and the resultant material was partitioned between 50 mL of Et_2O and 50 mL of water. The layers were separated, the aqueous phase was extracted 2 x 50 mL Et_2O, the combined organic phases were washed with 50 mL brine, dried Na_2SO_4, filtered through Celite and concentrated *in vacuo*. The resultant crude product was purified by column chromatography (10% EtOAc in hexanes) to give **2.27** (0.565 g, 50% Yield). ^{1}H NMR (500 MHz, $CDCl_3$) δ 5.70 (br s, 2H), 5.19 (br s, 1H), 4.36–4.29 (m, 2H), 2.72 (d, *J* = 5.1, 1H), 2.49 (s, 1H), 0.91 (s, 9H), 0.10 (s, 6H).

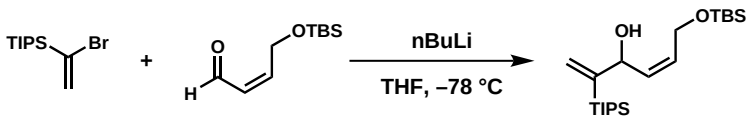

((*Z*))-6-((*tert*-butyldimethylsilyl)oxy)-2-(triisopropylsilyl)hexa-1,4-dien-3-ol (2.34):

Alkenyl bromide **2.33** (0.377 g, 1.43 mmol, synthesized as described by the Yamamoto group)[26] was diluted with 6 mL dry THF and cooled to –78 °C. *n*-BuLi (0.52 mL, 1.26 mmol) was added dropwise and the reaction mixture was stirred at –78 °C for 1 h. **2.25** (freshly made, $\leq$ 1.159 mmol) was added as a solution in 2 mL THF, the reaction mixture was stirred for another 1.5 h at –78 °C, and then quenched by pouring into 20 mL of ice and water. The resultant mixture was extracted 3 x 50 mL pentane, the combined organic phases were washed with 20 mL saturated aqueous $NaHCO_3$, 20 mL brine, dried with Na_2SO_4, filtered through Celite, concentrated *in vacuo*. The crude material was purified by column chromatography (10% EtOAc in hexanes) to give **2.34** (0.339 g, 76% Yield). ^{1}H NMR (600 MHz, $CDCl_3$) δ 6.11 (t, *J* = 1.6, 1H), 5.69 (dt, *J* = 11.6, 5.8, 1H), 5.56–5.53 (m, 2H), 5.03 (d, *J* = 7.7, 1H), 4.34 (ddd, *J* = 13.4, 6.2, 1.6, 1H), 4.22 (ddd, *J* = 13.4, 5.7, 1.1, 1H), 1.23–1.18 (m, 3H), 1.08 (d, *J* = 11.0) and 1.07 (d, *J* = 11.0) overlap total 18H, 0.90 (s, 9H), 0.08 (s, 6H); ^{13}C NMR (125 MHz, $CDCl_3$) δ 149.3, 134.0, 131.4, 128.0, 69.9, 59.8, 26.0, 18.9, 18.9, 18.4, 11.4, -5.1; HRMS (ESI/MeOH) *m* / *z* calcd for $C_{21}H_{44}O_2Si_2Na$ $(M+Na)^+$ 407.2778, found 407.2796.

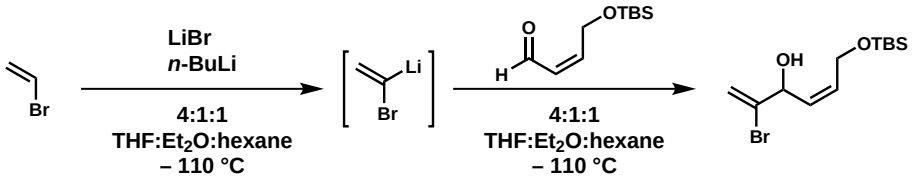

((*Z*))-2-bromo-6-((*tert*-butyldimethylsilyl)oxy)hexa-1,4-dien-3-ol (2.32): This procedure is based on the protocol reported by the Sampson group for preparation and use of 1-bromo-1-lithioethene.[27] Notable deviations from the Sampson protocol are: the use of a solvent mixture of 4:1:1 THF : Et_2O : n-hexane in place of 4:1:1 THF : Et_2O : pentane (Trapp mixture), the use of an Et_2O / liq. N_2 (–110 °C) cooling bath in place of a methylcyclohexane / liq. N_2 (–127 °C) cooling bath, mechanical stirring through a Teflon sealed adapter, and the absence of a specialized low temperature reactor vessel (**Figure 2.3**).

A large Dewar was equipped with a wind vane type stir bar and a heat exchanger (The bottom segment of a Schlenk trap was used, but any elongated piece of glassware will serve). The Dewar was filled with Et_2O, and the bath temperature was lowered to –100 °C by adding liquid nitrogen to the Dewar directly, after which the heat exchanger was repeated filled with liquid nitrogen until a shell of frozen Et_2O was observed around the heat exchanger. Temperature was maintained by stirring the coolant and periodically adding liquid nitrogen to the heat exchanger, resulting in the formation of a steadily increasing layer of solidified Et_2O while minimizing temperature gradients.

Lithium bromide (0.599 g wet, not reweighed, $\leq$0.333 mmol) was flame dried and degassed with argon, in triplicate, in a 500 mL three-neck flask equipped with a Teflon sealed mechanical stirrer. Modified Trapp mixture (4:1:1 THF : Et_2O : *n*-hexane, 30 mL) was added to the flask and the resulting solution was cooled to –110 °C, making sure that the flask was as deeply submerged in the coolant bath as possible without exposing the septum to the coolant bath. Vinyl bromide (6 mL, 84.6 mmol) was condensed at –78 °C, cannulated into the lithium bromide solution, and the condensing flask was rinsed with 1 mL modified Trapp mixture. To a separate flame dried flask was added 38 mL dry THF and 15 mL dry Et_2O, this solution was cooled to –78 °C and *n*-BuLi (13.0 mL, 29.4 mmol) was added, stirring by gently rocking the flask. The *n*-BuLi solution thus prepared was cannulated into the solution of vinyl bromide, dropwise, down the side of the flask over 55 min making sure that the cannula was immersed in the cooling bath as much as possible. The resultant cloudy suspension was stirred for 50 min at –110 °C. **2.25** (freshly prepared, $\leq$20.7 mmol) was diluted with 15 mL modified Trapp mixture, cannulated into the solution of 1-bromo-1-lithioethene over 10 min dropwise, down the side of the flask, the flask was rinsed with 0.5 mL modified Trapp mixture, and the reaction mixture was stirred at –110 °C for 1 h. The reaction was quenched by slow

addition of a –78 °C solution of glacial acetic acid (1.9 mL) in 22 mL Trapp mixture. When addition of the acetic acid was completed, the cold bath was removed, the reaction mixture was transferred to a separatory funnel, washed with 20 mL each 10% aqueous $NaHCO_3$ and brine, the organic layer was dried over Na_2SO_4, filtered through Celite, and concentrated in vacuo. Purification by column chromatography (0.5 âĂŞ 10% EtOAc in hexanes) gave **2.32** (4.668 g, 73% Yield). ^{1}H NMR (600 MHz, $CDCl_3$) δ 5.97 (s, 1H), 5.79 (dt, *J* = 11.4, 5.7, 1H), 5.60–5.57 (m, 2H), 4.99 (appar t, *J* = 6.12, 1H), 4.36 (ddd, *J* = 14.0, 6.1, 1.7, 1H), 4.28 (ddd, *J* = 14, 5.3, 1.4, 1H), 2.73 (dd, *J* = 4.8, 2.1, 1H), 2.04 (s, 1H), 1.53 (br s, 1H), 0.91 (s, 9H), 0.10 (s, 6H); ^{13}C NMR (125 MHz, $CDCl_3$) δ 135.3, 133.4, 130.0, 116.9, 72.2, 60.1, 36.0, 25.8, -5.1; HRMS (CI/DCM) *m* / *z* calcd for $C_{11}H_{20}O_2SiBr$ $(M–CH_3)^+$ 288.0545, found 288.0546.

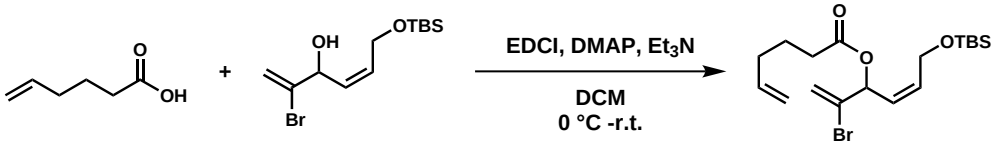

((*Z*))-2-bromo-6-((*tert*-butyldimethylsilyl)oxy)hexa-1,4-dien-3-yl hex-5-enoate (2.31): Alkenyl bromide **2.32** (1.533 g, 4.989 mmol) was diluted with 25 mL dry DCM and the solution was cooled to 0 °C. 5-hexenoic acid (0.750 g, 6.568 mmol, synthesized as reported by Starostin)[28] was added followed by DMAP (0.815 g, 6.673 mmol), Et_3N (1.1 mL, 7.89 mmol), and EDCI (1.205 g, 6.283 mmol). The resultant slightly yellow solution was stirred for 10 min at 0 °C, the cooling bath was removed and the reaction mixture was stirred for a further 3 h, diluted with 50 mL Et_2O, washed with 50 mL water, 50 mL 1M NaOH, 50 mL NH_4Cl, 50 mL brine, dried with Na_2SO_4, filtered through Celite, and concentrated *in vacuo*. The crude material was purified by filtering through silica gel (2% EtOAc in hexanes as eluent) to give **2.31** (1.780 g, 88% Yield). ^{1}H NMR (600 MHz, $CDCl_3$) δ 6.06 (d, *J* = 8.7, 1H), 5.93 (s, 1H), 5.84–5.74 (m, 2H), 5.62 (d, *J* = 1.9, 1H), 5.46 (ddt, *J* = 11.0, 8.93, 1.84, 1H), 5.03 (dd, *J* = 17, 1.04, 1H), 5.00 (d, *J* = 10.1, 1H), 4.39 (ddd, *J* = 14.1, 6.1, 1.5, 1H), 4.32 (ddd, *J* = 14, 5.3, 1.7, 1H), 2.36 (td, *J* = 7.5, 3.9, 2H),

2.10 (q, J = 7.1, 2H), 1.75 (dt, J = 14.6, 7.3, 2H), 1.53 (s, 1H), 0.90 (s, 9H), 0.08 (s, 3H), 0.08 (s, 3H); ^{13}C NMR (125 MHz, $CDCl_3$) δ 172.1, 137.7, 136.0, 130.7, 124.8, 119.0, 115.7, 72.3, 60.0, 33.7, 33.1, 26.0, 24.1, 18.5, -5.1; HRMS (ESI/MeOH) m / z calcd for $C_{18}H_{31}BrO_3SiNa$ $(M+Na)^+$ 425.1131, found 425.1124.

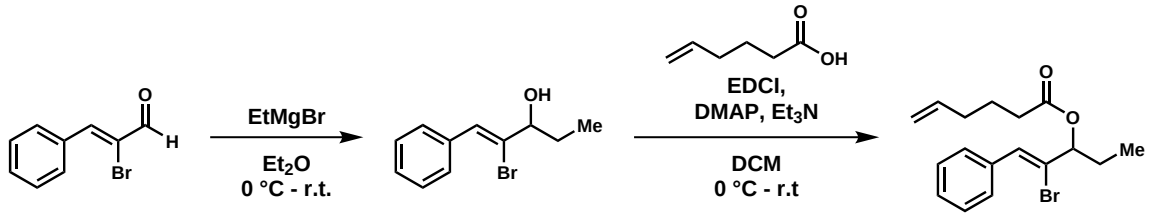

((*Z*))-2-bromo-1-phenylpent-1-en-3-ol (2.47): Commercially available α-bromocinnamaldehyde (2.019 g, 9.6 mmol) was dissolved in 25 mL dry Et_2O and cooled to 0 °C. Ethylmagnesium bromide (6.5 mL, 19.5 mmol) was added and the reaction mixture was stirred at 0 °C for 1.5 h before being quenched by slow addition of 20 mL saturated, aqueous NH_4Cl (Gas evolves). The resultant suspension was diluted with 10 mL of water, the layers were separated, the aqueous phase was extracted 2 x 20 mL Et_2O, the combined organic phases were dried with Na_2SO_4, filtered through Celite, and concentrated *in vacuo* to give **2.47** which was carried on without further purification.^{1}H NMR (MHz, $CDCl_3$) δ 7.61 (appar d, J = 7.1, 1H), 7.39-7.29 (m , 3H), 7.05 (br s , 1H), 4.18 (q , J = 6.4, 2H), 2.00 (d , J = 6.2, 1H), 1.86-1.73 (m , 2H), 0.97 (t , J = 7.4, 3H).

((*Z*))-2-bromo-1-phenylpent-1-en-3-yl hex-5-enoate (2.48): 5-hexenoic acid (0.204 g, 1.785 mmol, synthesized as reported by Starostin)[28] was diluted with 6.8 mL dry DCM and cooled to 0 °C. **2.47** (0.325 g, 1.346 mmol) was added followed by DMAP (0.218 g, 1.788 mmol), Et_3N (0.28 mL, 2.0 mmol), and EDCI (0.322 g, 1.677 mmol) and the resultant reaction mixture was allowed to warm to room temperature naturally, overnight. The reaction mixture was then diluted with 13 mL Et_2O and washed with 5 mL water, 5 mL 1M NaOH, 5 mL saturated aqueous NH_4Cl, 5 mL water, 5 mL brine.

The organic phase was dried with Na_2SO_4, filtered through Celite, and concentrated *in vacuo* to give **2.48** (0.2609 g, 57% Yield). ^{1}H NMR (600 MHz, $CDCl_3$) δ 7.62 (d , *J* = 7.4 , 2H), 7.36 (t , *J* = 7.4 , 2H), 7.31 (t , *J* = 7.3 , 1H), 7.07 (s , 1H), 5.78 (ddt , *J* = 17.0, 10.3, 6.7, 1H), 5.03 (dq , *J* = 17.1, 1.7 , 1H), 4.99 (dq , *J* = 10.2, 1.4 , 1H), 2.11 (qt , *J* = 7.1, 1.1 , 1H), 1.88 (tat , *J* = 31.5, 14.2, 7.3, 2H), 1.76 (dt , *J* = 14.9, 7.4 , 2H), 1.55 (s , 3H), 0.94 (t , *J* = 7.4 , 3H); ^{13}C NMR (125 MHz, $CDCl_3$) δ 172.8, 137.8, 135.0, 131.1, 129.4, 128.5, 128.3, 124.7, 115.6, 79.5, 33.9, 33.2, 26.4, 24.2, 9.6; HRMS (ESI/MeOH) *m / z* calcd for $C_{17}H_{21}BrO_2Na$ $(M+Na)^+$ 359.0623, found 359.0631.

Bibliography

(1) Gribble, G. W. *Environ. Chem.* **2015**, *12*, 396–405.

(2) Gribble, G. W. *Acc. Chem. Res.* **1998**, *31*, 141–152.

(3) Watanabe, K.; Miyakado, M.; Ohno, N.; Okada, A.; Yanagi, K.; Moriguchi, K. *Phytochemistry* **1989**, *28*, 77–78.

(4) Crews, P.; Myers, B. L.; Naylor, S.; Clason, E. L.; Jacobs, R. S.; Staal, G. B. *Phytochemistry* **1984**, *23*, 1449–1451.

(5) Fuller, R. W.; Cardellina, J. H.; Kato, Y.; Brinen, L. S.; Clardy, J.; Snader, K. M.; Boyd, M. R. *J. Med. Chem.* **1992**, *35*, 3007–3011.

(6) Fuller, R. W.; Cardellina, J. H.; Jurek, J.; Scheuer, P. J.; Alvarado-Lindner, B.; McGuire, M.; Gray, G. N.; Steiner, J. R.; Clardy, J. *J. Med. Chem.* **1994**, *37*, 4407–4411.

(7) Morinaka, B. I.; Molinski, T. F. *Org. Lett.* **2011**, *13*, 6338–6341.

(8) Matsumori, N.; Kaneno, D.; Murata, M.; Nakamura, H.; Tachibana, K. *J. Org. Chem.* **1999**, *64*, 866–876.

(9) Wang, X.; Duggan, B. M.; Molinski, T. F. *J. Am. Chem. Soc.* **2015**, *137*, 12343–12351.

(10) Alt, G. H.; Barton, D. H. R. *J. Chem. Soc.* **1954**, 4284–4294.

(11) Barton, D. H. R.; King, J. F. *J. Chem. Soc.* **1958**, 4398–4402.

(12) González, A. G.; Derias, J.; Martín, J. D.; Pérez, C. *Tetrahedron Lett.* **1974**, *15*, 1249–1250.

(13) Chung, W.-j.; Vanderwal, C. D. *Angew. Chem. Int. Ed.* **2016**, *55*, 4396–4434.

(14) Salvi, L.; Jeon, S.-J.; Fisher, E. L.; Carroll, P. J.; Walsh, P. J. *J. Am. Chem. Soc.* **2007**, *129*, 16119–16125.

(15) Li, H.; Carroll, P. J.; Walsh, P. J. *J. Am. Chem. Soc.* **2008**, *130*, 3521–3531.

(16) Kerrigan, M. H.; Jeon, S.-J.; Chen, Y. K.; Salvi, L.; Carroll, P. J.; Walsh, P. J. *J. Am. Chem. Soc.* **2009**, *131*, 8434–8445.

(17) Hussain, M. M.; Li, H.; Hussain, N.; Urenã, M.; Carroll, P. J.; Walsh, P. J. *J. Am. Chem. Soc.* **2009**, *131*, 6516–6524.

(18) Kim, H. Y.; Salvi, L.; Carroll, P. J.; Walsh, P. J. *J. Am. Chem. Soc.* **2009**, *131*, 954–962.

(19) Bhat, N. G.; Tamm, A.; Gorena, A. *Synlett* **2004**, *2004*, 297–298.

(20) Ma, S.; Liu, F.; Negishi, E.-i. *Tetrahedron Lett.* **1997**, *38*, 3829–3832.

(21) Kikukawa, K.; Umekawa, H.; Wada, F.; Matsuda, T. *Chem. Lett.* **1988**, *17*, 881–884.

(22) Faraoni, M. B.; Gerbino, D. C.; Podestá, J. C. *J. Organomet. Chem.* **2008**, *693*, 1877–1885.

(23) Hamze, A.; Provot, O.; Brion, J.-D.; Alami, M. *J. Org. Chem.* **2007**, *72*, 3868–3874.

(24) Takao, K.-i.; Hayakawa, N.; Yamada, R.; Yamaguchi, T.; Saegusa, H.; Uchida, M.; Samejima, S.; Tadano, K.-i. *J. Org. Chem.* **2009**, *74*, 6452–6461.

(25) Zhang, D.; Ready, J. M. *J. Am. Chem. Soc.* **2007**, *129*, 12088–12089.

(26) Usanov, D. L.; Yamamoto, H. *Org. Lett.* **2012**, *14*, 414–417.

(27) Novikov, Y. Y.; Sampson, P. *Org. Lett.* **2003**, *5*, 2263–2266.

(28) Starostin, E. K.; Furman, D. B.; Ignatenko, A. V.; Barkova, A. P.; Nikishin, G. I. *Russ. Chem. Bull.* **2006**, *55*, 2016–2019.

(29) Aird, J. I.; Hulme, A. N.; White, J. W. *Org. Lett.* **2007**, *9*, 631–634.

(30) Fürstner, A.; Jeanjean, F.; Razon, P.; Wirtz, C.; Mynott, R. *Chem.- Eur. J.* **2003**, *9*, 320–326.

(31) Fürstner, A. *Chem. Commun.* **2011**, *47*, 6505.

(32) Fürstner, A.; Thiel, O. R.; Lehmann, C. W. *Organometallics* **2002**, *21*, 331–335.

(33) Gatti, M.; Drinkel, E.; Wu, L.; Pusterla, I.; Gaggia, F.; Dorta, R. *J. Am. Chem. Soc.* **2010**, *132*, 15179–15181.

(34) Pentzer, E. B.; Gadzikwa, T.; Nguyen, S. T. *Org. Lett.* **2008**, *10*, 5613–5615.

(35) Ooi, T.; Maruoka, K.; Yamamoto, H. *Org. Synth.* **1993**, 95–95.

(36) Cai, Z.; Yongpruksa, N.; Harmata, M. *Org. Lett.* **2012**, *14*, 1661–1663.

(37) Seidl, F. J.; Burns, N. Z. *Beilstein J. Org. Chem.* **2016**, *12*, 1361–1365.

(38) Hu, D. X.; Seidl, F. J.; Bucher, C.; Burns, N. Z. *J. Am. Chem. Soc.* **2015**, *137*, 3795–3798.

(39) Bucher, C.; Deans, R. M.; Burns, N. Z. *J. Am. Chem. Soc.* **2015**, *137*, 12784–12787.

(40) Abdel-Baky, S.; Giese, R. W. *J. Org. Chem.* **1986**, *51*, 3390–3391.

(41) Negoro, T.; Ikeda, Y. *Bull. Chem. Soc. Jpn.* **1984**, *57*, 2111–2115.

Chapter 3:

Progress Toward the Synthesis of Crotogoudin

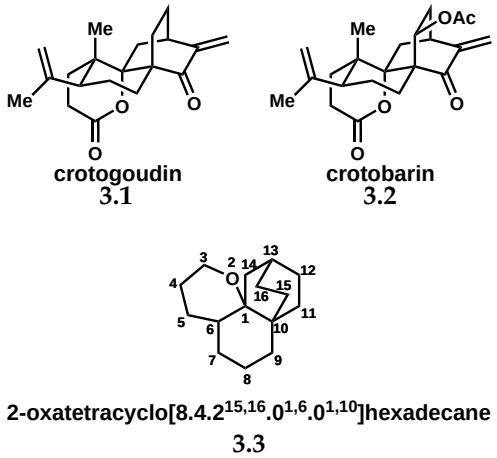

Figure 3.1: Crotogoudin and crotobarin.

(–)-Crotogoudin (**3.1**) is a 3,4-*seco*-atisane diterpene that has been shown to interrupt the cell cycles of several human cancer cell lines. The core structure is a stereochemically rich 2-oxatetracyclo[8.4.2^{15,16}.0^{1,6}.0^{1,10}]hexadecane (von Baeyer numbering, **3.3**). Of the four contiguous stereocenters, three are at bridgehead positions, two are quaternary carbons, and one is a fully substituted, and therefore labile, lactone. Furthermore, the bicyclo[2.2.2]octane moiety has an obligatory *syn*-pentane interaction with the axial methyl group which promised to complicate attempts at late stage bicycle formation. While the source of crotogoudin's cytotoxicity is not known, it is likely that the exocyclic enone may be responsible.[1] Because the majority of our synthetic work toward crotogoudin was conducted on racemic material, I represent crotogoudin and crotobarin as depicted in **Figure 3.1** despite the fact that the (+)-crotogoudin and (+)-crotobarin enantiomers shown represent the unnatural enantiomers of both **3.1** and **3.2**, as was established after our work began.

3.1 Biosynthesis of related *ent*-diterpene natural product families.

Despite the fact that they carry the *ent*- prefix, *ent*-beyerene, *ent*-atisane, *ent*-kaurene, and *ent*-trachylobane diterpenes (**Scheme 3.1**) are the more common

representatives of each of these natural product families. The nomenclature seems to stem from their shared biosynthetic origins, as all of these diterpenes are formed from *ent*-copalyl pyrophosphate (**3.5**) which is, in turn, made from geranylgeranyl pyrophosphate (**3.4**). Loss of the diphosphate in **3.5** generates an allylic carbocation that cyclizes to close the third ring of the system, forming the pimarenyl carbocation (**3.6**).

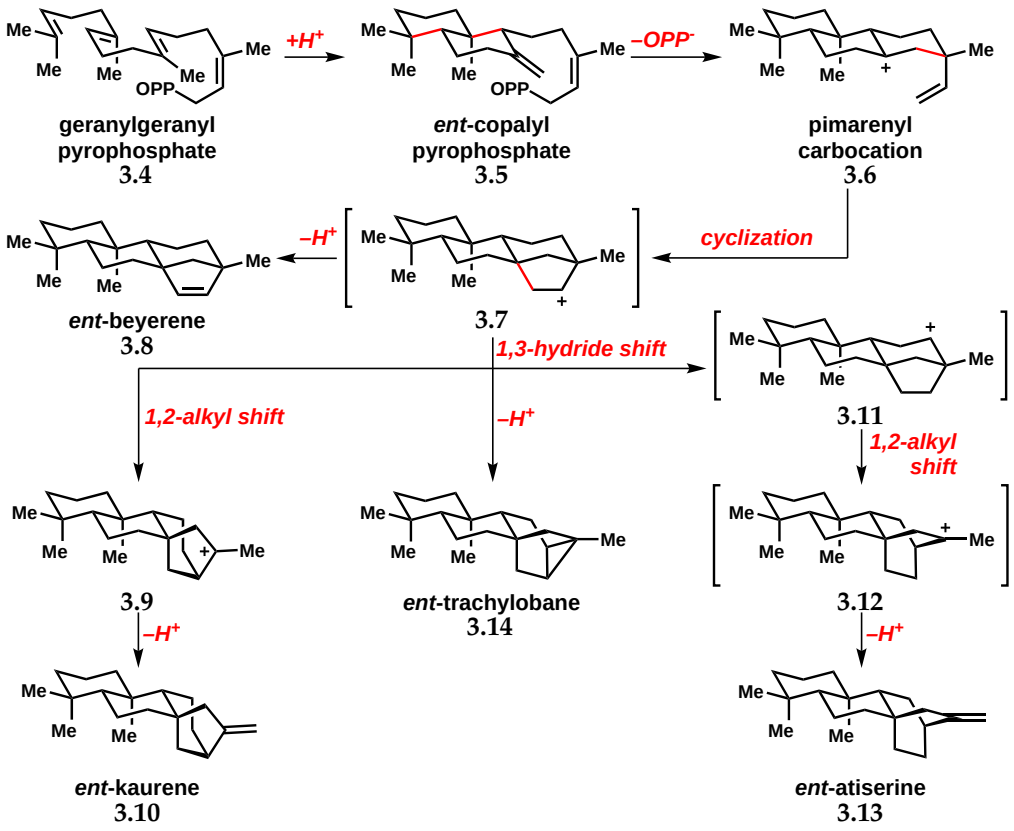

Scheme 3.1: Biosynthesis of *ent*-beyerene, *ent*-atisane, *ent*-kaurene, and *ent*-trachylobane diterpenes.

Classically, the proposed biosynthesis continues with an intramolecular cation-alkene cyclization using the nucleophilic alkenyl group of **3.6** to form the beyerenyl carbocation (**3.7**), which may be further deprotonated to form the skeleton of the *ent*-beyerene family of natural products (**3.8**). A Wagner–Meerwein rearrangement of **3.7** yields the more stable, tertiary kaurenyl carbocation (**3.9**) which, after elimination, leads to the *ent*-kaurene family of natural products (**3.10**). If instead a 1,3-hydride shift occurs forming secondary carbocation **3.11**, a subsequent 1,2-alkyl shift generates

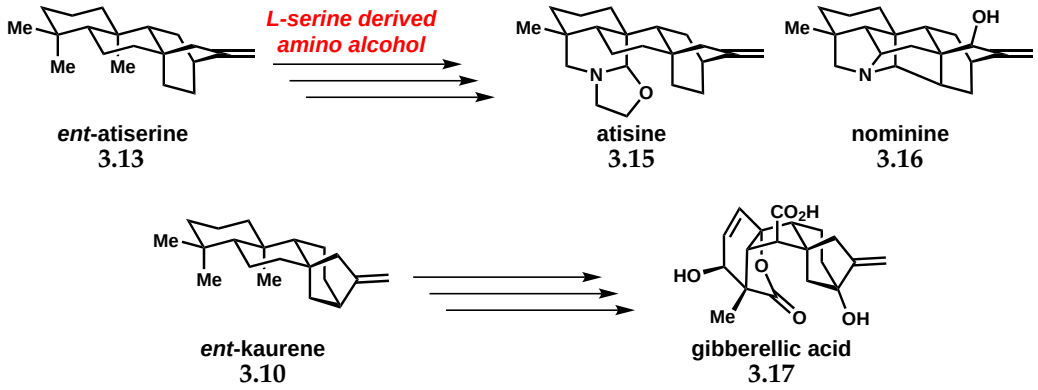

Scheme 3.2: Examples of diterpene alkaloids derived from atiserine and kaurene.

tertiary carbocation (**3.12**). Deprotonation of **3.12** then leads to the *ent*-atisane family of natural products (here represented by atiserine **3.13**). Deprotonation and cyclization of **3.7** is the generally accepted route to the *ent*-trachylobane family of natural products; however, it has been proposed that analogous reactions on **3.12** may also lead to the *ent*-trachylobane scaffold.[2–4] Further complexity can be biosynthetically added to these hydrocarbon scaffolds *via* oxidation and amination (**Scheme 3.2**), leading to diverse natural products which may closely resemble their parent diterpenes, such as atisine (**3.15**) and nominine (**3.16**), or skeletally rearranged compounds with excised carbon atoms such as gibberellic acid (**3.17**).[5,6]

While the biosynthesis presented in **Scheme 3.1** is appealing in the descriptive order of events, the formation of the unstable secondary beyerenyl carbocation (**3.7**), as well as the isomeric carbocation **3.11**, have led to contention concerning this biosynthetic proposal. Computational studies by the Tantillo group were unable to find energy minima corresponding to **3.7**, but showed that a similar structure is on the reaction coordinate between **3.7** and the **3.9**.[7,8] This computational result suggests that cyclization of **3.6** to form **3.7** and the 1,2-alkyl shift which forms **3.9** occur in a concerted, asynchronous reaction pathway. Surprisingly, a minimum could not be found for secondary carbocation **3.11** either. In this case, the lack of an energy minimum suggests that **3.12** is formed from **3.6** *via* a complex series of three concerted, asynchronous reactions. The suggestion, then, that the *ent*-beyerene and *ent*-trachylobane families are

made by deprotonation of **3.6** becomes surprising since both of these transformations necessarily involve an intermolecular deprotonation, which is expected to be several orders of magnitude slower than intramolecular carbocation rearrangements and hydride shifts.

3.2 Isolation of Crotogoudin

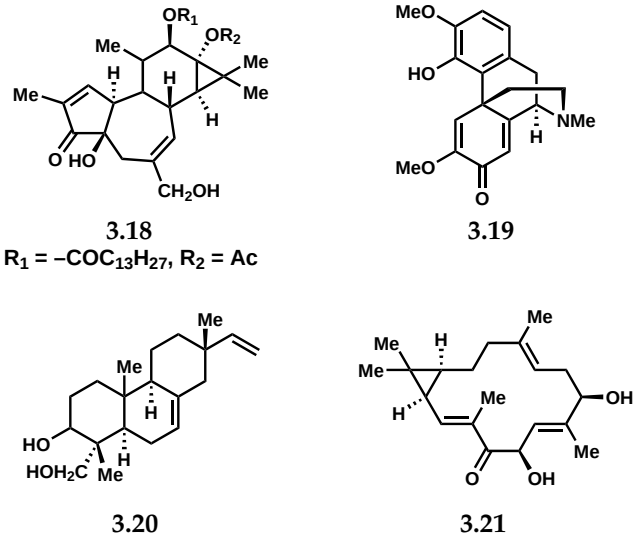

Figure 3.2: Examples of natural products isolated from the *Croton* plant genus.

The genus *Croton* includes over 500 species of flowering plants; at least 130 *Croton* species are known on Madagascar alone. Members of the *Croton* genus are prevalent in herbal medicine and are known to produce many bioactive compounds (**Figure 3.2**), such as the potent tumor promoter 12-O-tetradecanoyl-phorbol-13-acetate (**3.18**, *C. tiglium*),[9] salutaridine (**3.19**, *C. salutaris*),[10] 18-hydroxyisopimara-7,25-dien-3β-ol (**3.20**, *C. zambesicus*),[11] and 1,4-dihydroxy-2E,6E,12E-trien-5-one-casbane (**3.21**, *C. nepetaefoltus*), which prevents *Candida* biofilm formation.[12] However, an exhaustive assay of *Croton* derived natural products has not been performed.[9] Madagascan herbal medicine prescribes *Croton goudotii* (*C. goudotii*) to treat chronic blennorrhea, cough, and, ironically, as a purported aphrodisiac. *Croton barorum* is used for the treatment of cough and malaria.[13]

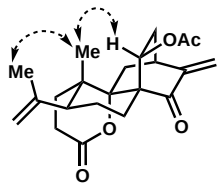

Figure 3.3: Key NOESY correlations observed by the Rasoanaivo group.

Cytotoxicity guided fractionation of the ethyl acetate extracts of *C. goudotii* and *C. barorum* gave crotogoudin (**3.1**) and crotobarin (**3.2**) in 1.2% and 0.8% yield, respectively, after chromatographic purification. High resolution mass spectrometry of **3.2** gave $[M+Na]^+$ 395.1849 corresponding to a molecular formula of $C_{22}H_{28}O_5$. The IR spectrum showed peaks at 1730 and 1238 cm^{-1} indicating the presence of a lactone and an ester. The ^{13}C NMR showed an α,β-unsaturated ketone at 195.1 ppm, as well as esters at 170.5 and 169.7 ppm. ^1H NMR showed two alkene methylenes at δ_H 5.91, 5.30 and 5.00, 4.86 ppm, respectively. Three distinct methyl groups were also apparent at δ_H 1.94, 1.82 and 1.23. These functional groups were organized using key HMBC correlations and the relative stereochemistry was determined by NOESY correlation (**Figure 3.3**) between the isopropylene methyl group, C6 methyl group, and bicyclo[2.2.2]octane bridge proton. The structure of **3.1** was assigned both by analogy to **3.2** and by independent NMR experiments. While the optical rotations for **3.1** and **3.2** were initially reported as $[\alpha]_D^{20}$ = 20 (*c* +7, 0.40)$CHCl_3$ and $[\alpha]_D^{20}$ = 20 (*c* –29.9, 0.05)$CHCl_3$, respectively, the absolute stereochemistry was not established until the Carreira group's synthesis of crotogoudin was completed.[13] Following Carreira's synthesis of (+)-crotogoudin (**3.1**), the Rasoanaivo group repeated their isolation of **3.1** and **3.2**, revising the optical rotations to be $[\alpha]_D^{20}$ = 20 (*c* –25.2, 0.04)$CHCl_3$ for **3.1** and $[\alpha]_D^{20}$ = 20 (*c* –23.8, 0.04)$CHCl_3$ for **3.2**. This finding demonstrates that natural crotogoudin is of the common *ent*-atisane series of natural products, and that the Carreira group made the unnatural (+)-enantiomer of **3.1**.[14]

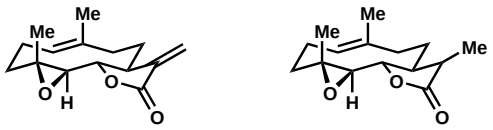

Figure 3.4: Parthenolide, a reported TCP inhibitor and its inactive derivative.

3.3 Bioactivity

Several anti-mitotic cancer therapies have targeted tubulin, the protein responsible for cell scaffolding, motility, and division. While some drugs, such as *vinca* alkaloids and colchicine, prevent tubulin from aggregating into microtubules, the taxane family of natural products stabilize the microtubule structure, preventing disassembly and causing misalignment in the microtubule framework. A third mechanism of action has been found which disrupts the microtubule framework by altering the balance been tyrosinated and detyrosinated tubulin reservoirs. Selective detyrosination of microtubules has been shown to direct chromosomes toward the poles of the mitotic spindle framework. Conversely, exhaustive detyrosination of tubulin results in transportation of chromosomes in random directions.[15] Though poorly understood, tubulin carboxypeptidase (TCP) is known to remove the carboxy-terminal tyrosine of tubulin, a reaction which is reversed by tubulin tyrosine ligase (TTL). TTL suppression has been linked with particularly aggressive metastatic tumors. Inhibition of TCP may thus be therapeutic, restoring the ratio of tyrosinated tubulin to detyrosinated tubulin, and limiting the tumor's spread. Since paclitaxel displays a phenotype similar to TTL inhibition, using TCP inhibitors in combination with taxane therapies may also be beneficial. Parthenolide (**3.22**, **Figure 3.4**), an anti-mitotic, anti-inflammatory, and anti-parasitic natural product, has been demonstrated to avoid build up of detyrosinated tubulin in cells treated with paclitaxel or a TTL specific antibody, suggesting that **3.22** acts as a TCP inhibitor. Interestingly, the hydrogenated dihydroparthenolide (**3.23**) shows no activity under the same experimental conditions, suggesting that the α-methylene lactone is required for TCP inhibition.[16]

Examining the structure of **3.1** and **3.2**, the most reactive functional group appears to be the exocyclic methylene α,β-unsaturated ketone. While conjugate addition of nucleophilic residues into the enone functional group may be unspecific, the efficacy of parthenolide is an encouraging result in support of using α,β-unsaturated carbonyls in drug molecules.

Table 3.1: Cytotoxicity of crotogoudin (**3.1**) and crotobarin (**3.2**).

			IC_{50} (μM)		
Entry	Source	Cell Line	crotogoudin	crotobarin	docetaxel
1	*Cervical*	KB	2.5 ± 0.10	1.5 ± 0.03	0.29 ± 0.03
2	*Colorectal*	HT29	2.1 ± 0.60	1.9 ± 0.25	0.92 ± 0.02
3	*Alveolar*	A549	0.79 ± 0.15	0.54 ± 0.02	0.37 ± 0.01
4	*Myeloid*	HL60	0.56 ± 0.02	0.49 ± 0.01	0.52 ± 0.02
5	*Lymphocyte (murine)*	P388	0.4 nM	0.4 nM	

The Rasoanaivo group isolated both **3.1** and **3.2** using a cytotoxicity guided fractionation procedure. Indeed, both **3.1** and **3.2** showed significant cytotoxicity against the murine P388 cancer cells as well as a variety of human tumor cell lines. In studies against the A549 alveolar cancer cell line (**Table 3.1**, Entry 3), crotogoudin and crotobarin both gave sub-micromolar IC_{50} values. In comparison, the anti-mitotic agent docetaxel was twice as potent as crotogoudin and 1.5 times more potent than crotobarin. The most promising activity was found against the HL60 myeloid tumor cell line (**Table 3.1**, Entry 4), as crotogoudin was only 40 nM less efficacious than docetaxel and crotobarin was slightly more cytotoxic than the positive control. Neither crotogoudin nor crotobarin showed high efficacy against KB cervical tumor cells or HT29 colorectal tumor cells (**Table 3.1**, Entries 1,2). This suggests that both crotogoudin and crotobarin may be selective chemotherapy agents, a point which must be stressed since cytotoxicity experiments with normal human cells were absent from this study.[13]

Measurement of cellular uptake of 5-bromo-2′-deoxyuridine and propidium iodide by K562 myeloid cells in the presence and absence of crotogoudin and crotobarin showed that 4 μM concentrations of either compound led to an increasing proportion of cells trapped in the G2 and mitosis stages of the cell cycle. The increasing number of cells stranded in, or just prior to, mitotic division, combined with subdiploid DNA content in all cells exposed to **3.1** and **3.2** supports the hypothesis that both **3.1** and **3.2** may act as TCP inhibitors and thus be valuable as anti-mitotic cancer treatments.[13,16]

3.4 Synthesis of bicyclo[2.2.2]octanes

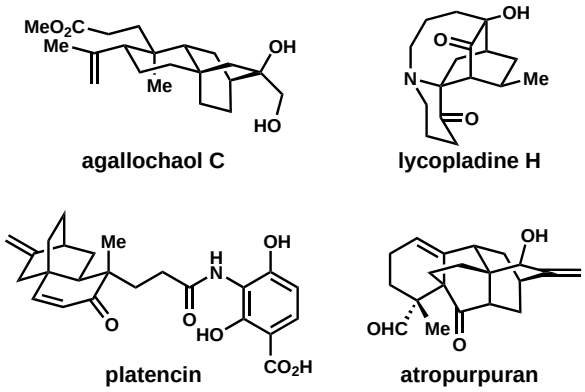

Figure 3.5: Bicyclo[2.2.2]octane containing natural products.

As the decorated bicyclo[2.2.2]octane moiety of crotogoudin promises to be the most challenging component to install, a discussion of prior art in the synthesis of this functional group is warranted. Though bicyclo[3.2.1]octanes are more prevalent than their isomeric bicyclo[2.2.2]octane cousins, several natural product families bear the functional group (**Figure 3.5**).[17–20]

3.4.1 Diels–Alder and double Michael strategies

Between a concerted, synchronous Diels–Alder and a double Michael addition is a continuum of concerted, asynchronous Diels–Alder reaction pathways. Since the concerted Diels–Alder and sequential double Michael reactions are related and often involve synthesis of similar starting materials, they are both discussed in this section.

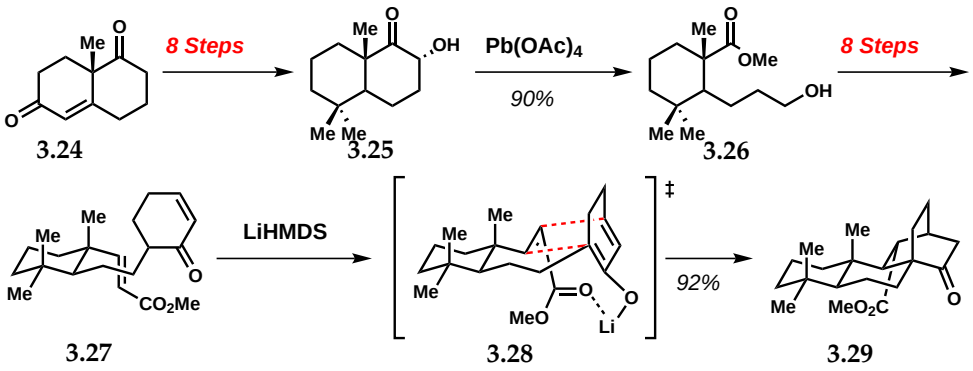

Scheme 3.3: Fukumoto's synthesis of (+)-atiserine.

In 1984, the Fukumoto group published its first paper describing the use of cross-conjugated cyclohexadienolates as the nucleophilic component of what he describes as intramolecular double Michael cyclizations, beginning an eight year foray into the synthesis of atisane diterpenes and diterpene alkaloids.[21–24] Two years later, this intramolecular double Michael reaction was employed in the enantioselective synthesis of (+)-atiserine (**Scheme 3.3**).[25] Starting from optically active Weiland–Miescher ketone **3.24**, a known, though lengthy, sequence of operations generated decalone **3.25**.[26] Exposing **3.25** to lead tetraacetate resulted in oxidative cleavage of the carbonyl-C_α bond to give ester **3.26** in 90% yield. Another extensive campaign of protections and functional group interconversions set the Fukumoto group up for their key intramolecular double Michael reaction. Treatment of enone **3.27** with lithium hexamethyldisilazide resulted in the formation of bicyclo[2.2.2]octane **3.29** in 92% yield. The complete diastereoselectivity observed in the reaction is attributed to lithium chelation between the methyl ester of the acryloyl component and the enolate oxygen, as shown in **3.28**.

The Fukumoto group also contributed a rapid entry into complex bicyclo[2.2.2]octanes *via* a retro-[2+2] cycloreversion (**Scheme 3.4**). Benzocyclobutane **3.30** was readily elaborated to enone **3.31** in four steps. Protection of the alkene with thiophenol *via* the thio-ene reaction and Wittig olefination gave exocyclic alkene **3.32**. Heating alkene **3.32** effected the 4π electrocyclic ring opening, forming the reactive *ortho*-xylylene, which underwent a Diels–Alder cycloaddition to give a 1:1

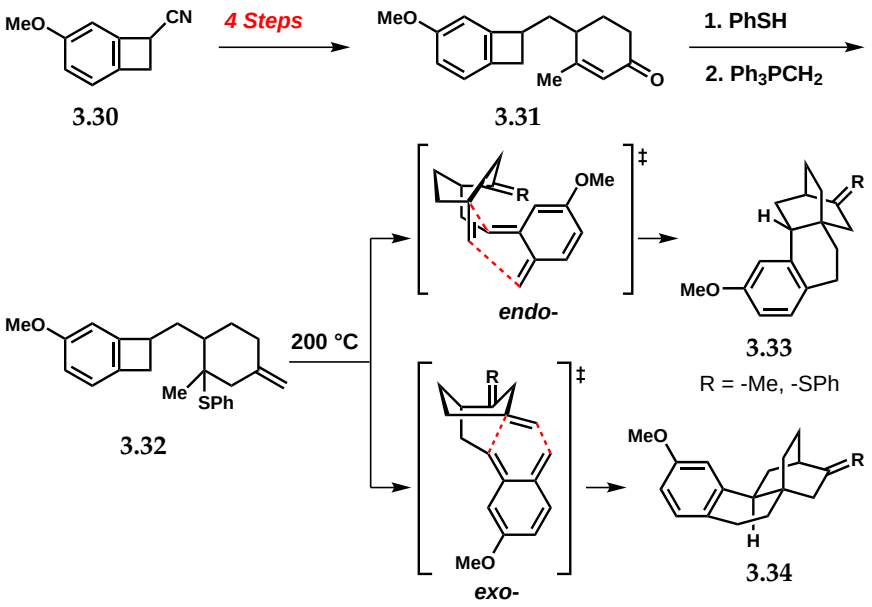

Scheme 3.4: The Fukumoto group's 4π electrocyclic ring opening/xylylene Diels–Alder strategy.

diastereomeric mixture of *syn*-(**3.33**) and *anti*-(**3.34**) bicyclooctanes resulting from the corresponding *endo*- and *exo*-Diels–Alder transition states. Experiments on the *des*-thiophenyl analog of **3.32** gave an 8:1 preference for the undesired, *endo*-Diels–Alder, which may explain why this methodology has not found use in the synthesis of bicyclo[2.2.2]octane containing natural products.[27]

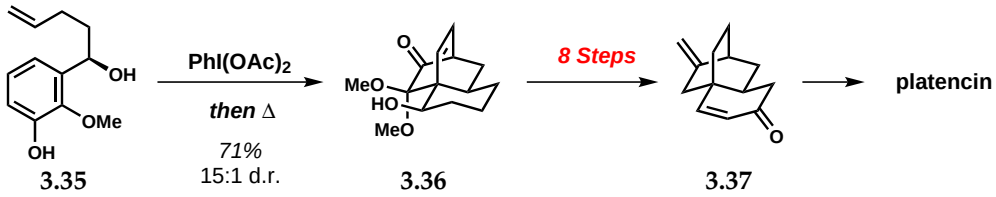

Scheme 3.5: Nicolaou's inverse electron demand Diels–Alder *en route* to platencin.

Starting from a variety of rapidly synthesized aromatic molecules, groups from around the world have taken advantage of the intramolecular inverse electron demand Diels–Alder reaction to form bicyclo[2.2.2]octanes while setting up to four stereocenters in a single transformation. Following their first synthesis of platencin,[28] the Nicolaou group published an alternative route to their key intermediate **3.37** (**Scheme 3.5**), constituting a formal synthesis of platencin **Figure 3.5**. Phenol **3.35**, synthesized in 90%

e.e. from the corresponding ketone, readily undergoes oxidative dearomatization with phenyliodonium diacetate to give bicycle **3.36**. While this route offers a rapid entry into enantioenriched bicyclooctanes, the high degree of oxidation is a nuisance when approaching the synthesis of hydrocarbons such as platencin and a large number of functional group interconversions were required to finish the platencin core **3.37**.[29]

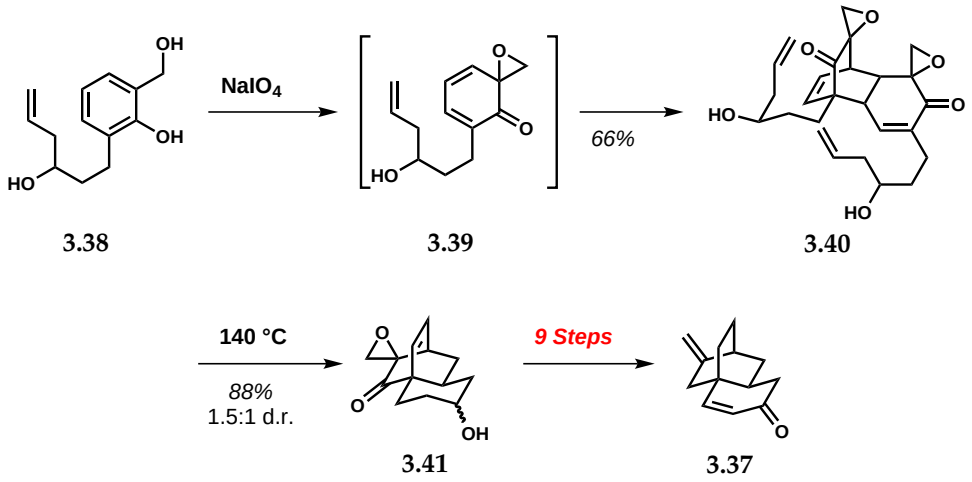

Scheme 3.6: The Singh group's oxidative dearomatization/oxidation approach to platencin.

Though the Singh group used a salicyl alcohol to perform a Becker-Adler oxidative dearomatization-epoxidation,[30–32] rather than a solvolytic oxidative dearomatization, the strategy employed (**Scheme 3.6**) mirrors that of Nicolaou's earlier work. Oxidation of phenolic methanol **3.38** gives epoxy-diene **3.39**; however, the intramolecular Diels–Alder reaction appears to be slow at room temperature as the only Diels–Alder product isolated was dimer **3.40**. Heating dimer **3.40** to 140 °C facilitates a retro-Diels–Alder, cleaving the dimer back to diene **3.39** which can, under the elevated temperatures undergo the desired [4+2] cyclization to give bicycle **3.41** as an inconsequential mixture of diastereomers at the alcohol stereocenter. While use of the inverse electron demand Diels–Alder reaction by Singh again gave a rapid entry into the desired bicyclic systems, the high degree of oxidation required for this methodology was again a handicap, requiring nine steps to reach the platencin core **3.37**.[33]

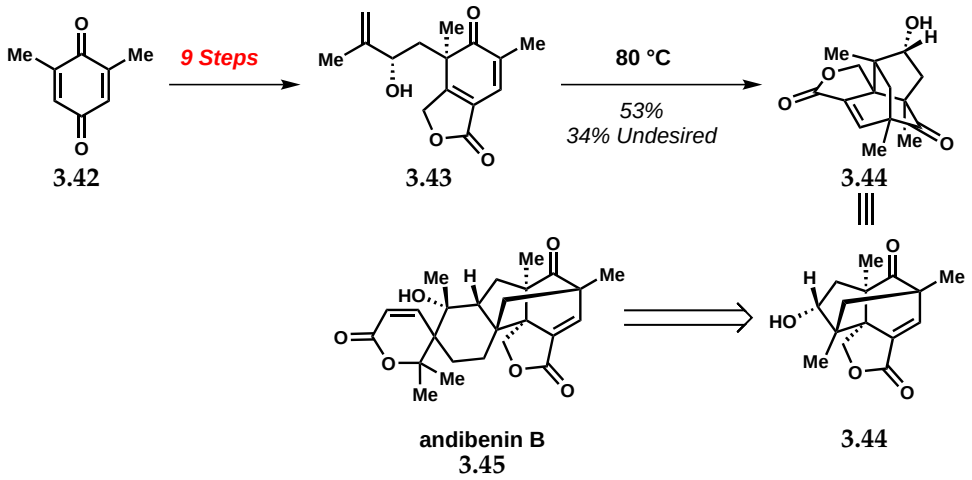

Scheme 3.7: Sorensen and Spangler's synthesis of eastern fragment of andibenin B.

While hydrocarbons such as platencin may be difficult targets for an inverse electron demand Diels–Alder reaction due the extensive reduction sequences required to remove the high degree of oxidation, a more oxidized natural product makes an appealing target for the strategy (**Scheme 3.7**). Elaboration of achiral paraquinone **3.42** provided Sorensen and Spangler with the doubly electron withdrawn diene **3.43**. Despite the sterically hindered nature of both the diene and dienophile, heating diene **3.43** gave both *endo*- and *exo*-Diels–Alder products, with the desired bicycle **3.44** as the major product. Sorensen's inverse electron demand Diels–Alder cycloaddition reaction set three stereocenters in a single step with complete diastereocontrol and **3.44** maps well onto the proposed target andibenin B (**3.45**); however, **3.44** lacks the functional handles to complete the natural product. Ideally, an elaborated dienophile would be installed such that the inverse electron demand Diels–Alder cycloaddition reaction would lead to **3.45** directly; however, the fact that no synthesis of andibenin B has been completed to date suggests that either the substrate is extremely challenging to make or that the increased steric demand of the substituted dienophile prevents the desired transformation.[20]

In one of the few syntheses that avoided making use of Nicolaou's platencin core **3.37** as an intermediate, the Banwell group made acetonide **3.46** *via* Stille coupling,

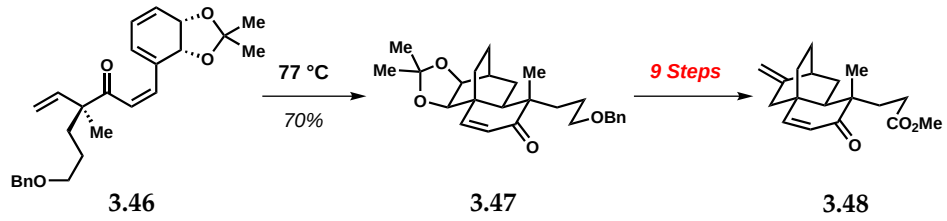

3.46 3.47 3.48

Scheme 3.8: Banwell group's approach to (–)-platencin.

which, on heating, underwent a Diels–Alder cycloaddition to give bicycle **3.47**. Though the diene of **3.46** is not as electron withdrawn as that of Sorensen's lactone **3.43**, the inductive electron withdrawing effect of the acetonide fused cyclohexadiene combined with distant, though conjugated, carbonyl, and the lack of electron withdrawing groups on the dienophile suggest that this Diels–Alder proceeds in the inverse electron demand manifold. Like other examples, the Banwell group's strategy suffers from the necessity of removing excess functionality, requiring nine steps to obtain alkene **3.48**.[34,35]

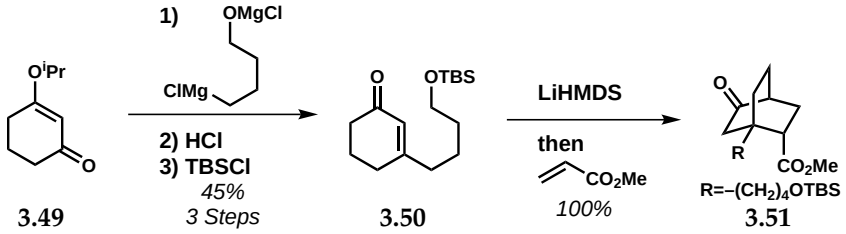

3.49 3.50 3.51

Scheme 3.9: The Maier group's approach to bicyclo[2.2.2]octanes.

Where intramolecular Diels–Alder reactions have been extensively used in the synthesis of bicyclo[2.2.2]octanes, the equivalent intermolecular reaction has not provided the same degree of utility. The Maier group installed their bicyclo[2.2.2]octane in the early stages of their work toward crotogoudin by an intermolecular double Michael reaction **Scheme 3.9**. After the alkylation and subsequent protection of vinylogous ester **3.49**, the enolate generated from **3.50** underwent the double Michael reaction with methyl acrylate in quantitative yield to give bicycle **3.51**.[36] Whereas the Yoshimitsu group was able to use a similar strategy to complete platencin,[37] the Maier group was unable to complete crotogoudin as they struggled to elaborate the under-functionalized ketone **3.51**. Similarly, the Snider group's early bicyclooctane

installation took advantage of MacMillan's asymmetric Diels–Alder reaction using a chiral imidazolidinone catalyst to reversibly generate the imine ion of acrolein (**Scheme 3.10**). Though the Diels–Alder reaction formed the desired *endo*-product preferentially, the bicycle **3.52** was obtained in only 32% yield and 87% e.e. after a five day reaction time. A further six steps were required to furnish enone **3.53**, which was elaborated to (–)-*nor*-platencin *via* precedented alkylation reactions.[38]

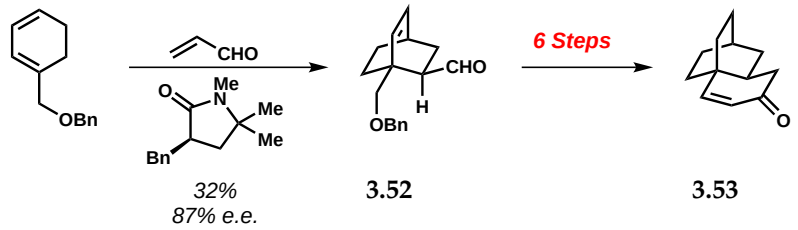

Scheme 3.10: Snider's approach to (–)-*nor*-platencin.

3.4.2 Radical cyclizations and rearrangements.

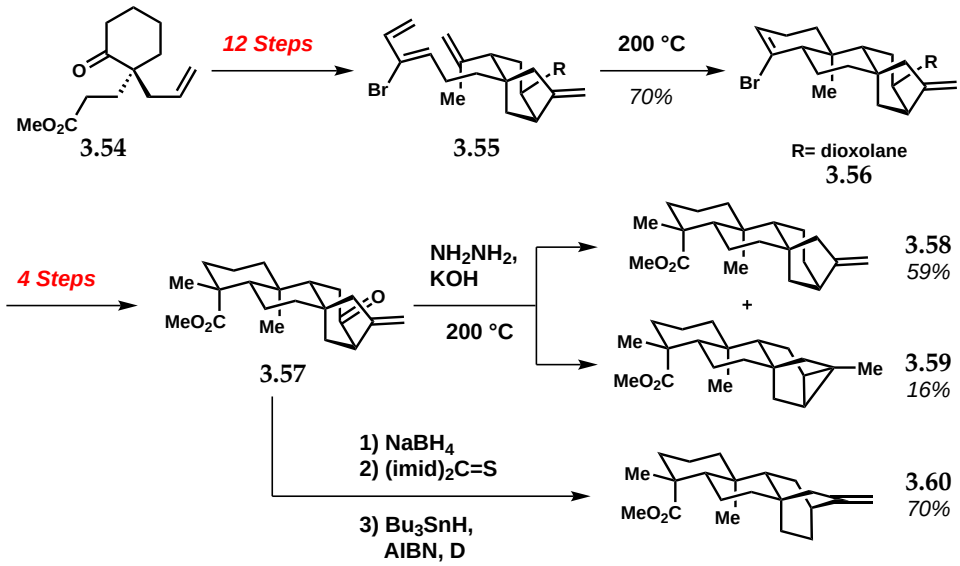

Scheme 3.11: Toyota's approach to (–)-methyl atisenoate.

The Toyota group has made use of the more readily available bicyclo[3.2.1]octane skeleton as an intermediate to methyl atisenoate (**3.60**) and serofendic acids A and B using a homoallylic radical rearrangement (**Scheme 3.11**),[39–41] a strategy that was later

employed in a variety of platencin syntheses including the Nicolaou group's original synthesis of platencin,[28,42] as well as by Maier and Yoshimitsu.[43,44] Enantioenriched ketone **3.54** was elaborated in twelve steps to triene **3.55**, which underwent an intramolecular Diels–Alder cycloaddition in 70% yield to give tetracycle **3.56**. While the majority of the kaurane skeleton is present in **3.54**, a four step sequence was required to furnish the key ketone **3.57**. Reduction of the ketone followed by Barton–McCombie deoxygenation gave (–)-methyl atisenoate (**3.60**) in 70% yield over three steps. Furthermore, subjecting **3.57** to Wolff–Kishner reduction gave a 3.7:1 mixture of (–)-methyl kaurenoate (**3.58**) and (–)-methyl trachylobanoate (**3.59**) (59% and 16% yield respectively).

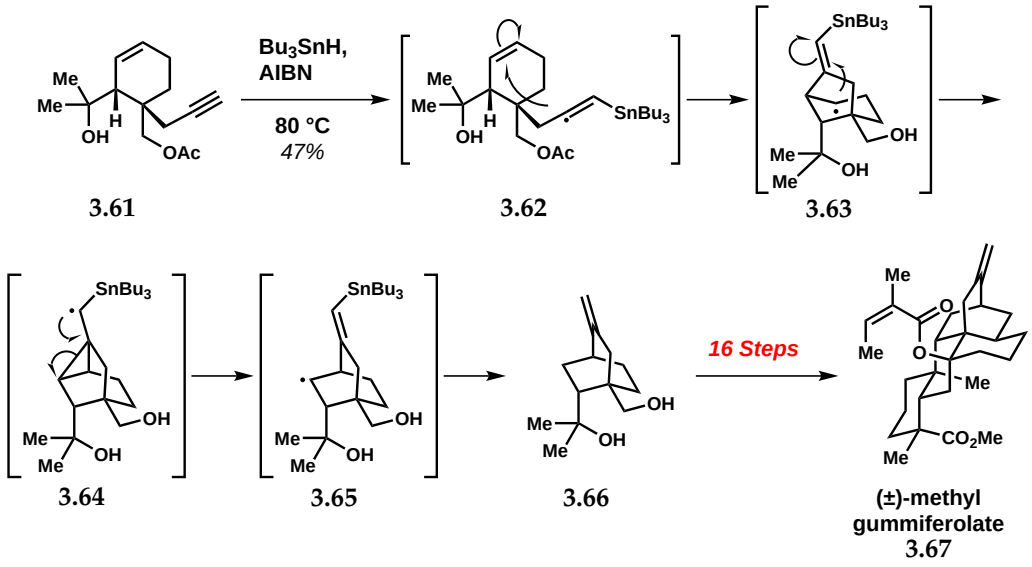

Scheme 3.12: Toyota's direct radical bicyclization *en route* to (±)-methyl gummiferolate.

The excellent regiocontrol seen in their radical rearrangements motivated the Toyota group to employ a direct radical bicyclization reaction in their synthesis of (±)-methyl gummiferolate (**3.67**, **Scheme 3.12**). Treatment of alkyne **3.61** with tri-*n*-butyltin hydride and AIBN at elevated temperature resulted in radical addition of the tri-*n*-butylstannyl radical to the alkyne to give the reactive vinyl radical **3.62**. While **3.62** may undergo direct 6-*exo*-trig cyclization to give the [2.2.2]-bicyclic radical **3.65**,

Toyota's earlier studies with other alkene isomers of **3.61** demonstrated that 1,5-hydrogen atom abstraction occurs faster than 6-*exo*-trig cyclization. As a result, it is likely that the vinyl radical **3.62** instead underwent the kinetically faster 5-*exo*-trig radical cyclization to give the [3.2.1]-bicyclic radical **3.63**. A 3-*exo*-trig cyclization gave cyclopropyl radical **3.64**, which underwent cyclopropane fragmentation to give the [2.2.2]-bicyclic radical **3.65**. The radical chain reaction was then propagated by hydrogen atom abstraction from another molecule of tributyltin hydride and mildly acidic work up with SiO_2 was sufficient to protonate the vinyl tin moiety to give bicycle **3.66** in 48% yield. Though this radical bicyclization is interesting, the relatively low yield is exacerbated by the 16 step sequence required to complete (±)-methyl gummiferolate (**3.67**).[45,46] A similar bicyclization strategy was employed by the Lee group in their synthesis of the platencin core,[47] while the Rawal group chose to approach the same disconnection *via* a nickel catalyzed 6-*exo*-Heck bicyclization reaction.[48] The Ghosh group avoided Toyota's low yielding radical cyclization by switching the radical donor and acceptor. Employing a cyclohexyl radical in a 6-*exo*-dig cyclization onto a pendant alkyne, the Ghosh group was able to close their bicyclooctane in 69% yield, though the Kaliappan group later reported only a 43% yield in a nearly identical transformation.[49,50]

3.4.3 Aldol strategies.

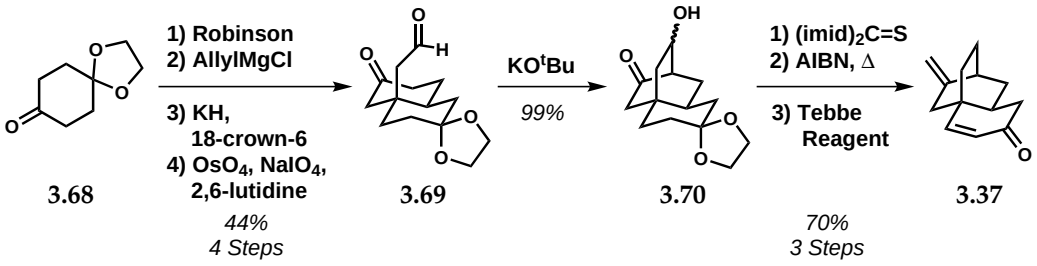

Scheme 3.13: Yadav's formal synthesis of platencin.

The efficiency of the Diels–Alder reaction and the ease of radical cyclizations has meant that relatively few groups have looked to aldol chemistry to install bicyclo[2.2.2]octanes. The relatively simple transformations employed by the Yadav

group allow them to intercept Nicolaou's platencin core **3.37** in eight steps (**Scheme 3.13**). Staring with protected diketone **3.68** a sequence of Robinson annulation, 1,2-addition of allyl Grignard, anionic oxy-Cope, and Johnson–Lemieux–Jin oxidation gave aldehyde **3.69**. Exposure to potassium *tert*-butoxide gave bicycle **3.70** as a diastereomeric mixture of alcohols which was immediately resolved *via* Barton–McCombie deoxygenation. Tebbe olefination of the resultant ketone and hydrolysis of the dioxolane in acidic work up gave **3.37** in 30% overall yield from ketone **3.68**.[51,52]

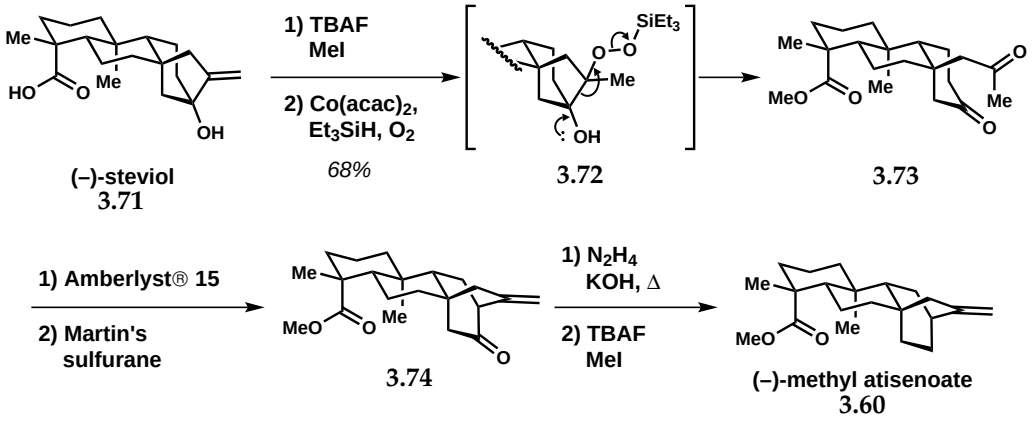

Scheme 3.14: Baran's semi-synthesis of atisane diterpenes.

The Baran group's work to create a unified approach to atisane and kaurene diterpenes represents the most centralized and modular synthesis of these classes of natural products (**Scheme 3.14**).[53] Starting from the readily available natural product (–)-steviol (**3.71**), methylation of the carboxylic acid followed by Mukaiyama hydration gave diketone **3.72**, likely *via* fragmentation of a peroxysilyl ether such as **3.73**.[54] Aldol addition using Amberlyst® 15 acidic resin followed by a well established dehydration with Martin's sulfurane gave bicycle **3.74**. Wolff–Kishner reduction and reinstallation of the methyl group gave (–)-methyl atisenoate (**3.60**) in 38% overall yield.

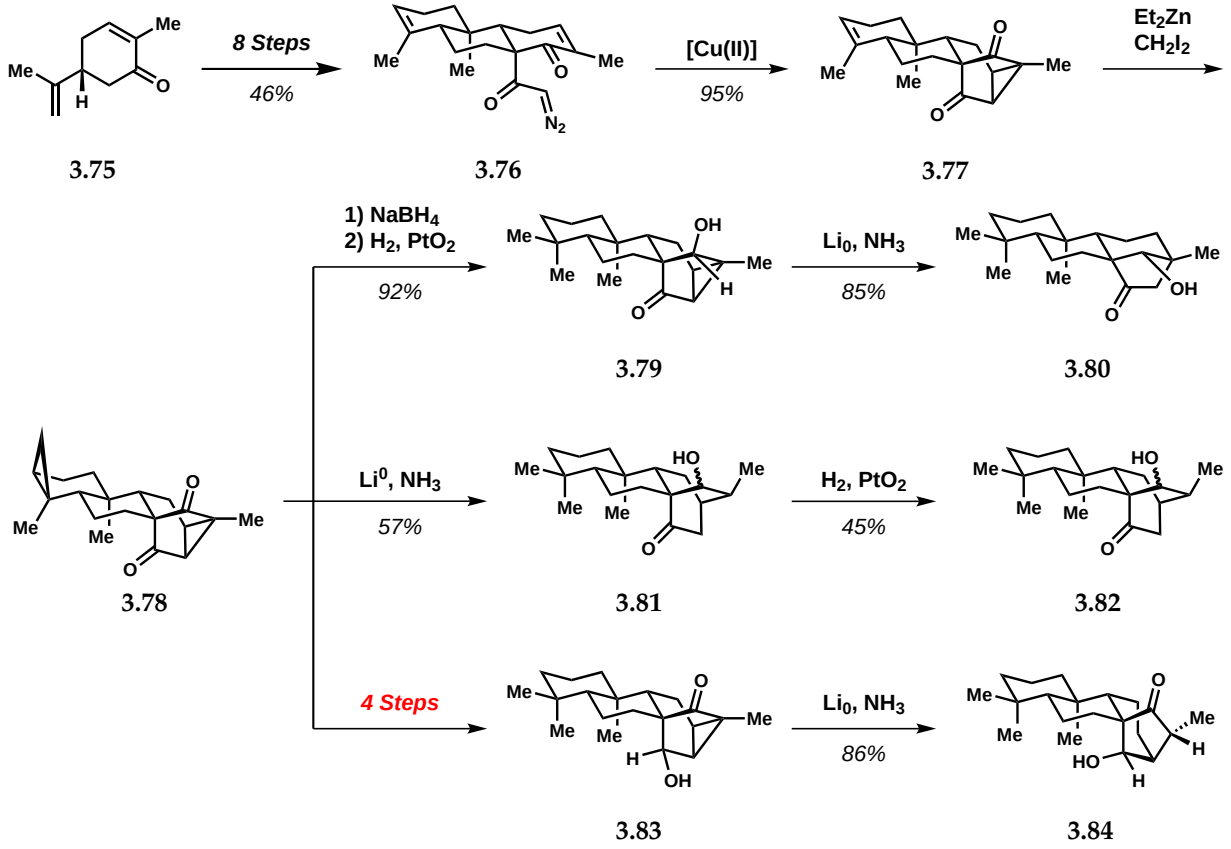

Scheme 3.15: The Abad group's unified strategy employs a carbene to access the trachylobane scaffold.

3.4.4 Miscellaneous strategies.

The Abad group pursued a unique carbene cyclization to access the *ent*-trachylobane and then demonstrates mastery of dissolving metal reductions, cleaving each bond in the trachylobane tricycle selectively to give *ent*-beyerane, *ent*-atisane, and *ent*-kaurane diterpenes.[55,56] Starting from (–)-carvone (**3.75**) and borrowing Toyota's intramolecular Diels–Alder strategy[40] to close their decalin ring, the Abad group generated α-diazo ketone **3.76** in eight steps. Exposure of diazo compound **3.76** to Cu(II) formed the copper carbene that cyclopropanated the pendant enone, giving diketone **3.77**. Further cyclopropanation of the remaining olefin of **3.77** forged the final carbon-carbon bond of the trachylobane scaffold to give the key bis-cyclopropane **3.78**. Sodium borohydride reduction of **3.78** was found to be regioselective for the doubly neopentylic ketone, while hydrogenation with Adam's catalyst regioselectively

reduced the alkyl cyclopropane in the presence of the cyclopropyl-diketone to give trachylobanol **3.79**. Dissolving metal reduction of **3.79** regioselectively formed the beyeranyl bicyclo[3.2.1]octane **3.80** in 85% yield.

Meanwhile, exposure of **3.78** to dissolving metal reduction regioselectively opened the cyclopropyl-diketone to give a bicyclo[2.2.2]octane **3.81**. Hydrogenation with Adam's catalyst then gave atisanol **3.82** as a 2:1 mixture of alcohol diastereomers. Having selectively fragmented two of the bonds of the trachylobanyl cyclopropane, the Abad group subjected diketone **3.78** to a four step sequence to switch the oxidation states in **3.79**, furnishing isomer **3.83**. Once more subjecting their material to a dissolving metal reduction, the Abad group selectively fragmented the cyclopropane of **3.83** giving the bicyclo[3.2.1]octane of the *ent*-kaurane family (**3.84**). While perhaps not the most efficient of syntheses, the Abad group demonstrated mastery in the understanding of cyclopropane electronics, regioselectively and sequentially reducing each bond of the cyclopropane **3.79** to provide a unified synthesis of four natural product families.[57,58]

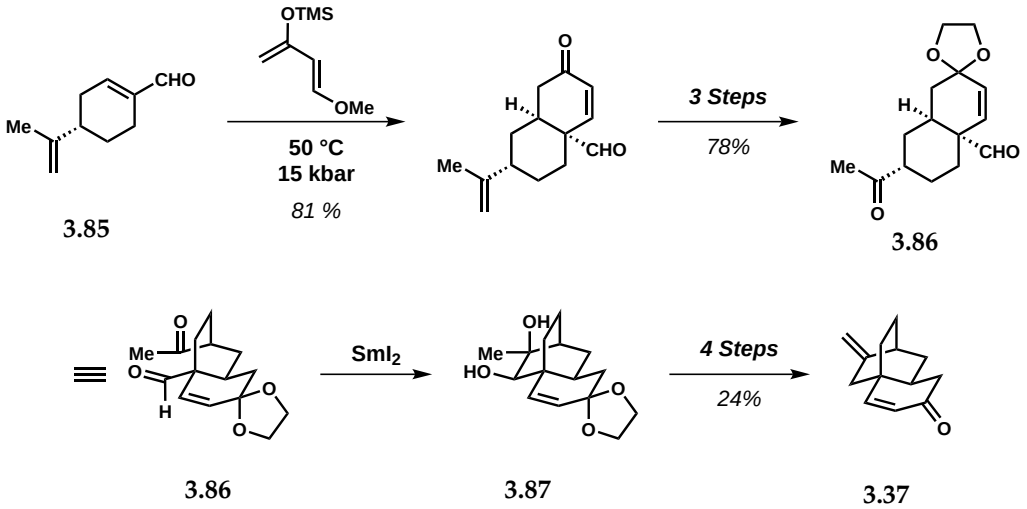

Scheme 3.16: Rutjes's formal synthesis of platencin.

The Rutjes group employed a samarium(II) iodide mediated pinacol coupling to complete their formal synthesis of platencin in nine steps by taking advantage of (–)-perillaldehyde (**3.85**) as a chiral starting material (**Scheme 3.16**). Diels–Alder

cycloaddition of Danishefsky's diene onto commercially available terpene **3.85** afforded the Rutjes group a rapid entry into platencin, setting all three stereocenters of the core in a single step. Protection of the aldehyde by olefination allowed selective protection of the unsaturated ketone as the dioxolane. Ozonolysis unveiled dicarbonyl **3.86**, which, on exposure to samarium(II) iodide readily underwent a pinacol coupling to give **3.87**. Deprotection of the ketone, acetylation of the secondary alcohol, dehydration of the tertiary alcohol with Burgess reagent, and de-acetylation *via* an allyl palladium complex gave the platencin core **3.37** in nine steps and 15% overall yield from **3.85**.[59]

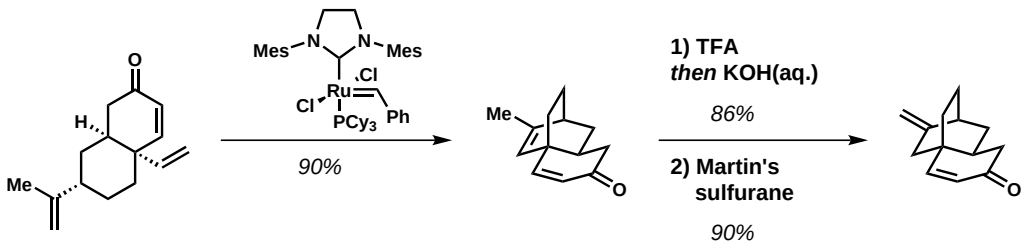

Scheme 3.17: The Mulzer group's rapid assembly of the platencin core.

While on par with work by Snider and Yadav, shorter than the syntheses by Nicolaou and Singh, and step-economical compared with Banwell's affair with the platencin core, the Rutjes group missed an opportunity to significantly shorten their formal synthesis of platencin (**Scheme 3.17**). Contemporaneously with the Rutjes group's work, the Mulzer group, pursuing similar inspiration, performed a Diels–Alder cycloaddition of Rawal's diene onto (–)-perillaldehyde (**3.85**) followed by Wittig olefination of the resultant decalin to give triene **3.88**. Treatment of triene **3.88** with Grubbs 2nd generation catalyst provided tricycle **3.89** in 90% yield. After extensively screening hydrohalogenation/elimination reactions, the Mulzer group found that hydration of alkene **3.89** *via* intermediacy of the trifluoroacetic acid ester and dehydration with Martin's sulfurane furnished the platencin core **3.37** in five steps and 38% overall yield, by far the shortest synthesis of the key tricycle.[60,61]

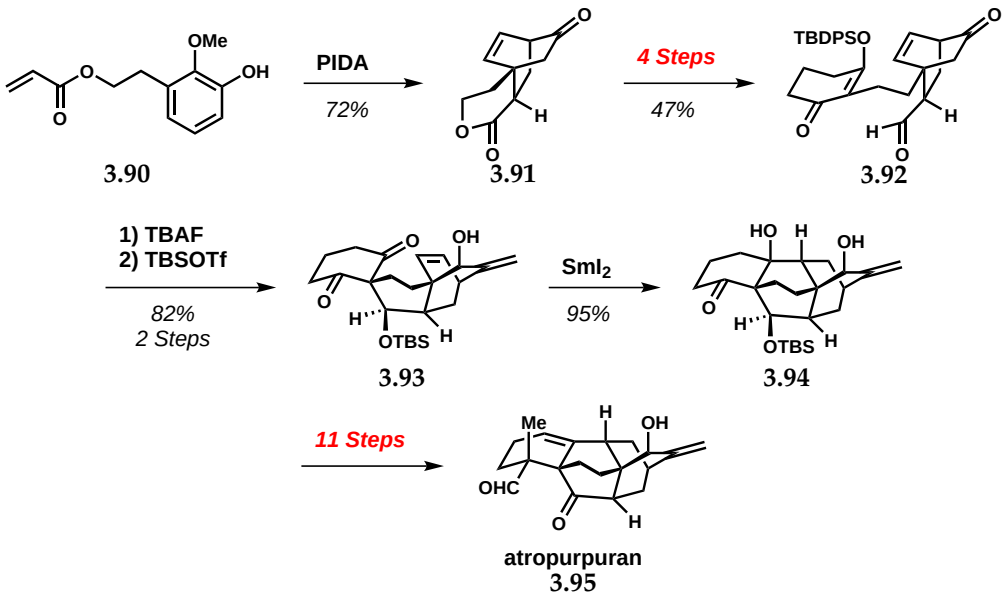

Scheme 3.18: First synthesis of an arcutane diterpene.

Gong, Chen, and Liu have completed the first synthesis to date of an arcutane diterpene **Scheme 3.18**.[62] The caged structure of atropurpuran (**3.95**) is a synthetic challenge for which the Gong group employed three different bicyclization strategies. Phenol **3.90** was subjected to oxidative dearomatization, forging bicyclo[2.2.2]octane **3.91** *via* an inverse electron demand Diels–Alder in 72% yield. In a four step synthesis lactone **3.91** was hydrolyzed, reduced, and condensed with 2,3-cyclohexanedione to give tricarbonyl **3.92**. Cleavage of the enoxysilane protecting group resulted in a Knoevenagel condensation of the dione moiety with the proximal aldehyde which, following TBS protection, gave spirocycle **3.93**. Having set the majority of desired stereocenters of the polycyclic framework, the Gong group's samarium(II) mediated 6-*exo*-trig radical cyclization benefited from the sterically hindered nature of spirocycle **3.93**, forming the arcutane core **3.94** in 92% yield. While the pentacycle **3.94** was synthesized effectively, the Gong group's synthesis does suffer from the extensive late stage functional group manipulation that was necessary to install the final two carbon atoms and properly set oxidation patterns. Nonetheless, the Gong group's synthesis works as an excellent review of bicyclization strategies. Whereas some syntheses make a point of showcasing

a single transformation, the Gong group flexibly used the tools at hand to rapidly build up the atropurpuran core.

3.5 Synthesis of (+)-crotogoudin by the Carreira group.

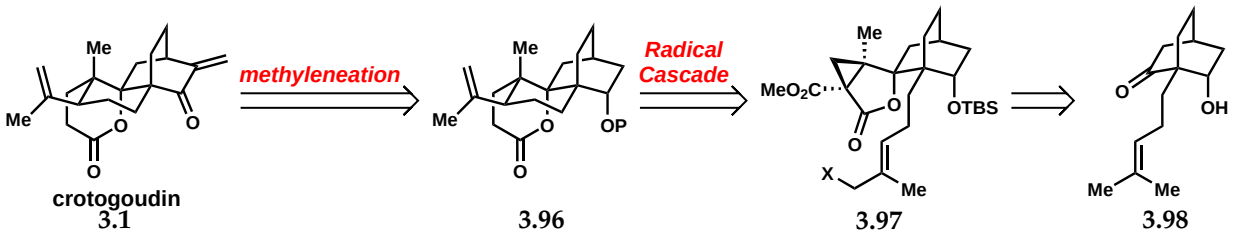

Scheme 3.19: Carreira's retrosynthetic analysis of (+)-crotogoudin.

The first synthesis of crotogoudin (**3.1**) was reported in 2013 by Carreira and Breitler.[14] Rather than attempt a late stage formation of the sterically encumbered bicyclo[2.2.2]octane, the Carreira group envisioned disconnecting the C6–C7 (von Baeyer numbering, **3.3**) bond of *seco*-*nor*-atisane **3.96** *via* a radical cascade which would terminate in formation of the C7 isopropylene. Spirocyclic lactone **3.97** would in turn be derived from *meso*-diketone **3.98** (**Scheme 3.19**).

Michael addition of β-ketoester **3.99** onto protected enal **3.100** followed by aldol condensation gave diene **3.101** in one pot (**Scheme 3.20**). The crude product was subjected to Krapcho decarboxylation, producing enone-aldehyde **3.102** in 60% yield over two steps. Deprotection of the benzyl alcohol *via* dissolving metal reduction also served to reduce the undesired alkene, giving diol **3.103**. Swern oxidation afforded ketoaldehyde **3.104** which underwent an aldol condensation to give bicyclooctane **3.105** as an inconsequential mixture of alcohol diastereomers. Finally, DMP oxidation produced *meso*-diketone **3.98** in 54% yield over four steps. Baker's yeast reduction was highly effective, desymmetrizing *meso*-diketone **3.98** to give the *endo*-alcohol **3.106** in 77% yield and >99% ee. Surprisingly, protection of alcohol **3.106** was found to prohibit nucleophile addition into the carbonyl. Reversing the order of operations, isopropenyl Grignard was added into ketone **3.106**. Diol **3.107** was isolated in 88% yield and

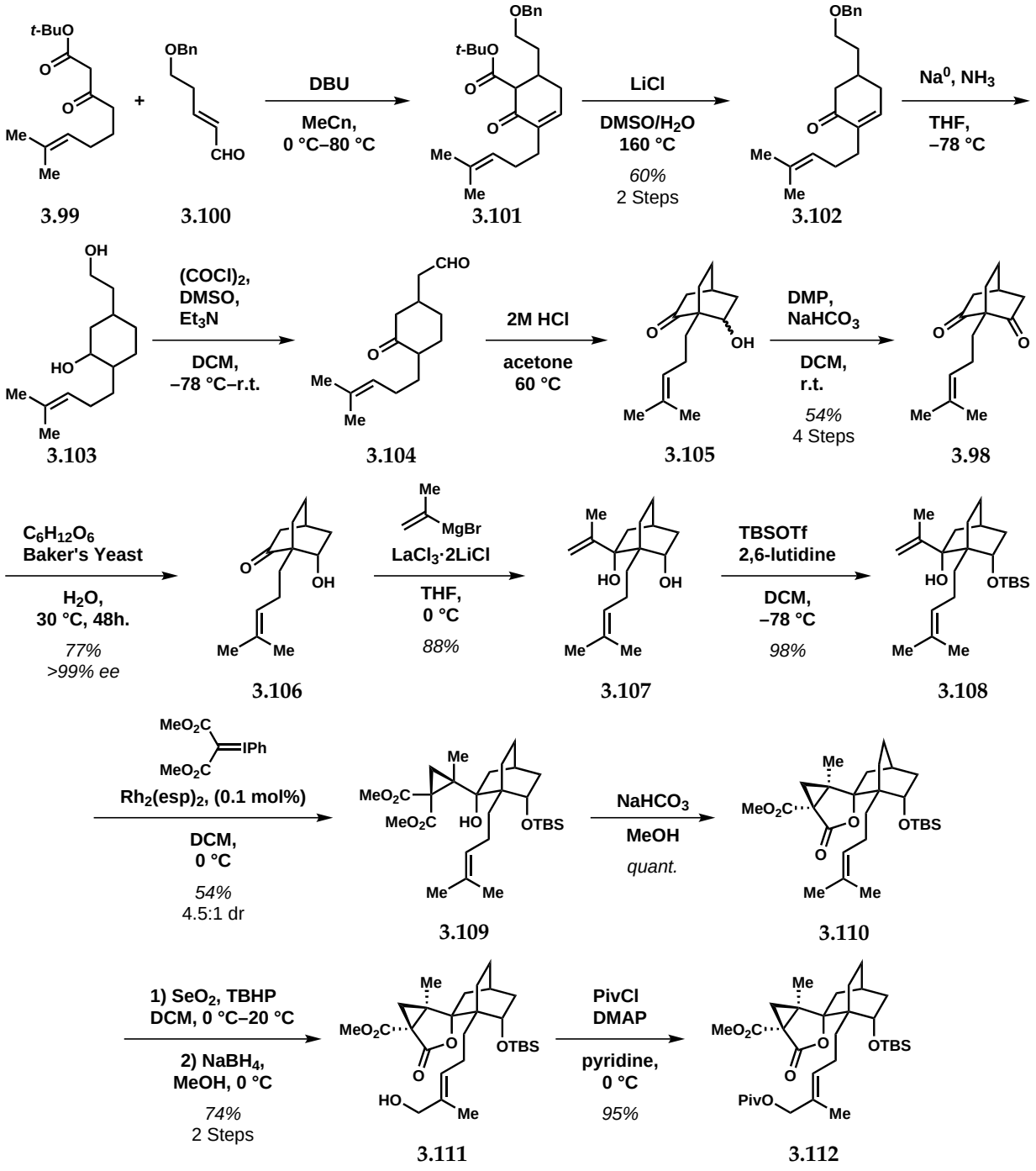

Scheme 3.20: Carreira's synthesis of the bicyclo[2.2.2]octane moiety of crotogoudin.

subjected to etherification with TBS-triflate, protecting the secondary alcohol in the presence of the tertiary in 98% yield (**3.108**). $Rh_2(esp)_2$ mediated cyclopropanation using the phenyl iodonium ylide of methyl malonate gave complete regiocontrol for the cyclopropanation of the less electron rich, disubstituted isopropylene in the presence of

the trisubstituted isoprenyl group. Having isolated the desired isopropyl diastereomer **3.110** in 54% yield from a 4.4:1 diastereomeric mixture of cyclopropanes, exposure of the diester to mildly basic conditions readily formed the key spirocyclic lactone **3.110**.

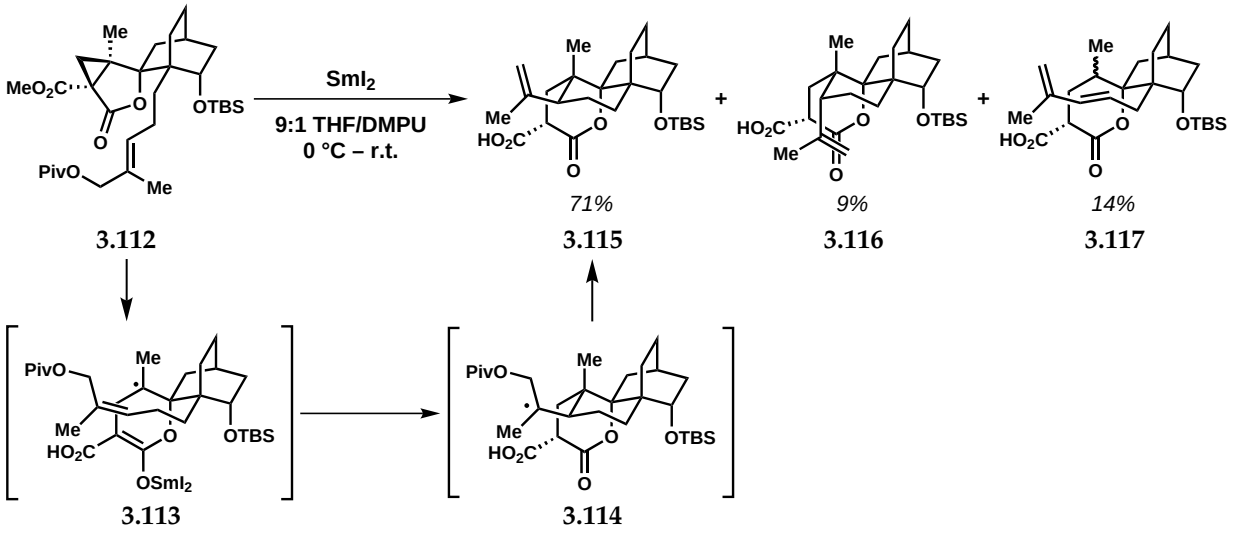

Scheme 3.21: Carreira's key radical cyclopropane fragmentation-cyclization cascade.

Attempts to effect the desired radical cascade cyclization on trisubstituted olefin **3.110** were proven ineffective, producing less than 10% of the desired isopropylene as well as the reduced isopropane product. The Carreira group thus resorted to installing a radical trap on the isoprenyl group in the hope of trapping out their desired cyclization product. Oxidation of the allylic methyl group to the methacrolein derivative was followed immediately by sodium borohydride reduction to allylic alcohol **3.111** in 74% yield over the two steps. Activation of the alcohol as the pivalate ester **3.112** proceeded in 95% yield, setting the stage for the desired radical cyclization (**Scheme 3.21**). Subjecting dicarbonyl **3.112** to samarium(II) iodide resulted in fragmentation of the cyclopropane, to give tertiary, neopentylic radical **3.116**. 6-exo-trig cyclization onto the activated isoprenyl group gave tertiary radical **3.117**. A second single electron reduction of **3.117** produced a tertiary anion that rapidly eliminated the adjacent pivaloyl group to give isopropylene **3.113** in 71% isolated yield. Despite the *syn*-pentane interaction, 9% of the *cis*-cyclized product was observed. 1,5-hydrogen atom abstraction of the allylic

proton in **3.116** further reduction of the allylic radical and elimination of the pivaloyl group produced side product **3.115** in 14% yield.

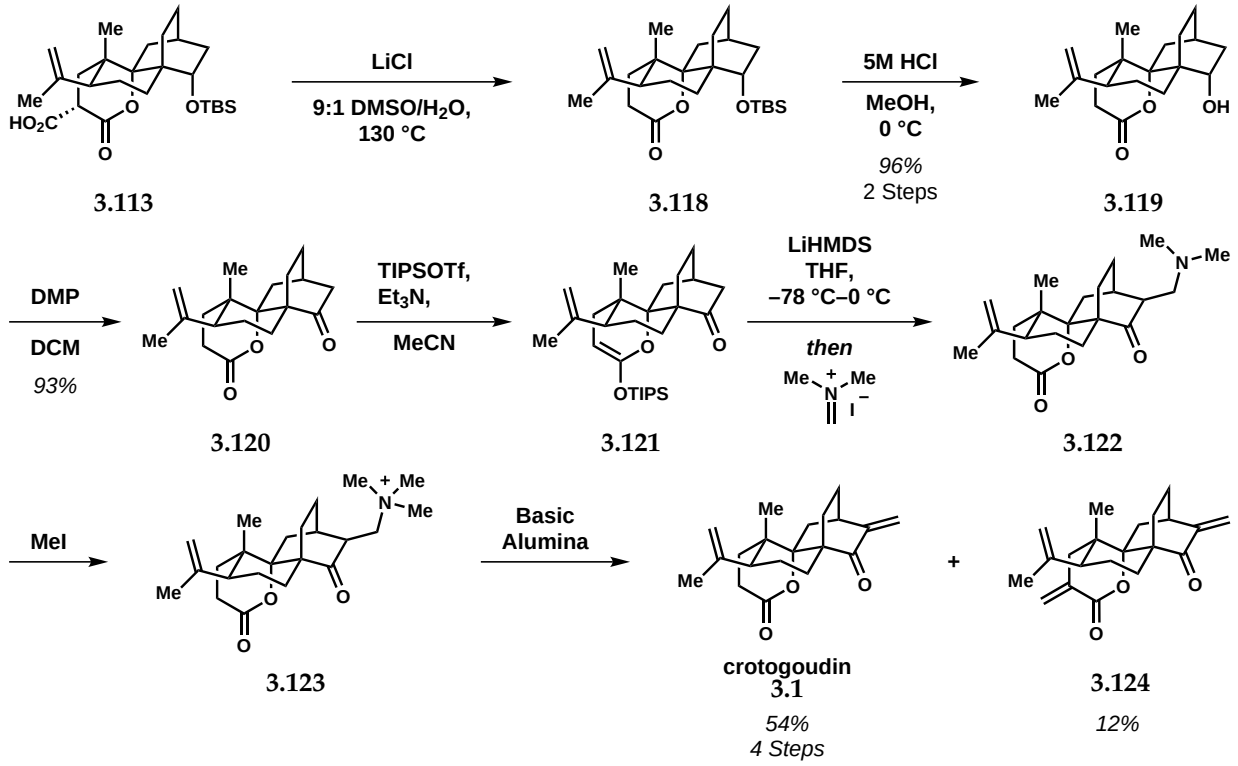

Scheme 3.22: Carreira's crotogoudin endgame.

With the *seco-nor*-atisane core of crotogoudin complete, Carreira's end game (**Scheme 3.22**) proceeded with Krapcho decarboxylation of the of spirocyclic lactone **3.113** and deprotection of the silyl ether **3.118** gave free alcohol **3.119** in 96% yield over two steps. DMP oxidation provided the ketone **3.120** in 93% yield; however, attempts at methylenation showed that the lactone of **3.120** underwent alkylation preferentially, likely due to the sterically hindered nature of the ketone enolate. Protection of the lactone as the TIPS enoxy-silane **3.121** followed by enolization with lithium hexamethyldisilazide and alkylation with Eschenmoser's salt gave dimethyl amine **3.122**. Methylation to the trimethyl ammonium salt **3.123** was followed by elimination on basic alumina to give crotogoudin **3.1** in 54% yield over four steps, or 2.8% overall yield and 22 steps from β-ketoester **3.99**.

Having completed the first synthesis of (+)-crotogoudin, the Carreira group was surprised to find that the optical rotation of their synthetic material ($[\alpha]_D^{20}$ = 20 (*c* +29.6, 0.4)$CHCl_3$) did not match that reported by Rasoanaivo ($[\alpha]_D^{20}$ = 20 (*c* +7, 0.40)$CHCl_3$). As bicycle **3.106** was desymmetrized in high ee and could not be racemized in following reactions, it was unlikely that Carreira's synthetic crotogoudin was a scalemic mixture. Reisolation of crotogoudin by the Rasoanaivo group allowed them to reassign the optical rotation to $[\alpha]_D^{20}$ = 20 (*c* −25.2, 0.4)$CHCl_3$. The natural configuration of crotogoudin was thus assigned to the common series of *ent*-atisanes. Overall, Carreira's synthesis featured an interesting desymmetrization reaction and a clever assembly of the C6-C7 bond *via* a radical cyclopropane fragmentation / cyclization cascade. Unfortunately the synthesis suffered from a high step count, a factor common to groups whose strategies involved early formation of the atisanyl bicyclo[2.2.2]octane. While far from poor, the native diastereocontrol provided by the bicyclic lactone was lacking, resulting in a total 40% loss of material as side products in the cyclopropanation and radical cyclization cascade steps. In addition, while protection of the lactone **3.119** as the TIPS enoxy-silane **3.121** allowed selective alkylation of the ketone enolate; however, the enoxy-silane remained an effective nucleophile, resulting in the formation of a doubly alkylated product, which led to the dimethylene **3.123** in 12% yield over the late stage four step methylenation.

3.6 Liu Synthesis of (±)-crotogoudin and (±)-crotobarin

In many respects, the Liu group adopted the same approach we ultimately pursued with a more biomimetic approach (**Scheme 3.23**). Observing that atisane and *seco*-atisane diterpenes are related by the oxidative cleavage of the atisane A-ring, the Liu group pursued the synthesis of crotogoudin starting with the alkylation of epoxy geranyl bromide **3.125** with the benzyllithium derived from 2,3-dimethoxytoluene **3.126**. Iron trichloride initiated cationic cascade cyclization of the resultant epoxide **3.127** gave the Liu group access to tricycle **3.128** in 39% over two steps. Though lacking three carbon atoms of the atisane framework, alcohol **3.128** is proposed to be a synthetic

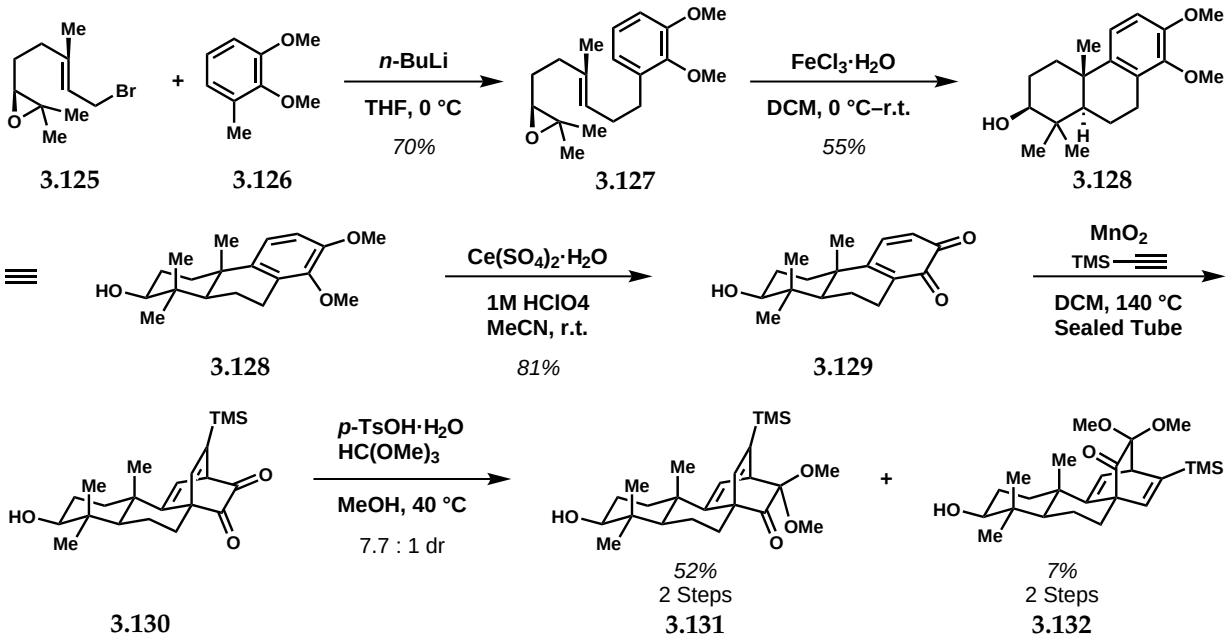

Scheme 3.23: Bicyclooctane formation in Liu's (±)-crotogoudin synthesis.

equivalent to the biosynthetic **3.6** cation intermediate. The Liu group is able to readily install the missing bicyclooctane bridge carbon atoms in a three step sequence. Oxidation of diether **3.128** with cerium(IV) sulfate gave orthoquinone **3.129** in 81% yield. Heating the electron poor diene **3.129** in the presence of TMS acetylene and manganese(IV)oxide provided the desired inverse electron demand Diels–Alder cycloaddition product **3.130** which was immediately protected as methylketal **3.131**.

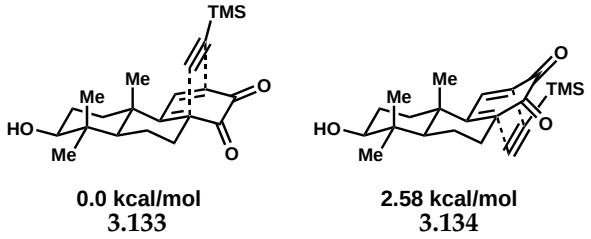

Scheme 3.24: M06-2X/6-31G(d,p) transition state energies for Liu's inverse electron demand Diels–Alder

Based on the structure of diene **3.130**, it is expected that the steric hindrance of the axial methyl group would bias the dienophile to approach from the bottom face of the molecule to give **3.132** *via* **3.134**. Surprisingly, isolation of the methylketal **3.131** showed a

7.7:1 dr favoring a *cis*- relationship between the newly installed bicyclooctane bridge and the axial methyl group (**3.131**), suggesting a late transition state. If that is the case, it is expected that to form bicyclooctane **3.132**, a large degree of the *syn*-pentane interaction would need to be built up between the axial methyl and the diketone. On the other hand, perturbations deflecting the ketone to the bottom face of the molecule would meet with less steric resistance and open a larger angle of approach for an incoming dienophile. Though this perturbation is not evident in the Liu group's computationally derived structures, gas phase calculations at the M06-2X/6-31G(d,p) level of theory showed transition state **3.133** to be over 40 kcal/mol lower in energy than the predicted alternative **3.134** (**Scheme 3.24**).

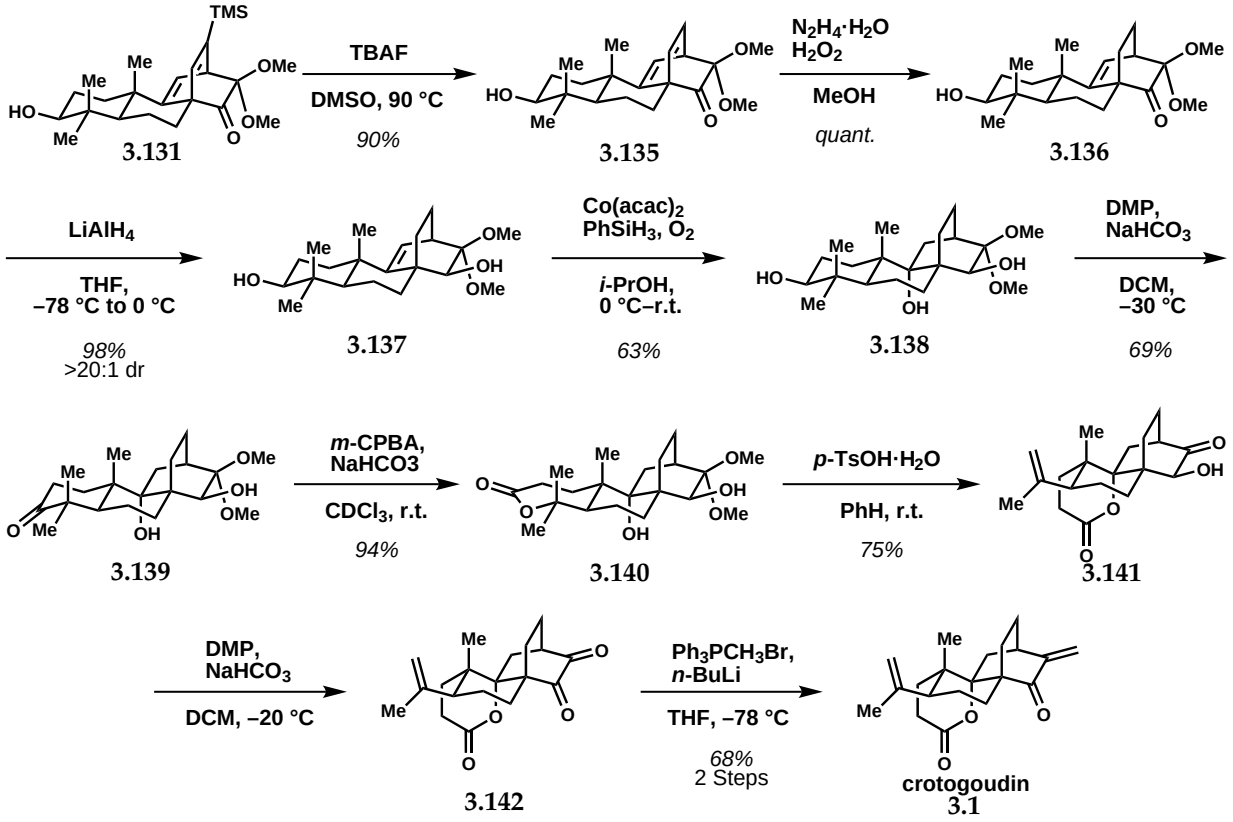

Scheme 3.25: Liu's crotogoudin end game.

Having constructed the bicyclo[2.2.2]octane atisane core, the Liu group's syntheses of crotogoudin and crotobarin diverged (**Scheme 3.25**). After removing the undesired

alkenyl TMS with TBAF, diazene reduction of diene **3.135** gave alkene **3.131** in 90% yield over two steps. Mukaiyama hydration using a cobalt(II) acetoacetate catalyst installed the tertiary alcohol **3.138** in 65% yield. DMP oxidation of the neopentyl alcohol **3.138** in the presence of the more sterically hindered alcohol of the bicyclooctane proceeded in 69% yield. Baeyer-Villiger oxidation to lactone **3.140** was followed by a tosic acid mediated one-pot E1 elimination, lactonization, and ketal deprotection to give *seco-nor*-atisane **3.141** in 71% yield over two steps. Learning from the difficulties faced by the Carreira group, Liu's group used a DMP oxidation of the remaining alcohol and a Wittig methylenation reaction to complete the synthesis of (±)-crotogoudin in 68% yield, or 3% yield over 14 steps from epoxy geranyl bromide.

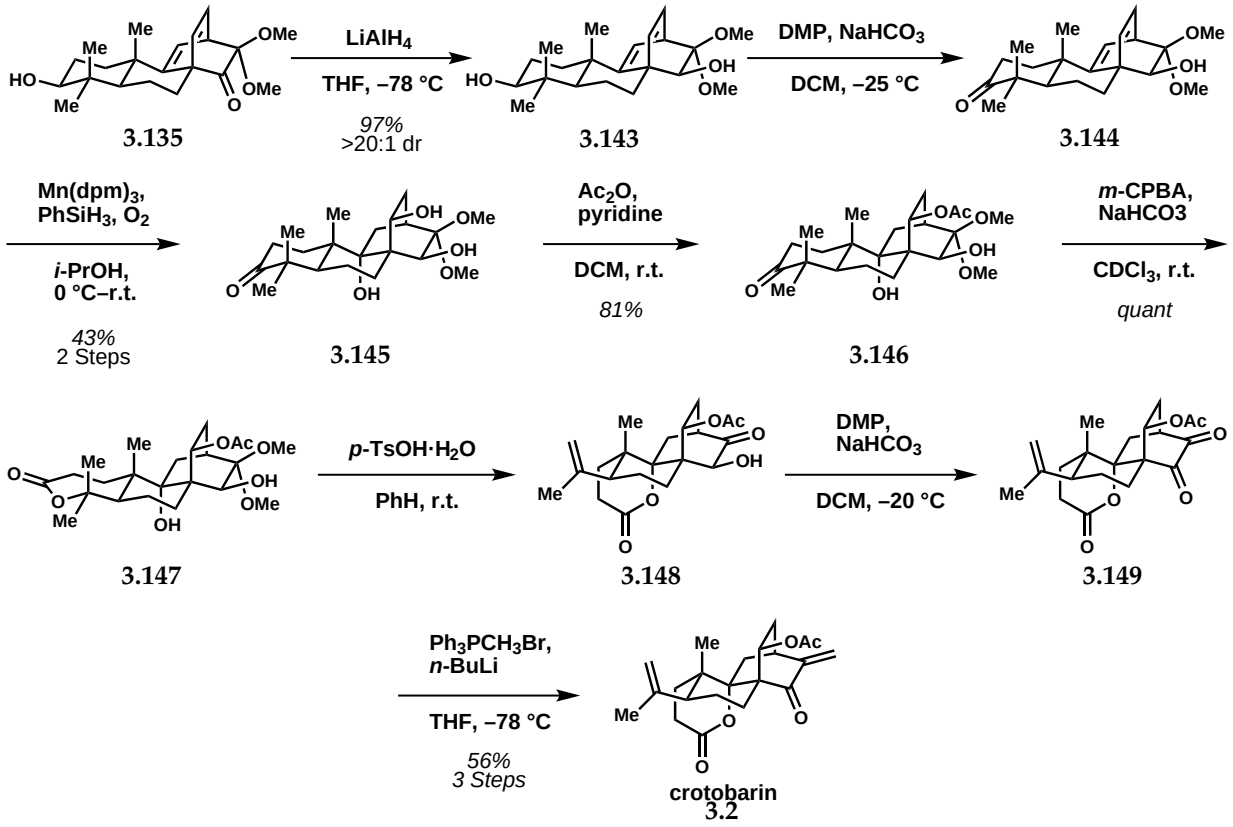

Scheme 3.26: Liu's crotobarin end game

While the construction of crotogoudin required the reduction of diene **3.135** to **3.136**, the synthesis of crotobarin benefited from the presence of the second alkene.

Reduction of ketone **3.135** in 97% yield followed by oxidation of the neopentylic alcohol **3.143** gave ketone **3.144** which was subjected to Mukaiyama hydration without purification. Hydration with a manganese(III) dpm catalyst gave diol **3.145** in 43% yield over two steps, with complete diastereocontrol. Acetylation of the less hindered secondary alcohol gave ketone **3.146** in 81% yield, installing the ester present in crotobarin and protecting the alcohol from further oxidation. Baeyer-Villiger oxidation followed by the same one-pot, tosic acid mediated E1 elimination, lactonization, ketal deprotection gave lactone **3.148** which was oxidized to diketone **3.149** and further methylenated to give crotobarin in 56% yield over four steps or 2.8% yield in 14 steps from geranyl bromide.

Of the two syntheses of crotogoudin, Liu's is by far superior. While the Liu group's synthesis was not enantioselective, it could easily be rendered so by the enantioselective installation of the epoxide of epoxy geranyl bromide *via* Sharpless asymmetric dihydroxylation of geranyl bromide followed by acid mediated epoxide closure. While Carreira's synthesis suffered from multiple moderately diastereoselective reactions, the Liu group's synthesis takes advantage of the known highly diastereoselective reactions performed on decalin and steroid scaffolds. Furthermore, though Carreira's Baker's yeast desymmetrization of *meso*-diketone **3.98** was well chosen and worked well with their reaction pathway, their key radical cyclization cascade can only be applied to *seco*-atisane diterpenes such as crotogoudin and crotobarin, while the Liu group's late stage fragmentation of the atisane A-ring potentially allows them entry into a wide variety of atisane diterpenes.

3.7 Efforts towards the synthesis of (±)-crotogoudin and a general synthesis of atisane diterpenes.

The Vanderwal group's synthetic efforts toward crotogoudin began with a high risk, high reward strategy (**Scheme 3.27**) which would, in a best case scenario give the skeleton of crotogoudin in a one-pot two step reaction. The crotogoudin methylene was

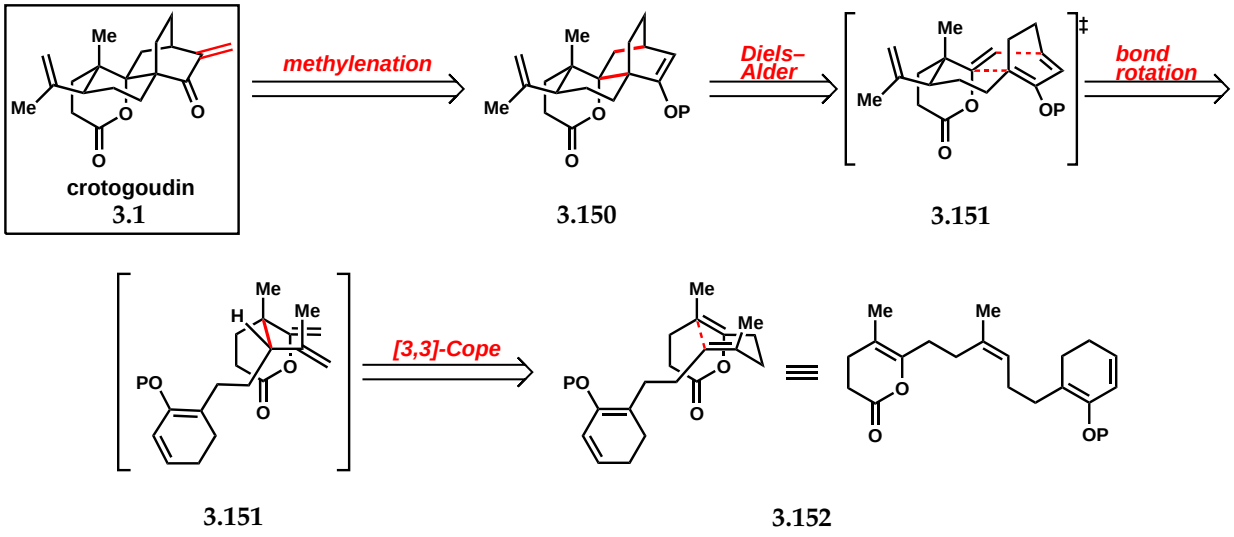

Scheme 3.27: Proposed one-pot assembly of the crotogoudin skeleton.

disconnected to give *seco-nor*-atisane **3.150**. An intramolecular Diels–Alder disconnection would give tetraene **3.151** which in turn would come from at [3,3]-Cope of enelactone **3.152**. While Dr. Peter Mai, the researcher originally working towards crotogoudin, was able to synthesize an enelactone such as **3.152**, the molecule was found to decompose on storage. Despite repeated attempts at the desired sigmatropic rearrangement/Diels–Alder sequence, no product of either reaction was observed. Calculations performed in collaboration with the Houk group showed that while our desired [3,3]-Cope was not impossible, there were several other reactions that had lower energy transition states and thus were more likely to happen.

3.8 A Biomimetic Approach

With the failure of the attractive yet risky one-pot polycyclization route, Dr. Mai proposed a biomimetic approach toward crotogoudin (**Scheme 3.28**). Dr. Mai's retrosynthesis called for bicyclooctane **3.153** to be synthesized from key enone **3.154** by any of a variety of methods, including double Michael addition or Diels–Alder cycloaddition. This key intermediate was proposed to come from the conjugate reduction of dienone **3.155**, which was the expected product of oxidative dearomatization performed on phenol **3.156**. The free acid of **3.156** was proposed to be

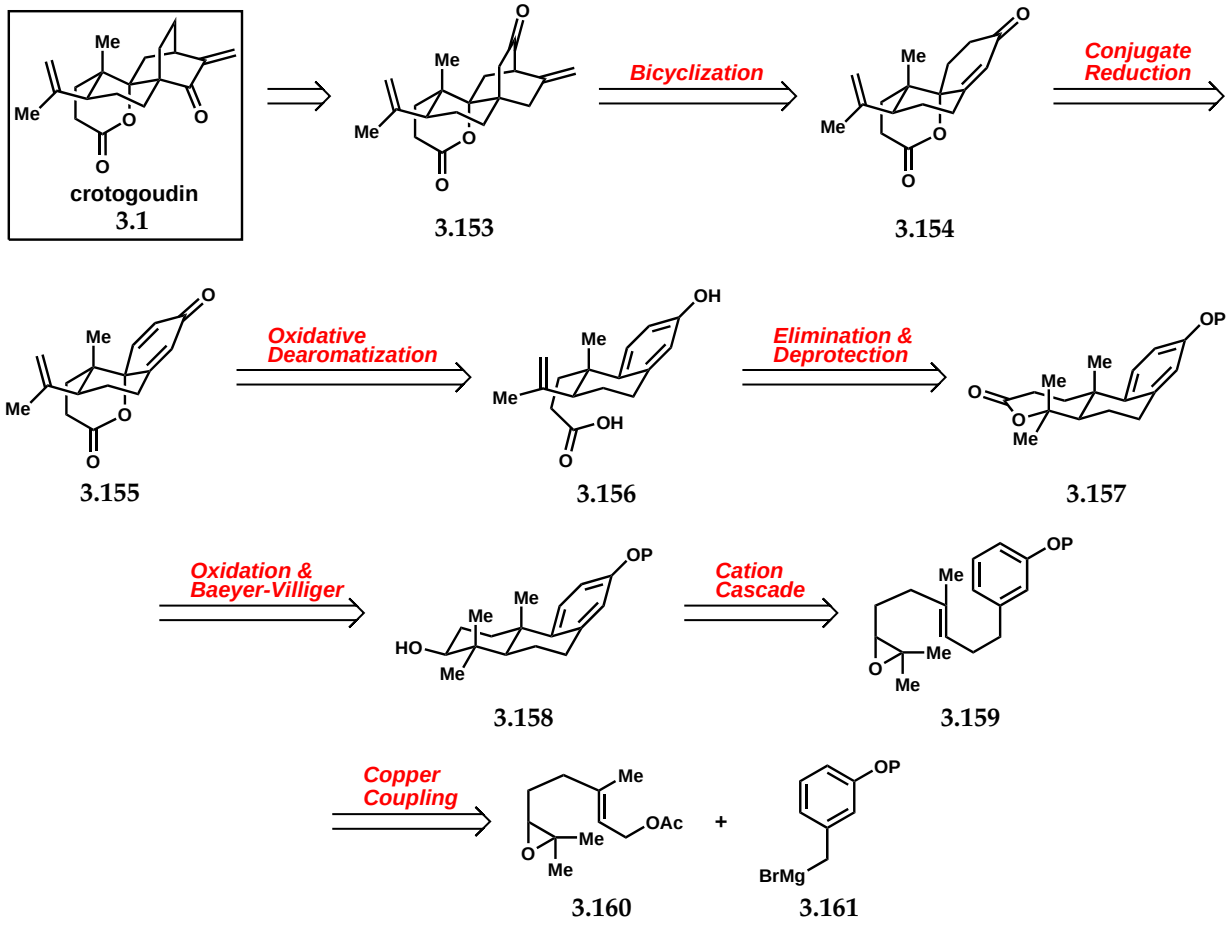

Scheme 3.28: Dr. Mai's retrosynthetic analysis of crotogoudin.

synthesized by a biomimetic sequence of oxidation, Baeyer-Villiger, and elimination from **3.158**. Tricycle **3.158** would be synthesized by well precedented cation cascade cyclization of epoxide **3.159** which, in turn, would be made by alkylation of epoxy geranyl acetate **3.160** with benzyl Grignard **3.161**.

In the forward sense (**Scheme 3.29**), TBDPS protected benzyl bromide **3.164** was obtained in three steps and 81% yield from 3-hydroxybenzaldehyde **3.162**.[63] Slow addition of the bromide **3.164** to excess magnesium metal in the presence of excess magnesium bromide diethyl etherate generated benzyl Grignard **3.166** with no observed dimerization due to Wurtz coupling. The allylic acetate of epoxy geranyl acetate **3.160** was displaced with the magnesium cuprate formed from Grignard **3.166** and Li_2CuCl_4 to give epoxide **3.167** in 67% yield.[64–66] Cation cascade cyclization with ethylaluminum

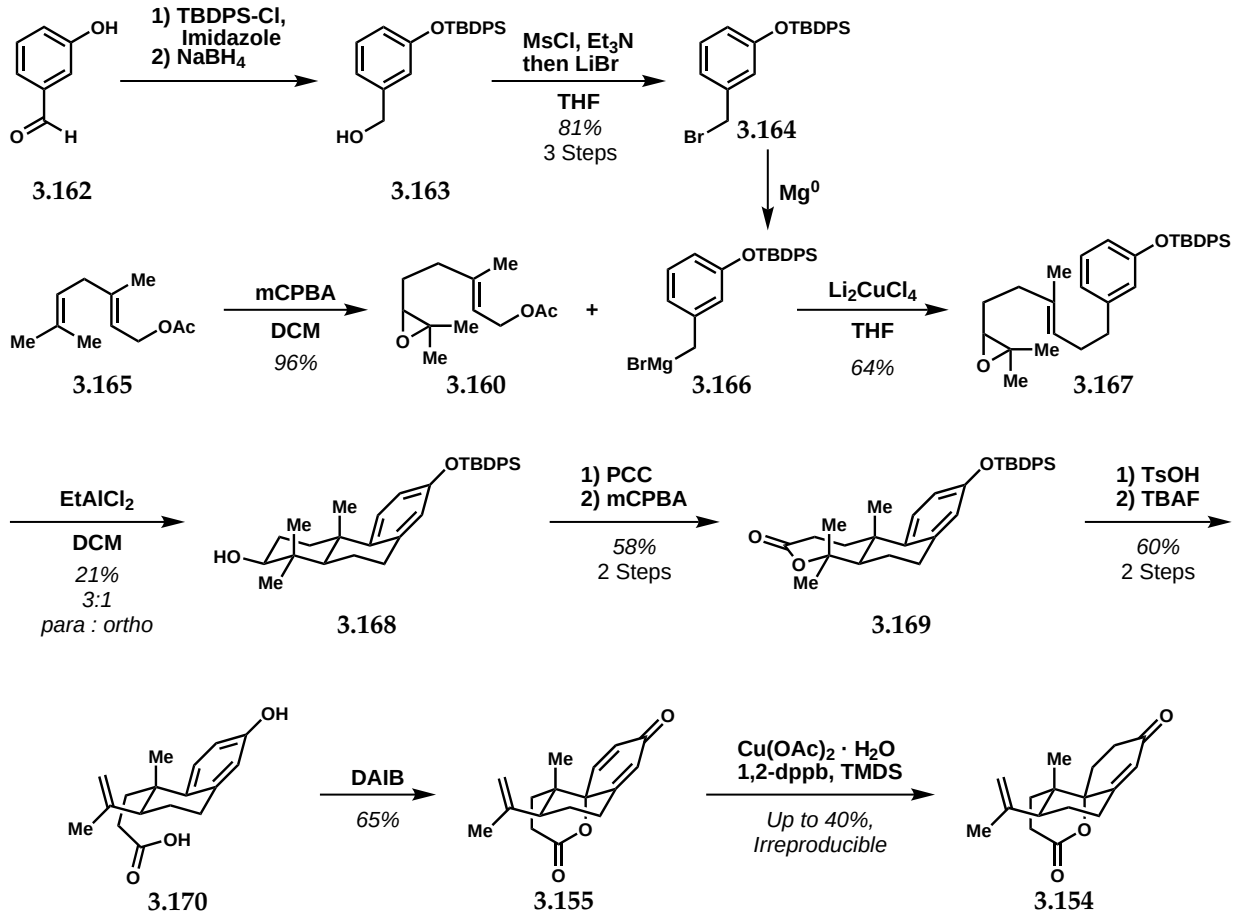

Scheme 3.29: A biomimetic approach to crotogoudin.

dichloride gave tricycle **3.168** in a rather disappointing 21% yield due to only a 3:1 selectivity for cyclization with the *para*-position versus with the *ortho*- position. This result is somewhat surprising as in several manuscripts, similar cation cascades have been carried out to high efficacy.[63,67] Disregarding, for the moment, the poor yield of the cation cascade, oxidation of alcohol **3.168** with pyridinium chlorochromate followed by Baeyer-Villiger oxidiation gave the seven memembered lactone **3.169** in 58% yield over two steps. Subsequent tosic acid mediated E1 elimination followed by deprotection of the TBDPS ether unveiled phenol **3.170** in 60% yield over two steps. Oxidative dearomatization with diacetoxyiodobenzene gave diene **3.155** in 65% yield.

3.9 Oxygen Dependence in Copper Hydride Reduction

Reduction of dienone **3.155** to enone **3.154** proved to be problematic. Despite many attempts at hydrogenation with various catalysts or conjugate reductions with copper hydride sources, all reactions were found to be ineffective or poorly selective, giving extensive over reduction. Stryker's reagent, for example, was found to be inactive toward dienone **3.155**; however, the "Hot Stryker's Reagent" reported by Lipshutz and coworkers gave some isolable enone product.[68]

Combining inexpensive copper(II) acetate with 1,2-bis(diphenylphosphino)benzene in the presence of polymethylhydrosiloxane, the Lipshutz group developed the new (BDP)-CuH reagent which was especially reactive in conjugate reduction reactions toward alkenes and alkynes activated by esters, ketones, aldehydes, or nitriles. While the Lipshutz group proposed the structure of (BDP)-CuH to be **3.171**, no characterization of the complex was attempted. Considering that copper(II) acetate is poorly soluble in the toluene used as the reaction solvent and that ten times more copper than ligand had been employed, it is not unreasonable to expect that the active hydride source may be bimetallic, polymeric, or heterogeneous in nature.

To this point, the synthesis was well precedented and reproducible. The low regiocontrol of the carbocation cyclization cascade limited the material throughput, but the irreproducibility of the conjugate reduction was the main stumbling block preventing us from pursuing the completion of crotogoudin. As such, when I took over the project from Dr. Mai, my first priority was to optimize or replace the dienone reduction. The conjugate reduction was irreproducible (**Table 3.2**, Entries 1-4) and could not be scaled up to provide adequate material to move forward efficiently. As the nature of (BDP)-CuH was unknown, optimization attempts would have to be based on experimentation alone. After carefully purifying all reagents, the reactants were loaded into a nitrogen filled glovebox for improved control over the reaction conditions. I was surprised to find that despite the care I had taken to ensure the purity of all reagents and

reactants, no product was observed from any conjugate reduction reactions performed in the glovebox (**Table 3.2**, Entry 5). Instead, the only observed products of the reaction were phenols, largely **3.170**. As this is an overall reduction of the dienone, I suspect that the desired conjugate reduction was occurring; however, under the reaction conditions it seems that the resultant enoxysilane undergoes an elimination reaction to give the more stable phenol or phenyl ether.

Table 3.2: Exploration of the oxygen dependence of Lipshutz's (BDP)-CuH conjugate reduction reaction.

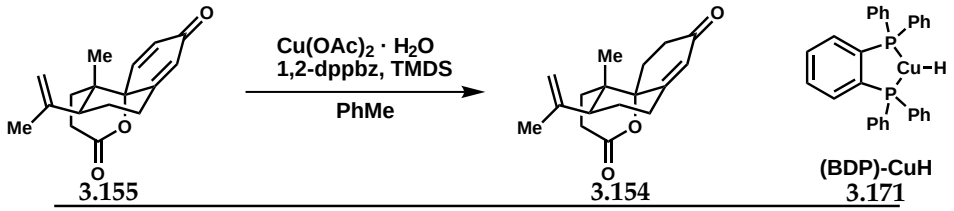

3.155 3.154 3.171

Entry	Conditions	%Pdt.	%ArOH[a]	%S.M.	Pdt.:S.M.	ArOH[a]:S.M.
1	Ar atm.	50	25	25	2	1
2	Ar atm.	59	12	29	2.0	0.4
3	Ar atm.	40	4	56	0.7	0.1
4	Ar atm.	59	35	6	9.8	5.8
5	Glovebox N_2 atm.	–	100	–	–	–
6	Stringently Degassed	–	100	–	–	–
7	Not Degassed	42	50	8	5.3	6.2
8	Ambient atm.	59	35	6	9.8	5.8

[a] ArOH refers to a combination of aromatic products, largely **3.170**.

As the (BDP)-CuH reduction reaction had worked previously, albeit in variable yield, it was surprising to find that I was obtaining only undesired side products after rigorously purifying all of the components of the reaction. To further explore this unexpected result, the Lipshutz's (BDP)-CuH conjugate reduction was repeated using stringently degassed solvents (**Table 3.2**, Entry 6). Again, only phenol products were observed suggesting that the reduction was followed by a rapid elimination reaction. Suspecting that perhaps a new batch of ligand or TMDS terminal reductant was at fault, I set out to reproduce my earlier results (Entries 1-4). To my amazement, when solvent

was used from the solvent system directly, without any further degassing, the (BDP)-CuH conjugate reduction again gave desired product (Entry 7). With only two data points, I could not say that I had an experimental trend, but on a whim, I ran the conjugate reduction in an open vial (Entry 8), providing the best yield of the desired enone **3.154** yet obtained. Considering the air sensitivity of Stryker's reagent, it seemed improbable that allowing ambient atmosphere into a conjugate reduction reaction would be in any way beneficial;[69] however, another data point could be readily obtained.

Table 3.3: Attempts to optimize (BDP)-CuH reduction under oxygen atmosphere.

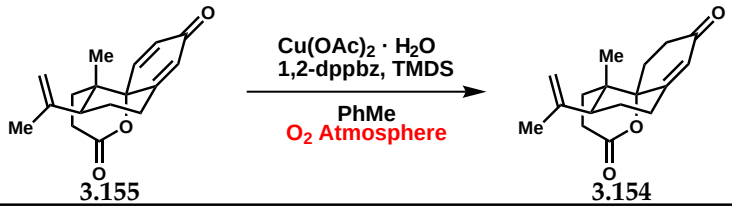

3.155 3.154

Entry	Conditions	%Pdt.	%OR[a]	%S.M.	Pdt.:S.M.	OR[a]:S.M.
9	O_2 atm.	42	4	54	0.8	0.1
10	4% Ligand	48	9	43	1.1	0.2
11	Continuous TMDS Addn.	40	5	55	0.7	0.1
12	Continuous Reagent Addn.	59	35	6	9.8	5.8
13	Batch-wise Reagent Addn.	88	3	9	9.8	0.3

[a] OR refers to over reduced ketone product obtained *via* a conjugate reduction of **3.154**.

(BDP)-CuH was complexed under argon and the atmosphere was exchanged for pure oxygen prior to the addition of dienone **3.155** (**Table 3.3**, Entry 9). After workup, the crude extract of this reaction mixture contained the desired enone **3.154** in approximately a 1:1 ratio with unreacted starting material as well as a small amount of over reduced product, but no phenol side-products were observed. This reaction was readily reproducible, but was found to stall after about two hours at 50% conversion. In an attempt to recover reactivity, experiments were conducted introducing secondary batches of each reagent separately, but no further conversion was observed. Increasing the ligand load of the reaction (Entry 10) gave a slightly higher conversion, but doubled

the amount of over reduction observed. Continuous addition of TMDS *via* syringe pump did not improve the conversion of the reaction, but did again increase the amount of over reduced product obtained. Continuous addition of a toluene solution of precomplexed (BDP)-CuH increased the reaction conversion significantly, but was deemed ineffective as over thirty percent of the obtained product was over reduced and the chromatographic separation of ketone from enone was unsuccessful. Of all attempts to break past the 50% conversion barrier, the most successful was the batch-wise addition of reagents, which gave conversion on par with continuous addition of (BDP)-CuH without increased over reduction; however, this method could not be readily reproduced.

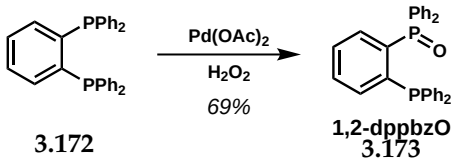

3.172 **1,2-dppbzO 3.173**

Scheme 3.30: Palladium catalyzed monooxidation of 1,2-dppbz

One possible role of oxygen in the (BDP)-CuH reaction was the oxidation of 1,2-dppbz **3.172** to the *bis*-phosphine monooxide 1,2-dppbzO **3.173** ligand, which would have a different bite angle, different electronics, and a therefore result in a copper complex with different reactivity. The monooxidation of 1,2-dppbz is known,[70] and was readily reproduced to give 1,2-dppbzO **3.174** in 69% yield (**Scheme 3.30**). Following the same procedures as those used for **Table 3.2** Entry 6, conjugate reductions were set up using stringently degassed solvents and reagents. Reactions were run under argon to avoid any unexpected oxygen inclusion. Under the standard reaction conditions (Entry 16), I observed successful production of enone **3.154**, but only at half the conversion of the analogous reaction with 1,2-dppbz ligand (Entry 9). Increasing the ligand load five fold (Entry 17) increased the conversion by a factor of two, but resulted in an increase in over reduction. Hoping that reducing the relative concentration of TMDS would slow

the over reduction while the increased ligand load would allow for continued conjugate reduction, the reaction was repeated with a five fold dilution (Entry 18). As may have been expected, the increased dilution slowed both the desired conjugate reduction and the over reduction, returning to the 25% conversion of Entry 16. While these experiments did not provide the solution for a selective, high yielding conjugate reduction reaction, the fact that the *bis*-phosphine monooxide ligand supports the desired reaction and does not result in the formation of phenols strongly suggests that this reagent is important to the observed (BDP)-CuH reduction under oxygen atmosphere. The fact that the conversion in this case is only half that observed with the 1,2-dppbz ligand demonstrates that there are more complicating factors that we have not addressed.

Table 3.4: Conjugate reductions using 1,2-dppbzO ligated CuH.

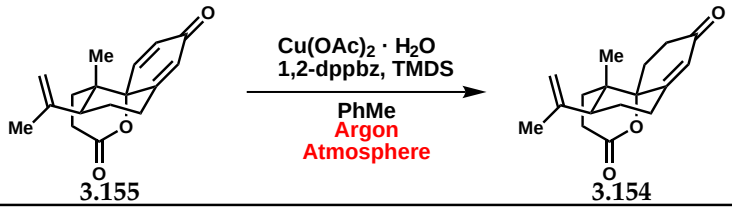

3.155 3.154

Entry	Conditions	%Pdt.	%OR[a]	%S.M.	Pdt.:S.M.	OR[a]:S.M.
16	2% 1,2-dppbzO	21	4	75	0.3	0.1
17	10% 1,2-dppbzO	53	11	37	1.4	0.3
18	10% 1,2-dppbzO diluted 5x	22	4	74	0.3	0.1

[a] OR refers to over reduced ketone product obtained *via* a conjugate reduction of **3.154**.

Over the course of many experiments it was observed that conversion and over reduction increased proportionally to each other. As such it was in some ways beneficial that the conjugate reduction stalled at a point where a significant amount of product had formed, but little over reduction had yet occurred. Unlike the over reduced ketone and enone **3.154**, the dienone **3.155** and enone **3.154** were readily separable by column chromatography, and the recovered starting material could be recycled to produce more of the desired enone **3.154**. Unfortunately, while the reaction was readily reproducible on the 10 mg scale, increasing the scale of the reaction three fold resulted in

irreproducibility. As starting material could be recycled and the reaction could be readily set up in multiple batches, optimization of the scaled up reaction was put off until the route to crotogoudin had been established.

3.10 Simple Ketones in Manganese Mediated Radical Cyclization

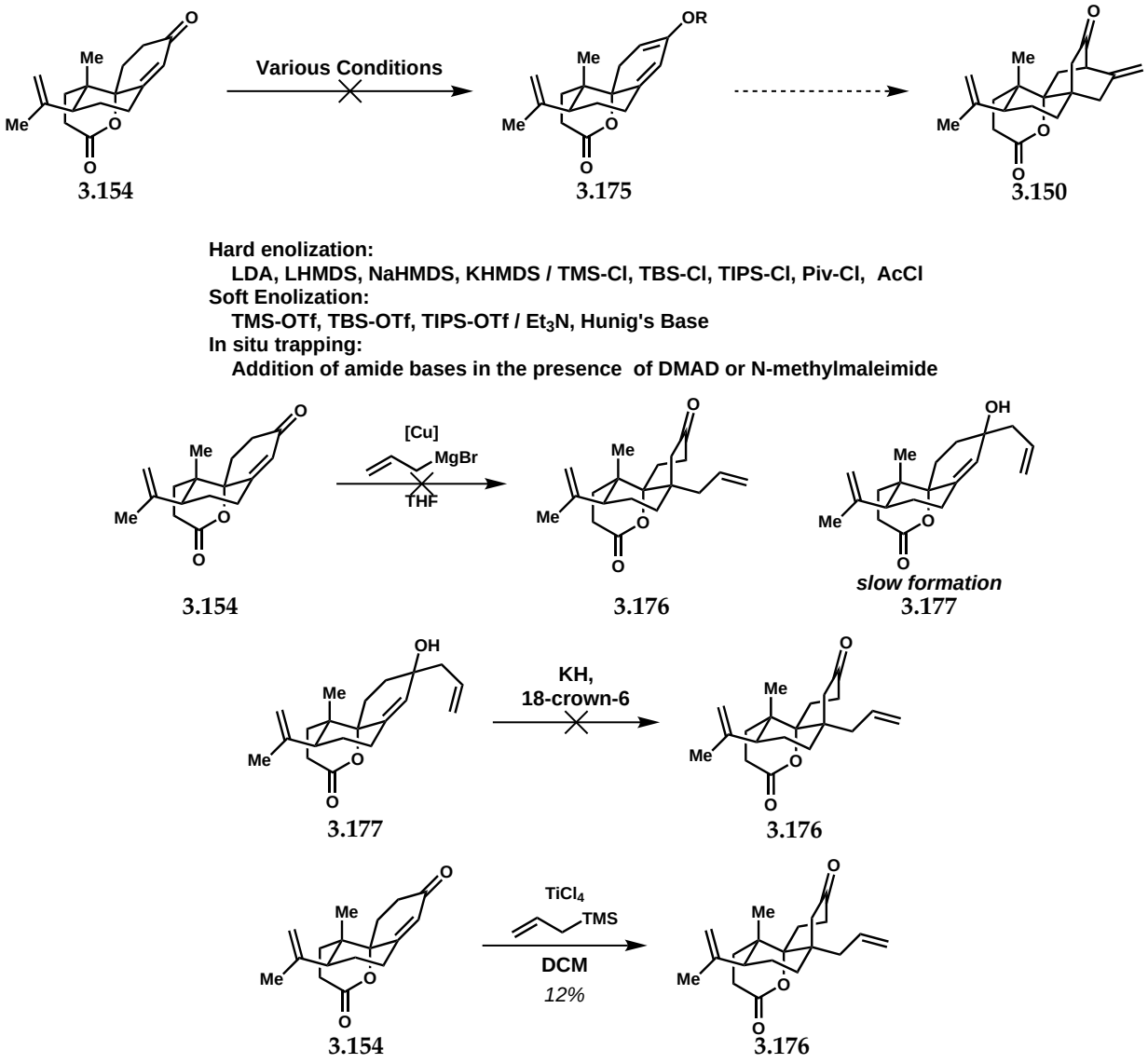

Scheme 3.31: Attempts at functionalization of enone **3.154**.

Having improved, though not solved, the problem of conjugate reduction with (BDP)-CuH, our next challenge was to perform a bicyclization to form the bicyclo[2.2.2]octane core of crotogoudin. Having installed the majority of the

crotogoudin framework we anticipated challenges inherent to the introduction of the *syn*-pentane interaction between the axial methyl group and the bicyclooctane bridge. Our first approach was to pursue a Diels–Alder disconnection by activating enone **3.154** as the dienolsilane **3.175**; however, neither hard nor soft enolization conditions with a variety of bases, silylchlorides, silyltriflates, and acid chlorides gave any desired product (**Scheme 3.31**). Instead, what we once again observed, aside from decomposition, was the expulsion of the spirocyclic lactone and formation of phenol **3.170**. As mentioned previously, we have proposed that this elimination occurs on the enolate or enol ether generated from **3.154**. As such, we attempted to trap this enolate *via* addition of DMAD or *N*-methylmaleimide after deprotonation, but to no avail. Furthermore, copper or cuprate catalyzed conjugate addition reactions failed to attack the sterically hindered trisubstituted enone alkene, though allowing the reaction to warm resulted in a slow 1,2-addition to the carbonyl.[71–78] Following the reactivity seemingly native to the molecule, we attempted an anionic oxy-cope [3,3]-sigmatropic rearrangement of doubly allylic alcohol **3.177**;[79–81] however, exposing doubly allylic alcohol **3.177** to potassium hydride and 18-crown-6 ether and slowly elevating the temperature resulted in eventual decomposition without observing any of the desired ketone **3.176**. Of the vast array of reactions attempted, only one gave any positive result. The Sakurai allylation of enone **3.154** with titanium tetrachloride and allyltrimethylsilane at room temperature gave ketone **3.176** in 12% yield.[82–85] We were excited by this observation since soon after obtaining this result, the Baran group published a synthesis of *ent*-kaurane diterpenoids in which they noted that in an attempt to make an analogous substrate, "…attempts to form this quaternary center failed, including: copper-, indium-, and tin- mediated 1,4-additions, Sakurai and Keck allylations, as well as intramolecular bond formations through sigmatropic rearrangements."[86] It certainly seemed like our system was favoring attack on the sterically hindered enone, perhaps due to a directing effect from the spirocyclic lactone moiety.

Obtaining small amounts of ketone **3.176**, we attempted a variety of reactions to close the second bond of the bicyclooctane; however, neither transition metal catalyzed rearrangements nor attempts at ene-reactions gave the desired product.[87–90] I found inspiration from the Snider group's work on manganese(III) mediated radical bicyclization reactions (**Scheme 3.32**).[91,92] Manganese(III) acetate abstracts a hydrogen atom α to the carbonyl **3.178**, providing a free radical enolate **3.179** which undergoes a reversible 6-*endo*-trig radical cyclization to give the more stable tertiary radical **3.180** which can perform a 5-*exo*-trig cyclization onto the pendant olefin to give primary radical **3.181**. Though **3.181** is the least stable of these intermediates, it is also most

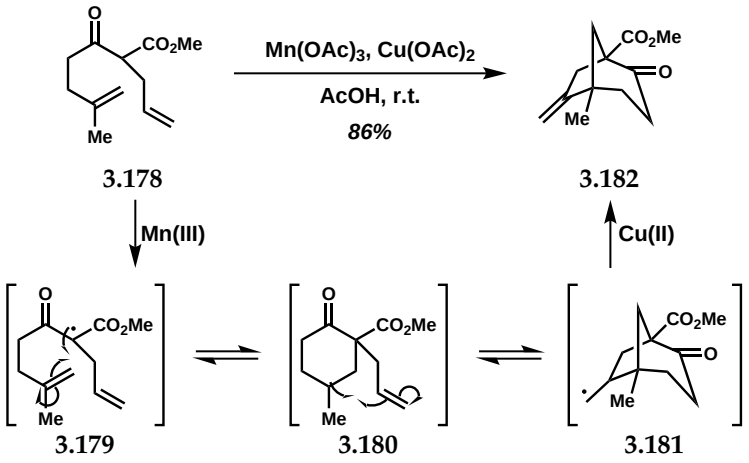

Scheme 3.32: Mn(III) mediated radical bicyclization reaction by Snider

reactive. *In situ* oxidation of radical bicycle **3.181** with copper(II) salts followed by β-hydride elimination gave bicycle **3.182** in 86% yield.[93] Though Snider and others have applied this manganese(III) mediated cyclization to many substrates including malonates,[94] β-ketoesters,[95,96] β-ketoamides,[95,97–99] and even β-ketosulfones,[100] and α-cyano ketones,[101] the strategy has almost exclusively been applied to weakly basic enolates. The only major use of unactivated ketones in manganese(III) mediated radical cyclization was published by Snider in his synthesis of gymnomitrol (**3.183**, **Scheme 3.33**), which required elevated temperatures compared to the more commonly employed β-ketoester and malonate substrates.[102,103] Using the α,α-disubstituted ketone **3.184** and

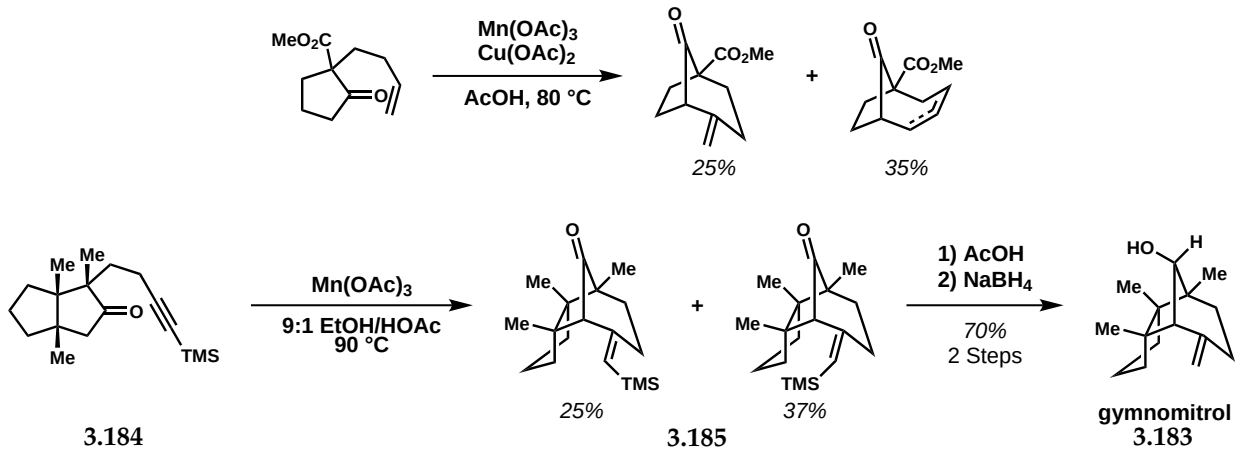

Scheme 3.33: Snider's approach to gymnomitrol.[102]

elevating the reaction temperature to 80 °C, Snider was able to regioselectively cyclize pentynone **3.184** to the corresponding bicyclo[3.2.1]octane **3.185** in a total 62% yield. While Snider's hydrocarbons may be able to withstand prolonged heating in acetic acid, many chemists would hesitate to subject their frontier material to such harsh conditions; however, the Burton group has demonstrated that the manganese(III) acetate mediated radical formation is equally effective in a variety of polar protic and polar aprotic solvents.[94,99,104–107]

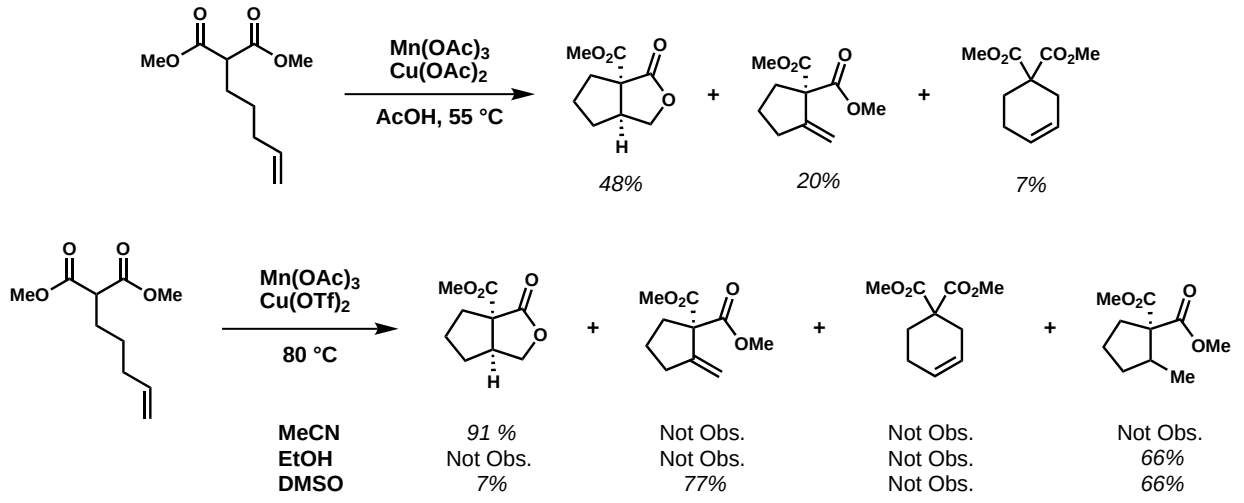

Scheme 3.34: Solvent effects on Mn(III) mediated free-radical cyclization. Snider's original acetic acid cyclizations (top) were non-selective; however, Burton's more recent work (bottom) demonstrates significant flexibility in the reaction.[104,107,108]

Table 3.5: Exploration of bicyclo[2.2.2]octane formation *via* Mn(III) mediate radical cyclization.

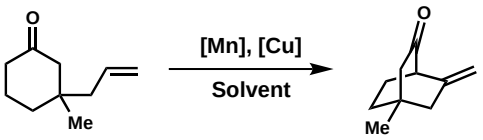

3.186 **3.187**

Entry	Solvent	[Mn] 2.2 equiv.	[Cu] 1 equiv.	Time	Temp.	Pdt.	:	S.M.
1	MeCN	$Mn(OAc)_3 \bullet 2H_2O$	$Cu(OTf)_2$	24 h	80 °C	2.2	:	1
2	DMF	$Mn(OAc)_3 \bullet 2H_2O$	$Cu(OTf)_2$	24 h	80 °C	6.1	:	1
3	DMSO	$Mn(OAc)_3 \bullet 2H_2O$	$Cu(OTf)_2$	24 h	80 °C	5.8	:	1
4	HMPA	$Mn(OAc)_3 \bullet 2H_2O$	$Cu(OTf)_2$	24 h	80 °C	2.6	:	1
5	Dioxane	$Mn(OAc)_3 \bullet 2H_2O$	$Cu(OTf)_2$	24 h	80 °C	1.9	:	1
6	PhH	$Mn(OAc)_3 \bullet 2H_2O$	$Cu(OTf)_2$	24 h	80 °C	1.0	:	1
1*	MeCN	$Mn(OAc)_3 \bullet 2H_2O$	$Cu(OTf)_2$	60 h	80 °C	3.3	:	1
2*	DMF	$Mn(OAc)_3 \bullet 2H_2O$	$Cu(OTf)_2$	60 h	80 °C	13.0	:	1
3*	DMSO	$Mn(OAc)_3 \bullet 2H_2O$	$Cu(OTf)_2$	60 h	80 °C	16.0	:	1
4*	HMPA	$Mn(OAc)_3 \bullet 2H_2O$	$Cu(OTf)_2$	60 h	80 °C	9.2	:	1
5*	Dioxane	$Mn(OAc)_3 \bullet 2H_2O$	$Cu(OTf)_2$	60 h	80 °C	3.2	:	1
6*	PhH	$Mn(OAc)_3 \bullet 2H_2O$	$Cu(OTf)_2$	60 h	80 °C	1.6	:	1
7	DMF	$Mn(OAc)_3 \bullet 2H_2O$	$Cu(OTf)_2$	12 h	80 °C	4.5	:	1
8	DMSO	$Mn(OAc)_3 \bullet 2H_2O$	$Cu(OTf)_2$	12 h	80 °C	2.3	:	1
9	DMSO	$Mn(III)acac_3$	$Cu(OTf)_2$	12 h	80 °C	0.1	:	1
10	DMSO	Mn_2O_3	$Cu(OTf)_2$	12 h	80 °C	0.1	:	1
11	DMSO	$Mn(OAc)_3 \bullet 2H_2O$	$Cu(OAc)_2 \bullet H_2O$	12 h	80 °C	2.7	:	1
12	DMSO	$Mn(OAc)_3 \bullet 2H_2O$	$CuCl_2$	12 h	80 °C	0.9	:	1
13	DMSO	$Mn(OAc)_3 \bullet 2H_2O$	$Cu(II)acac_2$	12 h	80 °C	0.5	:	1
14	DMSO	$Mn(OAc)_3 \bullet 2H_2O$	Cu(II)O	12 h	80 °C	0.4	:	1
15	DMF	$Mn(OAc)_3 \bullet 2H_2O$	$Cu(OAc)_2 \bullet H_2O$	12 h	40 °C	No Reaction		
16	DMF	$Mn(OAc)_3 \bullet 2H_2O$	$Cu(OAc)_2 \bullet H_2O$	12 h	40 °C	No Reaction		
			then	72 h	60 °C	2.5	:	1
17	DMF	$Mn(OAc)_3 \bullet 2H_2O$	$Cu(OAc)_2 \bullet H_2O$	87 h	r.t.	No Reaction		
18	DMSO	$Mn(OAc)_3 \bullet 2H_2O$	$Cu(OAc)_2 \bullet H_2O$	12 h	80 °C	1.5	:	1
19	DMF	$Mn(OAc)_3 \bullet 2H_2O$	$Cu(OAc)_2 \bullet H_2O$	12 h	80 °C	2.6	:	1
20	DMSO	$Mn(OAc)_3 \bullet 2H_2O$	$Cu(OAc)_2 \bullet H_2O$	14 h	80 °C	3.4	:	1
21	DMF	$Mn(OAc)_3 \bullet 2H_2O$	$Cu(OAc)_2 \bullet H_2O$	14 h	80 °C	1.5	:	1
22	DMSO	$Mn(OAc)_3 \bullet 2H_2O$	$Cu(OTf)_2$	14 h	80 °C	1.3	:	1
23	DMF	$Mn(OAc)_3 \bullet 2H_2O$	$Cu(OTf)_2$	14 h	80 °C	3.4	:	1

*An aliquot was taken after 24 h. Reaction was stopped after 60 h. Due to the heterogeneous nature of the reaction, reagent equivalents may not be accurate after the 24 h aliquot was removed.

With these examples in mind, ketone **3.186** was synthesized in 70% yield by Sakurai allylation of 3-methylcyclohexenone as a simple system to test bicyclization reactions (**Table 3.5**). A solvent screen (Entries 1-6, 1*-6*) first demonstrated the possible utility of this radical transformation. While even benzene (entry 6, 6*) gave some conversion, polar aprotic solvents performed best in the bicyclization reaction, though, surprisingly, the extremely polar HMPA was not as effective as DMSO or DMF which showed nearly complete conversion of ketone **3.186** to the bicyclooctane **3.187** after sixty hours. Since the extensive time required to achieve high conversions was not conducive to further screening efforts, the reaction time was reduced to twelve hours. Manganese(III) acetoacetate (Entry 9) and manganese(III) oxide (Entry 10) both gave small amounts of bicycle **3.187**; however, manganese(III) acetate was far superior. Screening copper sources, again showed that all copper sources, even the insoluble copper(II) oxide (Entry 14), were able to perform the terminal oxidation and elimination steps; however, only copper(II) acetate hydrate (Entry 11) showed reactivity on par with the significantly more expensive copper(II) triflate initially employed. Having already replaced acetic acid as a solvent of choice, I attempted to reduce the temperature of the reaction (Entries 15-17); however, no reaction was observed at either 40 °C or at room temperature. The reaction did not seem to be sensitive to heating for prolonged periods of time. Entry 16 showed no reaction after 12 h at 40 °C and was subsequently heated to 60 °C for three days, giving an appreciable amount of bicycle **3.187**. Finally, I worked to clarify whether DMSO or DMF were the better solvent for the manganese(III) mediated radical bicyclization reaction; however, as demonstrated by entries 18–23, the conversion after twelve or fourteen hours can vary. Snider and others have noted that the anhydrous manganese(III) acetate complex generally results in lower conversion and longer reaction times than the more commonly used manganese(III) acetate hydrate, implying that the hydration state of the complex is not innocent in the reaction dynamics.[91] Barton's procedure calls for the manganese and copper salts to be heated to

60 °C under high vacuum for several minutes prior to running a radical cyclization reaction. Following this procedure meant that variations in the vacuum pressure would have a significant impact on the amount of water in the reaction, a factor which may account for the irreproducible slow initiation of some of these reactions.

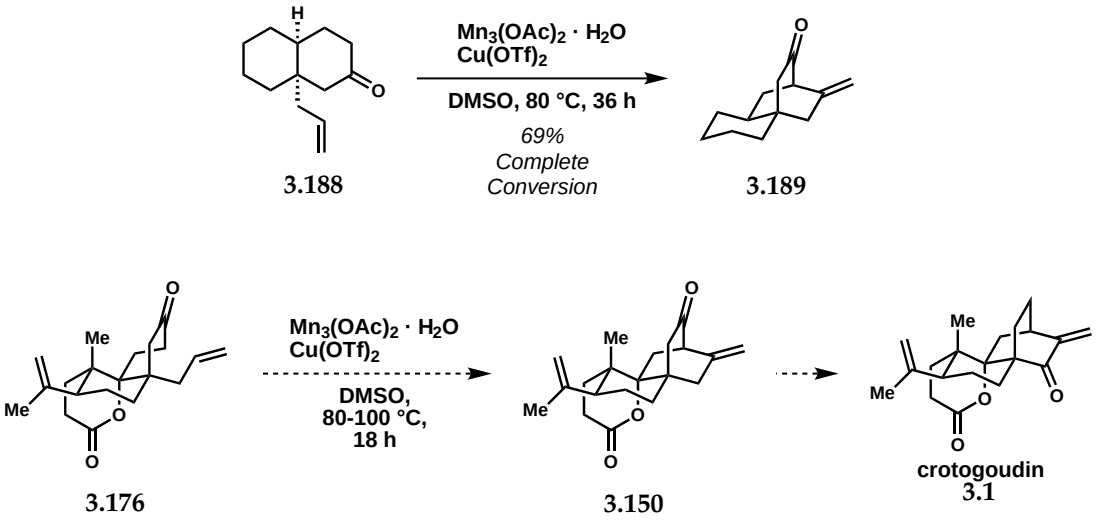

Scheme 3.35: Mn(III) radical bicyclization of allyl decalone and **3.176**

Satisfied that we had identified at least two sets of highly effective, if not optimal conditions, decalin **3.188** was synthesized *via* conjugate allylation of the corresponding enone as a model system for crotogoudin (**Scheme 3.35**). Subjecting decalone **3.188** to our optimized radical cyclization conditions gave bicycle **3.189** in complete conversion and 69% yield after thirty six hours. Unfortunately, when our frontier material **3.176** was subjected to the same conditions, no reaction was observed. Since only two milligrams of ketone **3.176** were available, the starting material was recovered and resubjected to the reaction conditions at an elevated temperature. After heating the reaction to 100 °C, NMR integration showed a loss of exocyclic alkene protons; however, due to the small amount of material in the reaction no product could be isolated.

3.11 A Scalable Synthesis

With a promising bicyclization reaction in hand, I resolved to find a scalable route to enone **3.154** (**Scheme 3.36**). Since the large TBDPS protecting group was insufficient to

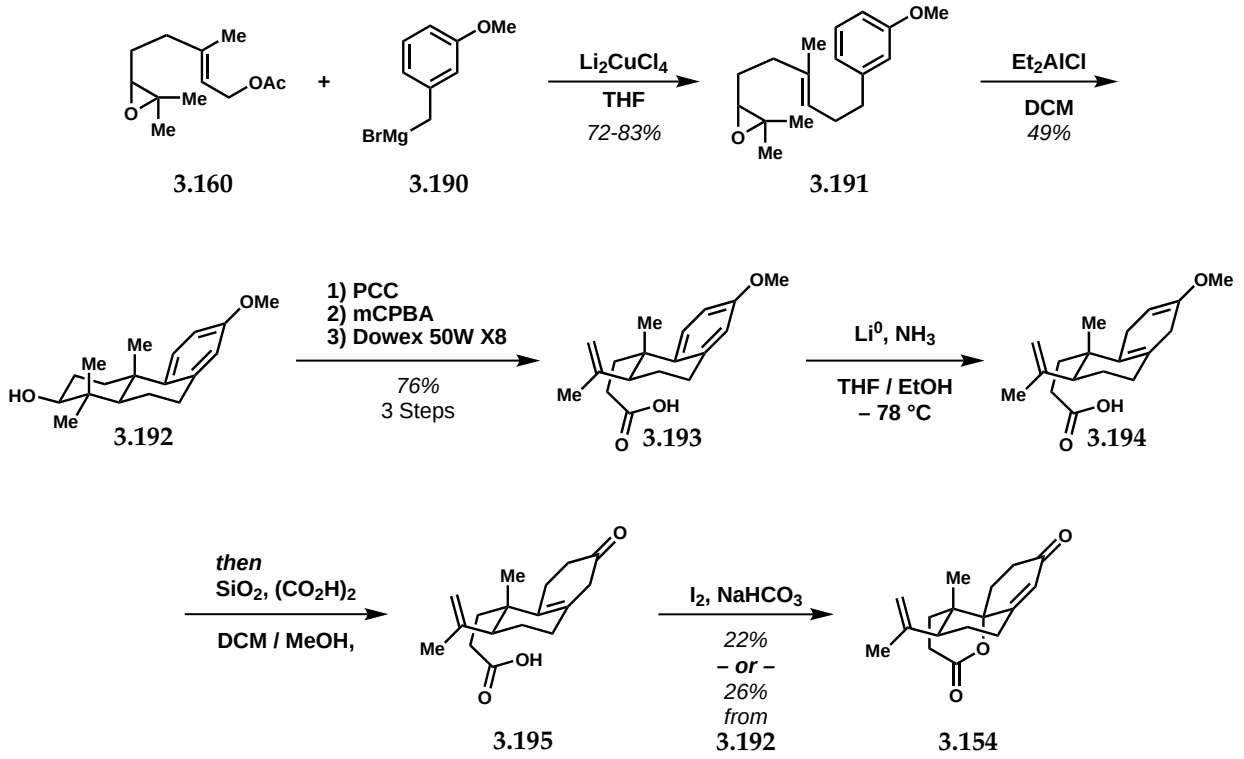

Scheme 3.36: An expedient synthesis of key enone **3.154**

avoid *ortho*- attack in our cation cyclization cascade, the synthesis instead began with the significantly cheaper 3-methoxybenzaldehyde, which was converted to Grignard **3.190** as in **Scheme 3.28**. Allylic acetate displacement was performed on up to twenty grams of geranyl acetate to give epoxide **3.191** in 72–91% yield. Cation cascade cyclization with diethylaluminum chloride gave tricycle **3.192** with 2:1 para:ortho selectivity. Whereas our previous synthesis required extensive chromatographic purification to isolate the desired *para*- cyclized product from the *ortho*-product and various alkenes resulting from early termination of the cation cascade, tricycle **3.192** could be isolated by careful recrystallization from a mixture of hexane, ethyl acetate, and toluene, significantly increasing the material throughput. PCC oxidation of alcohol **3.192** was followed by Baeyer-Villiger oxidation and E1 elimination on Dowex 50W X8 acidic resin to give carboxylic acid **3.193** in 76% yield over three steps. Birch reduction of anisole **3.192**, gave methyl enol ether **3.194**. A mild quench with methanol, oxalic acid, and silica gel in DCM followed by iodolactonization gave key enone **3.154** in 22% yield over two steps.

As deconjugated enone **3.195** slowly isomerized on storage or handling, attempts to isolate it resulted in significant reduction in yield. Shortly after this synthetic route was validated, I found that enone **3.154** could be synthesized from tricycle **3.192** in 26% yield over six steps without chromatographic purification of the intermediates.

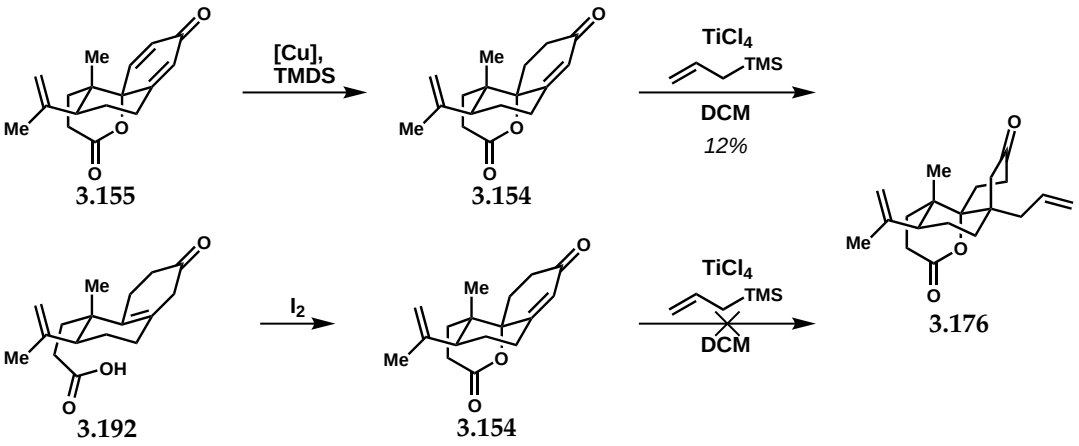

Scheme 3.37: Unexpected loss of reactivity in the Sakurai allylation.

With hundreds of milligrams of enone **3.154** in hand, we were excited about our prospects of completing crotogoudin; however, we were surprised to find that the product of iodolactonization did not undergo the previously observed Sakurai allylation (**Scheme 3.37**). Despite being identical in all analytical aspects, **3.154** derived from conjugate reduction gave allylated product **3.176** in 12% yield, while **3.154** derived from iodolactonization gave an identical decomposition profile, but no desired product. As the titanium(IV) chloride mediated conjugate allylation uses stoichiometric titanium and super stoichiometric allyltrimethylsilane, it seems unlikely that a catalytic impurity would be able to disable the Sakurai allylation. Instead, it seems more likely that an impurity carried on from our unprecedented oxygen dependent copper hydride reduction was enabling the observed allylation. Though largely unexplored, there are some examples of copper catalyzed alkylation with alkyl titanium species, but despite several attempts at doping the Sakurai allylation with copper, or ligands no conjugate allylation reactivity has been obtained from iodolactonization derived **3.154**.[109]

3.12 Conclusion

In summary, I have discovered an unprecedented oxygen dependence in the (BDP)-CuH conjugate reduction of dienones. While the function of oxygen in this reaction has yet to be elucidated, it seems that oxidation of the 1,2-dppbz ligand to the *bis*-phosphine monooxide **3.173** is at least in part responsible for the difference in reactivity. Furthermore, I have demonstrated a new implementation of Snider's manganese(III) radical enolate chemistry using unactivated ketones to form bicyclo[2.2.2]octanes in high yield and complete regiocontrol. While this method has not been successfully applied to the synthesis of crotogoudin, I was able to validate a cheap and rapid route to the key enone **3.154**. The unexpected failure of the Sakurai allylation on this material is in line with observations by other group.[86] and suggests that the successful allylation of conjugate reduction derived enone **3.154** is based on a heretofore unknown catalyst or mechanism.

3.13 Experimental Procedures

General Information

For General information please see Chapter 1.4.

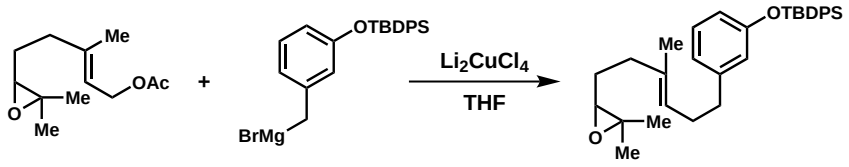

((*E*))-*tert*-butyl(3-(6-(3,3-dimethyloxiran-2-yl)-4-methylhex-3-en-1-yl)phenoxy)diphenyl-silane (3.167): Mg^0 (30.6 g, 1.26 mol) was flamed dried in round bottom flask. Once the solids cooled to room temperature 100 mL of dry Et_2O were added, the reaction mixture was cooled to 0 °C, and 1,2-dibromoethane (7.5 mL, 87 mmol) was added dropwise with stirring. Once ethylene evolution had ceased, a solution of **3.164** (26.8 g, 63.0 mmol) in 60 mL Et_2O was added in a rapid dropwise fashion until reflux was established at which point addition was slowed to maintain a gentle reflux. If reflux was not readily observed after ca. 2 mL of **3.164** solution was added, the addition was paused, the reaction mixture was warmed to room temperature, and heated with a heat gun until reflux began, at which point slow dropwise addition of **3.164** was resumed. Once it was clear that reflux could be maintained by addition of **3.164** solution, the 0 °C cooling bath was reintroduced and the addition of **3.164** was completed. Lithium chloride (0.032 g, 7.44 mmol) was flame dried three times under high vacuum, backfilling with nitrogen. Copper(II) chloride (0.50 g, 3.72 mmol) was added and the solids were degassed, backfilled with argon and suspended in 30 mL THF. The lithium chloride/copper(II) chloride solution was sonicated until a dark red solution (Li_2CuCl_4) was formed and no solids were observed. The **3.160** (7.9 g, 37.2 mmol) was diluted with 80 mL of dry THF, cooled to 0 °C, and the Li_2CuCl_4 solution was added *via* cannula. Benzyl Grignard **3.166** was rapidly cannulated into the solution of **3.160** and Li_2CuCl_4 and the resultant black reaction mixture was allowed to

warm naturally to room temperature over 12 h. The reaction mixture was then cooled to 0 °C and 200mL of saturated, aqueous ammonium chloride were added. The layers were separated and the aqueous phase was extracted 3 x 100 mL Et_2O. The combined organic phases were washed with 100 mL brine, dried with Na_2SO_4, filtered through a sintered glass funnel, and concentrated *in vacuo*. Purification of the crude residue by column chromatography (2%–10% EtOAc in hexanes) gave **3.167** (16.2 g, 89% Yield). ^{1}H NMR (500 MHz, $CDCl_3$) δ 7.72 (d, *J* = 6.7, 4H), 7.39 (dt, *J* = 28.7, 7.2, 6H), 6.97 (t, *J* = 7.8, 1H), 6.68 (d, *J* = 7.3, 1H), 6.61 (br s, 1H), 6.57 (d, *J* = 8.1, 1H), 5.14 (t, *J* = 6.3, 1H), 2.68 (t, *J* = 6.3, 1H), 2.45 (t, *J* = 7.8, 1H), 2.13–2.05 (m, 3H), 1.64–1.58 (m, 1H), 1.52 (br s, 3H), 1.29 (s, 3H), 1.25 (s, 3H), 1.10 (s, 9H); ^{13}C NMR (125 MHz, $CDCl_3$) δ 155.6, 143.7, 135.7, 134.8, 133.2, 129.9, 128.9, 127.8, 124.4, 121.4, 119.9, 117.2, 64.3, 58.5, 36.4, 36.0, 29.9, 27.6, 26.4, 25.0, 19.6, 18.6, 16.1; IR (thin film) 3071.3, 3048.7, 3030.5, 2958.8, 2930.9, 2857.5, 2896.3, 1602.6, 1583.7 cm^{-1}; HRMS (ESI/MeOH) *m* / *z* calcd for $C_{33}H_{42}O_2SiNa$ $(M+Na)^+$ 521.2852, found 521.2844.

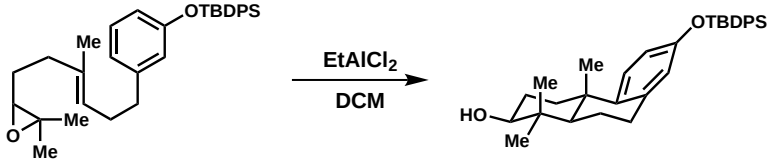

(2*S,4a*S**,10a*R**)-7-((*tert*-butyldiphenylsilyl)oxy)-1,1,4a-trimethyl-1,2,3,4,4a,9,10,10a-octahydrophenanthren-2-ol (3.168**): Epoxide **3.167** (60 g, 120 mmol) was dissolved in 120 mL DCM, cooled to –78 °C, ethylaluminum dichloride (120 mL, 120 mmol) was added *via* cannula, and the reaction mixture was stirred at –78 °C for 2 h. The reaction mixture was warmed to 0 °C and quenched by the addition of 300 mL of saturated, aqueous $NHCO_3$. The aqueous phase was separated and extracted 3 x 300 mL Et_2O. The combined organic phases were washed with 100 mL brine, dried over Na_2SO_4, and concentrated *in vacuo* to give the.21 crude product as a mix of *ortho*- and *para*- cyclization products along with various products of prematurely terminated cation cyclization cascades. Careful purification by column chromatography (5% EtOAc in hexanes) gave

3.168 as a white solid (28.9 g, 48% Yield). ^{1}H NMR (500 MHz, $CDCl_3$) δ 7.40 (dt, *J* = 29.1, 7.1, 4H), 6.91 (d, *J* = 8.9, 6H), 6.49 (s, 2H), 3.28 (dd, *J* = 11.3, 4.1, 1H), 2.78–2.64 (m, 2H), 2.19 (d, *J* = 13.2, 1H), 1.83–1.64 (m, 4H), 1.46 (td, *J* = 12.8, 2.6, 1H), 1.38 (br s, 1H), 1.27 (d, *J* = 12.2, 1H), 1.12 (s, 3H), 1.09 (s, 9H), 1.05 (s, 3H), 0.87 (s, 3H); ^{13}C NMR (125 MHz, $CDCl_3$) δ 153.1, 142.2, 136.2, 135.7, 133.4, 129.9, 127.8, 125.2, 119.3, 117.2, 78.9, 50.0, 39.1, 37.2, 37.1, 30.8, 28.3, 28.2, 26.7, 25.1, 19.6, 18.9, 15.5; IR (thin film) 3395.3, 3071.6, 2962.1, 2931.6, 160.5 cm^{-1}.

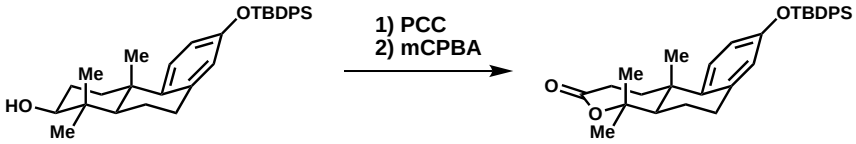

((4a*S,10a*R**)-7-((*tert*-butyldiphenylsilyl)oxy)-1,1,4a-trimethyl-3,4,4a,9,10,10a-hexahydrophenanthren-2(1*H*)-one:**Alcohol **3.168** (28.0 g, 56.1 mmol) diluted with 250 mL DCM and cooled to 0 °C. PCC (24.2 g, 112 mmol) was added, the cooling bath was removed and the initially red suspension was stirred until the reaction was complete by TLC (ca. 2 h). The resultant black suspension was diluted with 200 mL of Et_2O, filtered through SiO_2, and concentrated *in vacuo* to give the title ketone as an off white foam which was carried on without further purification. ^{1}H NMR (500 MHz, $CDCl_3$) δ 7.72 (d, *J* = 7.00, 4H), 7.40 (dt, *J* = 29.2, 7.2, 6H), 6.93 (d, *J* = 8.3, 1H), 6.52–6.50 (m, 2H), 2.77–2.62 (m, 3H), 2.57–2.52 (m, 1H), 2.40–2.34 (m, 2H), 1.90–1.84 (m, 2H), 1.75–1.68 (m, 2H), 1.22 (s, 3H), 1.14 (s, 3H), 1.11–1.10 (m, 12H); ^{13}C NMR (125 MHz, $CDCl_3$) δ 217.6, 153.3, 140.2, 136.0, 135.7, 133.3, 129.9, 127.8, 126.2, 119.3, 117.7, 50.7, 47.4, 37.7, 36.9, 34.8, 30.9, 26.9, 26.7, 24.8, 21.2, 20.3, 19.6; IR (thin film) 3071.6, 3049.4, 2960.5, 2933.0, 2894.7, 2858.4, 1706.6, 1606.6, 1496.8 cm^{-1}; HRMS (ESI/MeOH) *m / z* calcd for $C_{33}H_{40}O_2SiNa$ $(M+Na)^+$ 519.2695, found 519.2681.

(5a*R,11b*S**)-9-((*tert*-butyldiphenylsilyl)oxy)-5,5,11b-trimethyl-1,5,5a,6,7,11b-hexahydronaphtho[2,1-c]oxepin-3(2*H*)-one (3.169**): The ketone synthesized above

(23.0 g, 46.3 mmol) was dissolved in 230 mL DCM, cooled to 0 °C, and $NaHCO_3$ (19.4 g, 231 mmol) was added. *m*CPBA (16.0 g, 92.6 mmol) was dissolved in 230 mL DCM in a separatory funnel, the aqueous layer was removed, and the *m*CPBA solution was added slowly, over 30 min to the 0 °C solution of **3.169**. The resultant white suspension was allowed to warm to room temperature naturally overnight. The reaction mixture was diluted with 200 mL water, the layers were separated, and the aqueous phase was washed 3 x 50 mL Et_2O. The combined organic phases were washed with 200 mL brine, dried over Na_2SO_4, and concentrated *in vacuo*. Purification of the crude material by column chromatography (20% EtOAc in hexanes) gave **3.169** as a slightly yellow solid (20 g, 70% Yield over two steps). ^{1}H NMR (500 MHz, $CDCl_3$) δ 7.71 (d, *J* = 6.8, 4H), 7.40 (dt, *J* = 30.6, 7.3, 6H), 6.91 (d, *J* = 8.8, 1H), 6.54 (d, *J* = 6.6, 1H), 6.43 (s, 1H), 2.69–2.51 (m, 4H), 2.29–2.19 (m, 2H), 1.91–1.89 (m, 1H), 1.73–1.67 (m, 2H), 1.54 (s, 3H), 1.44 (s, 3H), 1.41 (s, 3H), 1.08 (s, 9H); ^{13}C NMR (125 MHz, $CDCl_3$) δ 174.4, 153.1, 141.4, 135.7, 135.5, 134.9, 133.2, 130.0, 128.1, 127.8, 118.5, 118.4, 86.0, 49.6, 39.3, 39.2, 32.9, 31.0, 30.4, 27.0, 26.8, 26.7, 26.5, 24.7, 19.6; IR (thin film) 3071.4, 3049.1, 2932.7, 2891.8, 2858.2, 1724.8, 1607.1, 1495.3, cm^{-1}; HRMS (ESI/MeOH) *m* / *z* calcd for $C_{33}H_{40}O_3SiNa$ $(M+Na)^+$ 535.2645, found 535.2642.

3-((1*S,2*S**)-6-((*tert*-butyldiphenylsilyl)oxy)-1-methyl-2-(prop-1-en-2-yl)-1,2,3,4-tetrahydronaphthalen-1-yl)propanoic acid:**Lactone **3.169** (20 g, 39 mmol) was dissolved in 200 mL THF, and *p*-TsOH•H_2O (74.2 g, 390 mmol) was added. The resultant solution was heated to 60 °C for 1 h, cooled to room temperature, diluted with 100 mL EtOAc and 100 mL hexanes, filtered through SiO_2. The filtrate was washed with water, the aqueous phase was removed and extracted 2 x 200 mL Et_2O. The combined organic

layers were washed with brine, dried over Na_2SO_4, filtered through cotton, and concentrated *in vacuo*. The resultant crude carboxylic acid was carried on without further purification. ^{1}H NMR (500 MHz, $CDCl_3$) δ 7.69 (d, *J* = 6.9, 4H), 7.38 (dt, *J* = 28.5, 7.0, 6H), 6.97 (d, *J* = 8.7, 1H), 6.54 (d, *J* = 8.3, 1H), 6.42 (s, 1H), 4.91 (s, 1H), 4.67 (s, 1H), 2.62–2.48 (m, 2H), 2.37 (d, *J* = 9.6, 1H), 2.13 (td, *J* = 13.7, 4.1, 1H), 2.05–1.91 (m, 2H), 1.86–1.71 (m, 2H), 1.74 (s, 3H); 1.13 (s, 3H); 1.07 (s, 9H); ^{13}C NMR (125 MHz, $CD3OD_3$) δ 177.9, 154.4, 148.2, 139.4, 137.1, 136.7, 134.3, 131.1, 128.8, 128.7, 120.4, 119.2, 114.7, 41.4, 36.1, 31.1, 30.4, 28.2, 27.0, 25.7, 23.2, 20.2, ; IR (thin film) 3071.3, 3050.0, 3028.1, 2960.6, 2931.5, 2857.8, 2891.2, 1735.6, 1707.1, 1606.9, 1496.3 cm^{-1}; HRMS (ESI/MeOH) *m / z* calcd for $C_{33}H_{40}O_3SiNa$ $(M+Na)^+$ 535.2645, found 535.2645.

3-((1*S,2*S**)-6-hydroxy-1-methyl-2-(prop-1-en-2-yl)-1,2,3,4-tetrahydronaphthalen-1-yl)propanoic acid (3.170**): The above synthesized carboxylic acid (14.4 g, 28.1 mmol) was dissolved in 60 mL THF and cooled to 0 °C. TBAF (84 mL, 84 mmol) was added dropwise over 15 min. The reaction mixture was stirred at 0 °C 15 min the the cooling bath was then removed and stirring was continued until no starting material was observed by TLC (ca. 1 h). The reaction mixture was cooled to 0 °C, slowly acidified *via* addition of 3M HCl, and diluted with water. The aqueous phase was separated and extracted 3 x 150 mL Et_2O. The combined organic phases were washed with brine, dried over Na_2SO_4, and concentrated *in vacuo*. The resultant crude material was purified by column chromatography (95:5:1 DCM:MeOH:AcOH) to give a yellow solid which was triturated with DCM to give **3.170** as a white powder (6.95 g, 64% Yield over two steps). ^{1}H NMR (500 MHz, $CDCl_3$) δ 7.08 (d, *J* = 8.6, 1H), 6.61 (dd, *J* = 8.6, 2.7, 1H), 6.46 (d, *J* = 2.7, 1H), 5.48 (s, 1H), 4.95 (s, 1H), 4.9 (br s, 2H), 4.72 (s, 1H), 2.78–2.67 (m, 2H), 2.44 (d, *J* = 11.5, 2.9, 1H), 2.21–2.16 (m, 1H), 2.05 (td, *J* = 11.9, 3.5, 2H), 1.93–1.75 (m, 2H), 1.80 (s, 3H); ^{13}C NMR (125 MHz, $CDCl_3$) δ 178.0, 155.8, 148.3, 139.4, 135.3, 128.8, 115.7, 114.8, 114.6, 41.4, 36.1, 31.4, 30.5, 28.5, 25.9, 23.3; IR (thin film) 3320.8, 3265.9, 3022.1, 2962.7, 1704.7,

1609.8, 1499.2 cm^{-1}; HRMS (ESI/MeOH) *m* / *z* calcd for $C_{17}H_{22}O_3Na$ $(M-H)^-$273.1491, found 273.1486.

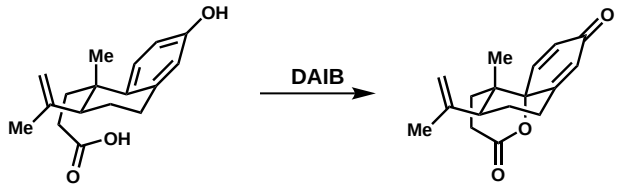

(4a*S,5*S**,11a*R**)-4a-methyl-5-(prop-1-en-2-yl)-3,4,4a,5,6,7-hexahydrobenzo[*i*]-chromene-2,9-dione (3.155)**: Phenol **3.170** (1.0 g, 3.65 mmol) was dissolved in 17 mL of CF_3CH_2OH and cooled to 0 °C. A solution of diacetoxyiodobenzene in 20 mL of CF_3CH_2OH was added dropwise over 30 min. The reaction mixture was stirred at 0 °C for 3 h, diluted with water, and extracted 3 x 100 mL DCM. The combined organic layers were dried with Na_2SO_4, filtered through cotton and concentrated *in vacuo*. The resultant crude dienone was purified by column chromatography (20% EtOAc in hexanes) to give **3.155** as a white solid (510 mg, 51% Yield). ^{1}H NMR (500 MHz, $CDCl_3$) δ 6.86 (d, *J* = 10.2, 1H), 6.33 (d, *J* = 10.2, 1H), 6.16 (s, 1H), 5.02 (s, 1H), 4.82 (s, 1H), 2.88–2.71 (m, 4H), 2.42 (d, *J* = 13.3, 1H), 2.02–1.83 (m, 4H), 1.77 (s, 3H), 0.89 (s, 3H); ^{13}C NMR (125 MHz, $CDCl_3$) δ 184.8, 169.9, 156.7, 144.1, 143.6, 131.1, 126.2, 116.3, 82.8, 44.0, 41.1, 31.8, 28.6, 28.0, 26.0, 23.3, 17.5; IR (thin film) 3076.5, 3053.0, 2969.4, 2948.7, 1740.6, 1674.2, 1640.2, 1614.9 cm^{-1}; HRMS (ESI/MeOH) *m* / *z* calcd for $C_{17}H_{20}O_3Na$ $(M+Na)^+$ 295.1310, found 295.1311.

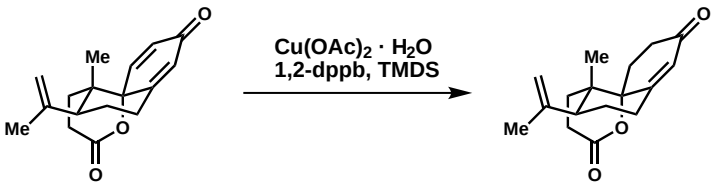

(4a*S,5*S**,11a*R**)-4a-methyl-5-(prop-1-en-2-yl)-3,4,4a,5,6,7,10,11-octahydrobenzo[*i*]-chromene-2,9-dione (3.154)**: To a one dram vial equipped with a magnetic stir bar was added, under argon, $Cu(OAc)_2 \bullet H_2O$ (0.001 g, 3.5 μmol) followed by 1,2-dppb (330 μg, 0.7 μmol) as a solution in 0.1 mL PhMe. The green suspension was stirred at room

temperature for 10 min, tetramethyldisilazane (TMDS, 7.7 μL, 44 μmol) was added as a solution in 0.1 mL PhMe, and the atmosphere was exchanged for O_2. The resultant yellow solution was stirred for stirred for 5 min and solid **3.155** (0.010 g, 39.3 μmol) was added followed by 0.2 mL PhMe. The resultant orange-brown reaction mixture was stirred for 2 h under O_2 atmosphere, quenched by addition of 1 mL 1M HCl, diluted with 2 mL water, and extracted 3 x 2 mL Et_2O. The combined organic phases were washed with $NaHCO_3$, brine, and dried over Na_2SO_4. The resultant crude material consisted of a ca. 1:1 ratio of **3.154**:**3.155**. As this reaction was found to be irreproducible when attempting to increase the scale, many different experiments were combined prior to purification by column chromatography (10%–30% EtOAc in hexanes) to give **3.154**. Recovered starting dienone could be readily resubmitted to obtain more product. Please see the appendix for comparison between **3.154** synthesized *via* conjugate reduction and that synthesized by iodolactonization.^{1}H NMR (500 MHz, $CDCl_3$) δ 5.98 (s, 1H), 5.04 (s, 1H), 4.84 (s, 1H), 2.79–2.61 (m, 5H), 2.45–2.38 (m, 3H), 2.17–2.13 (m, 1H), 1.95–1.86 (m, 3H), 1.83 (s, 3H), 1.03 (s, 3H); ^{13}C NMR (125 MHz, $CDCl_3$) δ 198.0, 170.7, 155.8, 144.9, 128.7, 116.2, 84.4, 44.1, 39.2, 33.6, 31.9, 29.8, 29.4, 27.1, 26.5, 26.2, 24.0, 18.9; IR (thin film) cm^{-1}; HRMS (ESI/MeOH) *m* / *z* calcd for $C_{17}H_{22}O_3Na$ $(M+Na)^+$ 297.1467, found 297.1461.

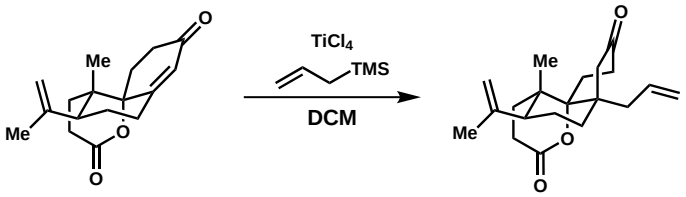

(4a*S,5*S**,7a*S**,11a*R**)-7a-allyl-4a-methyl-5-(prop-1-en-2-yl)decahydrobenzo[*i*]-chromene-2,9-dione (3.176**): Enone **3.154** (0.017 g, 0.063 mmol, concentrated from dry PhMe and stored over P_2O_5 on high vacuum overnight) was diluted with 0.8 mL dry DCM, and cooled to –78 °C. A solution of Titanium(IV) chloride (13 μL, 0.114 mmol, distilled) in 0.1 mL DCM was added dropwise. The resultant dark black reaction mixture

was stirred for 1 h at –78 °C and a solution of allyltrimethylsilane (15 μL, 0.0968 mmol) in 0.1 mL DCM was added. The cooling bath was removed, the reaction mixture was aged 6.5 h, cooled to 0 °C, quenched by addition of 2 mL 4:1:3 DCM:MeOH:Et_3N, and allowed to warm again to room temperature. 5 mL of water were added and the mixture was extracted 3 x 2 mL Et_2O. The combined organic phases were washed with 2 x 2 mL 1M HCl, 5 mL brine, dried over Na_2SO_4, filtered through cotton, and concentrated *in vacuo*. The crude material showed a great deal of decomposition, but the presence of a new terminal alkene was apparent by ^{1}H NMR. The crude material was purified by preparatory TLC (30% EtOAc in hexanes as eluent) to give **3.176** (0.0025 g, 12% Yield). ^{1}H NMR (600 MHz, $CDCl_3$) δ 5.87 (qt, *J* = 14.8, 7.5, 1H), 5.19 (dd, *J* = 10.1, 2.0, 1H), 5.14 (dd, *J* = 17.0, 0.9, 1H), 4.96 (s, 1H), 4.74 (s, 1H), 2.62 (dt, *J* = 19.6, 9.8, 1H), 2.52 (ddd, *J* = 19.5, 8.9, 1.4, 1H), 2.43 (dd, *J* = 12.8, 3.2, 1H), 2.22 (d, *J* = 7.6, 2H), 2.14 (s, 1H), 2.11–2.05 (m, 2H), 1.86–1.80 (m, 2H), 1.77 (s, 3H), 1.76–1.65 (m, 4H), 1.05 (s, 3H).

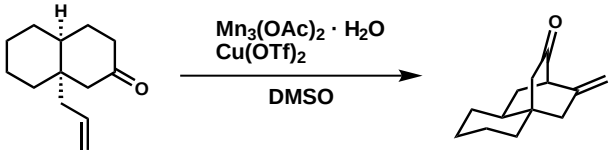

A representative procedure for Mn(III) acetate mediated radical bicyclization. **(2*R**,4a*S**,8a*S**)-10-methylenehexahydro-2*H*-2,4a-ethanonaphthalen-3(4*H*)-one (3.189)**: $Mn(OAc)_3$•$2H_2O$ (0.316 g, 1.18 mmol) and $Cu(OTf)_2$ (0.195 g, 0.539 mmol) were added to a flame dried vial, degassed in triplicate backfilling with argon, and suspended in 5.4 mL DMSO. Ketone **3.188** (0.103 g, 0.533 mmol) was added neat, *via* syringe, and the reaction mixture was heated to 80 °C in a preheated aluminum block for 36 h. The brown suspension was cooled to room temperature, diluted with 2 mL water, extracted with 2 x 2 mL DCM and 2 x 2 mL Et_2O. The combined organic phases were washed with $NaHCO_3$, water, brine, dried over Na_2SO_4, filtered through SiO_2, and concentrated *in vacuo*. The resultant crude material was purified by column chromatography (1%–3% EtOAc in hexanes) to give **3.189** (0.070 g, 69% Yield). ^{1}H NMR (600 MHz, $CDCl_3$) δ 4.92

(d, *J* = 0.7, 1H), 4.81 (d, *J* = 1.0, 1H), 2.85 (dd, *J* = 3.6, 2.2, 1H), 2.69 (dd, *J* = 19.1, 3.2, 1H), 2.23 (dd, *J* = 17.1, 2.3, 1H), 2.18–2.12 (m, 2H), 1.74 (dd, *J* = 19.2, 1.4, 1H), 1.73–1.62 (m, 2H), 1.60–1.48 (m, 3H), 1.37–1.16 (m, 4H), 1.08 (ddd, *J* = 35.7, 13.0, 3.5, 1H); ^{13}C NMR (125 MHz, $CDCl_3$) δ212.7, 143.3, 110.6, 55.0, 44.0, 42.9, 37.5, 36.3, 36.1, 32.9, 31.2, 26.2, 21.8; HRMS (CI/DCM) *m* / *z* calcd for $C_{13}H_{18}ONH_4$ $(M+NH_4)^+$ 208.1701, found 208.1703.

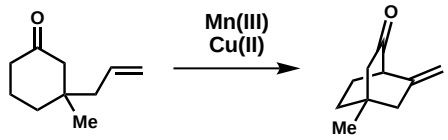

(1*R,4*S**)-4-methyl-6-methylenebicyclo[2.2.2]octan-2-one (3.187)**: **3.186** was readily synthesized by allylation of 3-methyl-cyclohex-2-enone and was used as the substrate of interest in exploring the manganese catalyzed cyclizations described in table **Table 3.5**. While a surprising large number of conditions gave some amount of product, the procedure above was settled on as the most reproducibly high yielding. As such, **3.187** was synthesized as described above for **3.189**. Crude material corresponds to literature spectra.[110] ^{1}H NMR (600 MHz, $CDCl_3$) δ 4.93 (s, 1H), 4.81 (s, 1H), 2.90 (t, *J* = 2.9, 1H), 2.33 (ddd, *J* = 17.1, 4.8, 2.4, 1H), 2.22 (ddd, *J* = 17.1, 5.0, 2.4, 1H), 2.10 (ddd, *J* = 25.2, 18.7, 2.6, 2H), 1.91 (td, *J* = 8.2, 2.8, 2H), 1.57–1.47 (m, 3H), 1.03 (s, 3H); ^{13}C NMR (125 MHz, $CDCl_3$) δ 212.8, 143.6, 110.6, 54.3, 50.4, 41.4, 33.5, 32.0, 26.5, 24.8.

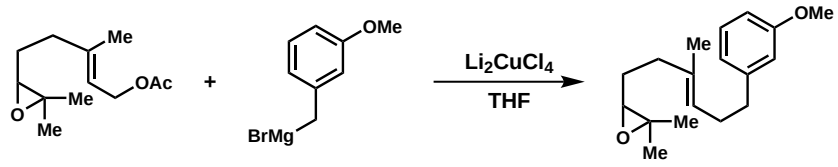

((*E*))-3-(6-(3-methoxyphenyl)-3-methylhex-3-en-1-yl)-2,2-dimethyloxirane (3.191): Flame dried magnesium metal powder (24 g, 1000 mmol) was suspended in 200 mL Et_2O, cooled to 0 °C, and 1,2-dibromoethane (10 mL, 120 mmol) was added dropwise over 30 min (1 mL bolus, then dropwise). When gas evolution ceased, a solution of 3-methoxybenzyl bromide (14 mL, 100 mmol) in 14 mL of Et_2O was added dropwise so

as to maintain a gentle reflux, and the solution was stirred 1 h further at 0 °C. During this time lithium chloride (0.512 g wet not reweighed, ≤0.25 mmol) was freshly fused three times, back filling with nitrogen. Copper(II) chloride (0.656 g, 4.88 mmol) was added to the dried lithium chloride, the solids were degassed, 40 mL dry THF were added, and the suspension was sonicated until it formed a clear red solution. This solution of Li_2CuCl_4 was cannulated into a 0 °C solution of **3.160** (10.29 g, 48.5 mmol) in 100 mL Et_2O. The resultant yellow solution was maintained at 0 °C while benzyl Grignard **3.190** was cannulated in rapidly. The resultant black reaction mixture was allowed to warm naturally overnight (12 h), cooled to 0 °C, and quenched by slow addition of saturated, aqueous NH_4Cl. The layers were separated, the aqueous phase was extracted 2 x 100 mL Et_2O, the combined organic phases were washed with brine, dried over $MgSO_4$, filtered through a sintered glass funnel, and concentrated *in vacuo*. The resultant crude product was purified by column chromatography (2% EtOAc, 49% PhMe, 49% hexanes) to give **3.196**diu13) (11.08 g, 83% Yield). The spectral data for **3.191** was in accordance with previous syntheses.[63,111] ^{1}H NMR (600 MHz, $CDCl_3$) δ 7.19 (t, *J* = 7.7, 1H), 6.78 (d, *J* = 7.6, 1H), 6.74–6.72 (m, 2H), 5.23 (td, *J* = 7.1, 1.0, 1H), 3.81 (s, 3H), 2.69 (t, *J* = 6.2, 1H), 2.62 (d, *J* = 15.7, 2H), 2.31 (q, *J* = 7.6, 2H), 2.18–2.07 (m, *J* =, 2H), 1.67–1.54 (m, *J* =, 2H), 1.58 (s, 3H), 1.30 (s, 3H), 1.26 (s, 3H); ^{13}C NMR (125 MHz, $CDCl_3$) δ 159.7, 144.1, 135.0, 129.3, 124.3, 121.0, 114.4, 111.1, 64.3, 58.5, 55.3, 36.4, 36.2, 30.0, 27.6, 25.0, 18.9, 16.1.

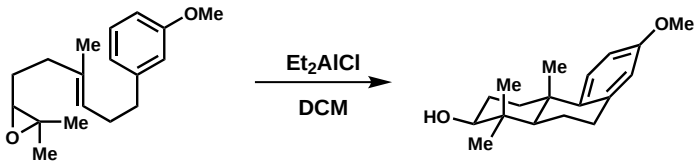

(2*S,4a*S**,10a*R**)-7-methoxy-1,1,4a-trimethyl-1,2,3,4,4a,9,10,10a-octahydrophenanthren-2-ol (3.192**): Diethylaluminum chloride (50 mL, 50 mmol) was added dropwise to a –78 °C solution of **3.191** in 200 mL dry DCM. The yellow solution was stirred at –78 °C for 3.5 h and was quenched by cannulating the reaction mixture onto a stirred mixture of 250 mL saturated aqueous $NaHCO_3$ and 300 mL of ice. The resultant white suspension

was warmed to room temperature, the layers were separated and the aqueous phase was extracted 3 x 100 mL DCM. The combined organic phases were dried over $MgSO_4$, filtered through a sintered glass funnel, and concentrated *in vacuo* to give **3.192** as a 2.5:1 mixture of para:ortho cyclization products along with contaminants resulting from premature E1 elimination. The crude mixture was purified by recrystallization. The white solids were suspended in 50 mL of hexanes, heated to 50 °C, and hot EtOAc was added dropwise with stirring until all solids were dissolved. A few drops of hot hexanes were then added and hot plate was turned off, allowing the solution to cool slowly to room temperature. The resultant white needles were found to be pure **3.192** (3.857 g, 35% Yield). The mother liquor was concentrated *in vacuo* and was found to consist of 23% **3.192**. This material could be recovered *via* further recrystallization or by column chromatography to give additional **3.192** (1.4 g, 14% Yield) for a total 49% Yield. Spectral data for **3.192** was in accordance with previous syntheses of the compound.[63,111] ^{1}H NMR (500 MHz, $CDCl_3$) δ 7.15 (d, *J* = 8.7, 1H), 6.70 (dd, *J* = 8.7, 2.7, 1H), 6.57 (d, *J* = 2.6, 1H), 3.76 (s, 3H), 3.30 (tt, *J* = 8.2, 5.6, 1H), 2.94 (dd, *J* = 16.9, 6.4, 2H), 2.84 (ddd, *J* = 17.6, 11.1, 6.9, 1H), 2.29 (dt, *J* = 13.1, 3.4, 1H), 1.91–1.70 (m, 4H), 1.50 (appar dd, *J* = 13.2, 4.2, 2H), 1.36 (d, *J* = 5.9, 1H), 1.31 (dd, *J* = 12.3, 2.1, 1H), 1.17 (s, 3H), 1.07 (s, 3H), 0.90 (s, 3H); ^{13}C NMR (150 MHz, $CDCl_3$) δ 157.3, 142.0, 136.5, 125.7, 113.3, 112.2, 78.9, 55.3, 50.2, 39.1, 37.3, 31.1, 28.3, 28.2, 25.1, 19.0, 15.5.

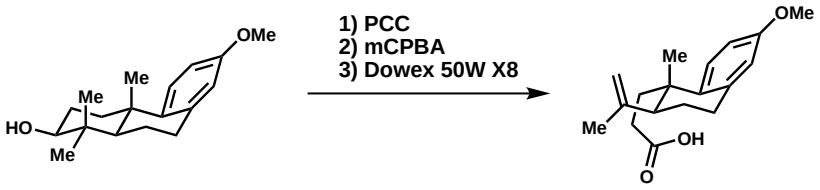

(4a*S,10a*R**)-7-methoxy-1,1,4a-trimethyl-3,4,4a,9,10,10a-hexahydrophenanthren-2(1*H*)-one:** A solution of alcohol **3.192** (0.4152 g, 1.51 mmol) in 7.5 mL DCM was added to a 0 °C suspension of PCC (0.70 g, 3.2 mmol) in 7.5 mL DCM. The resultant black suspension was allowed to warm naturally over 12 h, diluted with 20 mL Et_2O, filtered through

SiO_2, and concentrated *in vacuo* to give the title compound without the need for further purification. Spectral data was in accordance with previous synthesis of this ketone.[112,113] ^{1}H NMR (600 MHz, $CDCl_3$) δ 7.17 (d, *J* = 8.7, 1H), 6.73 (dd, *J* = 8.7, 2.6, 1H), 6.59 (d, *J* = 2.5, 1H), 3.77 (s, 3H), 2.94 (ddd, *J* = 16.9, 5.4, 1.8, 1H), 2.87 (ddd, *J* = 17.3, 11.1, 6.6, 1H), 2.69 (ddd, *J* = 15.9, 10.0, 7.5, 1H), 2.58 (ddd, *J* = 15.8, 7.6, 4.0, 1H), 2.46 (ddd, *J* = 13.1, 7.6, 4.1, 1H), 2.05–1.75 (m, 4H), 1.28 (s, 3H), 1.17 (s, 3H), 1.14 (s, 3H); ^{13}C NMR (150 MHz, $CDCl_3$) δ 217.3, 157.5, 139.9, 136.3, 126.6, 113.2, 112.6, 55.3, 50.9, 47.4, 37.8, 36.9, 34.8, 31.2, 29.8, 27.0, 24.8, 21.2, 20.3.

(5aR,11bS)-9-methoxy-5,5,11b-trimethyl-1,5,5a,6,7,11b-hexahydronaphtho[2,1-*c*]oxepin-3(2*H*)-one: $NaHCO_3$ (0.745 g, 8.87 mmol) was added to a 0 °C solution of the above ketone (0.4498 g, ≤1.65 mmol) in 15 mL DCM. *m*CPBA (1.49 g, 6.04 mmol) was added as a single portion and the reaction mixture was allowed to warm to room temperature naturally overnight. The resultant white suspension was diluted with 50 mL water and 50 mL DCM, the layers were separated, the aqueous phase was extracted 2 x 20 mL DCM. The combined organic layers were washed sequentially with saturated, aqueous $NaHCO_3$, water, brine, dried over $MgSO_4$, filtered through Celite and concentrated *in vacuo* to give the title compound without the need for further purification (0.4222 g, 1.463 mmol). ^{1}H NMR (600 MHz, $CDCl_3$) δ 7.15 (d, *J* = 8.8, 1H), 6.77 (dd, *J* = 8.7, 2.7, 1H), 6.53 (d, *J* = 2.7, 1H), 3.77 (s, 3H), 2.83 (ddd, *J* = 16.4, 4.6, 2.8, 1H), 2.78–2.67 (m, 2H), 2.57 (dt, *J* = 14.1, 4.2, 1H), 2.35 (td, *J* = 13.6, 4.3, 1H), 2.26 (dd, *J* = 11.7, 3.1, 1H), 1.96 (ddd, *J* = 14.2, 5.9, 4.1, 1H), 1.82–1.73 (m, 2H), 1.58 (s, 3H), 1.48 (s, 6H); ^{13}C NMR (125 MHz, $CDCl_3$) δ 174.2, 157.2, 141.0, 135.2, 128.3, 113.4, 112.3, 85.9, 55.3, 49.6, 39.4, 39.2, 32.9, 31.3, 30.5, 27.0, 26.6, 24.7; HRMS (ESI/MeOH) *m* / *z* calcd for $C_{18}H_{24}O_3Na$ $(M+Na)^+$ 311.1623, found 311.1626.

3-((1*S,2*S**)-6-methoxy-1-methyl-2-(prop-1-en-2-yl)-1,2,3,4-tetrahydronaphthalen-1-**

yl)propanoic acid (3.193): The above synthesized lactone (0.422 g, ≤1.46 mmol) was dissolved in 7.5 mL THF and *p*-TsOH•H_2O (2.827 g, 14.9 mmol) was added. The resultant orange solution was heated to 60 °C in an aluminum block for 3 h, cooled to room temperature, filtered through SiO_2 (eluted with EtOAc), and concentrated *in vacuo*. The resultant dark brown mixture was purified by column chromatography (20% EtOAc, 1% AcOH in hexanes) to give **3.193** as a yellow oil (0.3323 g, 76% Yield over three steps). Alternatively, the reaction was carried out using 4 weight equivalents of Dowex 50W X8-400 (acidic resin) in place of *p*-TsOH. The crude material was then isolated by filtration through Celite. The resultant cloudy oil was dried azeotropically and carried on without purification. ^{1}H NMR (600 MHz, $CDCl_3$) δ 7.16 (d, *J* = 8.7, 1H), 6.73 (dd, *J* = 8.7, 2.7, 1H), 6.56 (d, *J* = 2.7, 1H), 4.95 (s, 1H), 4.70 (s, 1H), 3.77 (s, 3H), 2.79–2.77 (m, *J* =, 2H), 2.40 (dd, *J* = 11.6, 2.9, 1H), 2.22 (ddd, *J* = 15.9, 11.5, 4.8, 1H), 2.14–.04 (m, 2H), 1.94–1.87 (m, 2H), 1.79 (s, 3H), 1.20 (s, 3H).

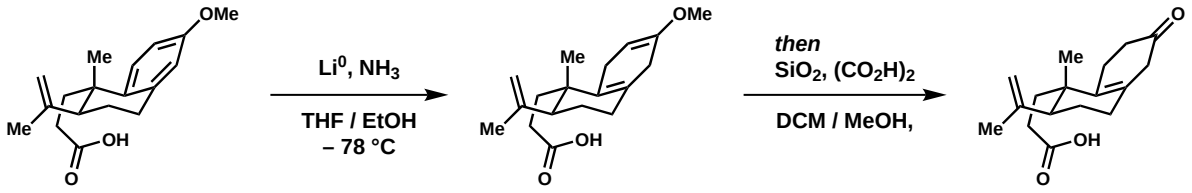

3-((1S,2S)-6-methoxy-1-methyl-2-(prop-1-en-2-yl)-1,2,3,4,5,8-hexahydronaphthalen-1-yl)propanoic acid (3.194): A solution of **3.193** (0.866 g, 3.00 mmol) in 40 mL THF was equipped with a glass coated stir bar, 4 mL ethanol were added, and the clear colorless solution was cooled to –78 °C. Gaseous ammonia (80 mL) was condensed directly into the solution. Lithium wire (0.2 g, ≤28 mmol), freshly scraped and not reweighed was added by cutting small pieces of the wire directly into the reaction mixture. Vigorous stirring gave a dark blue reaction mixture which became a white suspension after ca. 20 minutes despite the excess of lithium used. Additional lithium wire was added in ca. 0.2 g batches until the reaction mixture retained its deep blue color for 2 h. The deep blue reaction mixture was quenched by slow addition of solid NH_4Cl to give a white

suspension which was allowed to warm naturally to room temperature to allow excess ammonia to evaporate. Once no condensation was visible on the flask, the suspension diluted with 50 mL water, cooled to 0 °C, and the pH was adjusted to ca. pH 6 by dropwise addition of 6M HCl with vigorous stirring. Failure to adjust the pH resulted in dramatically diminished yield. The resultant mixture was extracted 3 x 50mL DCM. The combined organic phases were washed with brine, dried with Na_2SO_4, filtered through cotton and concentrated to give methyl enol ether **3.194** as a clear oil which was carried on. ^{1}H NMR (600 MHz, $CDCl_3$) δ 4.93 (s, 1H), 4.70 (s, 1H), 4.63 (s, 1H), 3.35 (s, 3H), 2.82–2.77 (m, 1H), 2.69–2.64 (m, 2H), 2.57–2.53 (m, 1H), 2.44–2.39 (m, 1H), 2.4 (dd, *J* = 12.2, 2.6, 1H), 2.06–2.01 (m, 2H), 1.90–1.75 (m, 4H), 1.17 (s, 3H), 0.98 (s, 3H).

3-((1*S,2*S**)-1-methyl-6-oxo-2-(prop-1-en-2-yl)-1,2,3,4,5,6,7,8-octahydronaphthalen-1-yl)propanoic acid (3.195**): Crude methyl enol ether **3.194** was diluted with 40 mL DCM, oxalic acid (0.481 g, 5.3 mmol) was added followed by 0.8 mL MeOH and SiO_2 (0.375 g, 0.43 mass equiv.). The resultant suspension was stirred at room temperature for 12 h, filtered through SiO_2 (eluted with EtOAc), and concentrated *in vacuo* to give **3.195**. Attempts to isolate **3.195** were unsuccessful and resulted in isomerization of the tetrasubstituted alkene into conjugation with the ketone. As a result in all further experiments, the β,γ-unsaturated ketone **3.195** was used immediately and without purification. ^{1}H NMR (500 MHz, $CDCl_3$) δ 4.92 (s, 1H), 4.70 (s, 1H), 3.65–3.56 (m, 2H), 2.77 (q, *J* = 18.9, 2H), 2.44–2.35 (m, 3H), 2.33–2.23 (m, 1H), 2.11–2.00 (m, 1H), 1.89–1.74 (m, 2H), 1.78 (s, 3H), 1.70–1.55 (m, 4H), 1.45–1.39 (m, 1H), 0.96 (m, 3H); ^{13}C NMR (125 MHz, $CDCl_3$) δ 211.8, 147.2, 135.3, 128.3, 114.1, 63.5, 46.6, 45.3, 41.5, 39.4, 32.8, 31.0, 28.0, 24.4, 24.4, 23.1, 22.9.

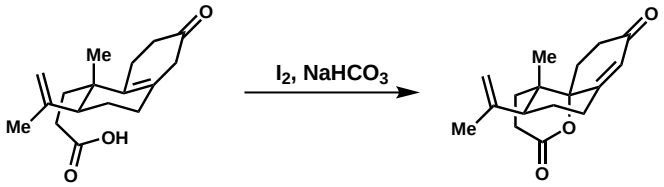

(4a*S,5*S**,11a*R**)-4a-methyl-5-(prop-1-en-2-yl)-3,4,4a,5,6,7,10,11-octahydrobenzo[*i*]-chromene-2,9-dione (3.154)**: β,γ-unsaturated ketone **3.195** (≤0.830 g, ≤3.00 mmol) was diluted with 21 mL DCM and 21 mL THF. Iodine (0.879 g, 3.46 mmol) was added immediately followed by 32 mL of saturated aqueous $NaHCO_3$. The resultant brown reaction mixture was stirred for 2-24 h shielded from light. The excess iodine was quenched with 30 mL of saturated aqueous $Na_2S_2O_3$, the reaction mixture was diluted with 40 mL DCM, the aqueous phase was separated and extracted 2 x 20mL DCM. The combined organic phases were dried with Na_2SO_4, filtered through cotton, and concentrated *in vacuo* to give a crude mixture of **3.195** and the conjugated isomer of **3.194**. Purification by column chromatography gave the desired enone **3.154** as a yellow solid (0.179 g, 22% Yield over two steps). Alternatively, employing Dowex resin in the synthesis of **3.193** and further carrying forward the crude β,γ-unsaturated ketone **3.195**, **3.154** was obtained in 26% yield over six steps from **3.192**. ^{1}H NMR (600 MHz, $CDCl_3$) δ 5.95 (s, 1H), 5.02 (s, 1H), 4.82 (s, 1H), 2.76–2.59 (m, 5H), 2.43–2.32 (m, 3H), 2.16–2.12 (m, 1H), 1.93–1.85 (m, 3H), 1.81 (s, 3H), 1.00 (s, 3H); ^{13}C NMR (125 MHz, $CDCl_3$) δ 197.8, 170.6, 155.7, 144.8, 128.5, 116.0, 84.2, 43.9, 39.0, 33.5, 31.7, 29.2, 27.0, 26.3, 26.1, 23.9, 18.7; HRMS (ESI/MeOH) *m* / *z* calcd for $C_{17}H_{22}O_3Na$ $(M+Na)^+$ 297.1467, found 297.1477.

Bibliography

(1) Gersch, M.; Kreuzer, J.; Sieber, S. A. *Nat. Prod. Rep.* **2012**, *29*, 659–682.

(2) Coates, R. M.; Cavender, P. L. *J. Am. Chem. Soc.* **1980**, *102*, 6358–6359.

(3) Roy, A.; Roberts, F. G.; Wilderman, P. R.; Zhou, K.; Peters, R. J.; Coates, R. M. *J. Am. Chem. Soc.* **2007**, *129*, 12453–12460.

(4) Xu, M.; Wilderman, P. R.; Peters, R. J. *Proc. Natl. Acad. Sci. U.S.A.* **2007**, *104*, 7397–7401.

(5) Fischbach, M. A.; Clardy, J. *Nat Chem Biol* **2007**, *3*, 353–355.

(6) Fraga, B. M.; Gonzalez, P.; Gonzalez-Vallejo, V.; Guillermo, R.; Diaz, L. N. *Phytochemistry* **2010**, *71*, 1313–1321.

(7) Hong, Y. J.; Tantillo, D. J. *Nat. Chem.* **2009**, *1*, 384–389.

(8) Hong, Y. J.; Tantillo, D. J. *J. Am. Chem. Soc.* **2010**, *132*, 5375–5386.

(9) Mishra, N. C.; Estensen, R. D.; Abdel-Monem, M. M. *Journal of Chromatography A* **1986**, *369*, 435–439.

(10) Barton, D. H. R.; Kirby, G. W.; Steglich, W.; Thomas, G. M.; Battersby, A. R.; Dobson, T. A.; Ramuz, H. *J. Chem. Soc.* **1965**, 2423–2438.

(11) Baccelli, C.; Block, S.; Holle, B. V.; Schanck, A.; Chapon, D.; Tinant, B.; Meervelt, L. V.; Morel, N.; Quetin-Leclercq, J. *Planta Med.* **2005**, *71*, 1036–1039.

(12) Vasconcelos, M. A.; Arruda, F. V. S.; Santos, H. S.; Rodrigues, A. S.; Bandeira, P. N.; Albuquerque, M. R. J. R.; Cavada, B. S.; Teixeira, E. H.; Henriques, M.; Pereira, M. O. *Industrial Crops and Products* **2014**, *61*, 499–509.

(13) Rakotonandrasana, O. L.; Raharinjato, F. H.; Rajaonarivelo, M.; Dumontet, V.; Martin, M.-T.; Bignon, J.; Rasoanaivo, P. *J. Nat. Prod.* **2010**, *73*, 1730–1733.

(14) Breitler, S.; Carreira, E. M. *Angew. Chem. Int. Ed.* **2013**, *52*, 11168–11171.

(15) Barisic, M.; e Sousa, R. S.; Tripathy, S. K.; Magiera, M. M.; Zaytsev, A. V.; Pereira, A. L.; Janke, C.; Grishchuk, E. L.; Maiato, H. *Science* **2015**, *348*, 799–803.

(16) Fonrose, X.; Ausseil, F.; Soleilhac, E.; Masson, V.; David, B.; Pouny, I.; Cintrat, J.-C.; Rousseau, B.; Barette, C.; Massiot, G.; Lafanechère, L. *Cancer Res.* **2007**, *67*, 3371–3378.

(17) Jayasuriya, H.; Herath, K.; Zhang, C.; Zink, D.; Basilio, A.; Genilloud, O.; Diez, M.; Vicente, F.; Gonzalez, I.; Salazar, O.; Pelaez, F.; Cummings, R.; Ha, S.; Wang, J.; Singh, S. *Angew. Chem. Int. Ed.* **2007**, *46*, 4684–4688.

(18) Ishiuchi, K.; Kubota, T.; Hayashi, S.; Shibata, T.; Kobayashi, J. *Tetrahedron Lett.* **2009**, *50*, 6534–6536.

(19) Wang, Z. C.; Lin, Y.; Feng, D. Q.; Ke, C. H.; Lin, P.; Yan, C. L.; Chen, J. D. *Molecules* **2009**, *14*, 414–422.

(20) Spangler, J. E.; Sorensen, E. J. *Tetrahedron* **2009**, *65*, 6739–6745.

(21) Ihara, M.; Toyota, M.; Fukumoto, K.; Kametani, T. *Tetrahedron Lett.* **1984**, *25*, 2167–2170.

(22) Ihara, M.; Toyota, M.; Fukumoto, K.; Kametani, T. *Tetrahedron Lett.* **1984**, *25*, 3235–3238.

(23) Ihara, M.; Suzuki, M.; Fukumoto, K.; Kametani, T.; Kabuto, C. *J. Am. Chem. Soc.* **1988**, *110*, 1963–1964.

(24) Ihara, M.; Hirabayashi, A.; Taniguchi, N.; Fukumoto, K. *Tetrahedron* **1992**, *48*, 5089–5098.

(25) Ihara, M.; Toyota, M.; Fukumoto, K.; Kametani, T. *J. Chem. Soc., Perkin Trans. 1* **1986**, 2151–2161.

(26) Sondheimer, F.; Elad, D. *J. Am. Chem. Soc.* **1957**, *79*, 5542–5546.

(27) Nemoto, H.; Hashimoto, M.; Kurobe, H.; Fukumoto, K.; Kametani, T. *J. Chem. Soc., Perkin Trans. 1* **1985**, 927–934.

(28) Nicolaou, K. C.; Tria, G.; Edmonds, D. *Angew. Chem. Int. Ed.* **2008**, *47*, 1780–1783.

(29) Nicolaou, K. C.; Toh, Q.-Y.; Chen, D. Y.-K. *J. Am. Chem. Soc.* **2008**, *130*, 11292–11293.

(30) Singh, V.; Sahu, P. K.; Sahu, B. C.; Mobin, S. M. *J. Org. Chem.* **2009**, *74*, 6092–6104.

(31) Singh, V.; Das, B.; Mobin, S. M. *Synlett* **2013**, *24*, 1583–1587.

(32) Singh, V.; Bhalerao, P.; Sahu, B. C.; Mobin, S. M. *Tetrahedron* **2013**, *69*, 137–146.

(33) Singh, V.; Sahu, B. C.; Bansal, V.; Mobin, S. M. *Org. Biomol. Chem.* **2010**, *8*, 4472–4481.

(34) Austin, K. A. B.; Banwell, M. G.; Willis, A. C. *Org. Lett.* **2008**, *10*, 4465–4468.

(35) Chang, E. L.; Schwartz, B. D.; Draffan, A. G.; Banwell, M. G.; Willis, A. C. *Chem. Asian J.* **2015**, *10*, 427–439.

(36) Ushakov, D. B.; Maier, M. E. *Synlett* **2013**, *24*, 705–708.

(37) Moustafa, G. A. I.; Saku, Y.; Aoyama, H.; Yoshimitsu, T. *Chem. Commun.* **2014**, *50*, 15706–15709.

(38) Barykina, O. V.; Rossi, K. L.; Rybak, M. J.; Snider, B. B. *Org. Lett.* **2009**, *11*, 5334–5337.

(39) Toyota, M.; Wada, T.; Fukumoto, K.; Ihara, M. *J. Am. Chem. Soc.* **1998**, *120*, 4916–4925.

(40) Toyota, M.; Wada, T.; Ihara, M. *J. Org. Chem.* **2000**, *65*, 4565–4570.

(41) Toyota, M.; Asano, T.; Ihara, M. *Org. Lett.* **2005**, *7*, 3929–3932.

(42) Nicolaou, K. C.; Tria, G. S.; Edmonds, D. J.; Kar, M. *J. Am. Chem. Soc.* **2009**, *131*, 15909–15917.

(43) Varseev, G.; Maier, M. *Angew. Chem. Int. Ed.* **2009**, *48*, 3685–3688.

(44) Yoshimitsu, T.; Nojima, S.; Hashimoto, M.; Tanaka, T. *Org. Lett.* **2011**, *13*, 3698–3701.

(45) Toyota, M.; Yokota, M.; Ihara, M. *J. Am. Chem. Soc.* **2001**, *123*, 1856–1861.

(46) Toyota, M.; Yokota, M.; Ihara, M. *Org. Lett.* **1999**, *1*, 1627–1629.

(47) Yun, S.; Zheng, J.-C.; Lee, D. *Angew. Chem. Int. Ed.* **2008**, *47*, 6201–6203.

(48) Hayashida, J.; Rawal, V. *Angew. Chem. Int. Ed.* **2008**, *47*, 4373–4376.

(49) Ghosh, A.; Xi, K. *Angew. Chem. Int. Ed.* **2009**, *48*, 5372–5375.

(50) Palanichamy, K.; Subrahmanyam, A. V.; Kaliappan, K. P. *Org. Biomol. Chem.* **2011**, *9*, 7877–7886.

(51) Yadav, J. S.; Goreti, R.; Pabbaraja, S.; Sridhar, B. *Org. Lett.* **2013**, *15*, 3782–3785.

(52) Li, P.; Yamamoto, H. *Chem. Commun.* **2010**, *46*, 6294–6295.

(53) Cherney, E. C.; Lopchuk, J. M.; Green, J. C.; Baran, P. S. *J. Am. Chem. Soc.* **2014**, 12592–12595.

(54) Isayama, S.; Mukaiyama, T. *Chem. Lett.* **1989**, *18*, 1071–1074.

(55) Abad, A.; Agulló, C.; Cuñat, A. C.; Navarro, I. *Tetrahedron Lett.* **2001**, *42*, 8965–8968.

(56) Abad, A.; Agulló, C.; Cuñat, A. C.; Navarro, I.; de Arellano, M. C. R. *Synlett* **2001**, *2001*, 349–352.

(57) Abad, A.; Agulló, C.; Cuñat, A. C.; de Alfonso Marzal, I.; Navarro, I.; Gris, A. *Tetrahedron* **2006**, *62*, 3266–3283.

(58) Abad, A.; Agulló, C.; Cuñat, A. C.; de Alfonso Marzal, I.; Gris, A.; Navarro, I.; Ramírez de Arellano, C. *Tetrahedron* **2007**, *63*, 1664–1679.

(59) Waalboer, D.; Schaapman, M.; van Delft, F.; Rutjes, F. *Angew. Chem. Int. Ed.* **2008**, *47*, 6576–6578.

(60) Tiefenbacher, K.; Mulzer, J. *Angew. Chem. Int. Ed.* **2008**, *47*, 6199–6200.

(61) Tiefenbacher, K.; Mulzer, J. *J. Org. Chem.* **2009**, *74*, 2937–2941.

(62) Gong, J.; Chen, H.; Liu, X.-Y.; Wang, Z.-X.; Nie, W.; Qin, Y. *Nat. Commun.* **2016**, *7*, 12183.

(63) Zhao, J.-F.; Zhao, Y.-J.; Loh, T.-P. *Chem. Commun.* **2008**, 1353–1355.

(64) Tamura, M.; Kochi, J. *Synthesis* **1971**, *1971*, 303–305.

(65) Backvall, J.-E.; Sellen, M. *J. Chem. Soc. Chem. Commun.* **1987**, 827.

(66) Gansauer, A.; Justicia, J.; Rosales, A.; Rinker, B. *Synlett* **2005**, 1954–1956.

(67) Gansauer, A.; Justicia, J.; Rosales, A.; Worgull, D.; Rinker, B.; Cuerva, J. M.; Oltra, J. E. *Eur. J. Org. Chem.* **2006**, *2006*, 4115–4127.

(68) Baker, B. A.; Bošković, Ž. V.; Lipshutz, B. H. *Org. Lett.* **2008**, *10*, 289–292.

(69) Deutsch, C.; Krause, N.; Lipshutz, B. H. *Chem. Rev.* **2008**, *108*, 2916–2927.

(70) Grushin, V. V. *Organometallics* **2001**, *20*, 3950–3961.

(71) Breit, B.; Schmidt, Y. *Chem. Rev.* **2008**, *108*, 2928–2951.

(72) Harutyunyan, S. R.; den Hartog, T.; Geurts, K.; Minnaard, A. J.; Feringa, B. L. *Chem. Rev.* **2008**, *108*, 2824–2852.

(73) Alexakis, A.; Bäckvall, J. E.; Krause, N.; Pàmies, O.; Diéguez, M. *Chem. Rev.* **2008**, *108*, 2796–2823.

(74) Lipshutz, B. H. *Tetrahedron Lett.* **1983**, *24*, 127–130.

(75) Lipshutz, B. H.; Ellsworth, E. L.; Dimock, S. H.; Smith, R. A. J. *J. Am. Chem. Soc.* **1990**, *112*, 4404–4410.

(76) Lipshutz, B. H.; Hackmann, C. *J. Org. Chem.* **1994**, *59*, 7437–7444.

(77) Lipshutz, B. H.; Huang, S.; Leong, W. W. Y.; Zhong, G.; Isley, N. A. *J. Am. Chem. Soc.* **2012**, *134*, 19985–19988.

(78) Yamamoto, Y.; Yamada, S.; Nishiyama, H. *Chem. Eur. J.* **2012**, *18*, 3153–3156.

(79) Paquette, L. A. *Synlett* **1990**, *1990*, 67–73.

(80) Paquette, L. A. *Tetrahedron* **1997**, *53*, 13971–14020.

(81) Nielsen, D. K.; Nielsen, L. L.; Jones, S. B.; Toll, L.; Asplund, M. C.; Castle, S. L. *J. Org. Chem.* **2009**, *74*, 1187–1199.

(82) Lee, P. H.; Seomoon, D.; Kim, S.; Nagaiah, K.; Damle, S. V.; Lee, K. *Synthesis* **2003**, 2189–2193.

(83) Lee, P. H.; Ahn, H.; Lee, K.; Sung, S.-y.; Kim, S. *Tetrahedron Lett.* **2001**, *42*, 37–39.

(84) Rossiter, B. E.; Swingle, N. M. *Chem. Rev.* **1992**, *92*, 771–806.

(85) Takuwa, A.; Nishigaichi, Y.; Iwamoto, H. *Chem. Lett.* **1991**, *20*, 1013–1016.

(86) Cherney, E. C.; Green, J. C.; Baran, P. S. *Angew. Chem. Int. Ed.* **2013**, *52*, 9019–9022.

(87) Kennedy-Smith, J. J.; Staben, S. T.; Toste, F. D. *J. Am. Chem. Soc.* **2004**, *126*, 4526–4527.

(88) Gao, Q.; Zheng, B.-F.; Li, J.-H.; Yang, D. *Org. Lett.* **2005**, *7*, 2185–2188.

(89) Corkey, B. K.; Toste, F. D. *J. Am. Chem. Soc.* **2005**, *127*, 17168–17169.

(90) Xiao, Y.-P.; Liu, X.-Y.; Che, C.-M. *Angew. Chem. Int. Ed.* **2011**, *50*, 4937–4941.

(91) Snider, B. B. *Tetrahedron* **2009**, *65*, 10738–10744.

(92) Haney, B. P.; Curran, D. P. *J. Org. Chem.* **2000**, *65*, 2007–2013.

(93) Dombroski, M. A.; Kates, S. A.; Snider, B. B. *J. Am. Chem. Soc.* **1990**, *112*, 2759–2767.

(94) Curry, L.; Hallside, M. S.; Powell, L. H.; Sprague, S. J.; Burton, J. W. *Tetrahedron* **2009**, *65*, 10882–10892.

(95) Cossy, J.; Bouzide, A. *Tetrahedron* **1999**, *55*, 6483–6496.

(96) Zhou, N.; Xie, T.; Liu, L.; Xie, Z. *J. Org. Chem.* **2014**, *79*, 6061–6068.

(97) Cossy, J.; Bouzide, A.; Leblanc, C. *J. Org. Chem.* **2000**, *65*, 7257–7265.

(98) Bouhlel, A.; Curti, C.; Dumètre, A.; Laget, M.; Crozet, M. D.; Azas, N.; Vanelle, P. *Bioorg. Med. Chem.* **2010**, *18*, 7310–7320.

(99) Logan, A. W. J.; Sprague, S. J.; Foster, R. W.; Marx, L. B.; Garzya, V.; Hallside, M. S.; Thompson, A. L.; Burton, J. W. *Org. Lett.* **2014**, *16*, 4078–4081.

(100) Curti, C.; Crozet, M. D.; Vanelle, P. *Tetrahedron* **2009**, *65*, 200–205.

(101) Wong, Y.-C.; Kao, T.-T.; Huang, J.-K.; Jhang, Y.-W.; Chou, M.-C.; Shia, K.-S. *Adv. Synth. Catal.* **2014**, *356*, 3025–3038.

(102) O'Neil, S. V.; Quickley, C. A.; Snider, B. B. *J. Org. Chem.* **1997**, *62*, 1970–1975.

(103) Liu, X.; Wang, L.; Zou, J. *Chin. J. Chem.* **2011**, *29*, 2097–2100.

(104) Logan, A. W.; Parker, J. S.; Hallside, M. S.; Burton, J. W. *Org. Lett.* **2012**, *14*, 2940–2943.

(105) Keane, H. A.; Hess, W.; Burton, J. W. *Chem. Commun.* **2012**, *48*, 6496–6498.

(106) Davies, J. J.; Krulle, T. M.; Burton, J. W. *Org. Lett.* **2010**, *12*, 2738–2741.

(107) Powell, L. H.; Docherty, P. H.; Hulcoop, D. G.; Kemmitt, P. D.; Burton, J. W. *Chem. Commun.* **2008**, 2559–2561.

(108) Snider, B. B.; Merritt, J. E.; Dombroski, M. A.; Buckman, B. O. *J. Org. Chem.* **1991**, *56*, 5544–5553.

(109) Arai, M.; Lipshutz, B. H.; Nakamura, E. *Tetrahedron* **1992**, *48*, 5709–5718.

(110) Paquette, L. A.; Sturino, C. F.; Wang, X.; Prodger, J. C.; Koh, D. *J. Am. Chem. Soc.* **1996**, *118*, 5620–5633.

(111) Tian, Y.; Xu, X.; Zhang, L.; Qu, J. *Org. Lett.* **2016**, *18*, 268–271.

(112) Stork, G.; Meisels, A.; Davies, J. E. *J. Am. Chem. Soc.* **1963**, *85*, 3419–3425.

(113) Prestwich, G. D.; Labovitz, J. N. *J. Am. Chem. Soc.* **1974**, *96*, 7103–7105.

Appendix A:

NMR Data for Chapter 1

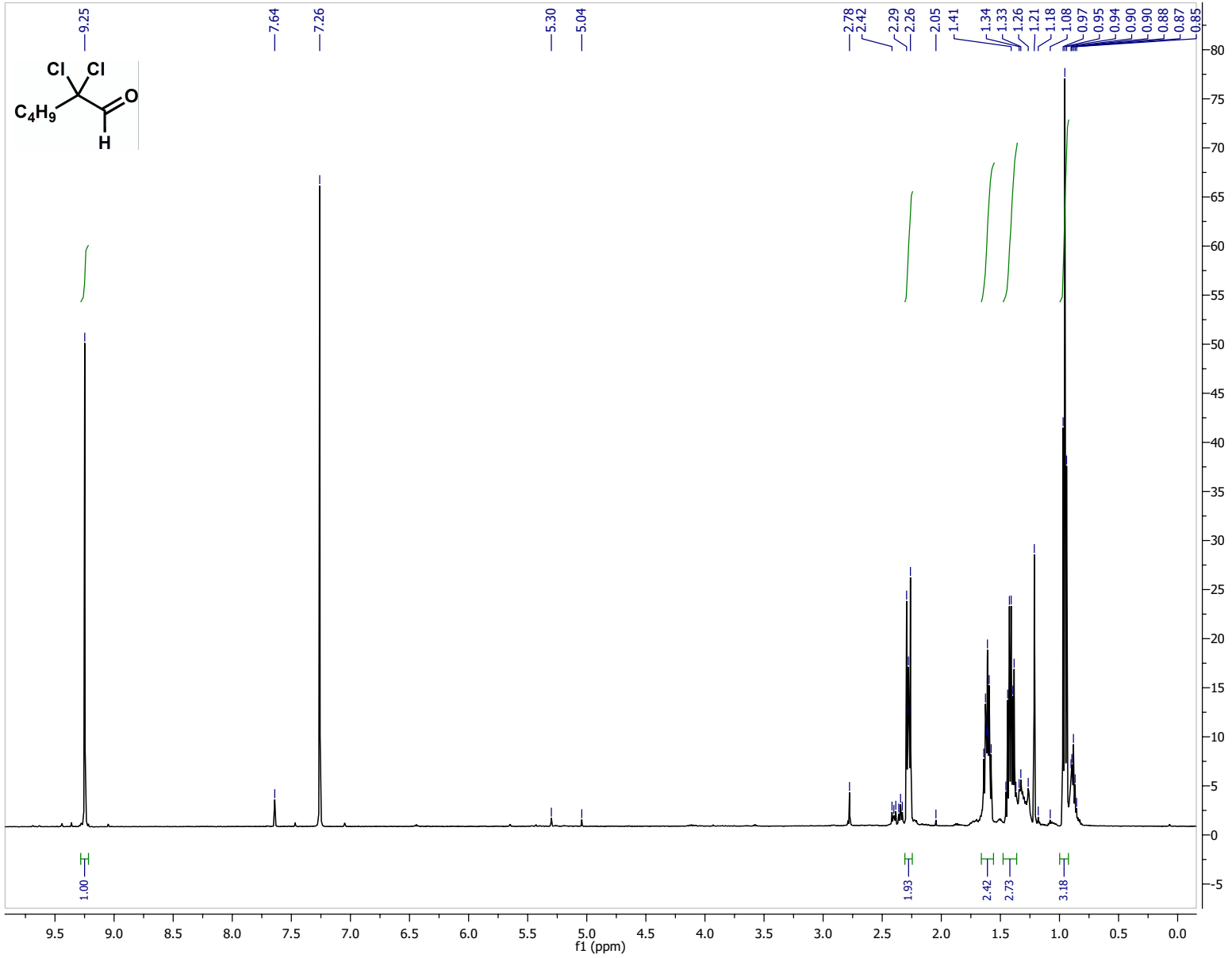
9.25
7.64
7.26
5.30
5.04
2.78
2.42
2.29
2.26
2.05
1.41
1.34
1.33
1.26
1.21
1.18
1.08
0.97
0.95
0.94
0.90
0.90
0.88
0.87
0.85
Cl
Cl
O
C4H9
H
1.00
1.93
2.42
2.73
3.18
f1 (ppm)

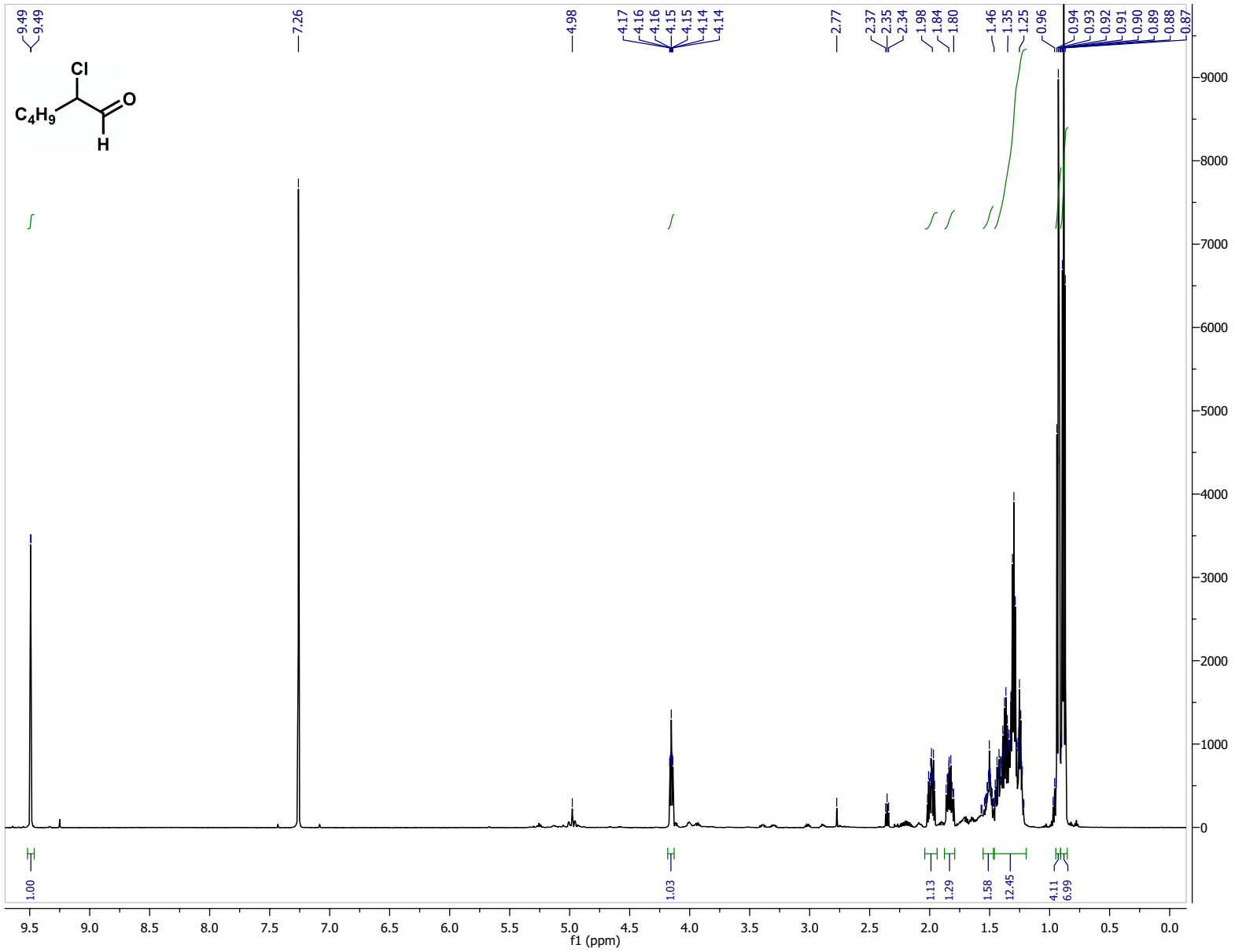
9.49
9.49
7.26
4.98
4.17
4.16
4.16
4.15
4.15
4.14
4.14
2.77
2.37
2.35
2.34
1.98
1.84
1.80
1.46
1.35
1.25
0.96
0.94
0.93
0.92
0.91
0.90
0.89
0.88
0.87
Cl
O
H
C_4H_9
9000
8000
7000
6000
5000
4000
3000
2000
1000
0
1.00
1.03
1.13
1.29
1.58
12.45
4.11
6.99
9.5
9.0
8.5
8.0
7.5
7.0
6.5
6.0
5.5
5.0
4.5
4.0
3.5
3.0
2.5
2.0
1.5
1.0
0.5
0.0
f1 (ppm)

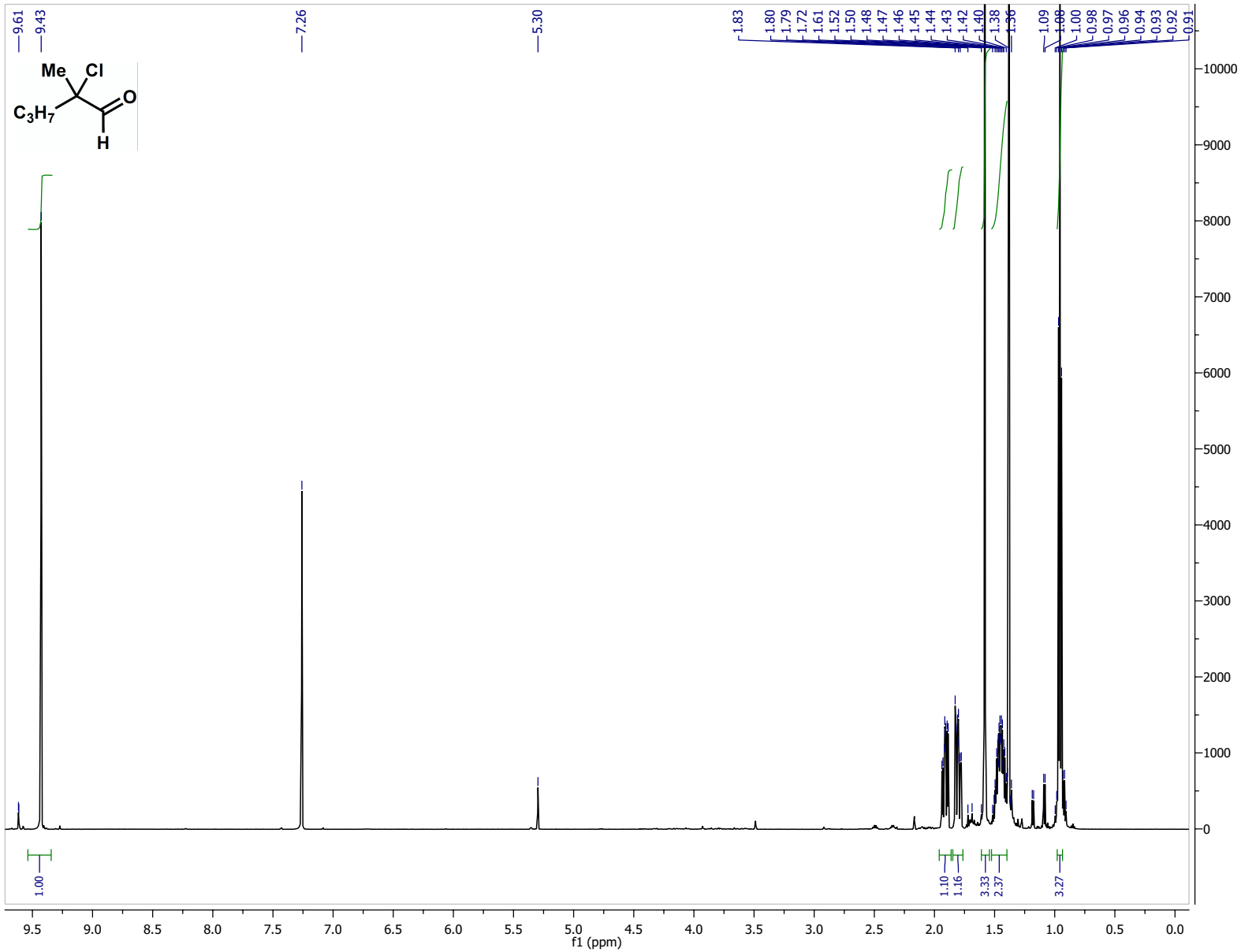
9.61
9.43
7.26
5.30
1.83
1.80
1.79
1.72
1.61
1.52
1.50
1.48
1.47
1.46
1.45
1.44
1.43
1.42
1.40
1.38
1.36
1.09
1.08
1.00
0.98
0.97
0.96
0.94
0.93
0.92
0.91
Me
Cl
C3H7
O
H
10000
9000
8000
7000
6000
5000
4000
3000
2000
1000
0
1.00
1.10
1.16
3.33
2.37
3.27
9.5
9.0
8.5
8.0
7.5
7.0
6.5
6.0
5.5
5.0
4.5
4.0
3.5
3.0
2.5
2.0
1.5
1.0
0.5
0.0
f1 (ppm)

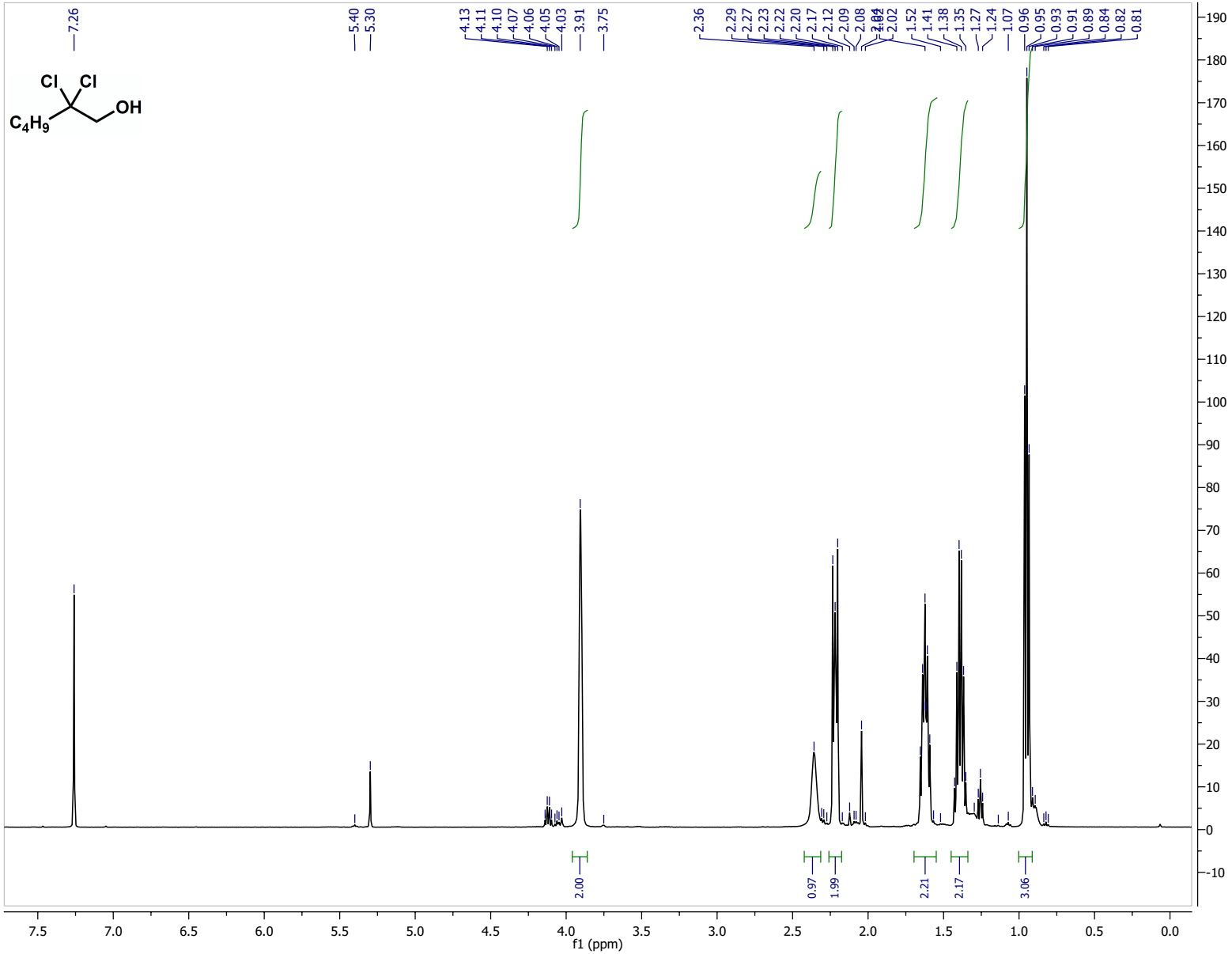
Cl
Cl
OH
C4H9
7.26
5.40
5.30
4.13
4.11
4.10
4.07
4.06
4.05
4.03
3.91
3.75
2.36
2.29
2.27
2.23
2.22
2.20
2.17
2.12
2.09
2.08
2.02
1.52
1.41
1.38
1.35
1.27
1.24
1.07
0.96
0.95
0.93
0.91
0.89
0.84
0.82
0.81
2.00
0.97
1.99
2.21
2.17
3.06
f1 (ppm)

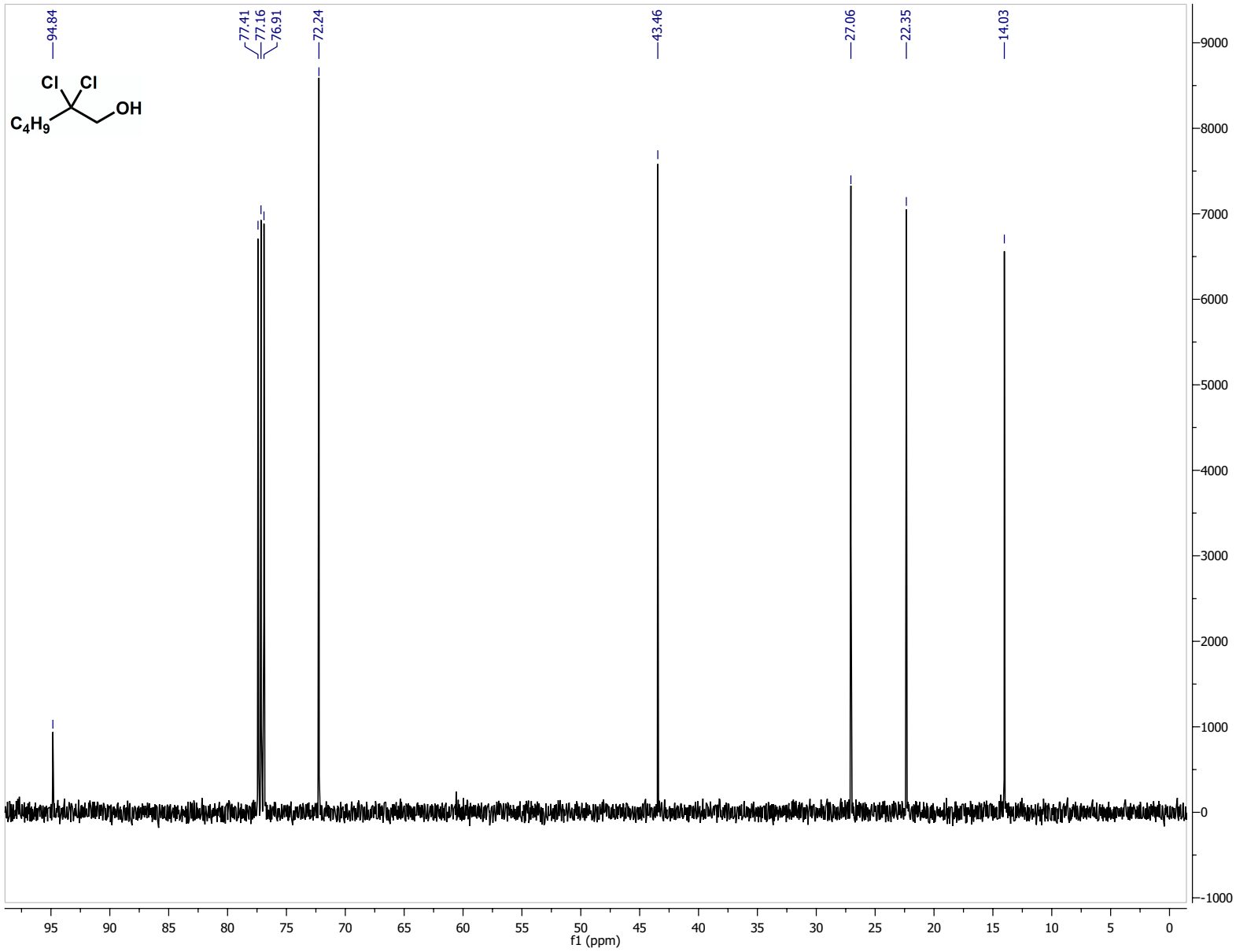
94.84
77.41
77.16
76.91
72.24
43.46
27.06
22.35
14.03
Cl
Cl
OH
C4H9
9000
8000
7000
6000
5000
4000
3000
2000
1000
0
-1000
95
90
85
80
75
70
65
60
55
50
45
40
35
30
25
20
15
10
5
0
f1 (ppm)

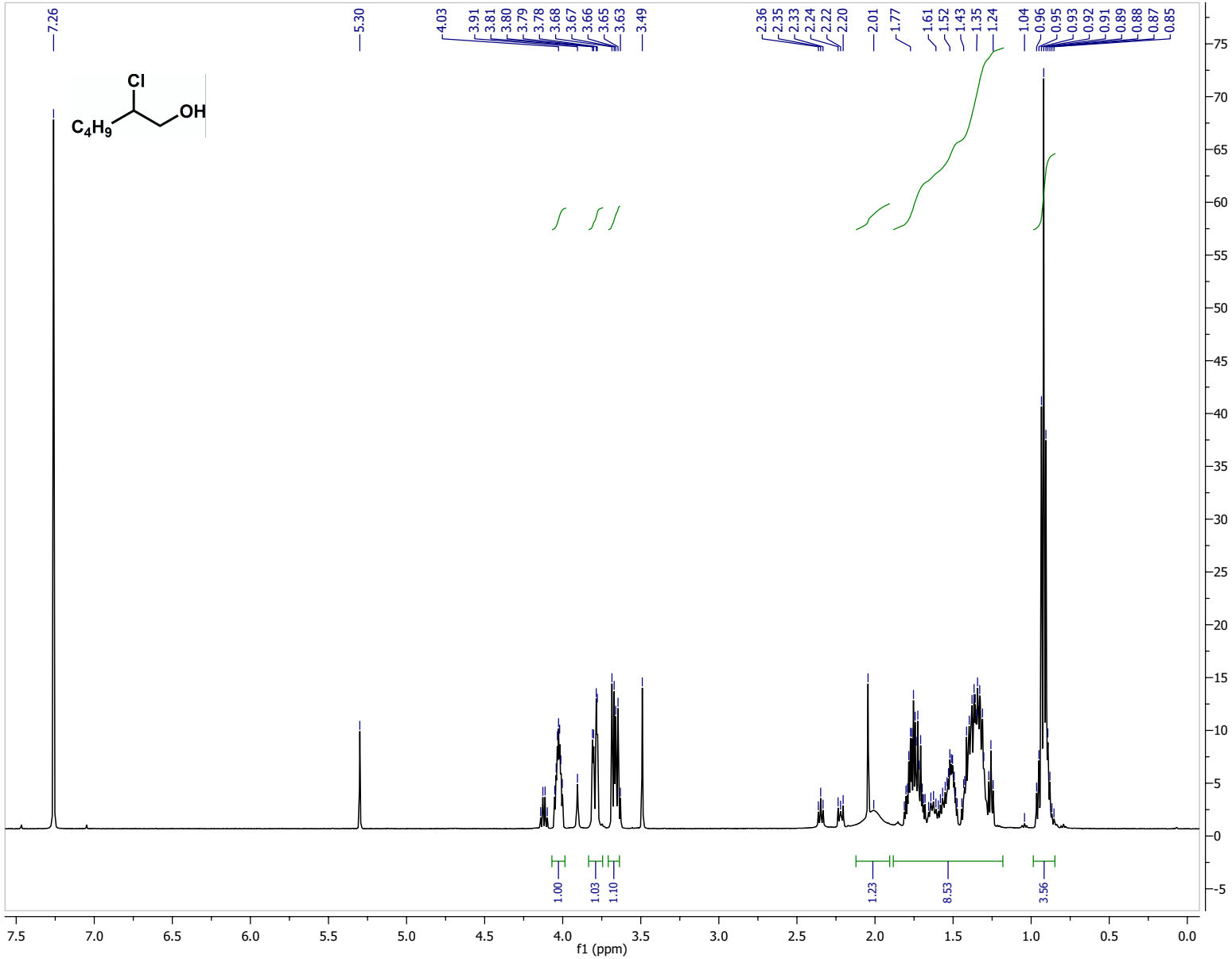
7.26
5.30
4.03
3.91
3.81
3.80
3.79
3.78
3.68
3.67
3.66
3.65
3.63
3.49
2.36
2.35
2.33
2.24
2.22
2.20
2.01
1.77
1.61
1.52
1.43
1.35
1.24
1.04
0.96
0.95
0.93
0.92
0.91
0.89
0.88
0.87
0.85
Cl
OH
C4H9
1.00
1.03
1.10
1.23
8.53
3.56
f1 (ppm)

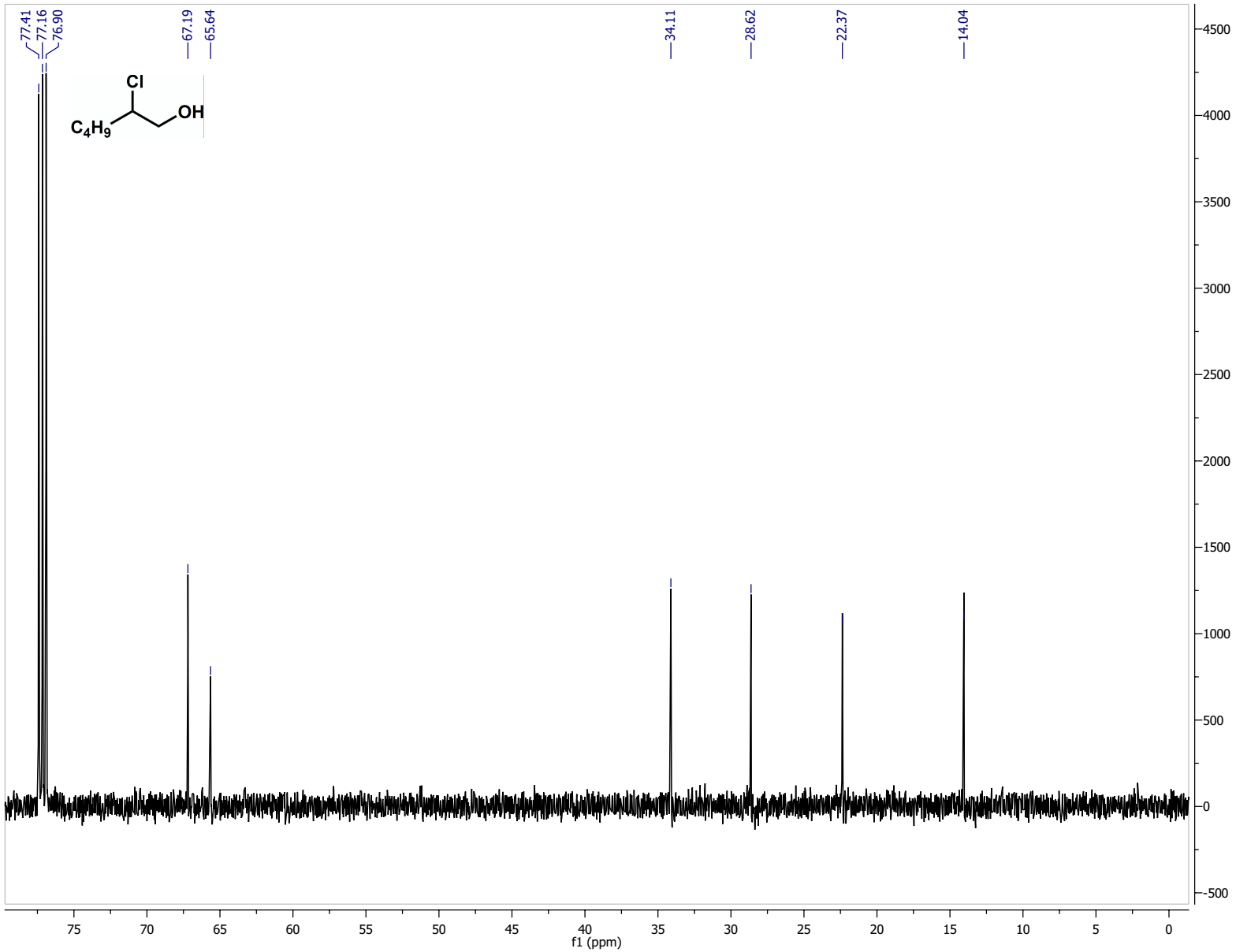
77.41
77.16
76.90
67.19
65.64
34.11
28.62
22.37
14.04
Cl
OH
C_4H_9
4500
4000
3500
3000
2500
2000
1500
1000
500
0
-500
75
70
65
60
55
50
45
40
35
30
25
20
15
10
5
0
f1 (ppm)

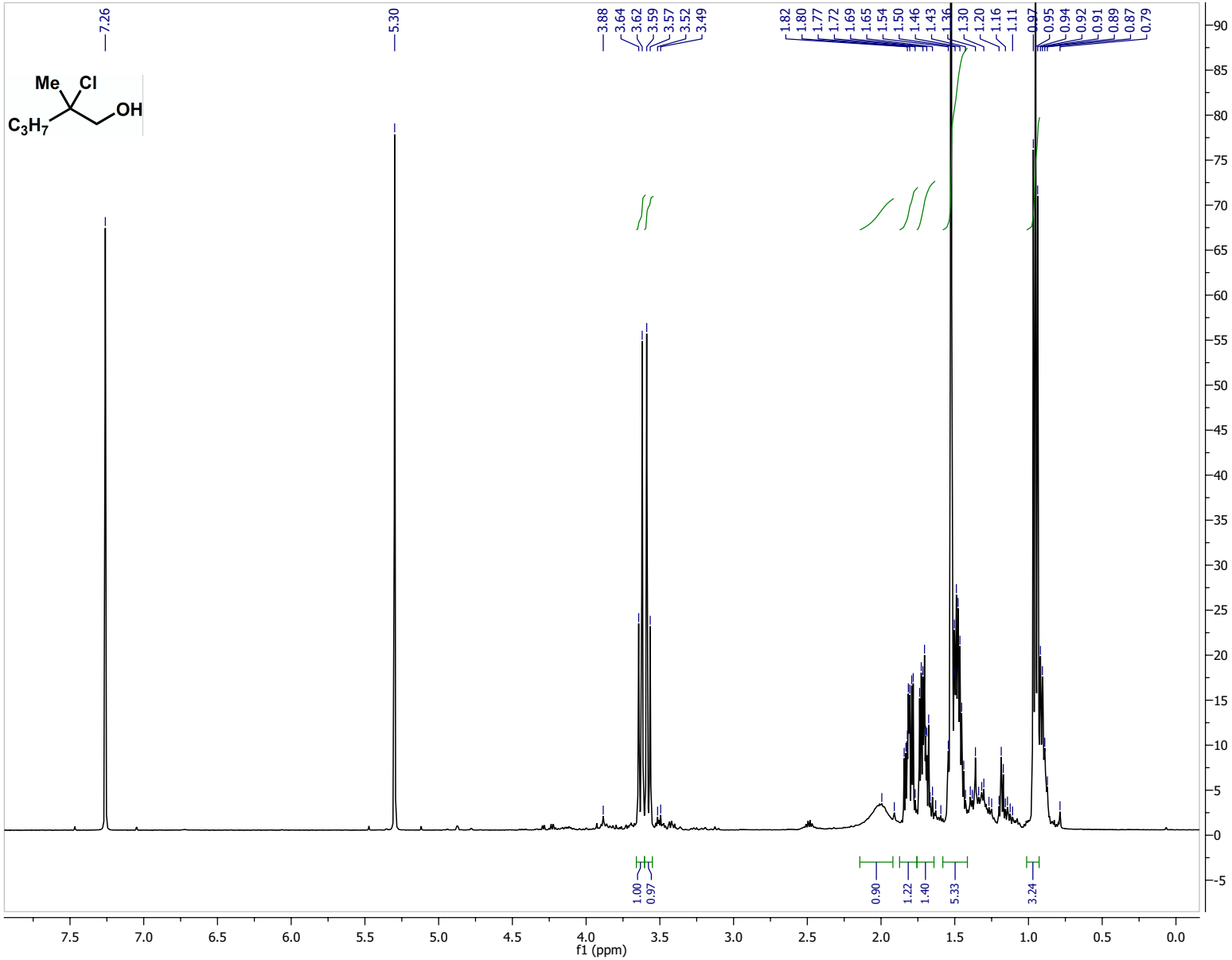
7.26
5.30
3.88
3.64
3.62
3.59
3.57
3.52
3.49
1.82
1.80
1.77
1.72
1.69
1.65
1.54
1.50
1.46
1.43
1.36
1.30
1.20
1.16
1.11
0.92
0.95
0.94
0.92
0.91
0.89
0.87
0.79
Me
Cl
OH
C3H7
1.00
0.97
0.90
1.22
1.40
5.33
3.24
f1 (ppm)

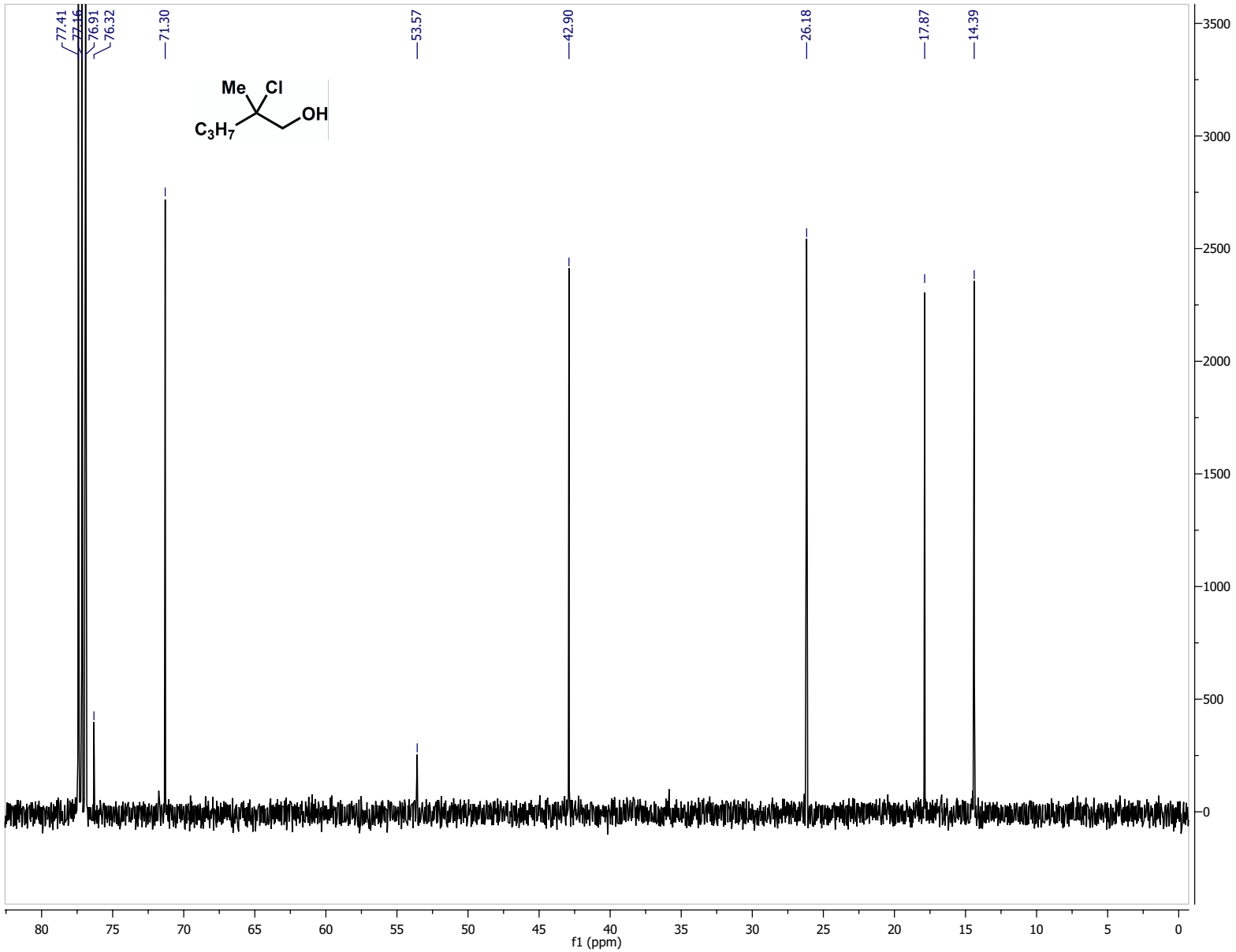
77.41
77.16
76.91
76.32
71.30
53.57
42.90
26.18
17.87
14.39
Me
Cl
OH
C3H7
3500
3000
2500
2000
1500
1000
500
0
80
75
70
65
60
55
50
45
40
35
30
25
20
15
10
5
0
f1 (ppm)

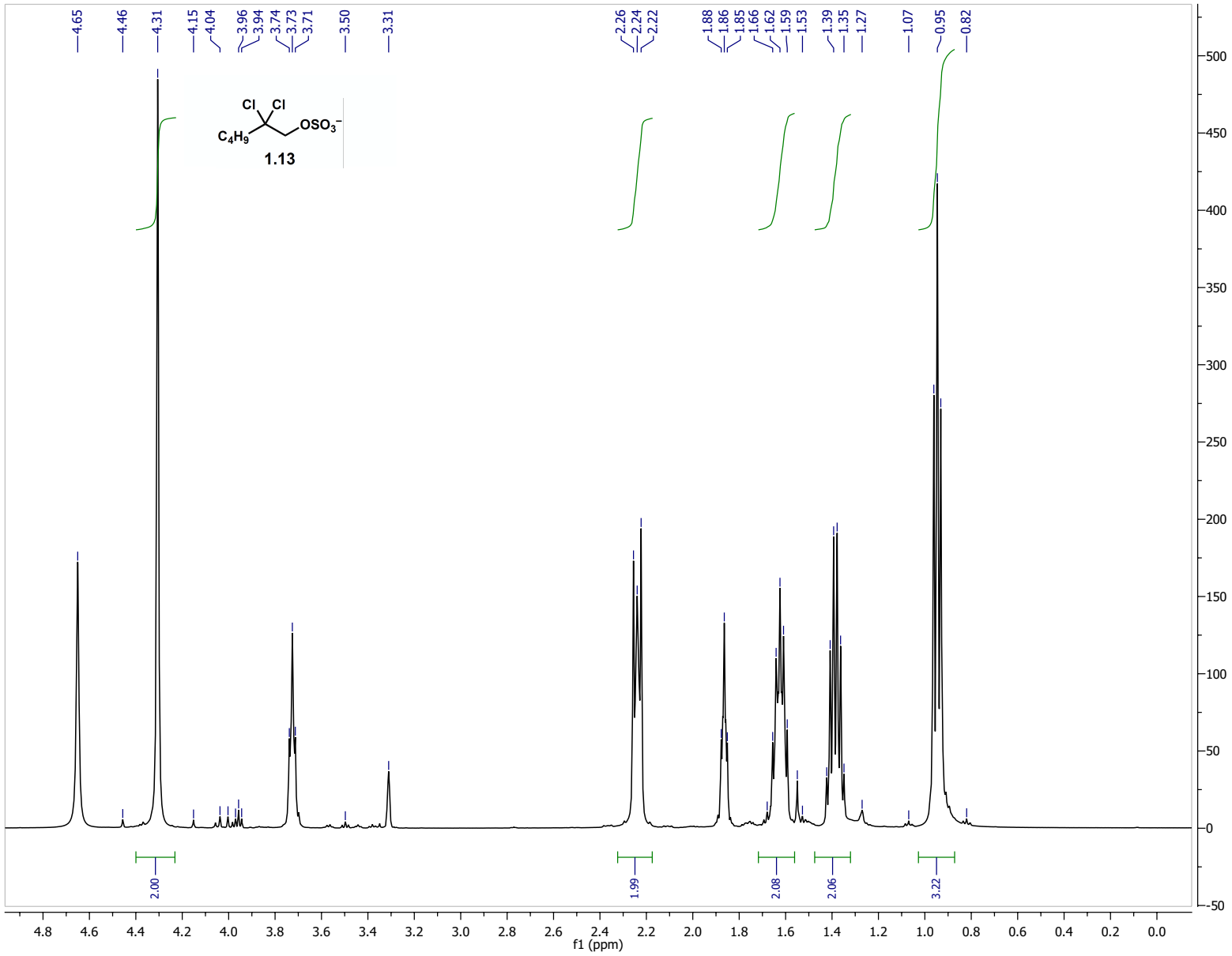
4.65
4.46
4.31
4.15
4.04
3.96
3.94
3.74
3.73
3.71
3.50
3.31
2.26
2.24
2.22
1.88
1.86
1.85
1.66
1.62
1.59
1.53
1.39
1.35
1.27
1.07
0.95
0.82
Cl
Cl
OSO3−
C4H9
1.13
2.00
1.99
2.08
2.06
3.22
f1 (ppm)

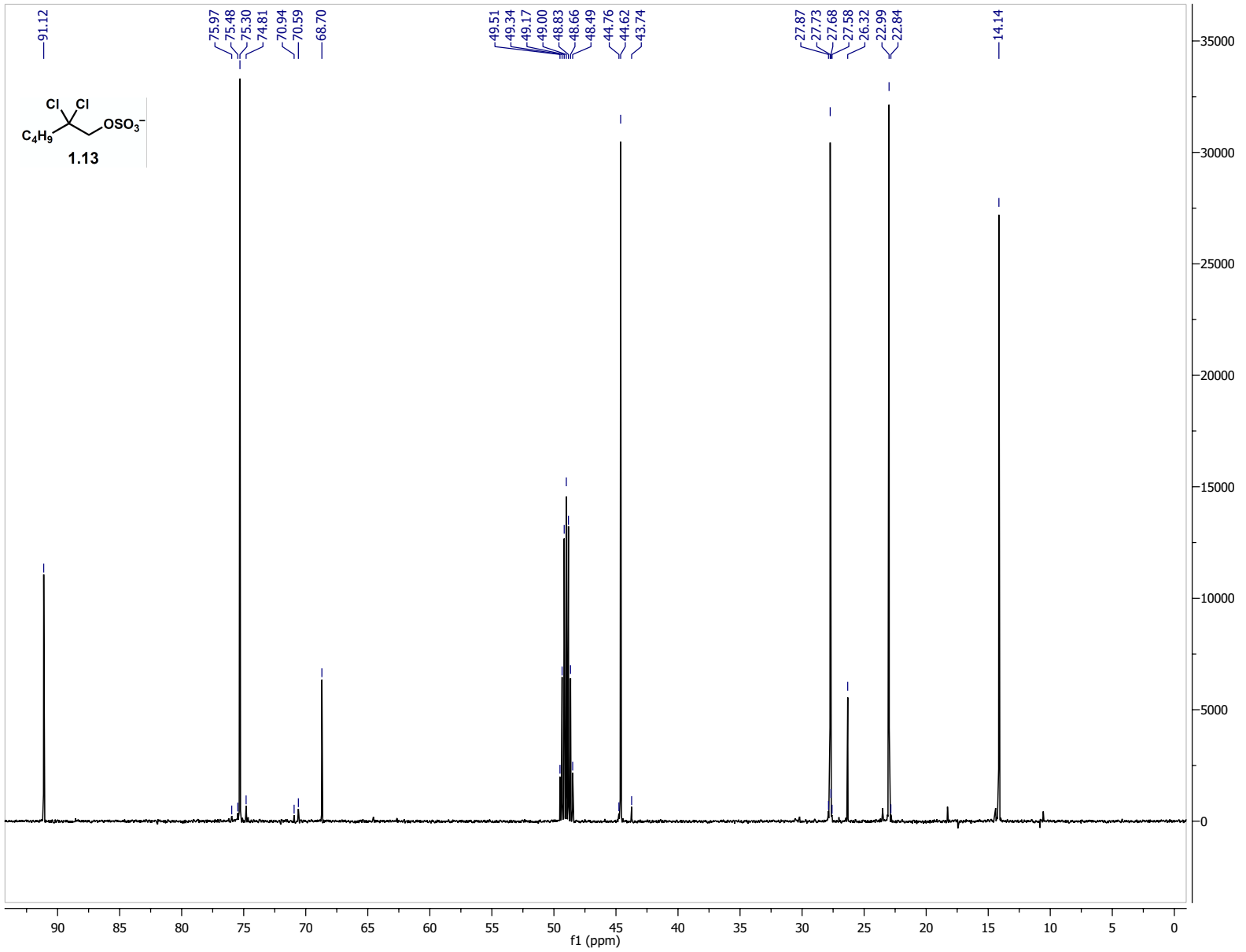
91.12
75.97
75.48
75.30
74.81
70.94
70.59
68.70
49.51
49.34
49.17
49.00
48.83
48.66
48.49
44.76
44.62
43.74
27.87
27.73
27.68
27.58
26.32
22.99
22.84
14.13
Cl
Cl
OSO3−
C4H9
1.13
35000
30000
25000
20000
15000
10000
5000
0
90
85
80
75
70
65
60
55
50
45
40
35
30
25
20
15
10
5
0
f1 (ppm)

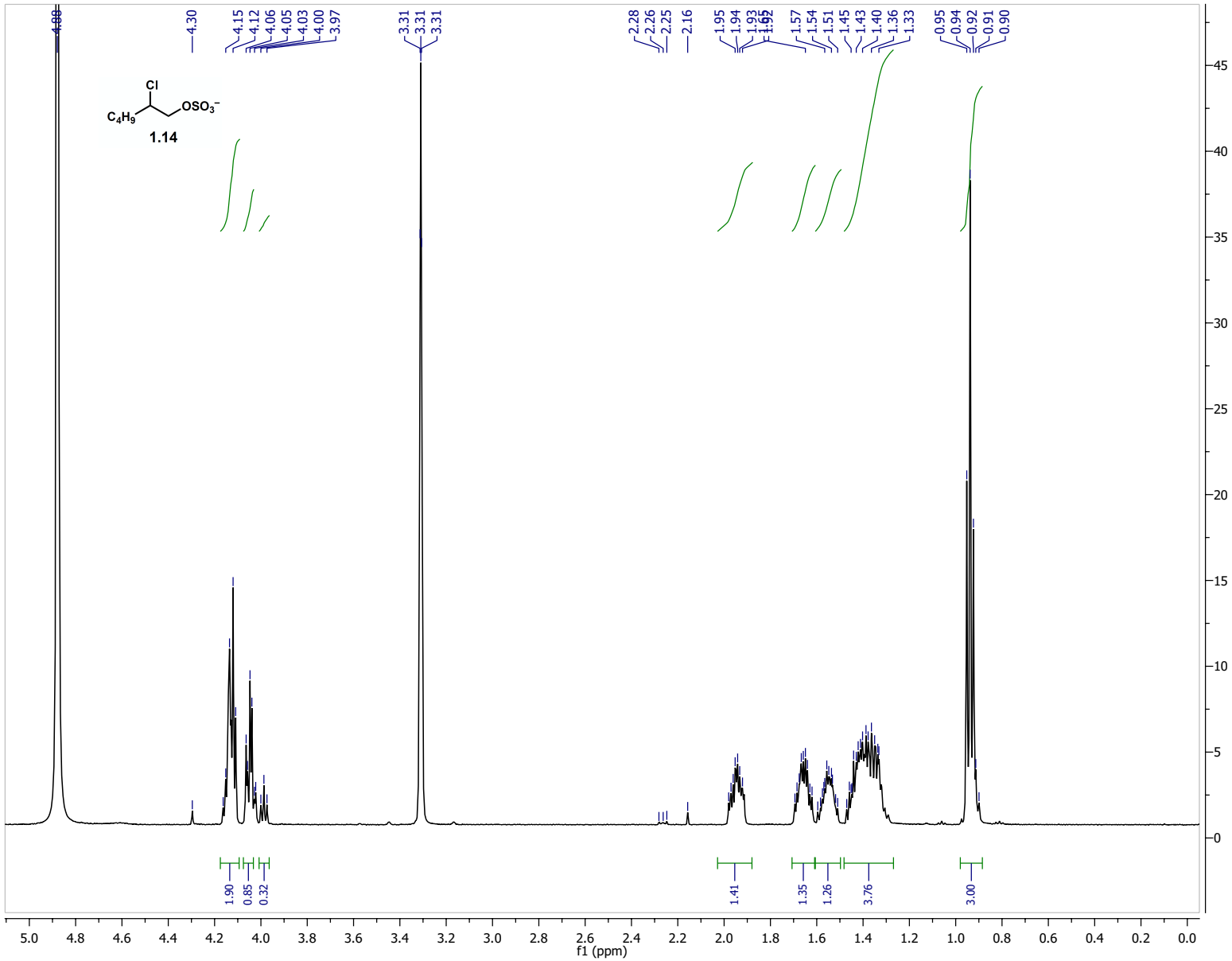
Cl
C_4H_9
OSO_3^-
1.14
4.88
4.30
4.15
4.12
4.06
4.05
4.03
4.00
3.97
3.31
3.31
3.31
2.28
2.26
2.25
2.16
1.95
1.94
1.93
1.57
1.54
1.51
1.45
1.43
1.40
1.36
1.33
0.95
0.94
0.92
0.91
0.90
1.90
0.85
0.32
1.41
1.35
1.26
3.76
3.00
f1 (ppm)

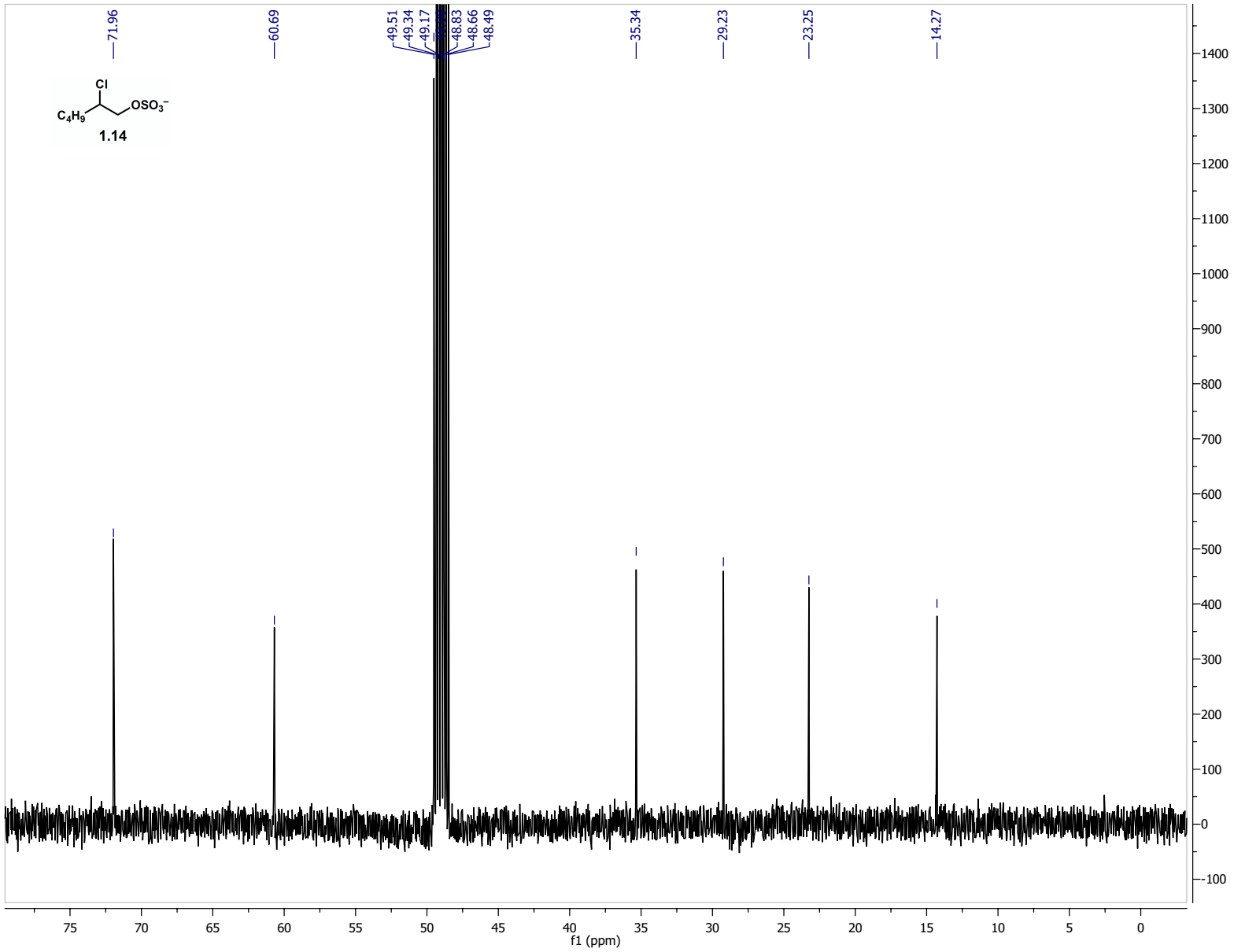
71.96
60.69
49.51
49.34
49.17
48.83
48.66
48.49
35.34
29.23
23.25
14.27
Cl
C4H9
OSO3−
1.14
f1 (ppm)

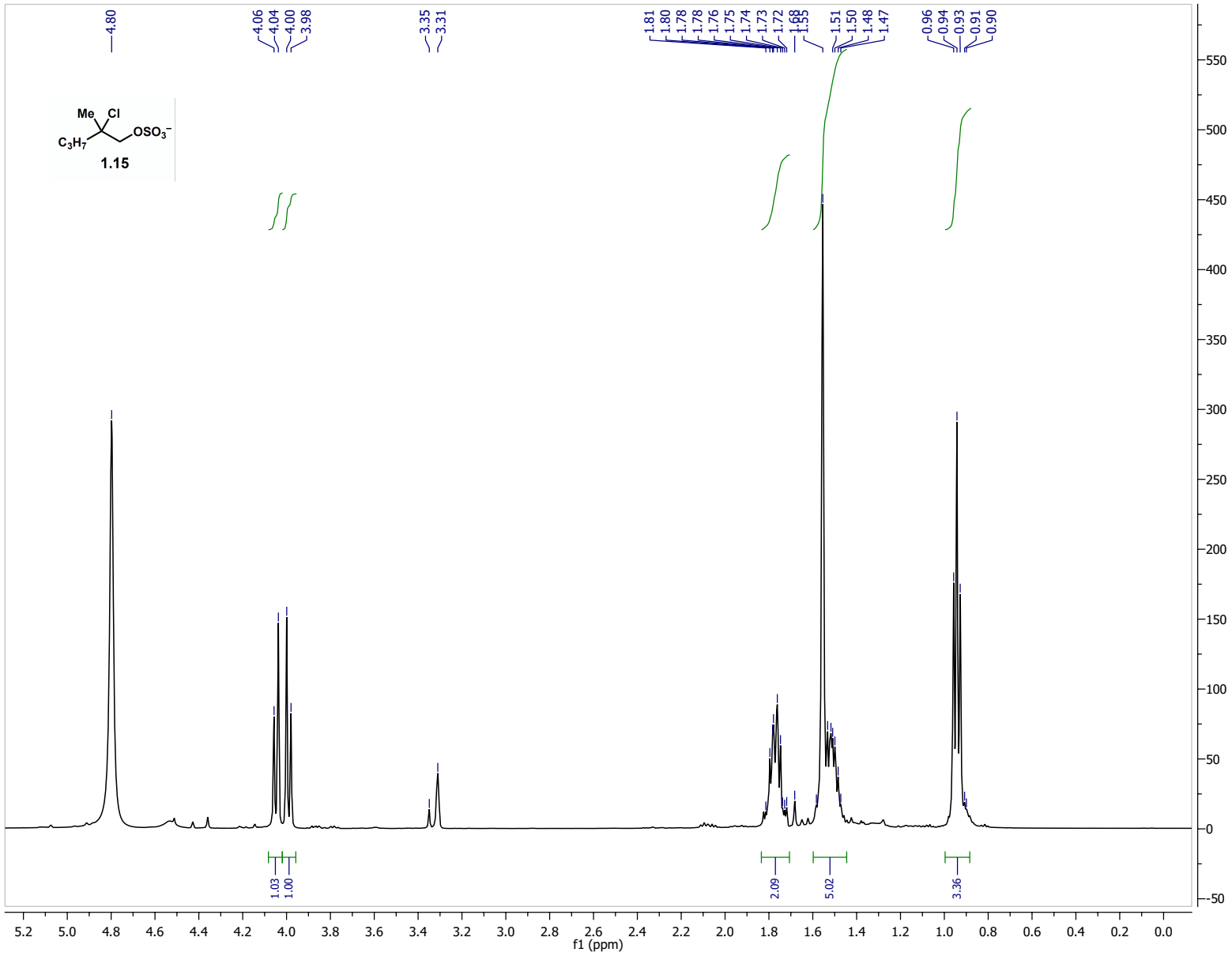
4.80
4.06
4.04
4.00
3.98
3.35
3.31
1.81
1.80
1.78
1.78
1.76
1.75
1.74
1.73
1.72
1.68
1.55
1.51
1.50
1.48
1.47
0.96
0.94
0.93
0.91
0.90
Me
Cl
C_3H_7
OSO_3^-
1.15
1.03
1.00
2.09
5.02
3.36
f1 (ppm)

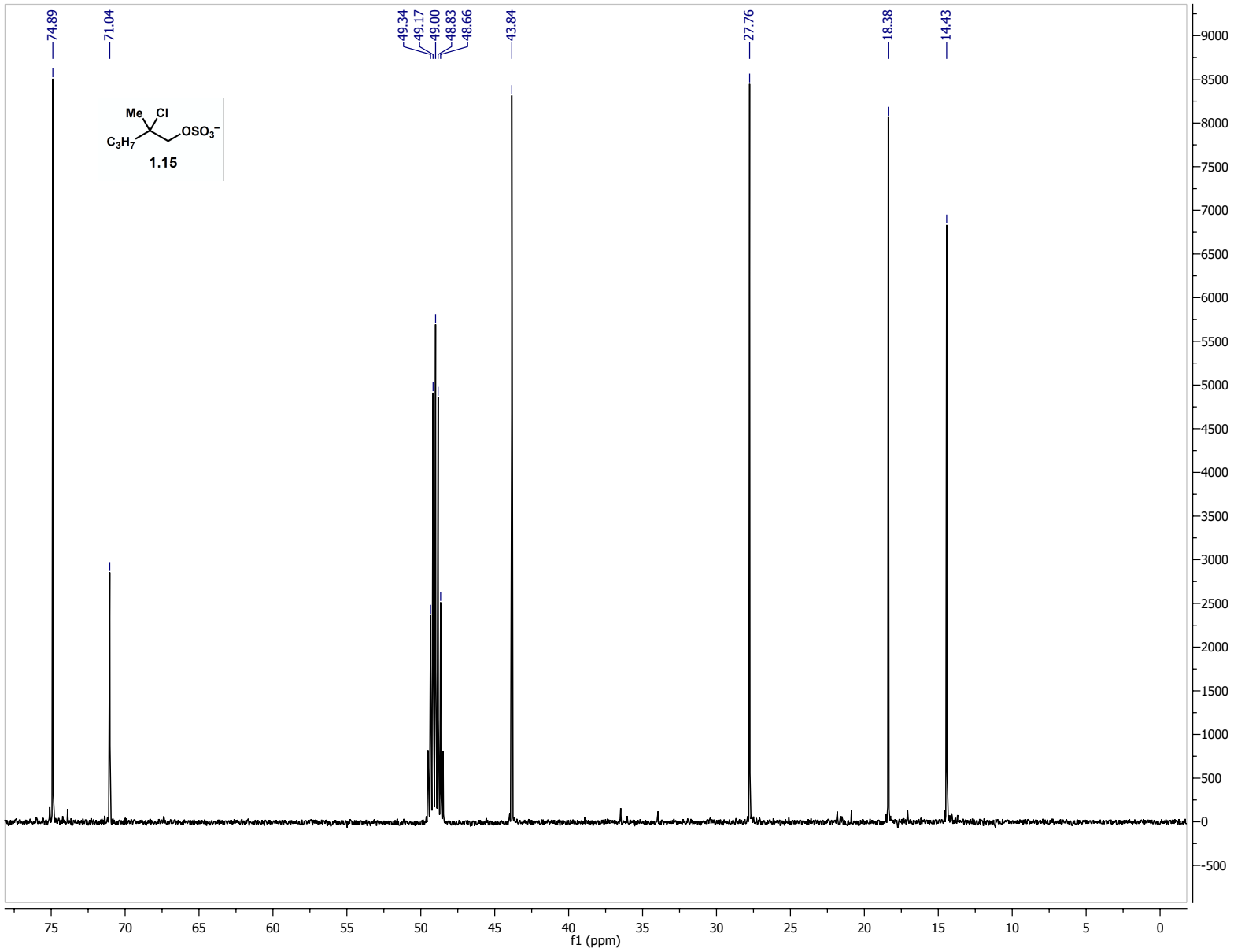
74.89
71.04
49.34
49.17
49.00
48.83
48.66
43.84
27.76
18.38
14.43
Me
Cl
C3H7
OSO3−
1.15
f1 (ppm)

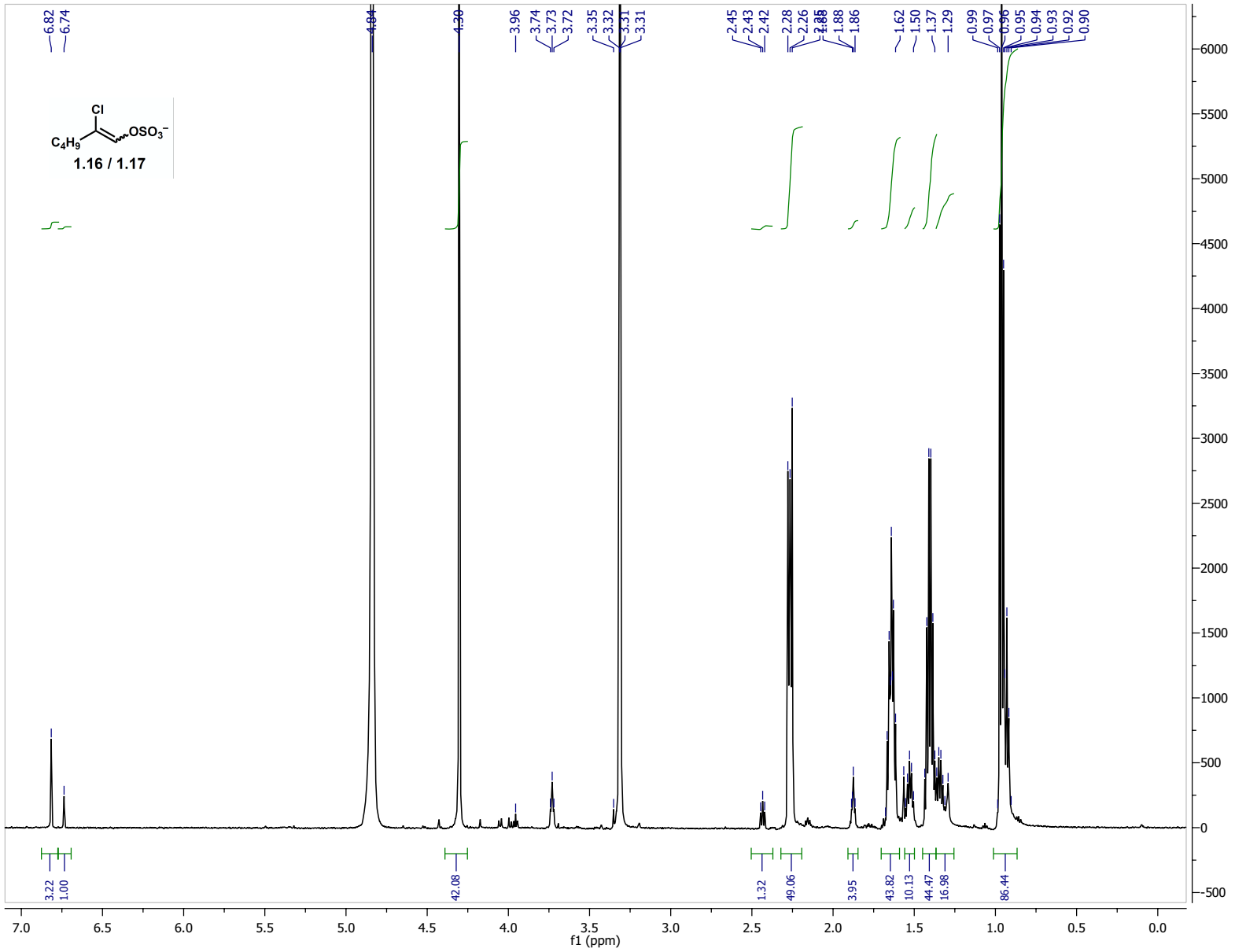
Cl
OSO3−
C4H9
1.16 / 1.17
6.82
6.74
4.94
4.90
3.96
3.74
3.73
3.72
3.35
3.32
3.31
3.31
2.45
2.43
2.42
2.28
2.26
1.88
1.86
1.62
1.50
1.37
1.29
0.99
0.97
0.96
0.95
0.94
0.93
0.92
0.90
3.22
1.00
42.08
1.32
49.06
3.95
43.82
10.13
44.47
16.98
86.44
f1 (ppm)

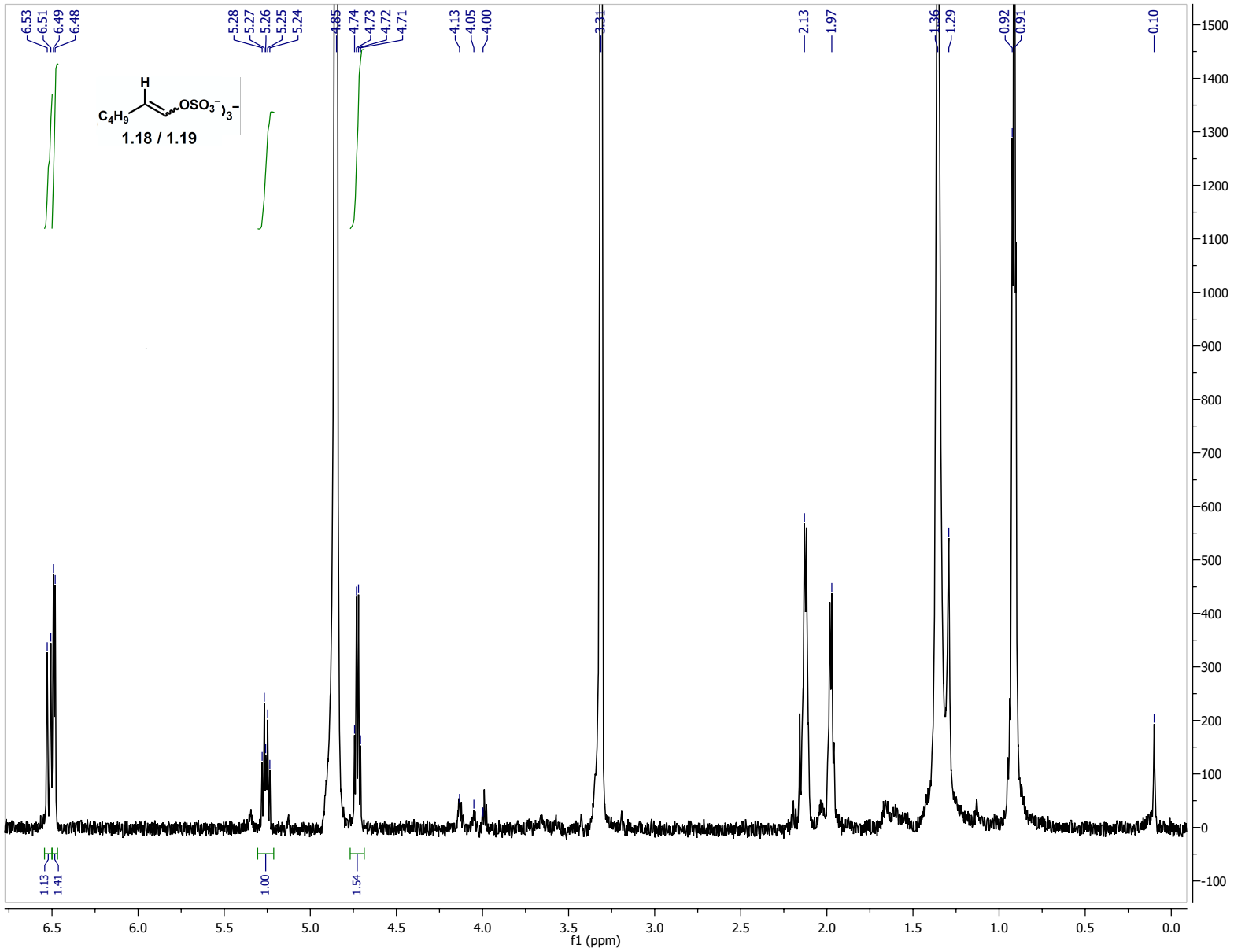
6.53
6.51
6.49
6.48
5.28
5.27
5.26
5.25
5.24
4.85
4.74
4.73
4.72
4.71
4.13
4.05
4.00
3.33
2.13
1.97
1.36
1.29
0.92
0.91
0.10
1.18 / 1.19
1.13
1.41
1.00
1.54
f1 (ppm)

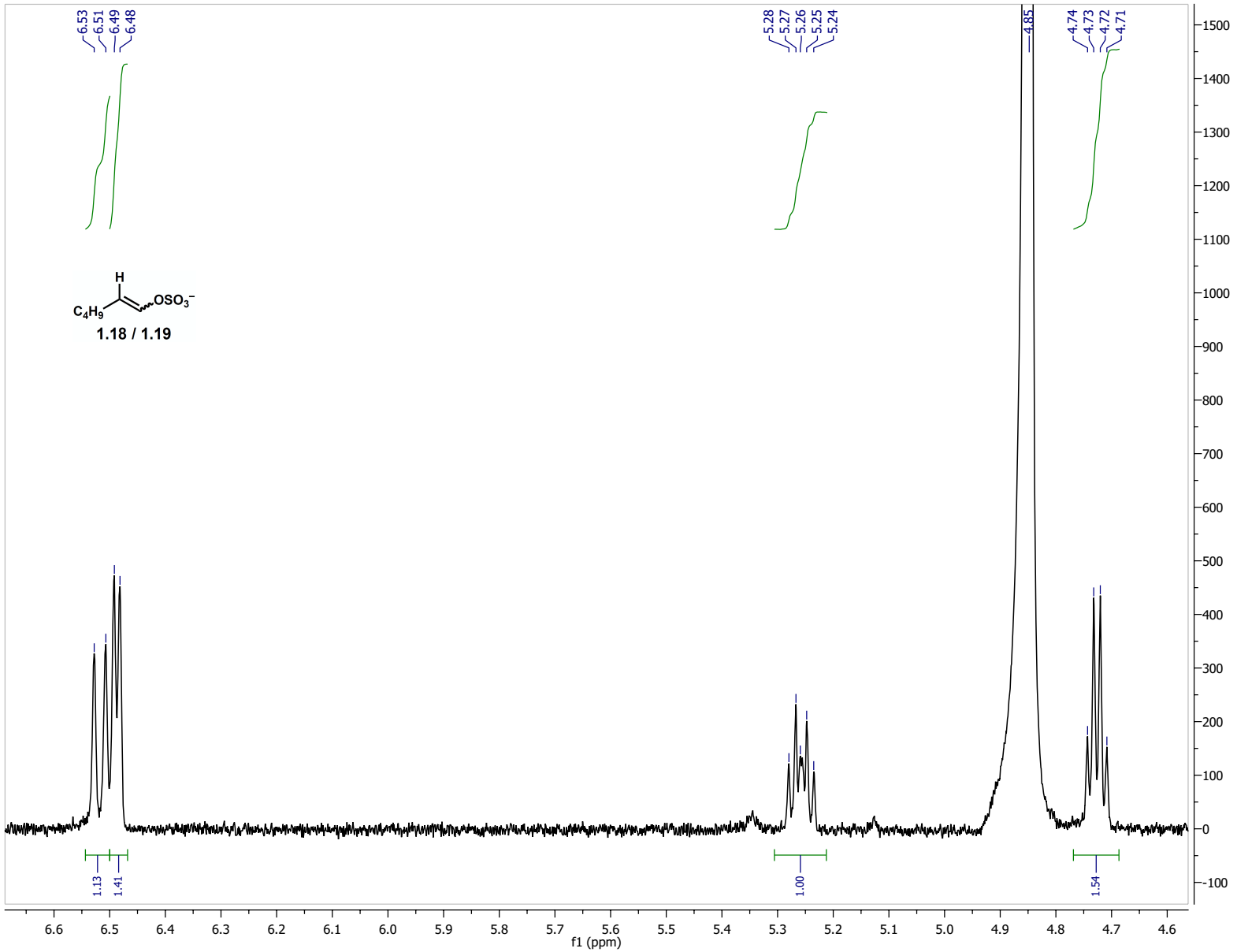
6.53
6.51
6.49
6.48
5.28
5.27
5.26
5.25
5.24
4.85
4.74
4.73
4.72
4.71
H
C4H9
OSO3−
1.18 / 1.19
1.13
1.41
1.00
1.54
f1 (ppm)

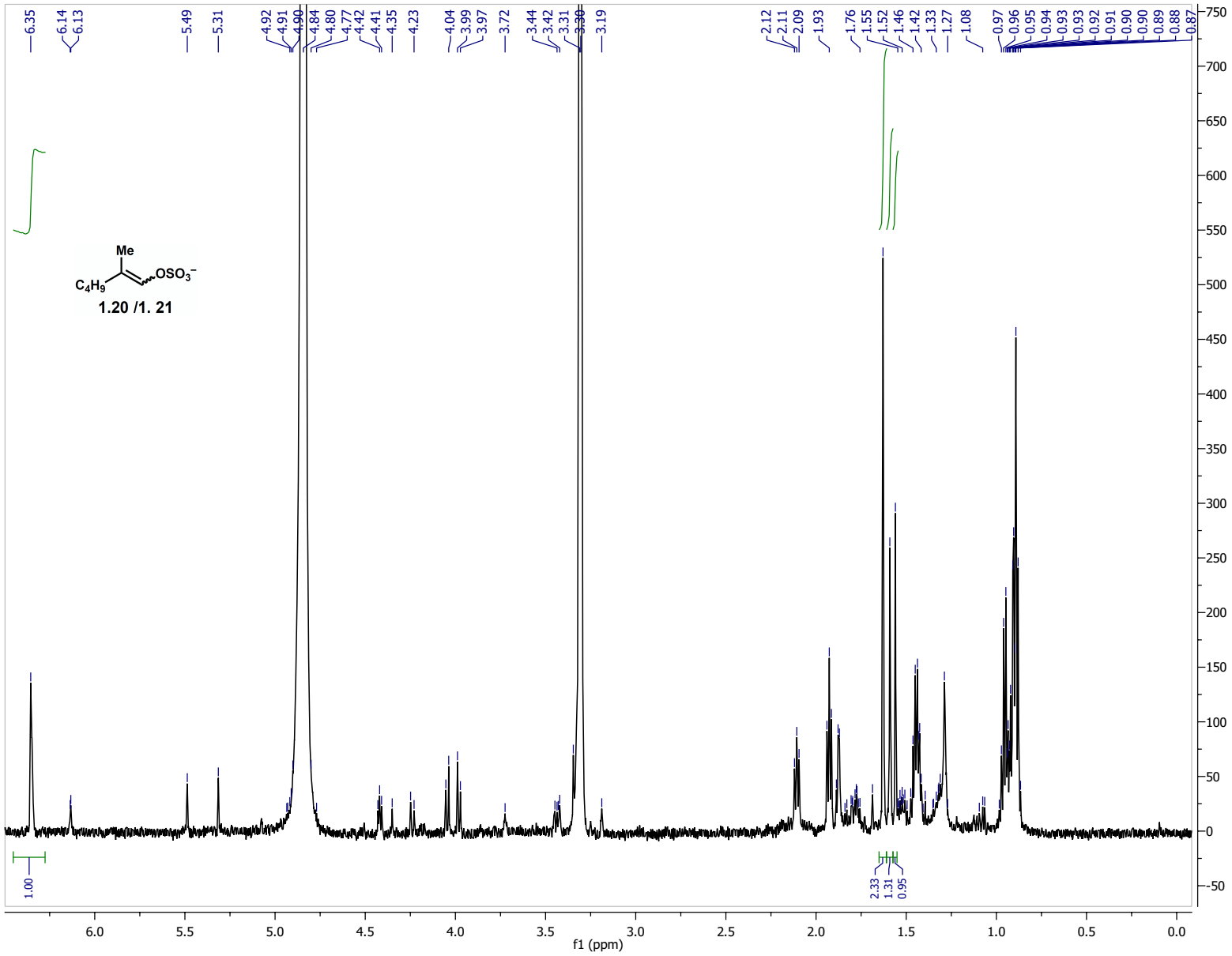
6.35
6.14
6.13
5.49
5.31
4.92
4.91
4.90
4.84
4.80
4.77
4.42
4.41
4.35
4.23
4.04
3.99
3.97
3.72
3.44
3.42
3.31
3.30
3.19
2.12
2.11
2.09
1.93
1.76
1.55
1.52
1.46
1.42
1.33
1.27
1.08
0.97
0.96
0.95
0.94
0.93
0.93
0.92
0.91
0.90
0.90
0.89
0.88
0.87
Me
C4H9
OSO3−
1.20 /1. 21
1.00
2.33
1.31
0.95
f1 (ppm)

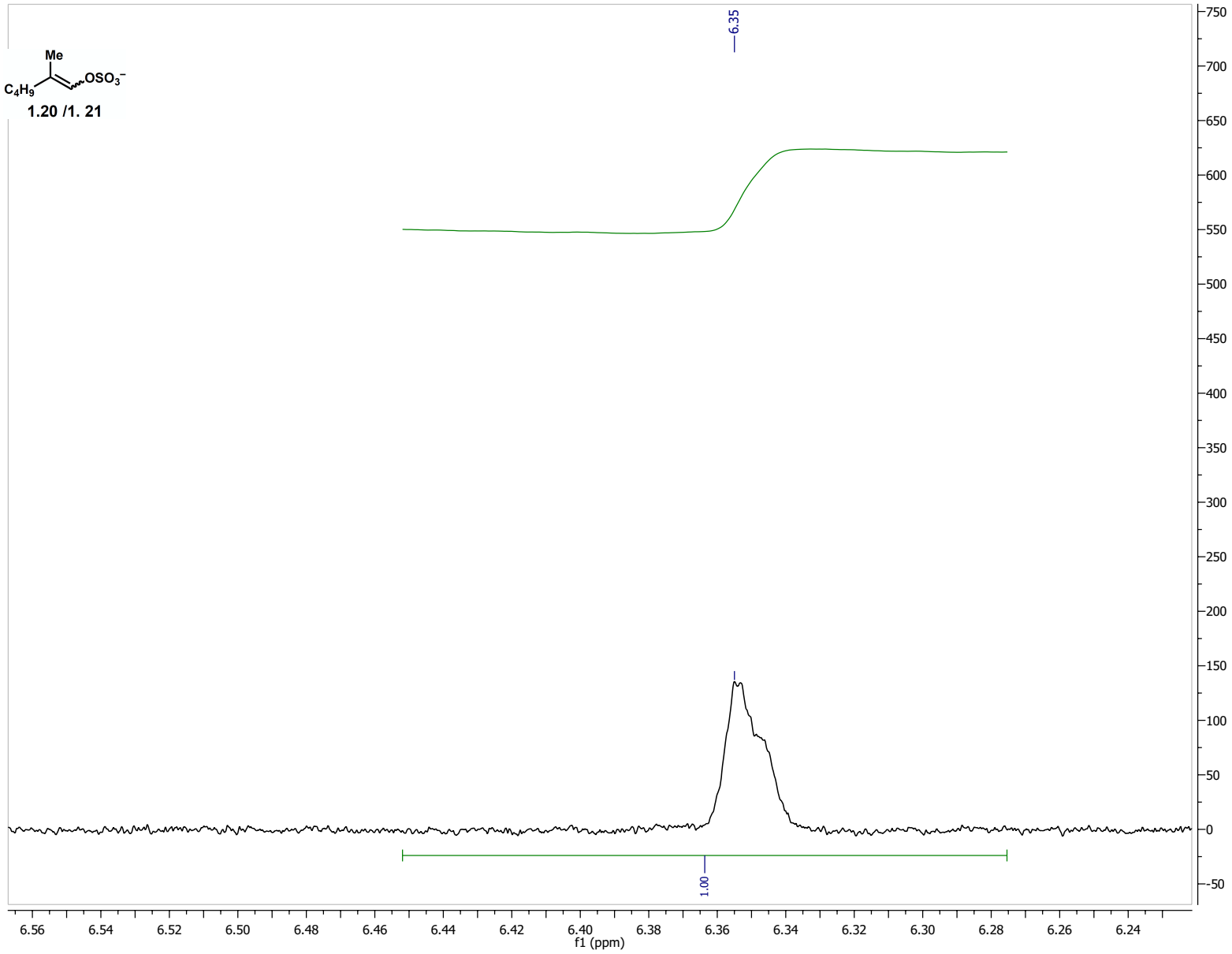
Me
C4H9
OSO3−
1.20 /1. 21
6.35
1.00
6.56
6.54
6.52
6.50
6.48
6.46
6.44
6.42
6.40
6.38
6.36
6.34
6.32
6.30
6.28
6.26
6.24
f1 (ppm)
750
700
650
600
550
500
450
400
350
300
250
200
150
100
50
0
-50

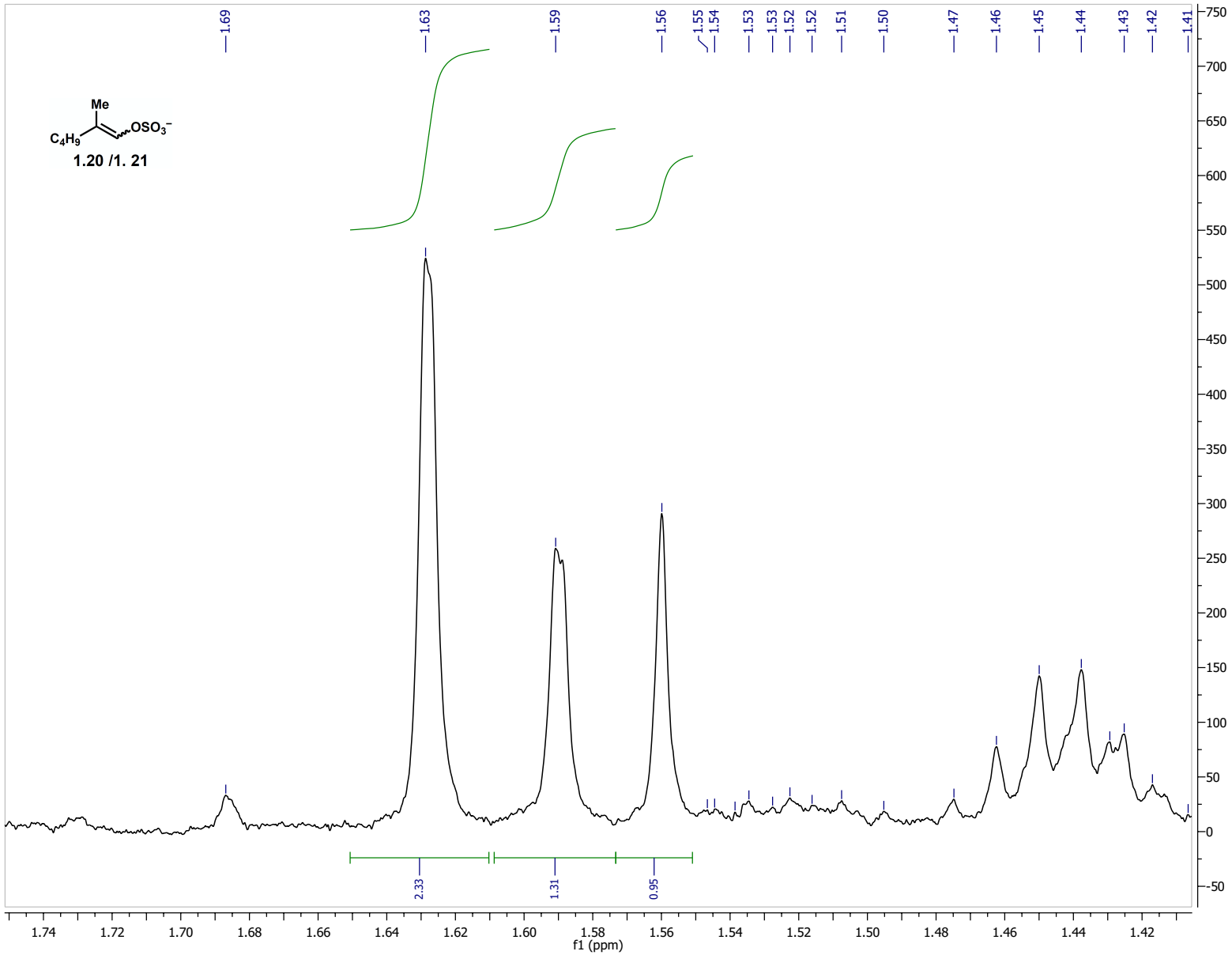
Me
C4H9
OSO3−
1.20 /1. 21
1.69
1.63
1.59
1.56
1.55
1.54
1.53
1.53
1.52
1.52
1.51
1.50
1.47
1.46
1.45
1.44
1.43
1.42
1.41
2.33
1.31
0.95
f1 (ppm)

Appendix B:

NMR Data for Chapter 2

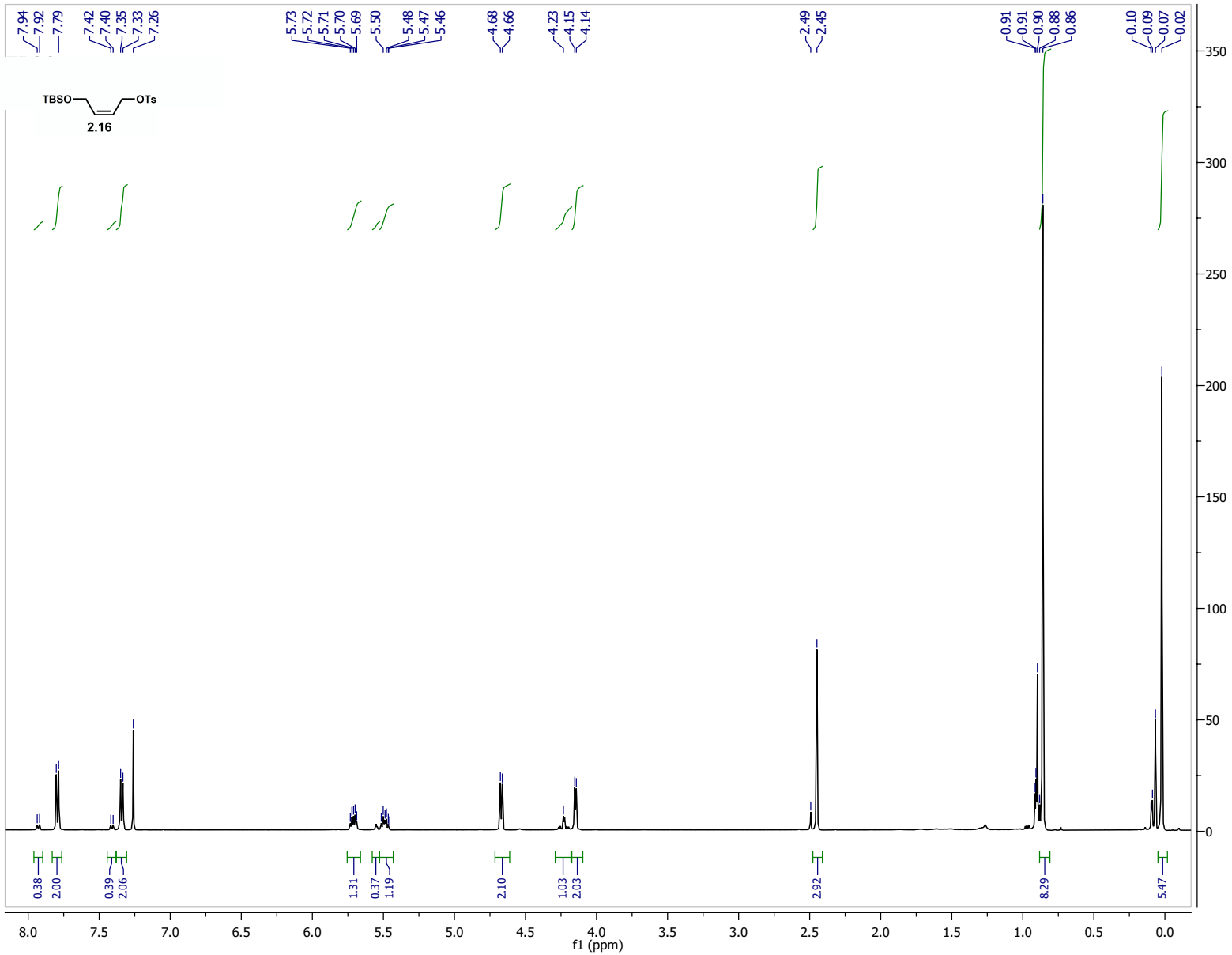
7.94
7.92
7.79
7.42
7.40
7.35
7.33
7.26
5.73
5.72
5.71
5.70
5.69
5.50
5.48
5.47
5.46
4.68
4.66
4.23
4.15
4.14
2.49
2.45
0.91
0.91
0.90
0.88
0.86
0.10
0.09
0.07
0.02
TBSO
OTs
2.16
0.38
2.00
0.39
2.06
1.31
0.37
1.19
2.10
1.03
2.03
2.92
8.29
5.47
f1 (ppm)

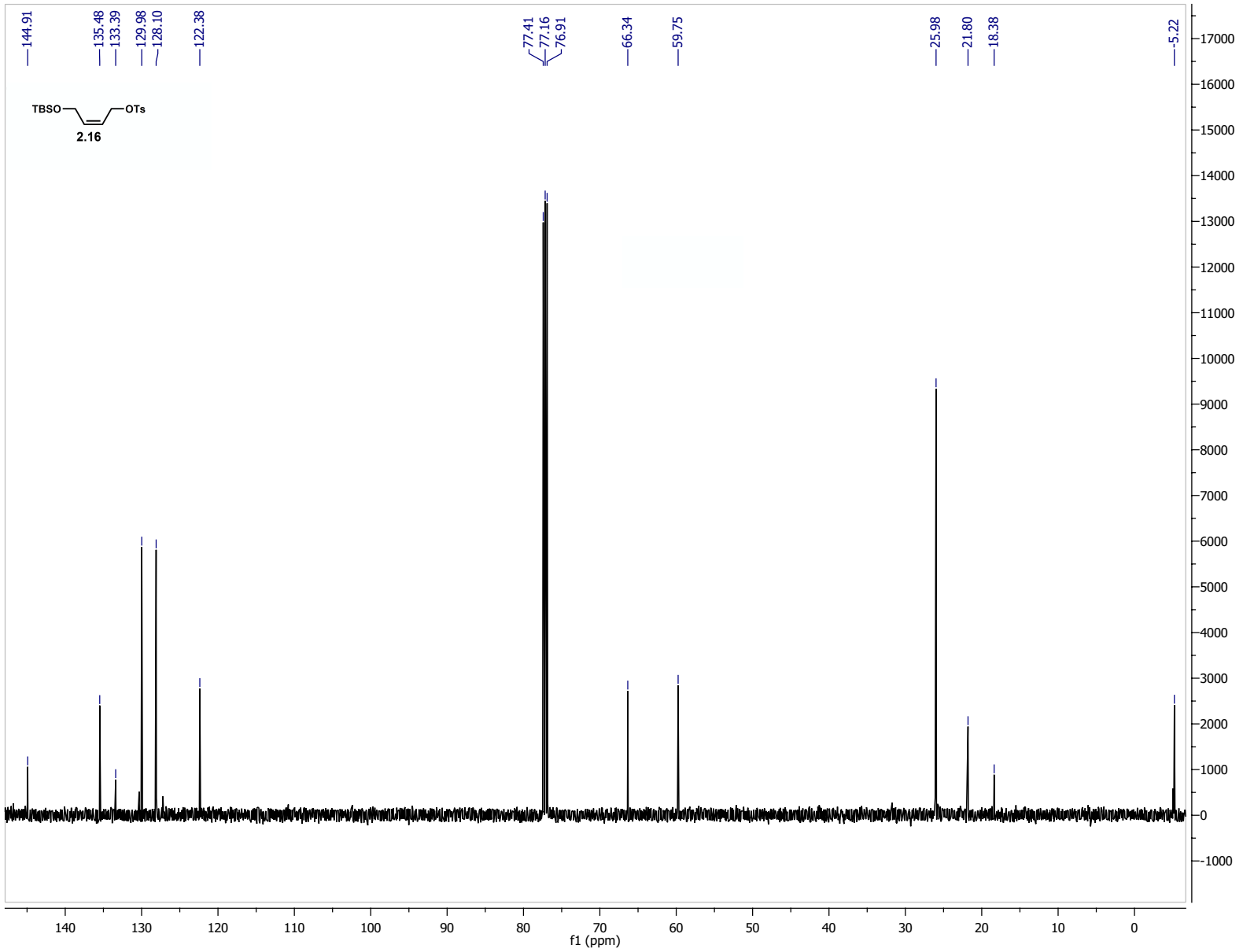
144.91
135.48
133.39
129.98
128.10
122.38
77.41
77.16
76.91
66.34
59.75
25.98
21.80
18.38
-5.22
TBSO
OTs
2.16
f1 (ppm)

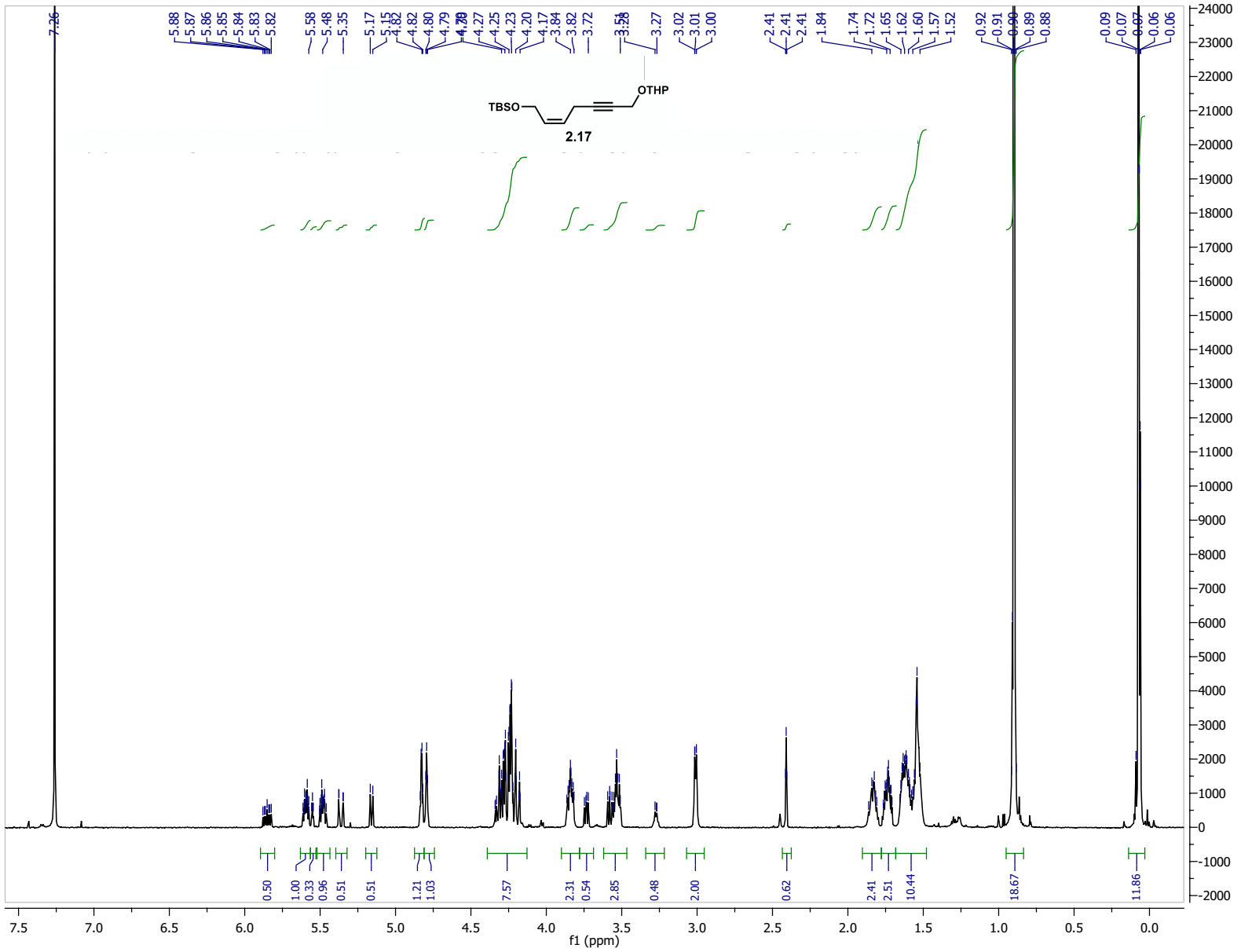
TBSO
OTHP
2.17
f1 (ppm)

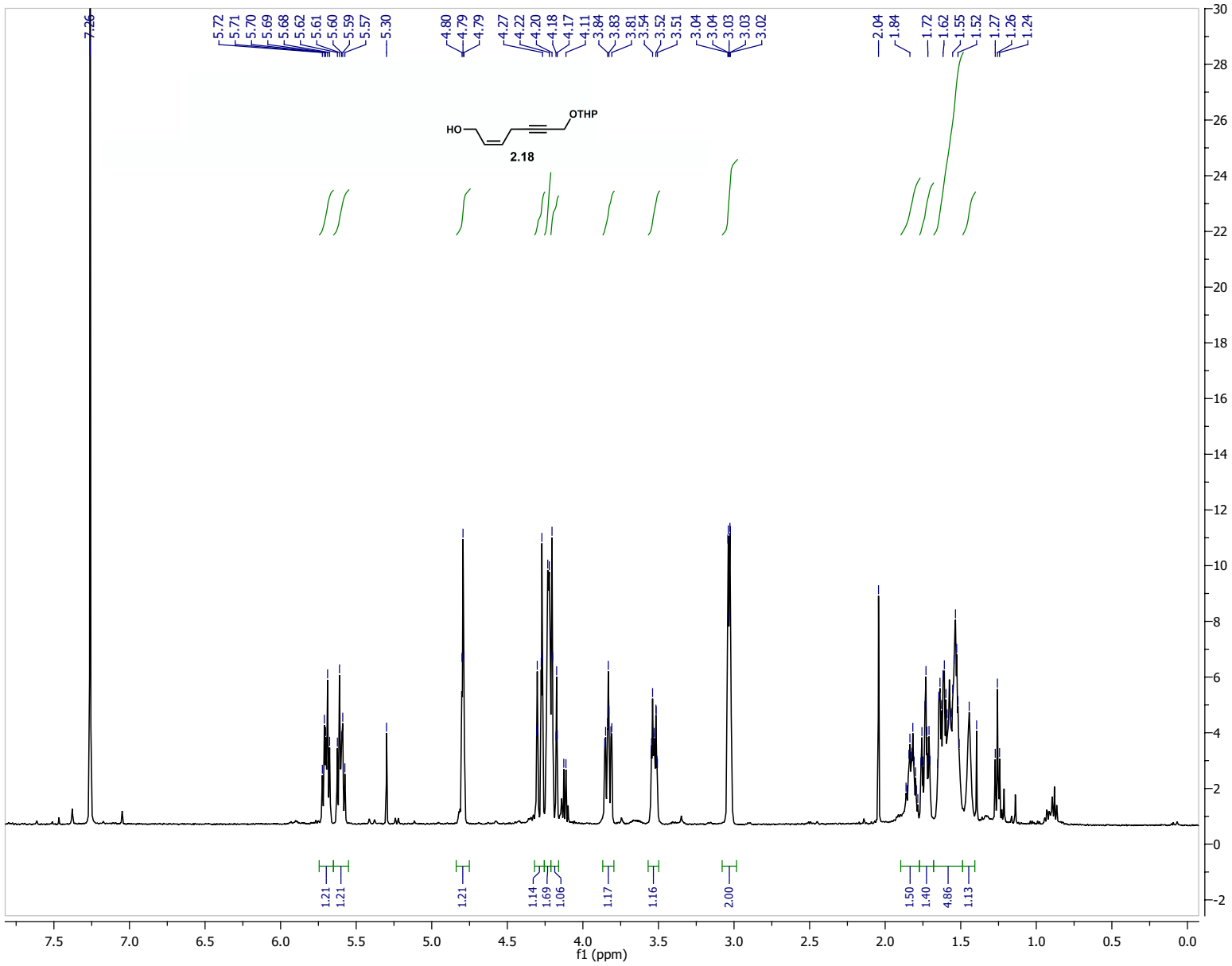
7.26
5.72
5.71
5.70
5.69
5.68
5.62
5.61
5.60
5.59
5.57
5.30
4.80
4.79
4.79
4.27
4.22
4.20
4.18
4.17
4.11
3.84
3.83
3.81
3.54
3.52
3.51
3.04
3.04
3.03
3.03
3.02
2.04
1.84
1.72
1.62
1.55
1.52
1.27
1.26
1.24
HO
OTHP
2.18
1.21
1.21
1.21
1.14
1.69
1.06
1.17
1.16
2.00
1.50
1.40
4.86
1.13
f1 (ppm)

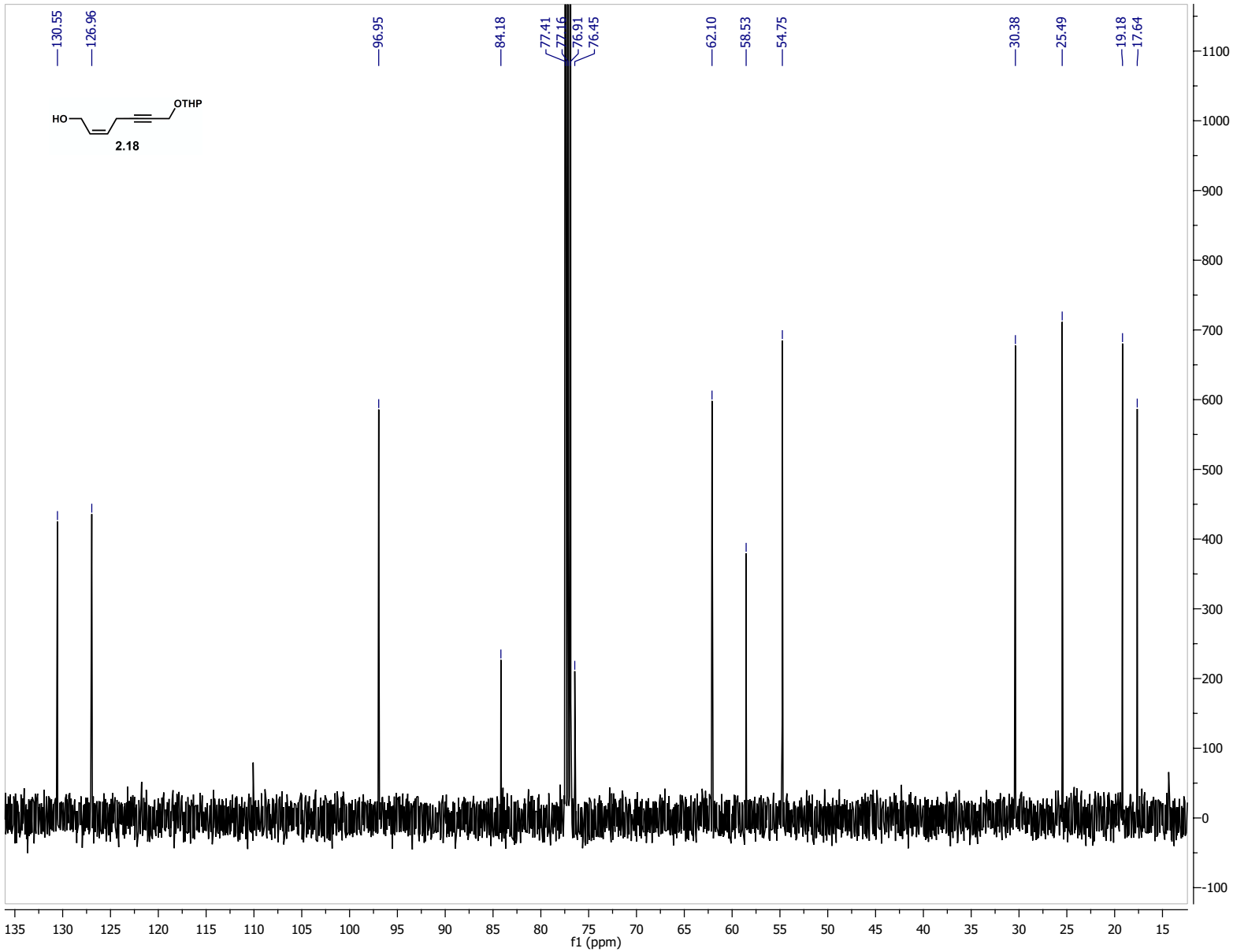
130.55
126.96
96.95
84.18
77.41
77.16
76.91
76.45
62.10
58.53
54.75
30.38
25.49
19.18
17.64
HO
OTHP
2.18
f1 (ppm)

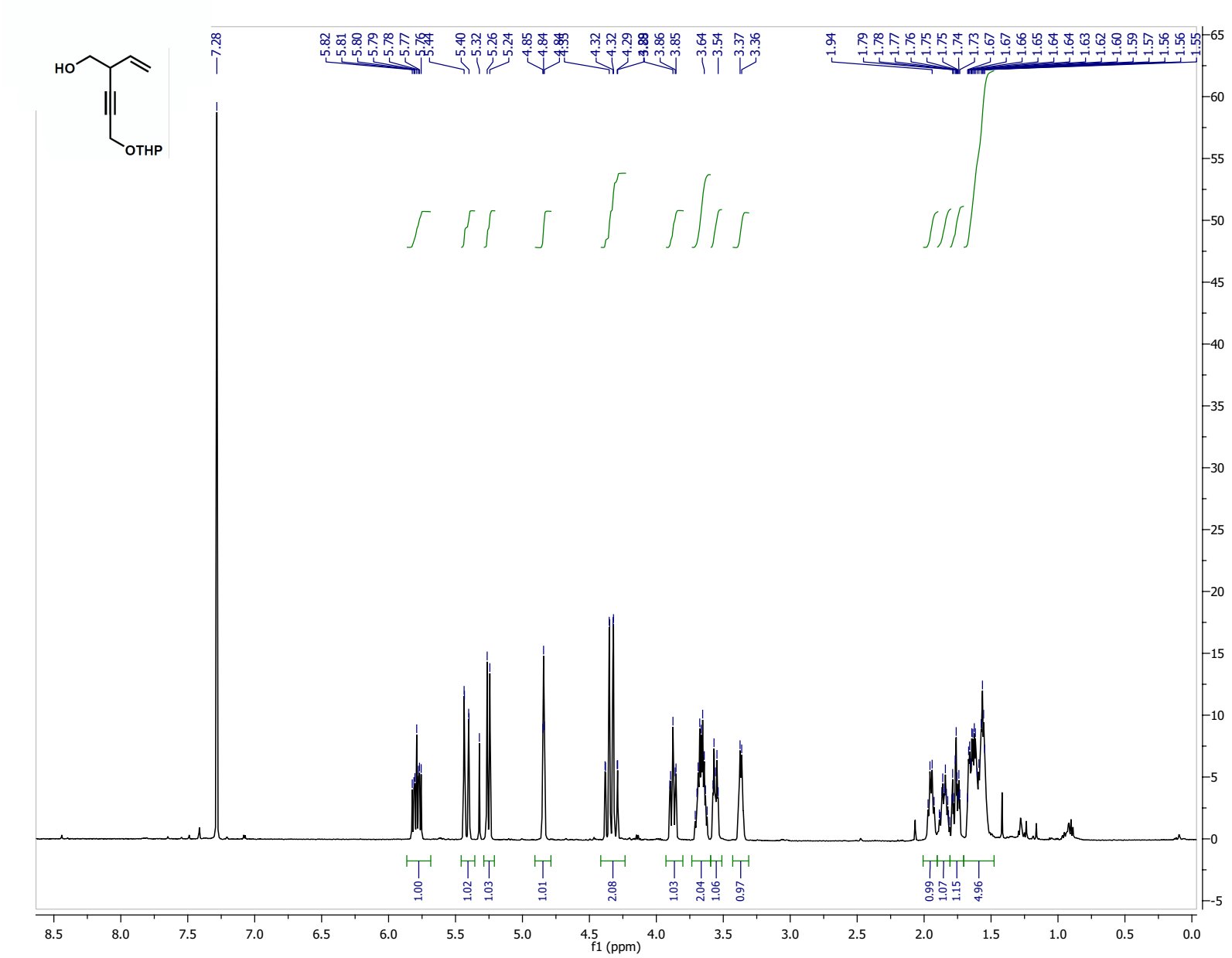
HO
OTHP
7.28
5.82
5.81
5.80
5.79
5.78
5.77
5.40
5.32
5.26
5.24
4.85
4.84
4.32
4.32
4.29
3.86
3.85
3.64
3.54
3.37
3.36
1.94
1.79
1.78
1.77
1.76
1.75
1.75
1.74
1.73
1.67
1.67
1.66
1.65
1.64
1.64
1.63
1.62
1.60
1.59
1.57
1.56
1.55
1.00
1.02
1.03
1.01
2.08
1.03
2.04
1.06
0.97
0.99
1.07
1.15
4.96
f1 (ppm)

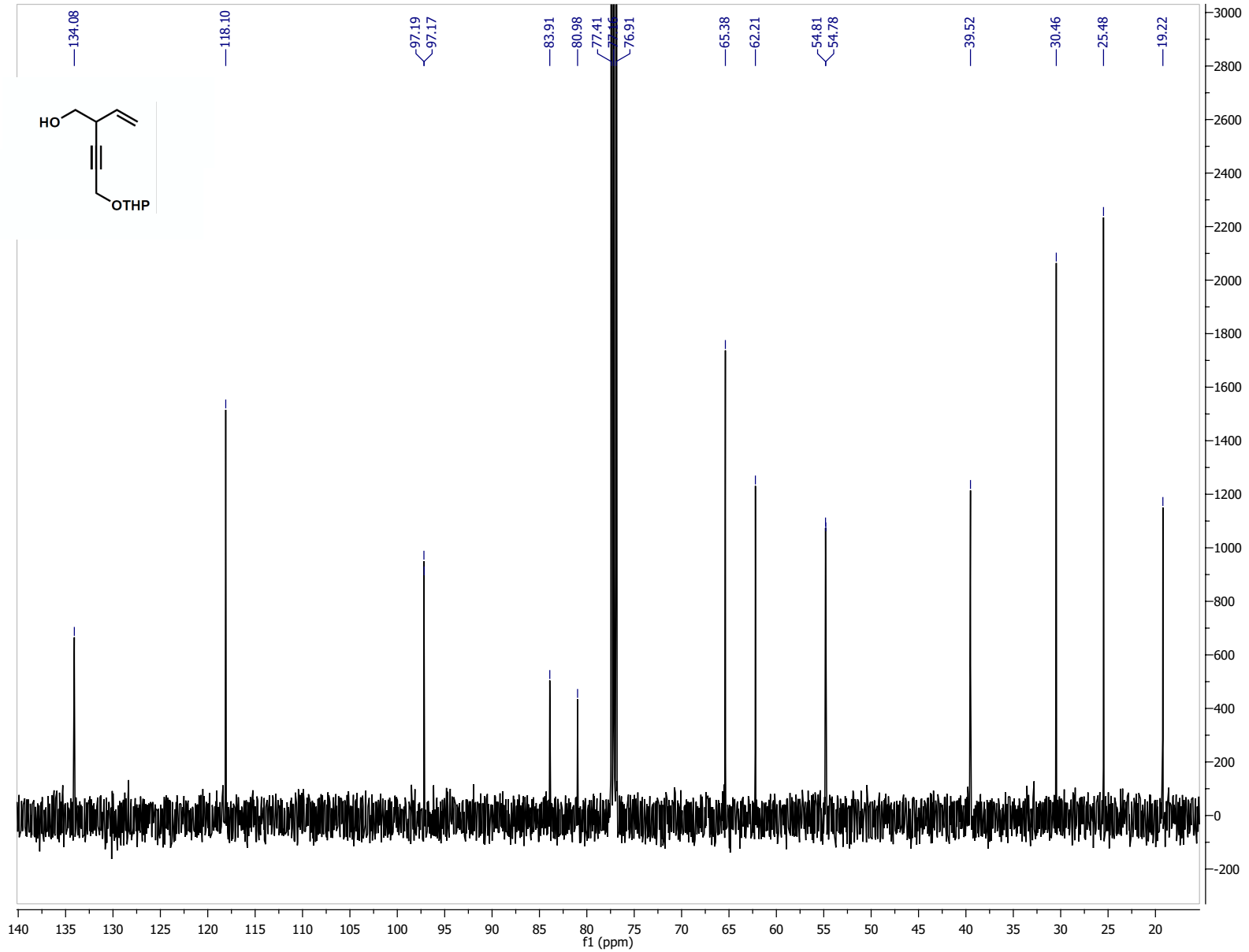
134.08
118.10
97.19
97.17
83.91
80.98
77.41
76.91
65.38
62.21
54.81
54.78
39.52
30.46
25.48
19.22
HO
OTHP
f1 (ppm)

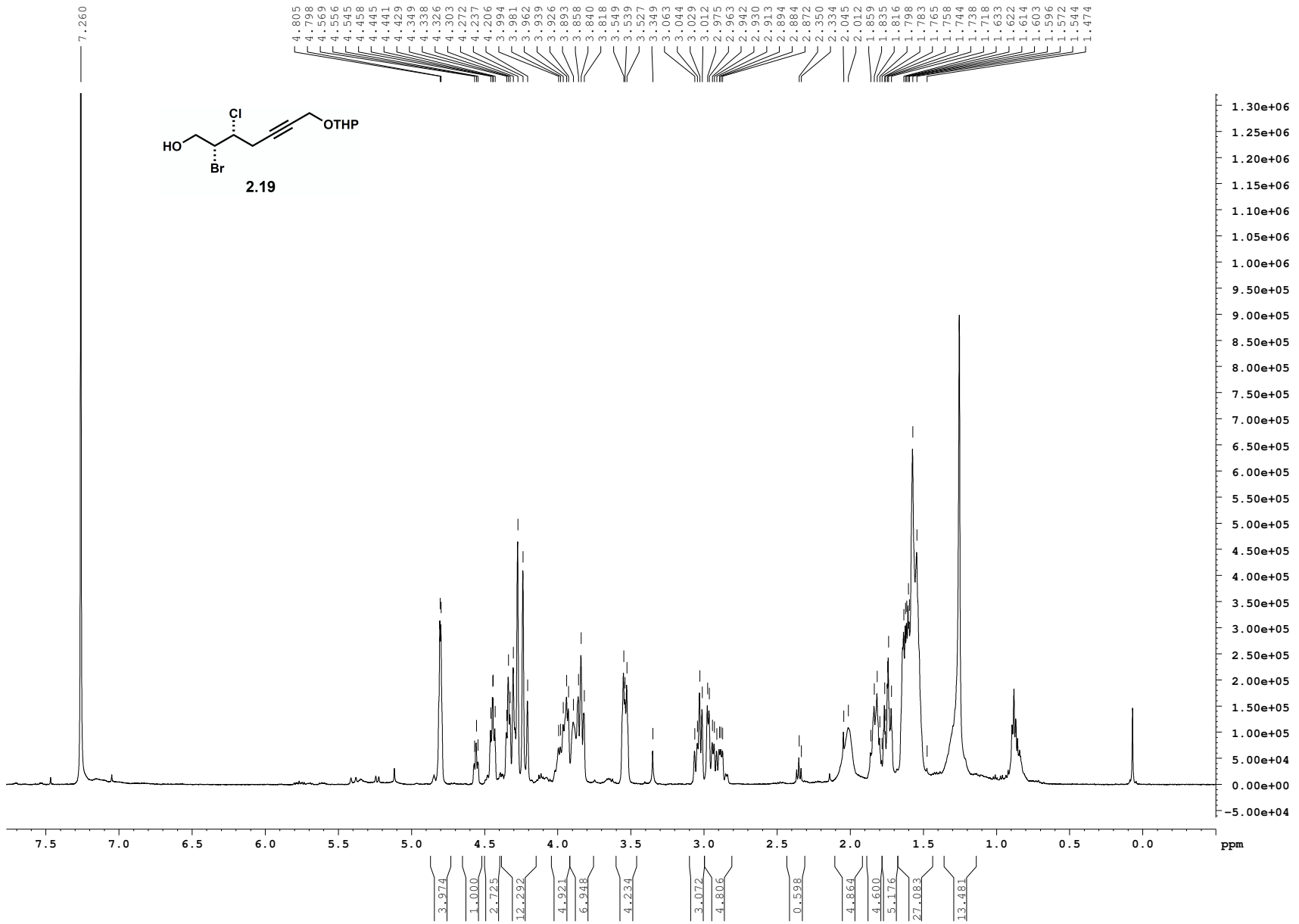
7.260
4.805 4.798 4.569 4.556 4.545 4.458 4.445 4.441 4.429 4.349 4.338 4.326 4.303 4.272 4.237 4.206 3.994 3.981 3.962 3.939 3.926 3.893 3.858 3.840 3.818 3.549 3.539 3.527 3.349 3.063 3.044 3.029 3.012 2.975 2.963 2.942 2.930 2.913 2.894 2.884 2.872 2.350 2.334 2.045 2.012 1.859 1.835 1.816 1.798 1.783 1.765 1.758 1.744 1.738 1.718 1.633 1.622 1.614 1.603 1.596 1.572 1.544 1.474
Cl
OTHP
HO
Br
2.19
1.30e+06
1.25e+06
1.20e+06
1.15e+06
1.10e+06
1.05e+06
1.00e+06
9.50e+05
9.00e+05
8.50e+05
8.00e+05
7.50e+05
7.00e+05
6.50e+05
6.00e+05
5.50e+05
5.00e+05
4.50e+05
4.00e+05
3.50e+05
3.00e+05
2.50e+05
2.00e+05
1.50e+05
1.00e+05
5.00e+04
0.00e+00
-5.00e+04
7.5 7.0 6.5 6.0 5.5 5.0 4.5 4.0 3.5 3.0 2.5 2.0 1.5 1.0 0.5 0.0
ppm
3.974 1.000 2.725 12.292 4.921 6.948 4.234 3.072 4.806 0.598 4.864 4.600 5.176 27.083 13.481

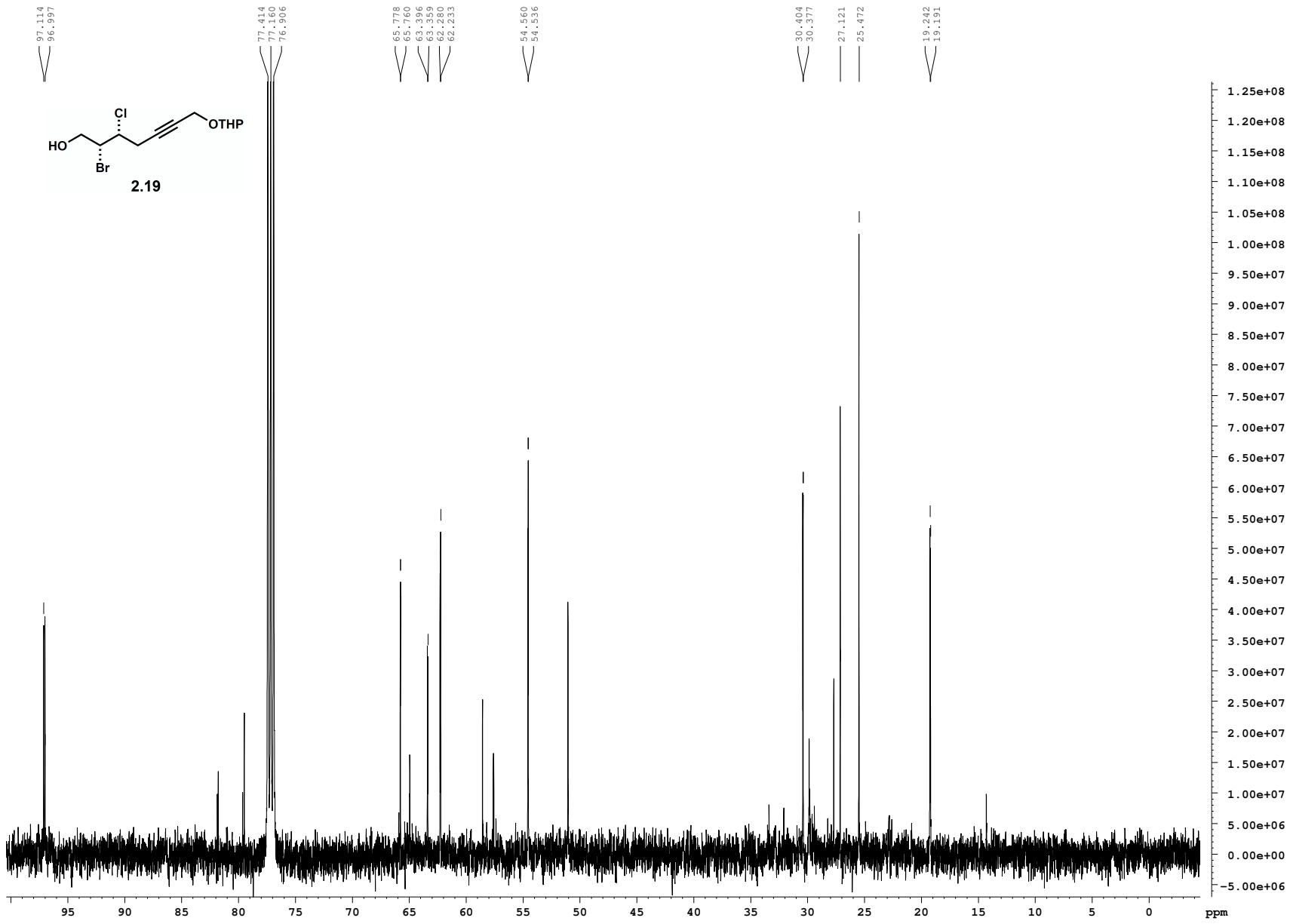
97.114
96.997
77.414
77.160
76.906
65.778
65.760
63.396
63.359
62.280
62.233
54.560
54.536
30.404
30.377
27.121
25.472
19.242
19.191
Cl
OTHP
HO
Br
2.19
1.25e+08
1.20e+08
1.15e+08
1.10e+08
1.05e+08
1.00e+08
9.50e+07
9.00e+07
8.50e+07
8.00e+07
7.50e+07
7.00e+07
6.50e+07
6.00e+07
5.50e+07
5.00e+07
4.50e+07
4.00e+07
3.50e+07
3.00e+07
2.50e+07
2.00e+07
1.50e+07
1.00e+07
5.00e+06
0.00e+00
-5.00e+06
95
90
85
80
75
70
65
60
55
50
45
40
35
30
25
20
15
10
5
0
ppm

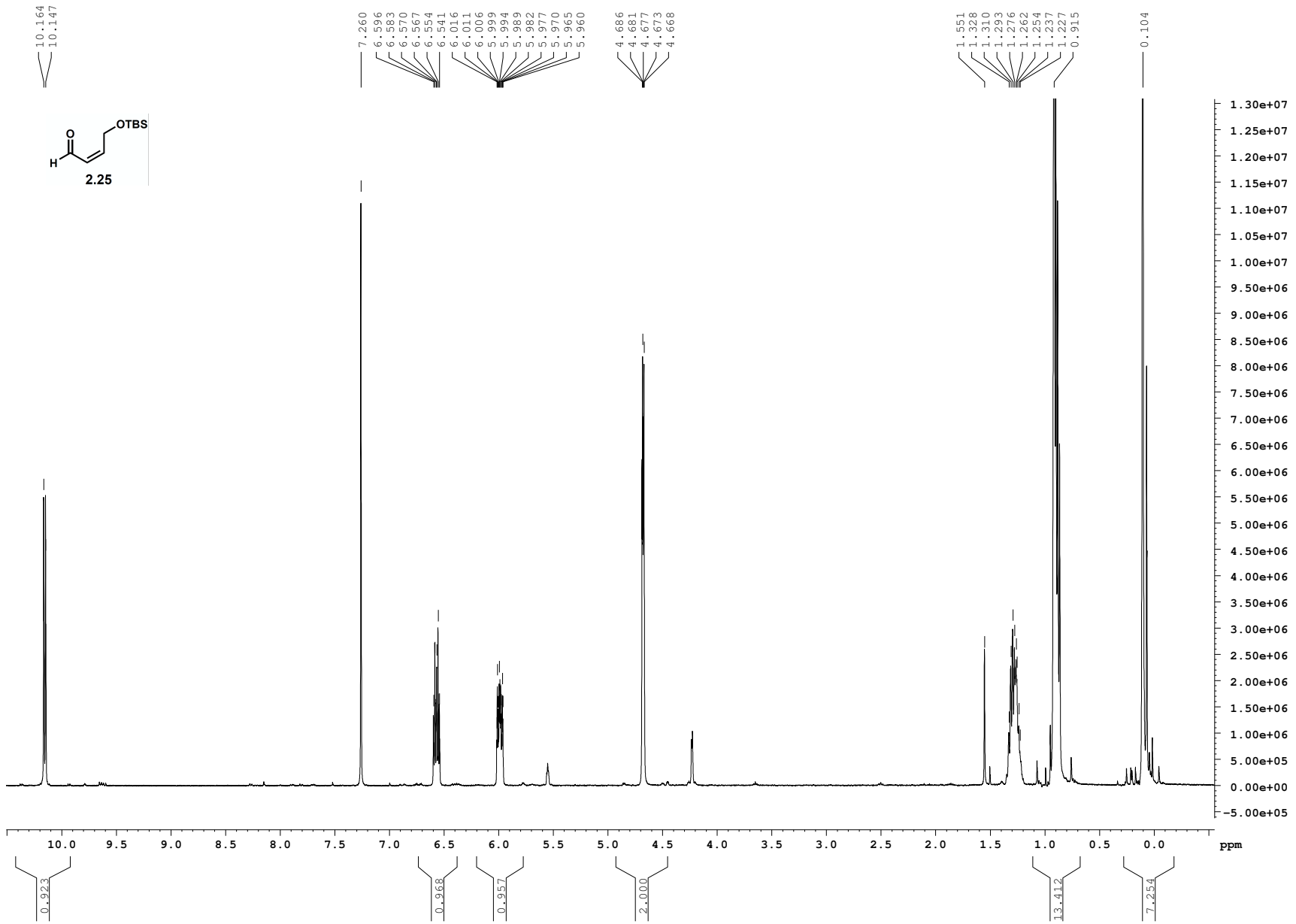
10.164
10.147
7.260
6.596
6.583
6.570
6.567
6.554
6.541
6.016
6.011
6.006
5.999
5.994
5.989
5.982
5.977
5.970
5.965
5.960
4.686
4.681
4.677
4.673
4.668
1.551
1.328
1.310
1.293
1.276
1.262
1.254
1.237
1.227
0.915
0.104
OTBS
O
H
2.25
ppm
0.923
0.968
0.957
2.000
13.412
7.254

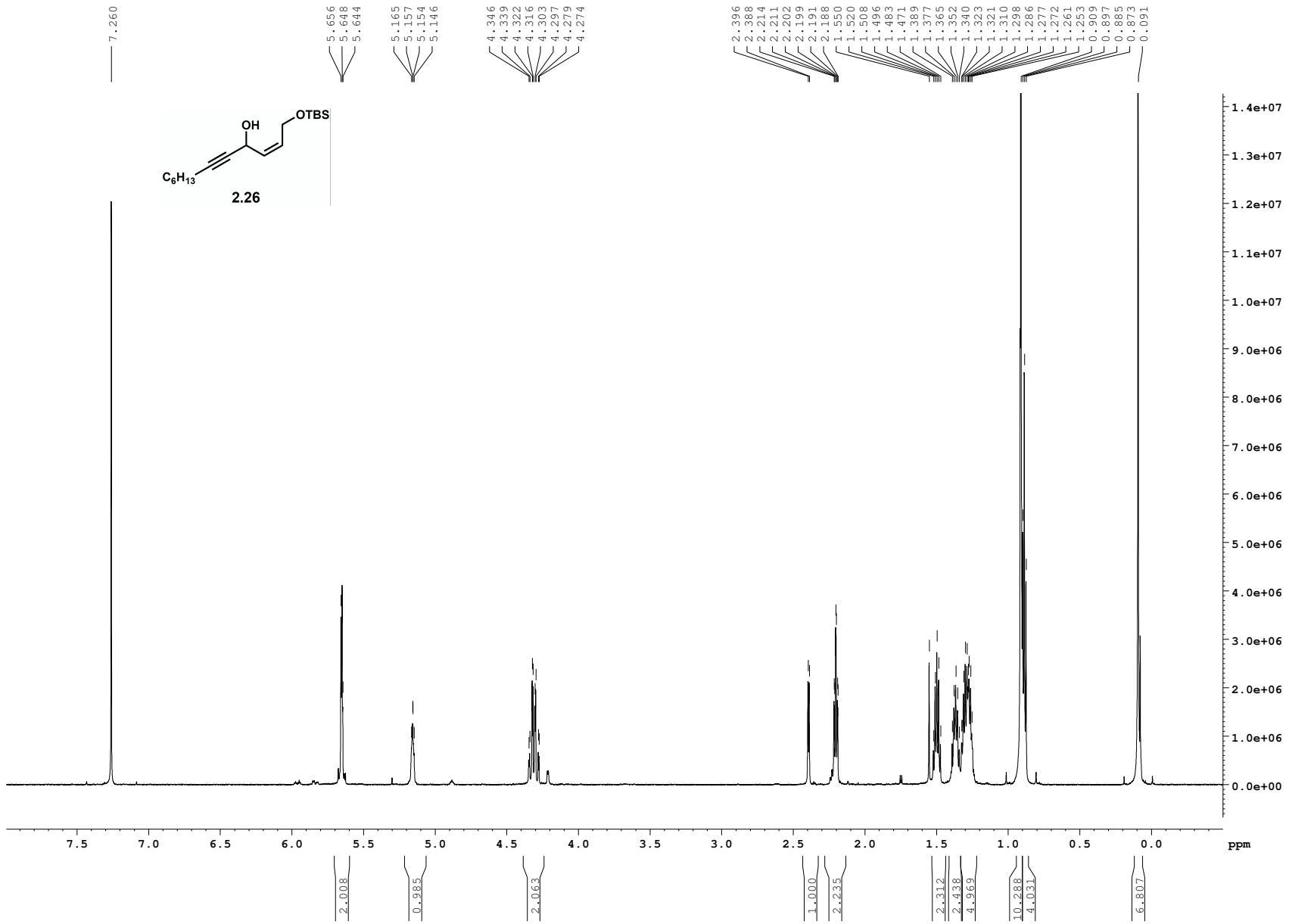
7.260
5.656
5.648
5.644
5.165
5.157
5.154
5.146
4.346
4.339
4.322
4.316
4.303
4.297
4.279
4.274
2.396
2.388
2.214
2.211
2.202
2.199
2.191
2.188
1.550
1.520
1.508
1.496
1.483
1.471
1.389
1.377
1.365
1.352
1.340
1.323
1.321
1.310
1.298
1.286
1.277
1.272
1.261
1.253
0.909
0.897
0.885
0.873
0.091
OH
OTBS
C6H13
2.26
1.4e+07
1.3e+07
1.2e+07
1.1e+07
1.0e+07
9.0e+06
8.0e+06
7.0e+06
6.0e+06
5.0e+06
4.0e+06
3.0e+06
2.0e+06
1.0e+06
0.0e+00
7.5
7.0
6.5
6.0
5.5
5.0
4.5
4.0
3.5
3.0
2.5
2.0
1.5
1.0
0.5
0.0
ppm
2.008
0.985
2.063
1.000
2.235
2.312
2.438
4.969
10.288
4.031
6.807

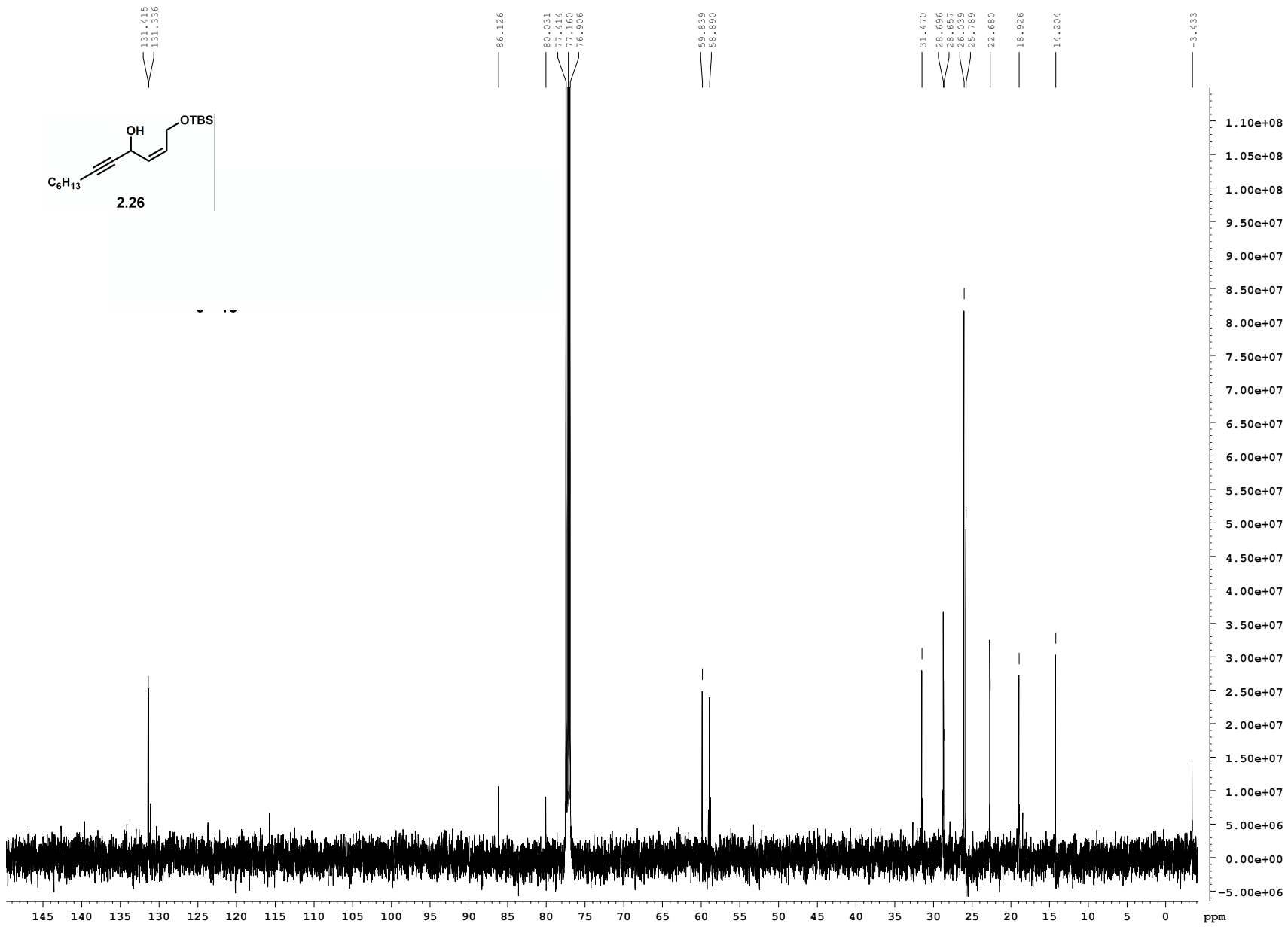
131.415
131.336
86.126
80.031
77.414
77.160
76.906
59.839
58.890
31.470
28.696
28.657
26.039
25.789
22.680
18.926
14.204
-3.433
OH
OTBS
C6H13
2.26
1.10e+08
1.05e+08
1.00e+08
9.50e+07
9.00e+07
8.50e+07
8.00e+07
7.50e+07
7.00e+07
6.50e+07
6.00e+07
5.50e+07
5.00e+07
4.50e+07
4.00e+07
3.50e+07
3.00e+07
2.50e+07
2.00e+07
1.50e+07
1.00e+07
5.00e+06
0.00e+00
-5.00e+06
145 140 135 130 125 120 115 110 105 100 95 90 85 80 75 70 65 60 55 50 45 40 35 30 25 20 15 10 5 0
ppm

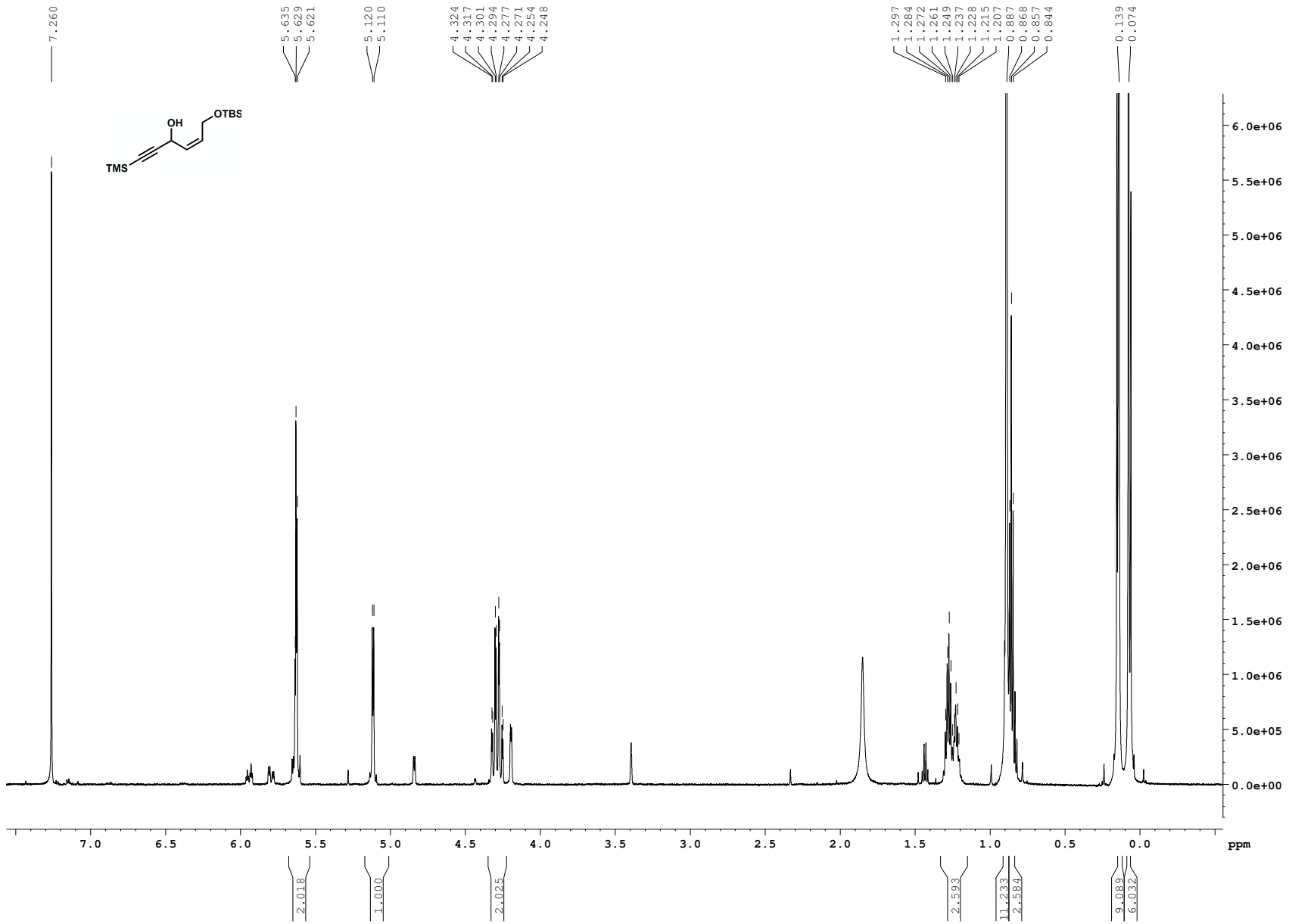
7.260
5.635
5.629
5.621
5.120
5.110
4.324
4.317
4.301
4.294
4.277
4.271
4.254
4.248
1.297
1.284
1.272
1.261
1.249
1.237
1.228
1.215
1.207
0.887
0.868
0.857
0.844
0.139
0.074
OH
OTBS
TMS
6.0e+06
5.5e+06
5.0e+06
4.5e+06
4.0e+06
3.5e+06
3.0e+06
2.5e+06
2.0e+06
1.5e+06
1.0e+06
5.0e+05
0.0e+00
7.0
6.5
6.0
5.5
5.0
4.5
4.0
3.5
3.0
2.5
2.0
1.5
1.0
0.5
0.0
ppm
2.018
1.000
2.025
2.593
11.233
2.584
9.089
6.032

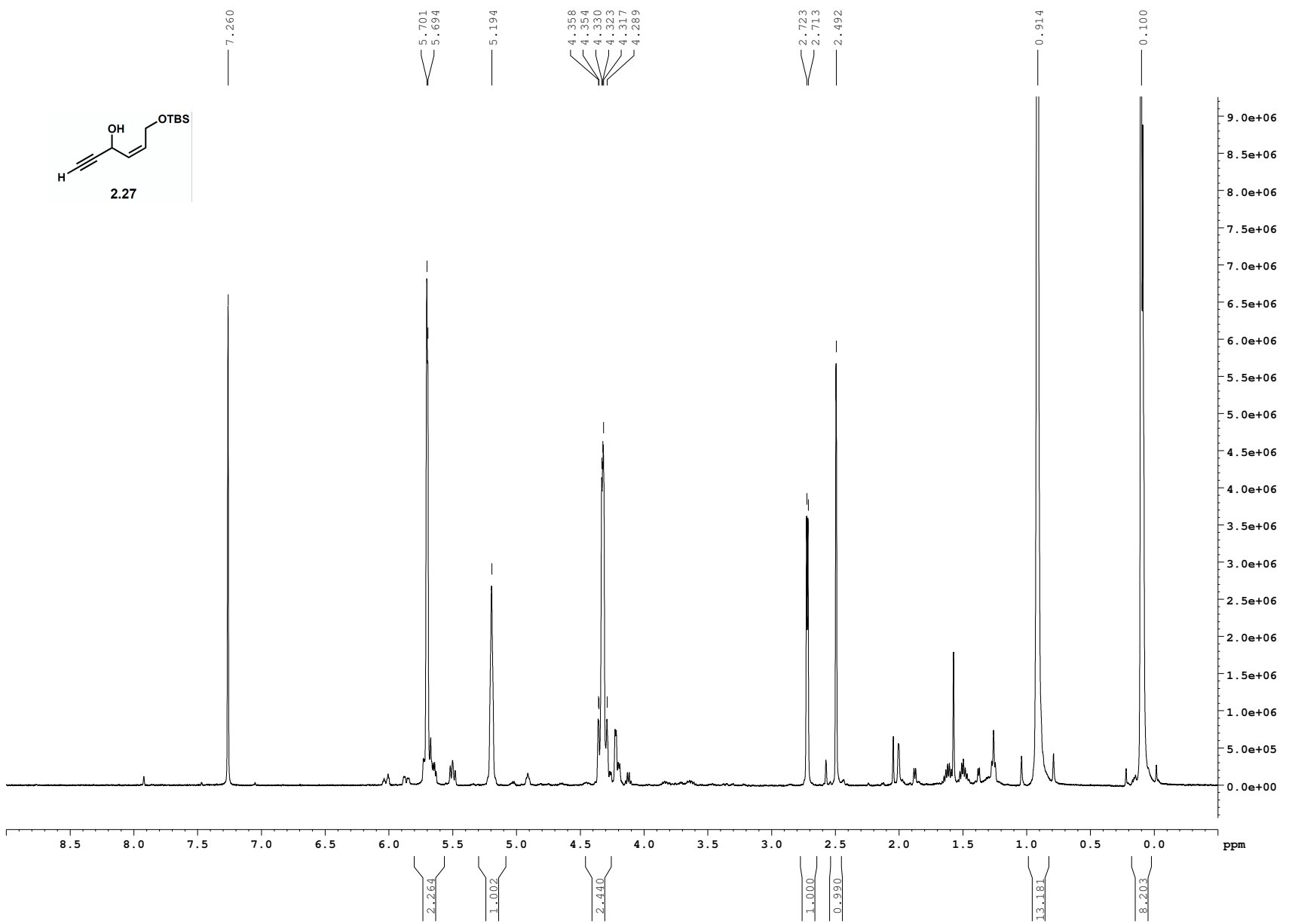
7.260
5.701
5.694
5.194
4.358
4.354
4.330
4.323
4.317
4.289
2.723
2.713
2.492
0.914
0.100
OH
OTBS
H
2.27
ppm
2.264
1.002
2.440
1.000
0.990
13.181
8.203

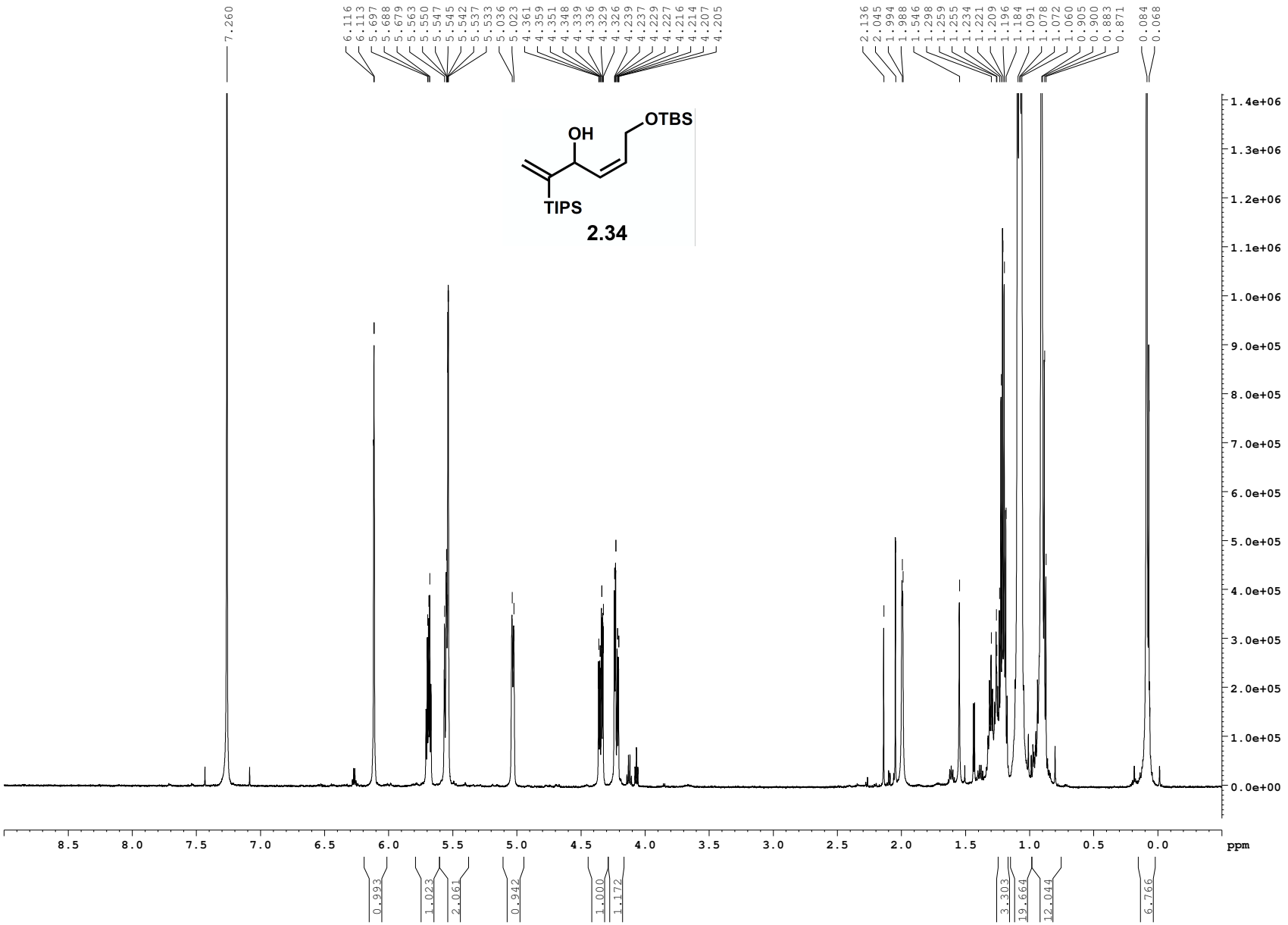
7.260
6.116
6.113
5.697
5.688
5.679
5.563
5.550
5.547
5.545
5.542
5.537
5.533
5.036
5.023
4.361
4.359
4.351
4.348
4.339
4.336
4.329
4.326
4.239
4.237
4.229
4.227
4.216
4.214
4.207
4.205
2.136
2.045
1.994
1.988
1.546
1.298
1.259
1.255
1.234
1.221
1.209
1.196
1.184
1.091
1.078
1.072
1.060
0.905
0.900
0.883
0.871
0.084
0.068
OTBS
OH
TIPS
2.34
1.4e+06
1.3e+06
1.2e+06
1.1e+06
1.0e+06
9.0e+05
8.0e+05
7.0e+05
6.0e+05
5.0e+05
4.0e+05
3.0e+05
2.0e+05
1.0e+05
0.0e+00
8.5
8.0
7.5
7.0
6.5
6.0
5.5
5.0
4.5
4.0
3.5
3.0
2.5
2.0
1.5
1.0
0.5
0.0
ppm
0.993
1.023
2.061
0.942
1.000
1.172
3.303
19.664
12.044
6.766

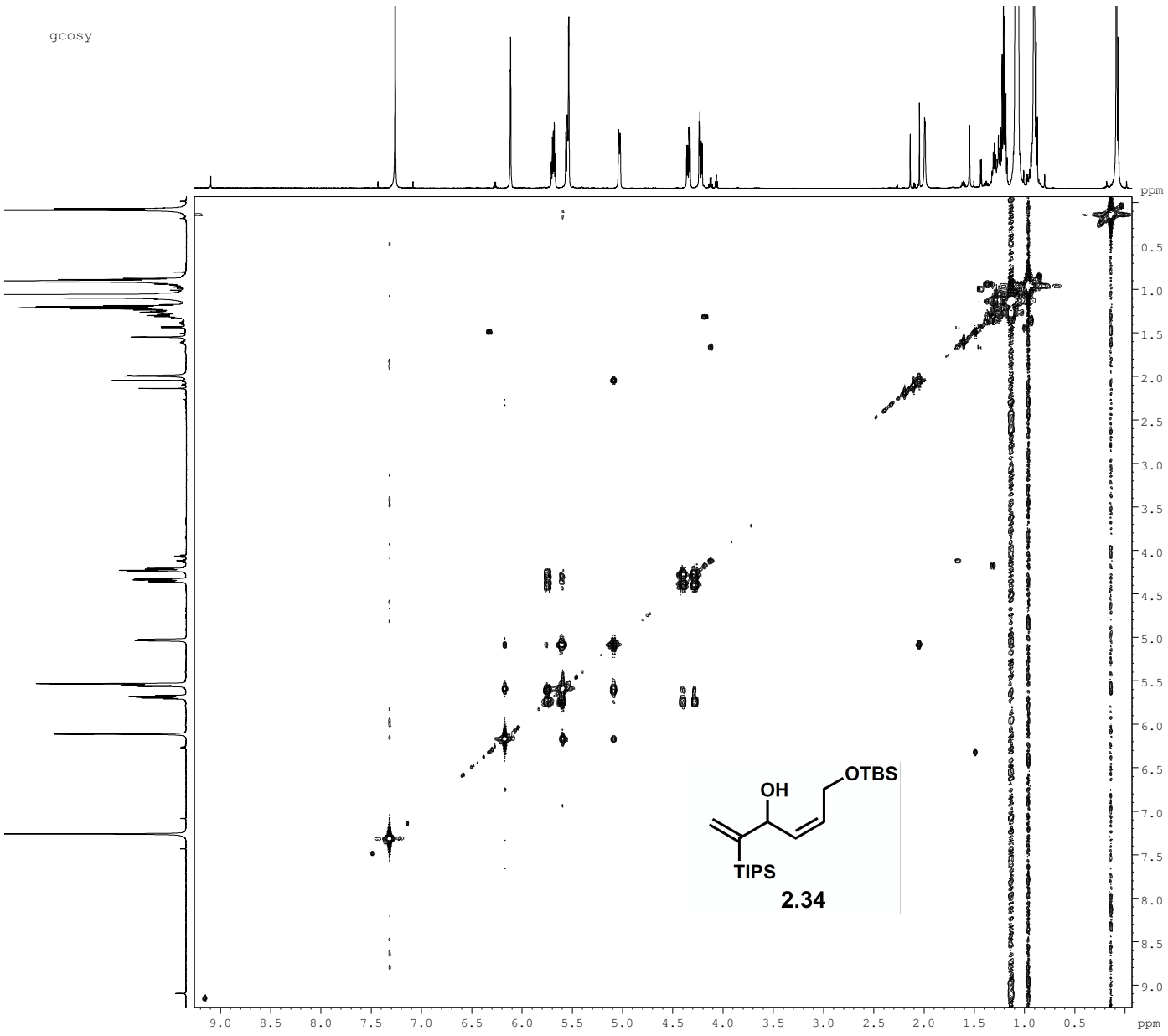
gcosy
OH
OTBS
TIPS
2.34
ppm
9.0 8.5 8.0 7.5 7.0 6.5 6.0 5.5 5.0 4.5 4.0 3.5 3.0 2.5 2.0 1.5 1.0 0.5
ppm

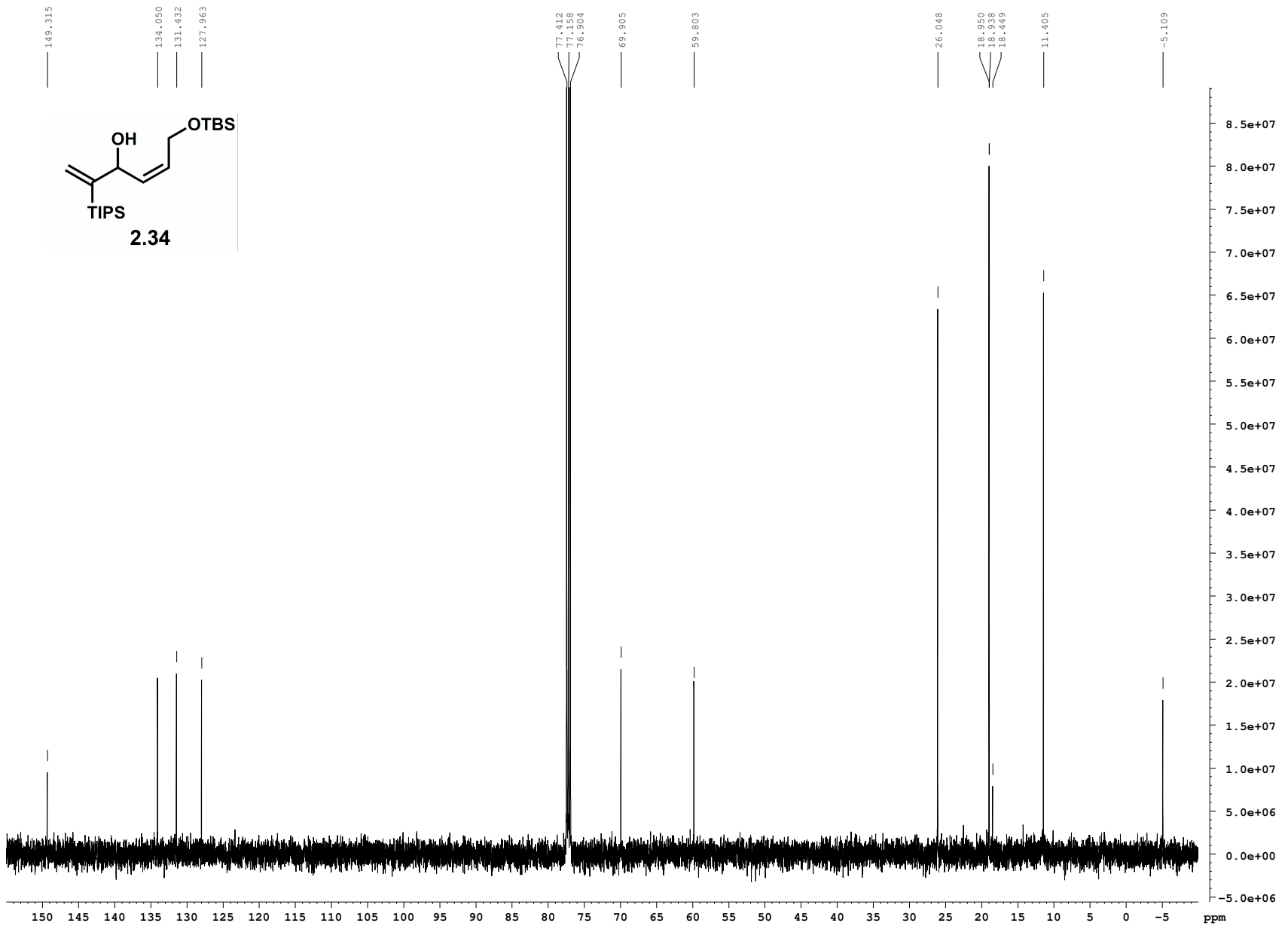
149.315
134.050
131.432
127.963
77.412
77.158
76.904
69.905
59.803
26.048
18.950
18.938
18.449
11.405
-5.109
OTBS
OH
TIPS
2.34
8.5e+07
8.0e+07
7.5e+07
7.0e+07
6.5e+07
6.0e+07
5.5e+07
5.0e+07
4.5e+07
4.0e+07
3.5e+07
3.0e+07
2.5e+07
2.0e+07
1.5e+07
1.0e+07
5.0e+06
0.0e+00
-5.0e+06
150 145 140 135 130 125 120 115 110 105 100 95 90 85 80 75 70 65 60 55 50 45 40 35 30 25 20 15 10 5 0 -5
ppm

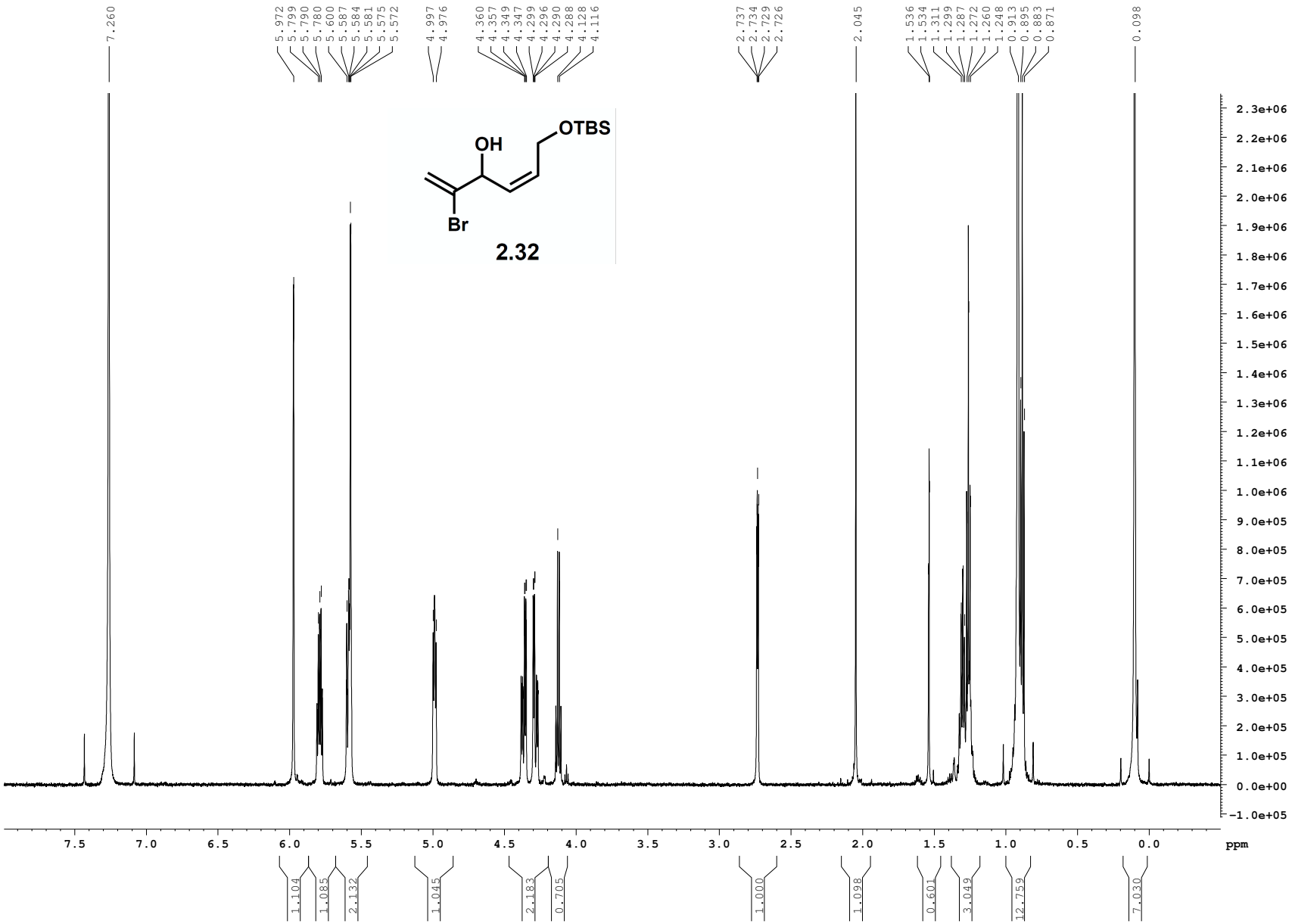
7.260
5.972
5.799
5.790
5.780
5.600
5.587
5.584
5.581
5.575
5.572
4.997
4.976
4.360
4.357
4.349
4.347
4.299
4.296
4.290
4.288
4.128
4.116
2.737
2.734
2.729
2.726
2.045
1.536
1.534
1.311
1.299
1.287
1.272
1.260
1.248
0.913
0.895
0.883
0.871
0.098
OH
OTBS
Br
2.32
ppm
1.104
1.085
2.132
1.045
2.183
0.705
1.000
1.098
0.601
3.049
12.759
7.030

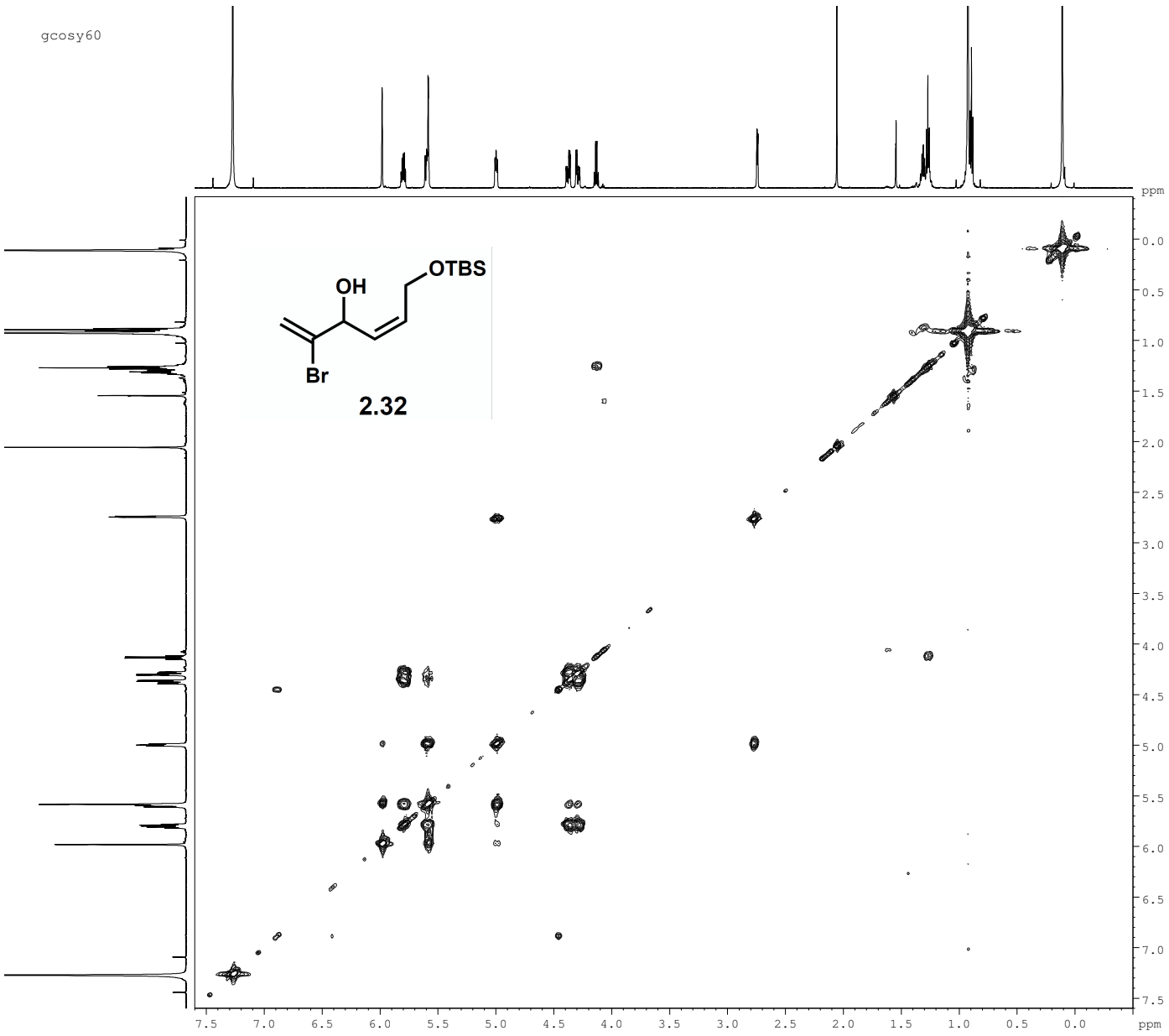
gcosy60
OTBS
OH
Br
2.32
ppm
7.5 7.0 6.5 6.0 5.5 5.0 4.5 4.0 3.5 3.0 2.5 2.0 1.5 1.0 0.5 0.0
ppm

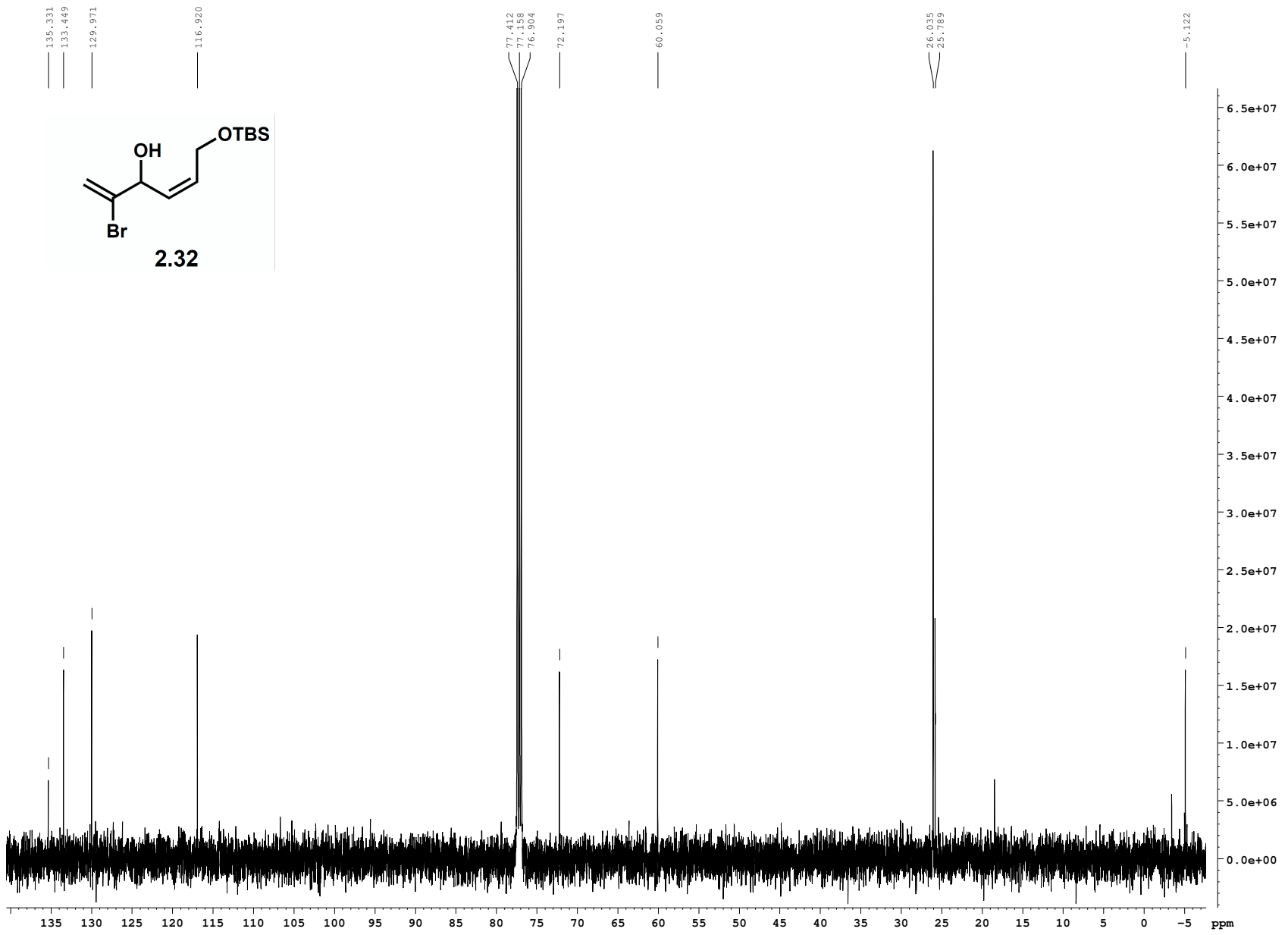
135.331
133.449
129.971
116.920
77.412
77.158
76.904
72.197
60.059
26.035
25.789
-5.122
OTBS
OH
Br
2.32
6.5e+07
6.0e+07
5.5e+07
5.0e+07
4.5e+07
4.0e+07
3.5e+07
3.0e+07
2.5e+07
2.0e+07
1.5e+07
1.0e+07
5.0e+06
0.0e+00
135 130 125 120 115 110 105 100 95 90 85 80 75 70 65 60 55 50 45 40 35 30 25 20 15 10 5 0 -5
ppm

7.260
6.063
6.049
5.935
5.838
5.828
5.819
5.809
5.798
5.791
5.786
5.780
5.769
5.763
5.757
5.752
5.741
5.620
5.617
5.479
5.464
5.461
5.446
5.046
5.044
5.017
5.015
4.999
4.982
4.408
4.406
4.398
4.395
4.385
4.382
4.375
4.372
4.339
4.337
4.331
4.328
4.316
4.313
4.307
4.304
2.379
2.373
2.367
2.360
2.354
2.348
2.119
2.107
2.095
2.083
2.045
1.775
1.763
1.751
1.739
1.727
1.533
0.900
0.083
0.077
O
O
OTBS
Br
2.31
7.5e+06
7.0e+06
6.5e+06
6.0e+06
5.5e+06
5.0e+06
4.5e+06
4.0e+06
3.5e+06
3.0e+06
2.5e+06
2.0e+06
1.5e+06
1.0e+06
5.0e+05
0.0e+00
.945
.965
.982
.960
.964
.000
.007
.031
.983
.009
.918
.908
.038

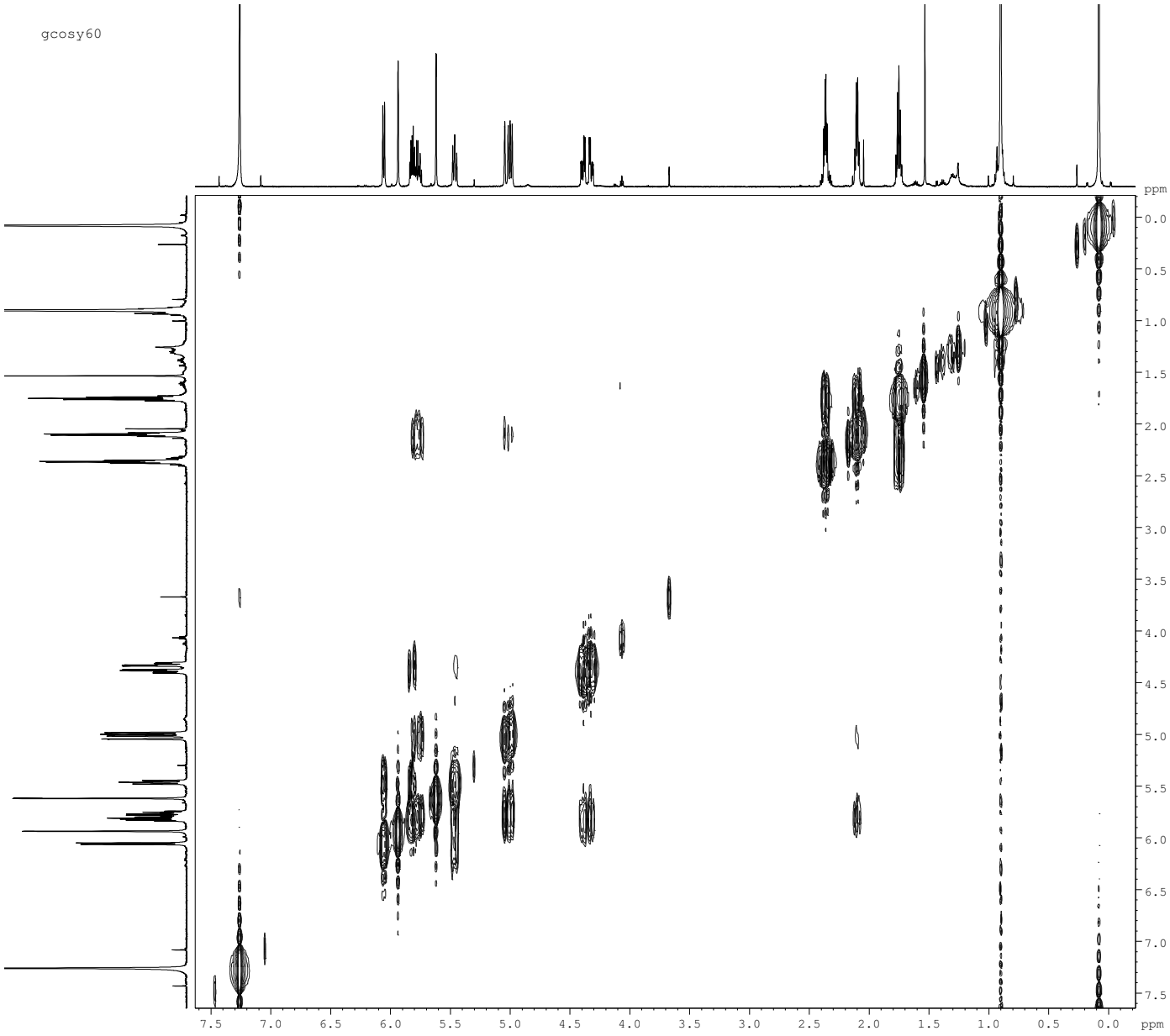
gcosy60
ppm
0.0
0.5
1.0
1.5
2.0
2.5
3.0
3.5
4.0
4.5
5.0
5.5
6.0
6.5
7.0
7.5
7.5
7.0
6.5
6.0
5.5
5.0
4.5
4.0
3.5
3.0
2.5
2.0
1.5
1.0
0.5
0.0
ppm

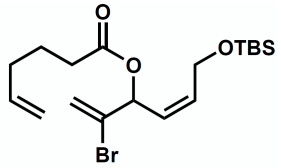
O
O
OTBS
Br

2.31

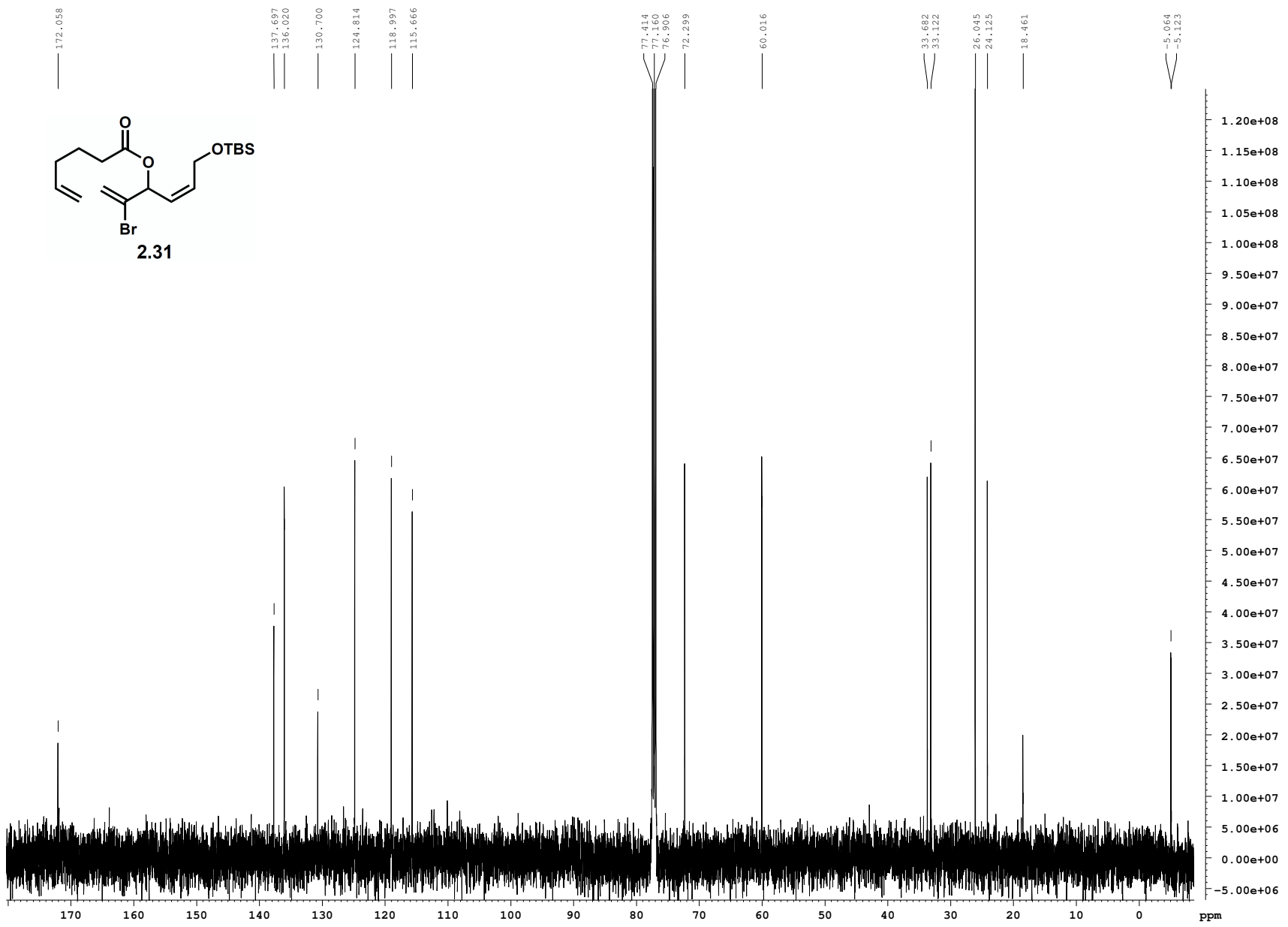
172.058
137.697
136.020
130.700
124.814
118.997
115.666
77.414
77.160
76.906
72.299
60.016
33.682
33.122
26.045
24.125
18.461
-5.064
-5.123
O
O
OTBS
Br
2.31
1.20e+08
1.15e+08
1.10e+08
1.05e+08
1.00e+08
9.50e+07
9.00e+07
8.50e+07
8.00e+07
7.50e+07
7.00e+07
6.50e+07
6.00e+07
5.50e+07
5.00e+07
4.50e+07
4.00e+07
3.50e+07
3.00e+07
2.50e+07
2.00e+07
1.50e+07
1.00e+07
5.00e+06
0.00e+00
-5.00e+06
170
160
150
140
130
120
110
100
90
80
70
60
50
40
30
20
10
0
ppm

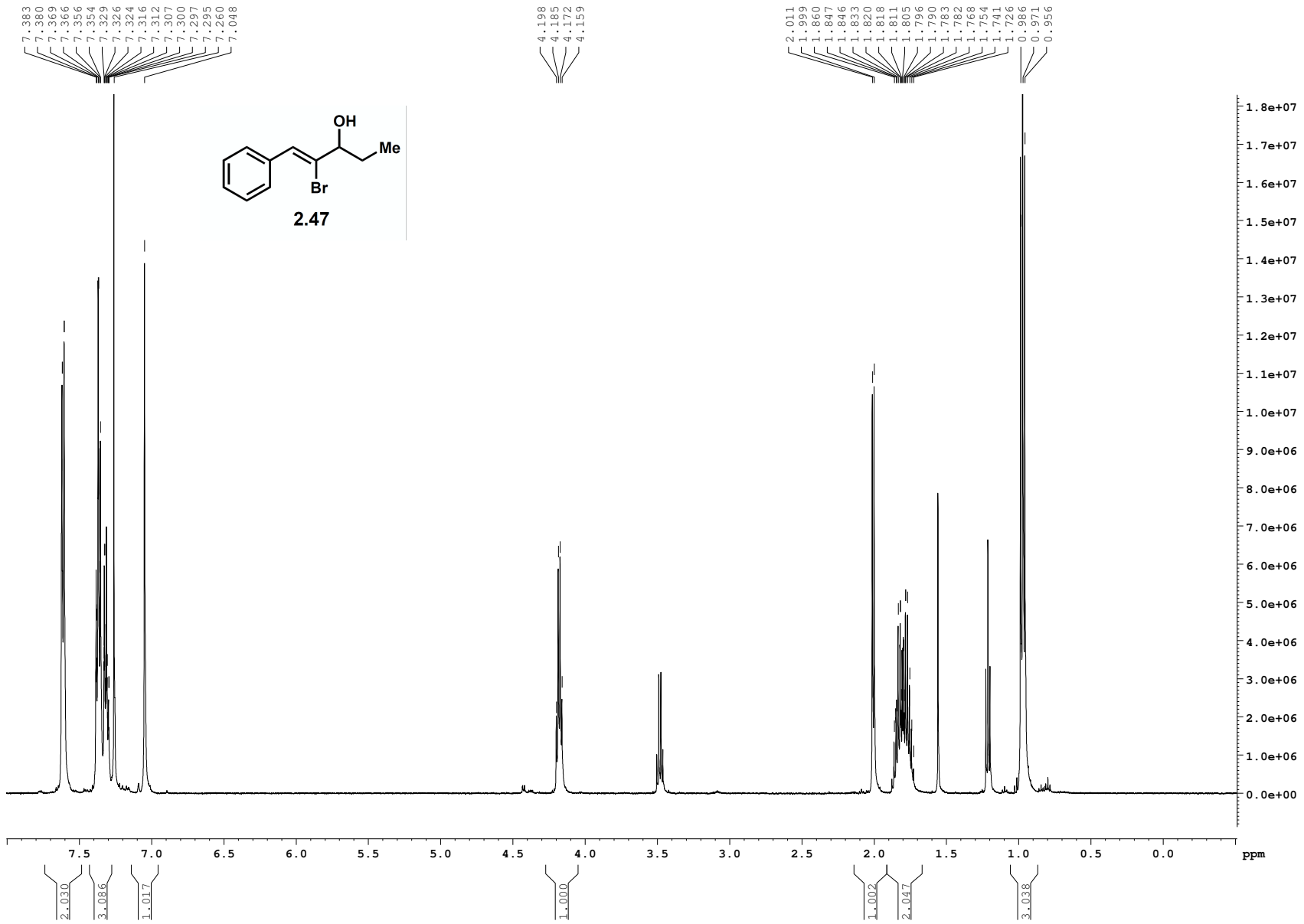
7.383
7.380
7.369
7.366
7.356
7.354
7.329
7.326
7.324
7.316
7.312
7.307
7.300
7.297
7.295
7.260
7.048
4.198
4.185
4.172
4.159
2.011
1.999
1.860
1.847
1.846
1.833
1.820
1.818
1.811
1.805
1.796
1.790
1.783
1.782
1.768
1.754
1.741
1.726
0.986
0.971
0.956
OH
Me
Br
2.47
1.8e+07
1.7e+07
1.6e+07
1.5e+07
1.4e+07
1.3e+07
1.2e+07
1.1e+07
1.0e+07
9.0e+06
8.0e+06
7.0e+06
6.0e+06
5.0e+06
4.0e+06
3.0e+06
2.0e+06
1.0e+06
0.0e+00
7.5
7.0
6.5
6.0
5.5
5.0
4.5
4.0
3.5
3.0
2.5
2.0
1.5
1.0
0.5
0.0
ppm
2.030
3.086
1.017
1.000
1.002
2.047
3.038

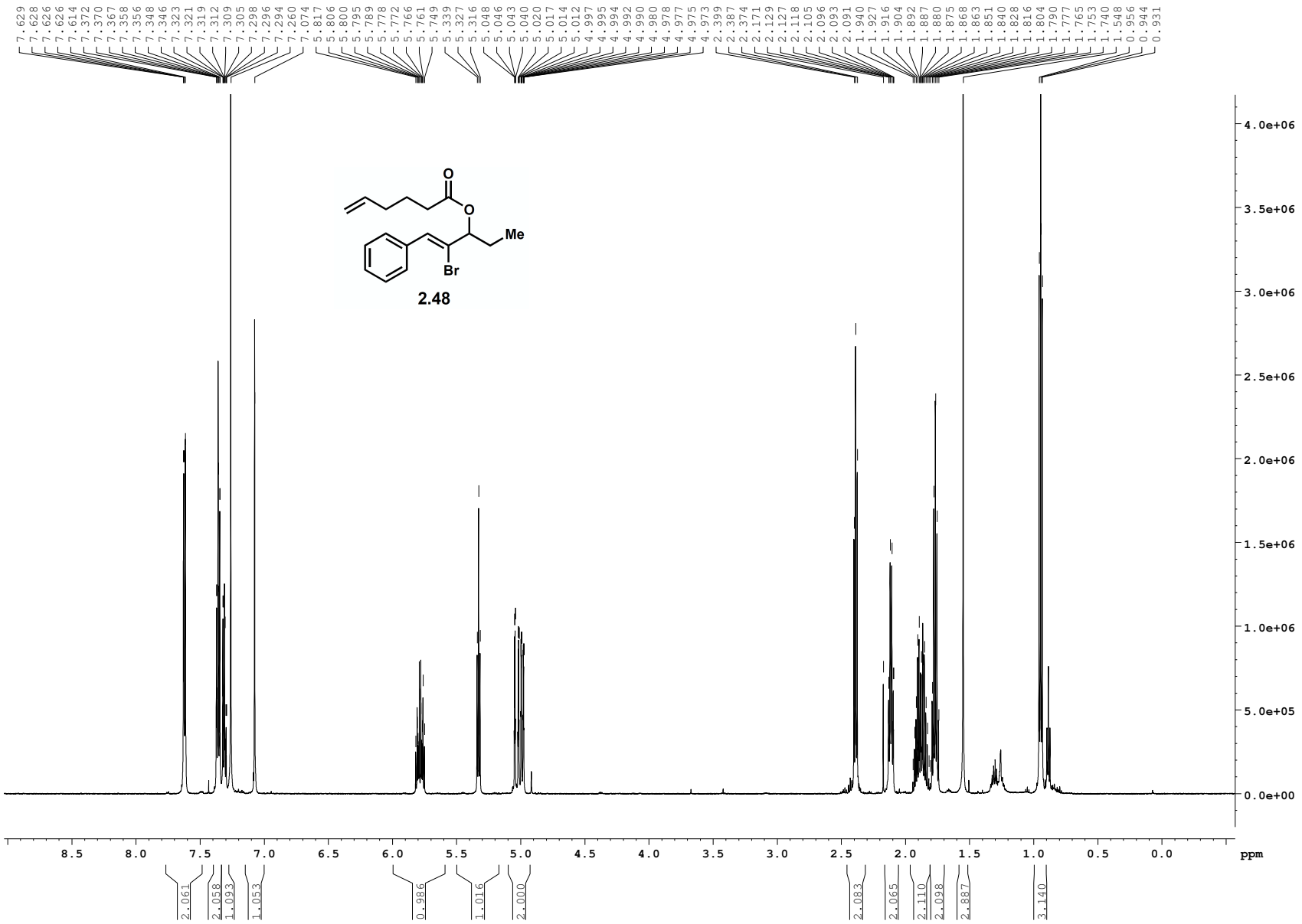
7.629
7.628
7.626
7.626
7.626
7.614
7.372
7.370
7.367
7.358
7.356
7.348
7.346
7.323
7.321
7.319
7.312
7.309
7.305
7.298
7.296
7.294
7.260
7.074
5.817
5.806
5.800
5.795
5.789
5.778
5.772
5.766
5.761
5.749
5.339
5.327
5.316
5.048
5.046
5.043
5.040
5.020
5.017
5.014
5.012
4.997
4.995
4.994
4.992
4.990
4.980
4.978
4.977
4.975
4.973
2.399
2.387
2.374
2.171
2.129
2.127
2.118
2.105
2.096
2.093
2.091
1.940
1.927
1.916
1.904
1.892
1.887
1.880
1.875
1.868
1.863
1.851
1.840
1.828
1.816
1.804
1.790
1.777
1.765
1.753
1.740
1.548
0.956
0.944
0.931
O
O
Me
Br
2.48
4.0e+06
3.5e+06
3.0e+06
2.5e+06
2.0e+06
1.5e+06
1.0e+06
5.0e+05
0.0e+00
8.5
8.0
7.5
7.0
6.5
6.0
5.5
5.0
4.5
4.0
3.5
3.0
2.5
2.0
1.5
1.0
0.5
0.0
ppm
2.061
2.058
1.093
1.053
0.986
1.016
2.000
2.083
2.065
2.110
2.098
2.887
3.140

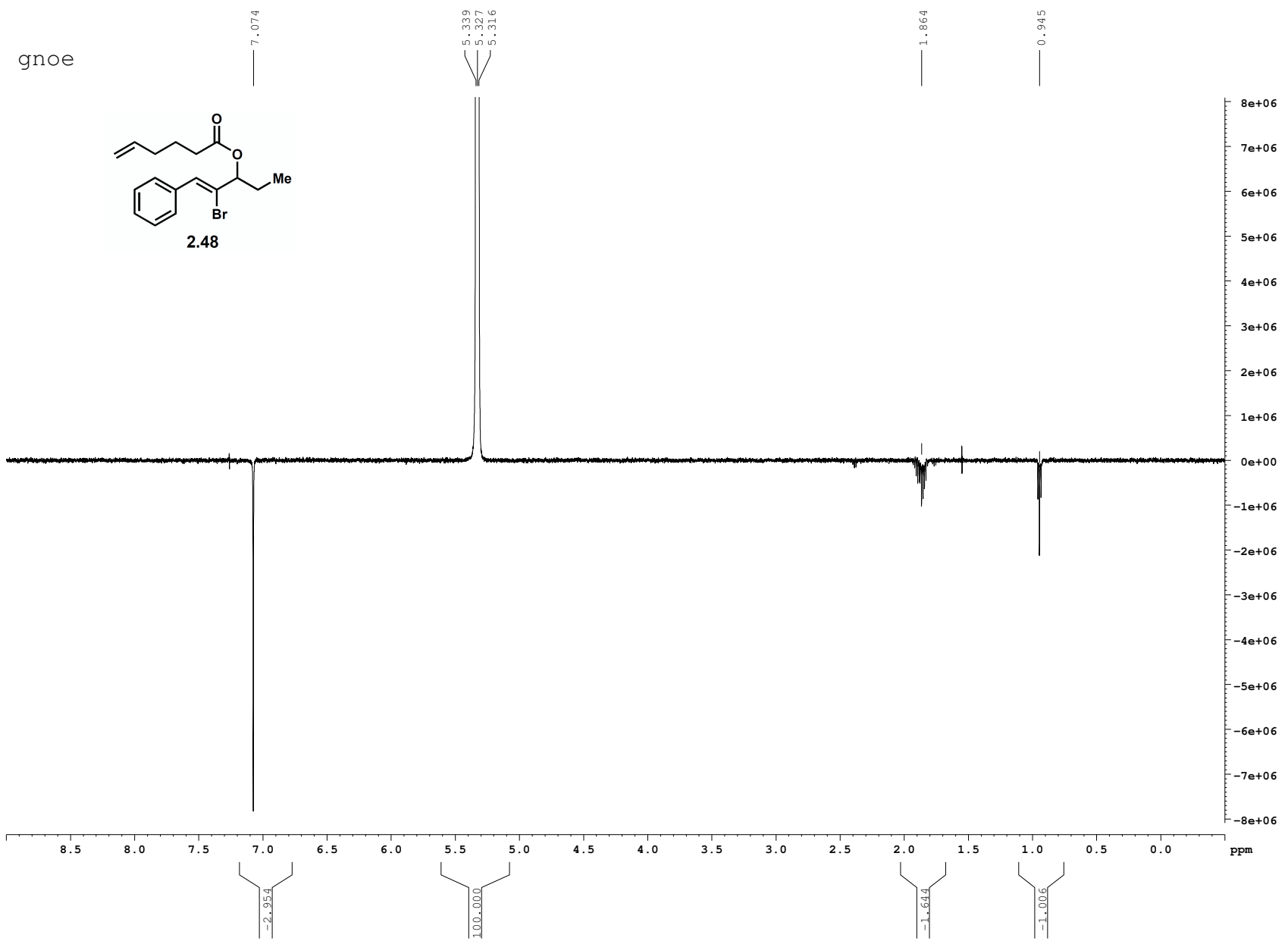
gnoe
7.074
5.339
5.327
5.316
1.864
0.945
O
O
Me
Br
2.48
8e+06
7e+06
6e+06
5e+06
4e+06
3e+06
2e+06
1e+06
0e+00
-1e+06
-2e+06
-3e+06
-4e+06
-5e+06
-6e+06
-7e+06
-8e+06
8.5
8.0
7.5
7.0
6.5
6.0
5.5
5.0
4.5
4.0
3.5
3.0
2.5
2.0
1.5
1.0
0.5
0.0
ppm
-2.954
100.000
-1.644
-1.006

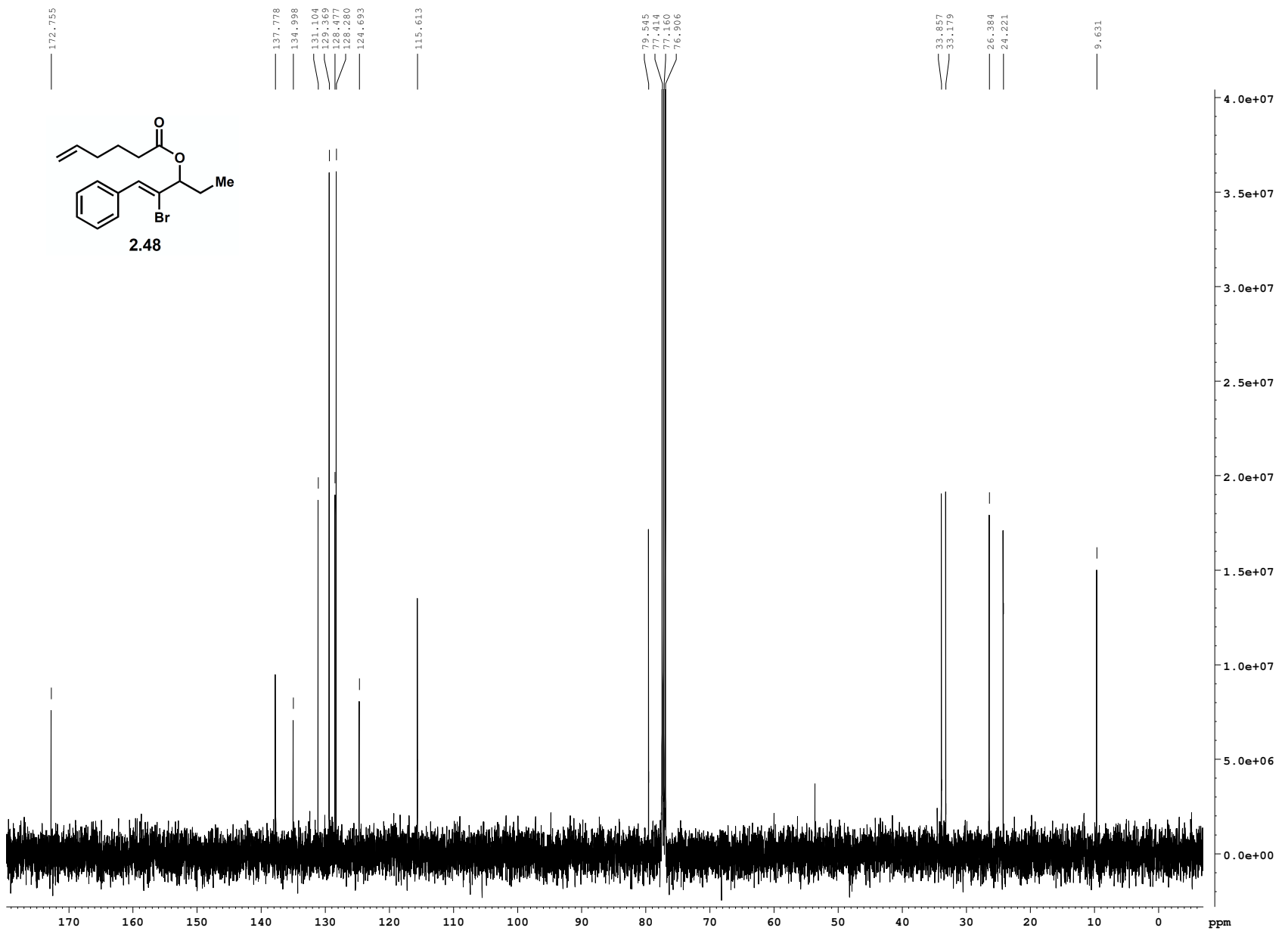
172.755
137.778
134.998
131.104
129.369
128.477
128.280
124.693
115.613
79.545
77.414
77.160
76.906
33.857
33.179
26.384
24.221
9.631
O
O
Me
Br
2.48
4.0e+07
3.5e+07
3.0e+07
2.5e+07
2.0e+07
1.5e+07
1.0e+07
5.0e+06
0.0e+00
170
160
150
140
130
120
110
100
90
80
70
60
50
40
30
20
10
0
ppm

Appendix C:

NMR Data for Chapter 3

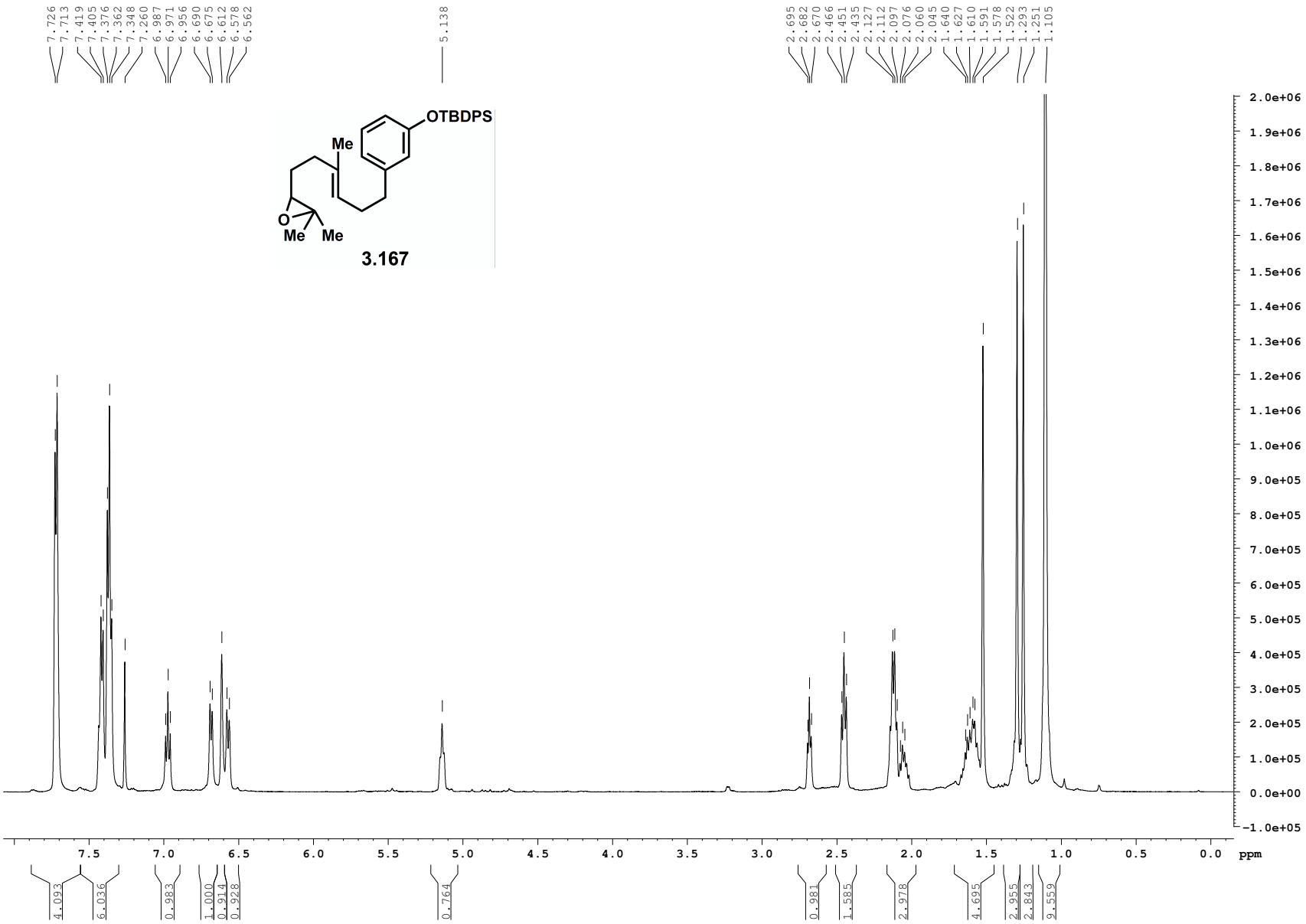
7.726
7.713
7.419
7.405
7.376
7.362
7.348
7.260
6.987
6.971
6.956
6.690
6.675
6.612
6.578
6.562
5.138
2.695
2.682
2.670
2.466
2.451
2.435
2.127
2.112
2.097
2.076
2.060
2.045
1.640
1.627
1.610
1.591
1.578
1.522
1.293
1.251
1.105
OTBDPS
Me
O
Me
Me
3.167
ppm
4.093
6.036
0.983
1.000
0.914
0.928
0.764
0.981
1.585
2.978
4.695
2.955
2.843
9.559

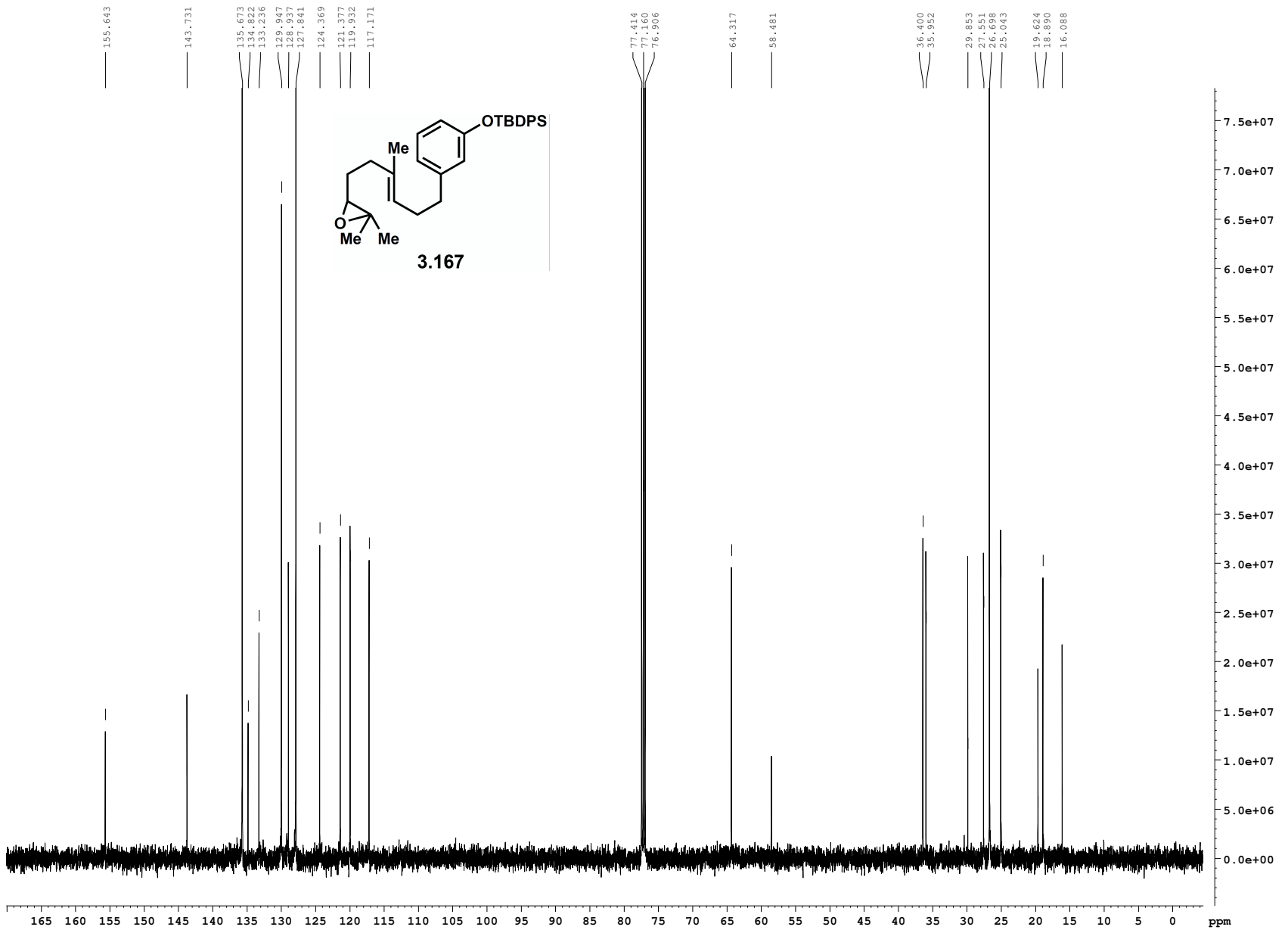
155.643
143.731
135.673
134.822
133.236
129.947
129.937
127.841
124.369
121.377
119.932
117.171
77.414
77.160
76.906
64.317
58.481
36.400
35.952
29.853
27.551
26.698
25.043
19.624
18.890
16.088
OTBDPS
Me
O
Me
Me
3.167
7.5e+07
7.0e+07
6.5e+07
6.0e+07
5.5e+07
5.0e+07
4.5e+07
4.0e+07
3.5e+07
3.0e+07
2.5e+07
2.0e+07
1.5e+07
1.0e+07
5.0e+06
0.0e+00
165 160 155 150 145 140 135 130 125 120 115 110 105 100 95 90 85 80 75 70 65 60 55 50 45 40 35 30 25 20 15 10 5 0
ppm

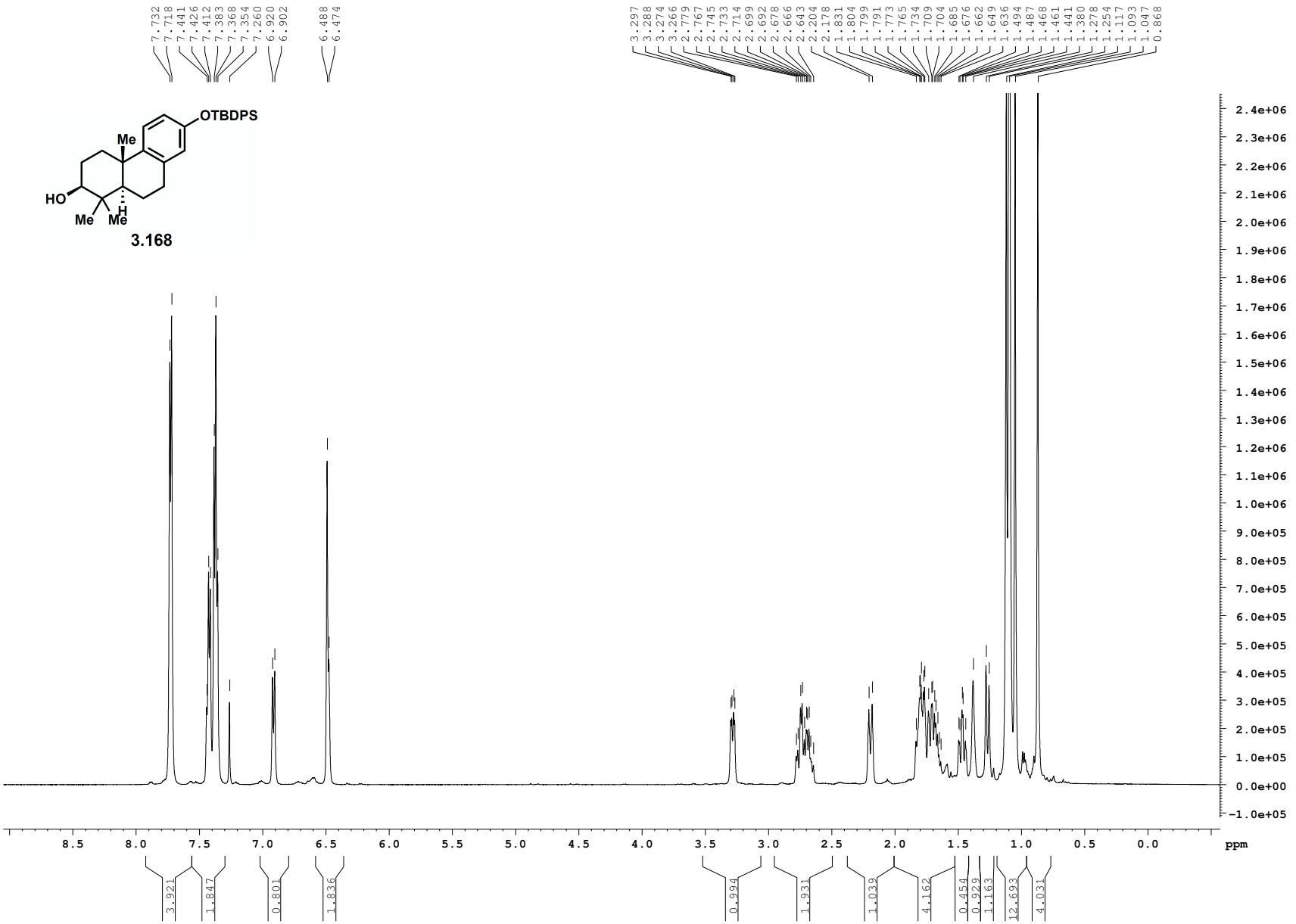
7.732
7.718
7.441
7.426
7.412
7.383
7.368
7.354
7.260
6.920
6.902
6.488
6.474
3.297
3.288
3.274
3.266
2.779
2.767
2.745
2.733
2.714
2.699
2.692
2.678
2.666
2.643
2.204
2.178
1.831
1.804
1.799
1.791
1.773
1.765
1.734
1.709
1.704
1.685
1.676
1.662
1.649
1.636
1.494
1.487
1.468
1.461
1.441
1.380
1.278
1.254
1.117
1.093
1.047
0.868
OTBDPS
Me
HO
Me
Me
H
3.168
ppm
3.921
1.847
0.801
1.836
0.994
1.931
1.039
4.162
0.454
0.329
1.163
12.693
4.031

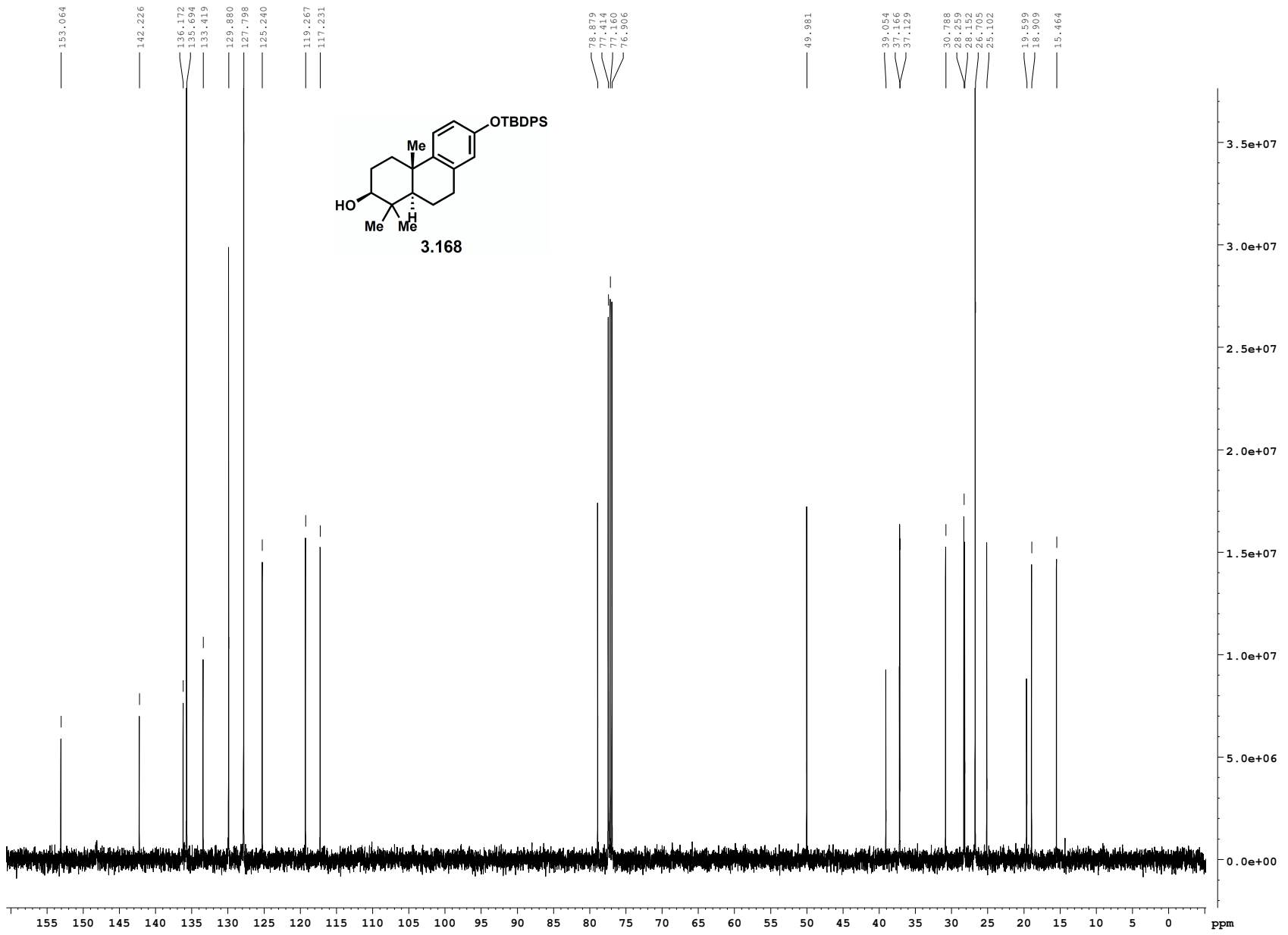
153.064
142.226
136.172
135.694
133.419
129.880
127.798
125.240
119.267
117.231
78.879
77.414
77.160
76.906
49.981
39.054
37.166
37.129
30.788
28.259
28.132
26.705
25.102
19.599
18.909
15.464
OTBDPS
Me
HO
Me
Me
H
3.168
3.5e+07
3.0e+07
2.5e+07
2.0e+07
1.5e+07
1.0e+07
5.0e+06
0.0e+00
155 150 145 140 135 130 125 120 115 110 105 100 95 90 85 80 75 70 65 60 55 50 45 40 35 30 25 20 15 10 5 0
ppm

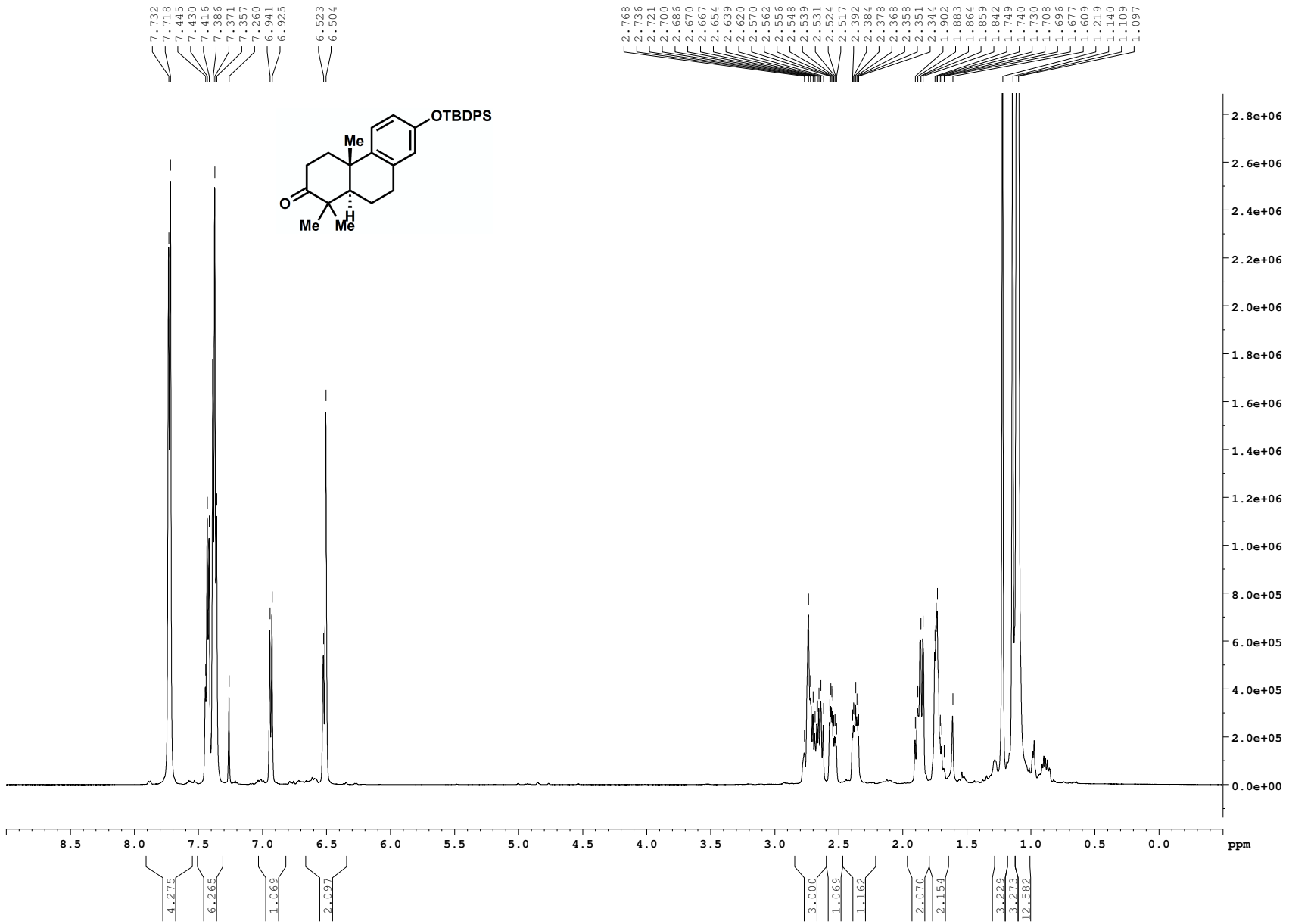
7.732
7.718
7.445
7.430
7.416
7.386
7.371
7.357
7.260
6.941
6.925
6.523
6.504
2.768
2.736
2.721
2.700
2.686
2.670
2.667
2.654
2.639
2.620
2.570
2.562
2.556
2.548
2.539
2.531
2.524
2.517
2.392
2.384
2.378
2.368
2.358
2.351
2.344
1.902
1.883
1.864
1.859
1.842
1.749
1.740
1.730
1.708
1.696
1.677
1.609
1.219
1.140
1.109
1.097
OTBDPS
Me
O
Me
Me
H
2.8e+06
2.6e+06
2.4e+06
2.2e+06
2.0e+06
1.8e+06
1.6e+06
1.4e+06
1.2e+06
1.0e+06
8.0e+05
6.0e+05
4.0e+05
2.0e+05
0.0e+00
8.5
8.0
7.5
7.0
6.5
6.0
5.5
5.0
4.5
4.0
3.5
3.0
2.5
2.0
1.5
1.0
0.5
0.0
ppm
4.275
6.265
1.069
2.097
3.000
1.069
1.162
2.070
2.154
3.229
3.273
12.582

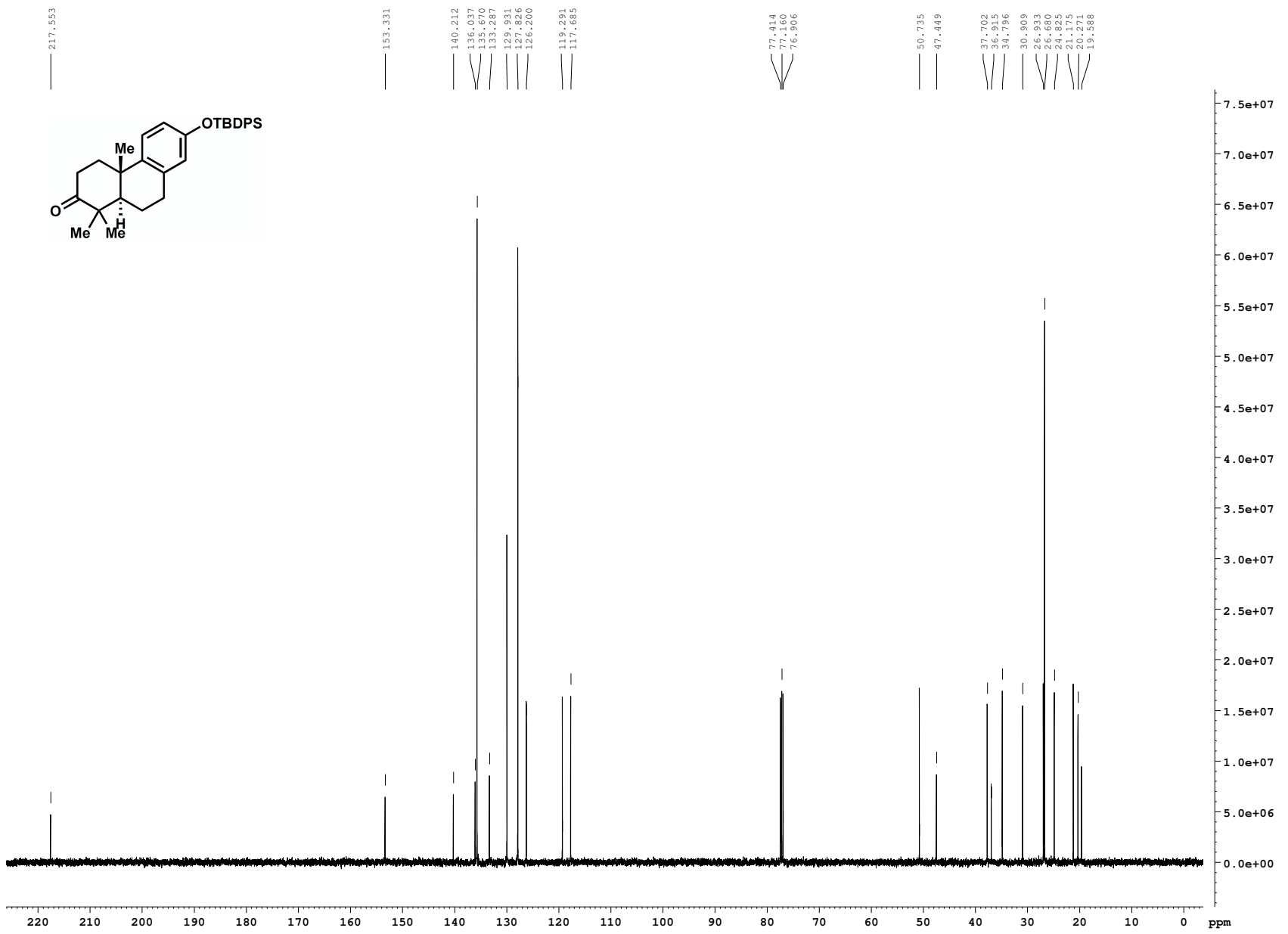
217.553
153.331
140.212
136.037
135.670
133.287
129.931
127.826
126.200
119.291
117.685
77.414
77.160
76.906
50.735
47.449
37.702
36.915
34.796
30.909
26.933
26.680
24.825
21.175
20.271
19.588
OTBDPS
Me
O
Me
Me
H
7.5e+07
7.0e+07
6.5e+07
6.0e+07
5.5e+07
5.0e+07
4.5e+07
4.0e+07
3.5e+07
3.0e+07
2.5e+07
2.0e+07
1.5e+07
1.0e+07
5.0e+06
0.0e+00
220
210
200
190
180
170
160
150
140
130
120
110
100
90
80
70
60
50
40
30
20
10
0
ppm

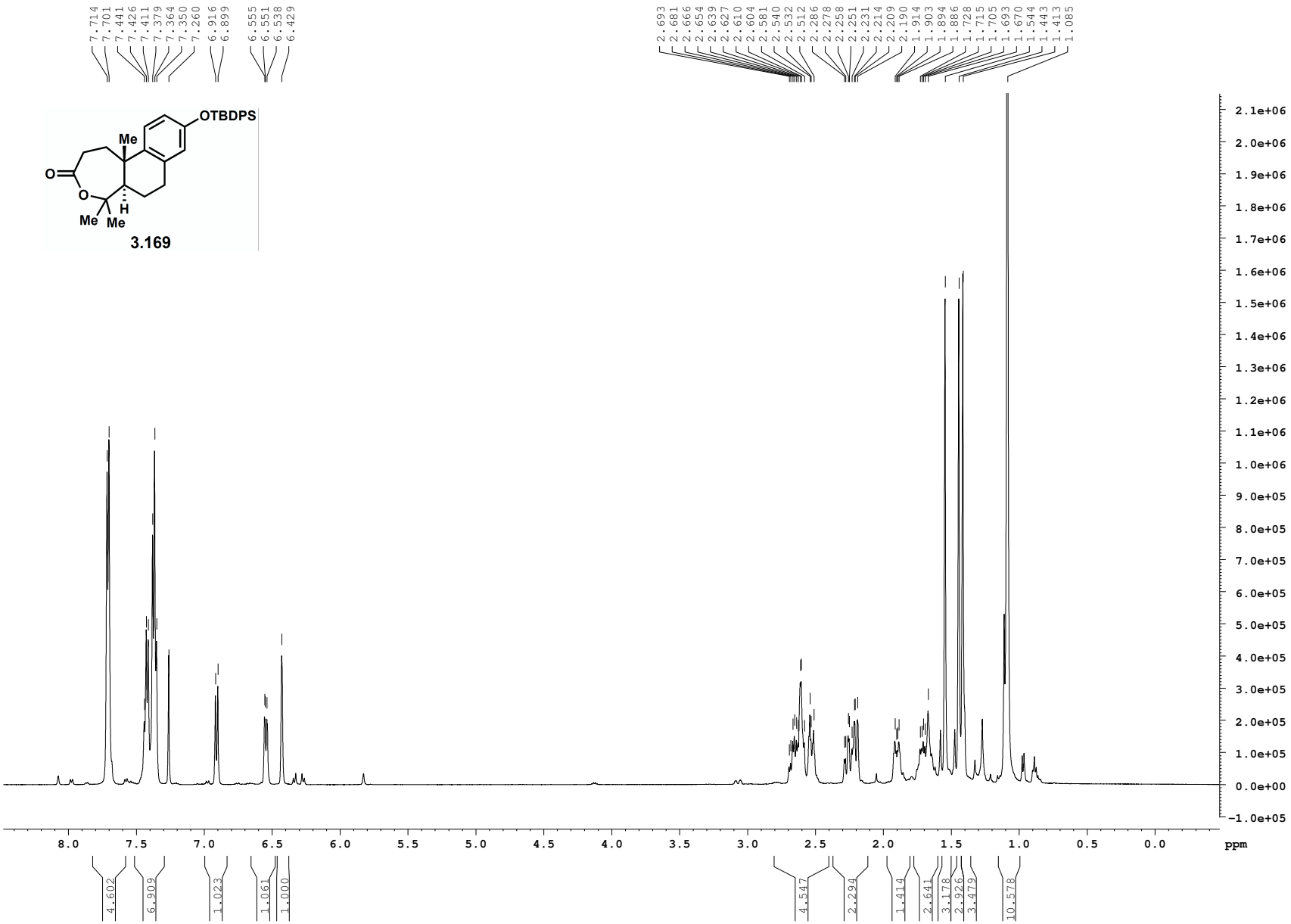
7.714
7.701
7.441
7.426
7.411
7.379
7.364
7.350
7.260
6.916
6.899
6.555
6.551
6.538
6.429
2.693
2.681
2.666
2.654
2.639
2.627
2.610
2.604
2.581
2.540
2.532
2.512
2.286
2.278
2.258
2.251
2.231
2.214
2.209
2.190
1.914
1.903
1.894
1.886
1.728
1.715
1.705
1.693
1.670
1.544
1.443
1.413
1.085
OTBDPS
Me
O
O
Me
Me
H
3.169
ppm
4.602
6.909
1.023
1.061
1.000
4.547
2.294
1.414
2.641
3.178
2.926
3.479
10.578

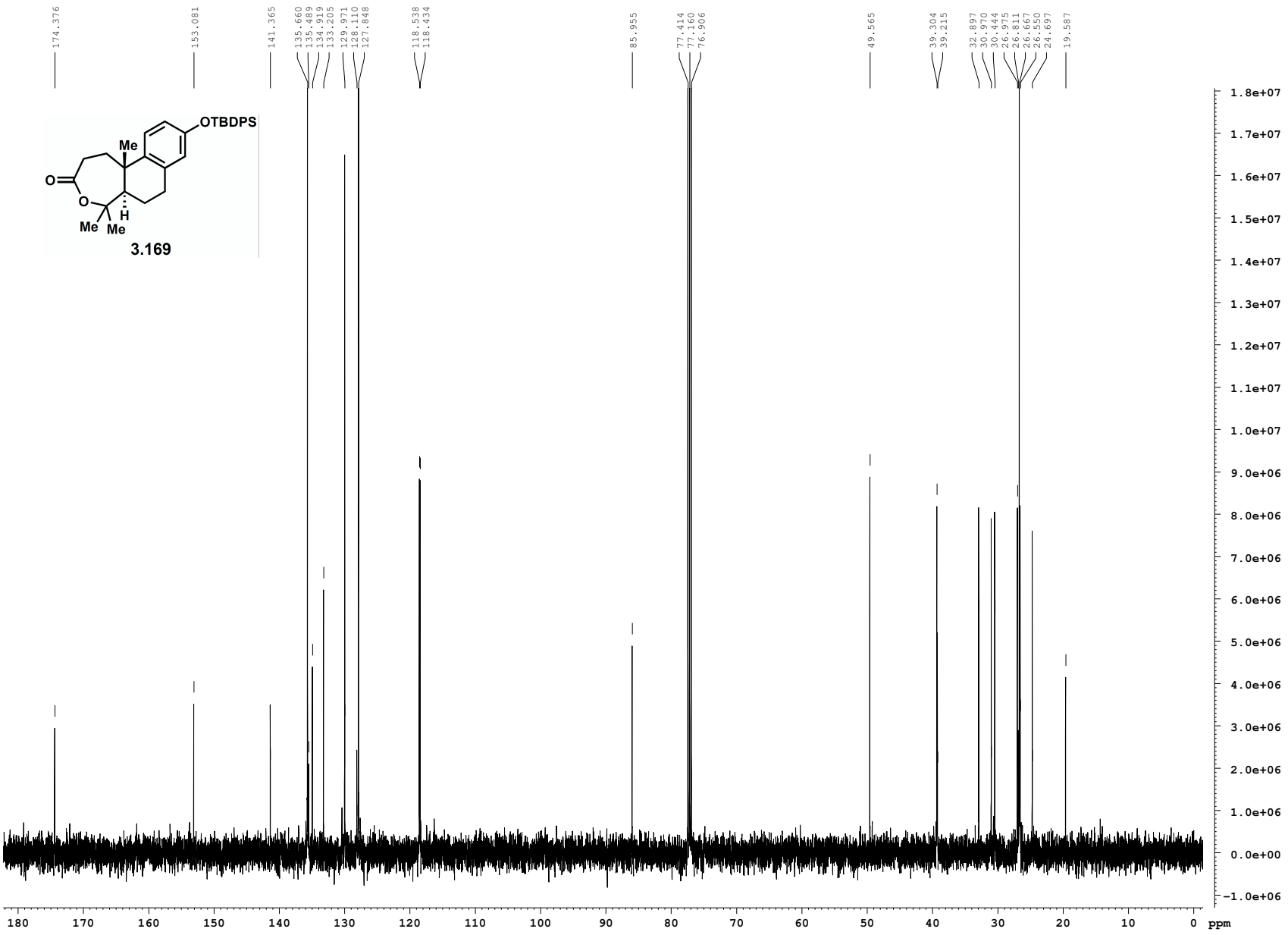
174.376
153.081
141.365
135.660
135.489
134.919
133.205
129.971
128.110
127.848
118.538
118.434
85.955
77.414
77.160
76.906
49.565
39.304
39.215
32.897
30.970
30.444
26.975
26.811
26.667
26.550
24.697
19.587
OTBDPS
Me
O
O
Me
Me
H
3.169
1.8e+07
1.7e+07
1.6e+07
1.5e+07
1.4e+07
1.3e+07
1.2e+07
1.1e+07
1.0e+07
9.0e+06
8.0e+06
7.0e+06
6.0e+06
5.0e+06
4.0e+06
3.0e+06
2.0e+06
1.0e+06
0.0e+00
-1.0e+06
180
170
160
150
140
130
120
110
100
90
80
70
60
50
40
30
20
10
0
ppm

7.697
7.683
7.424
7.410
7.397
7.368
7.353
7.339
6.976
6.958
6.552
6.536
6.422
4.910
4.673
3.310
2.583
2.515
2.378
2.359
2.126
2.025
2.002
1.972
1.965
1.944
1.807
1.797
1.761
1.741
1.709
1.126
1.102
1.074
OTBDPS
Me
HO
O
H
Me
ppm
4.331
6.380
1.031
1.007
1.000
3.332
1.103
2.144
1.184
1.105
2.274
1.402
5.202
4.011
9.375

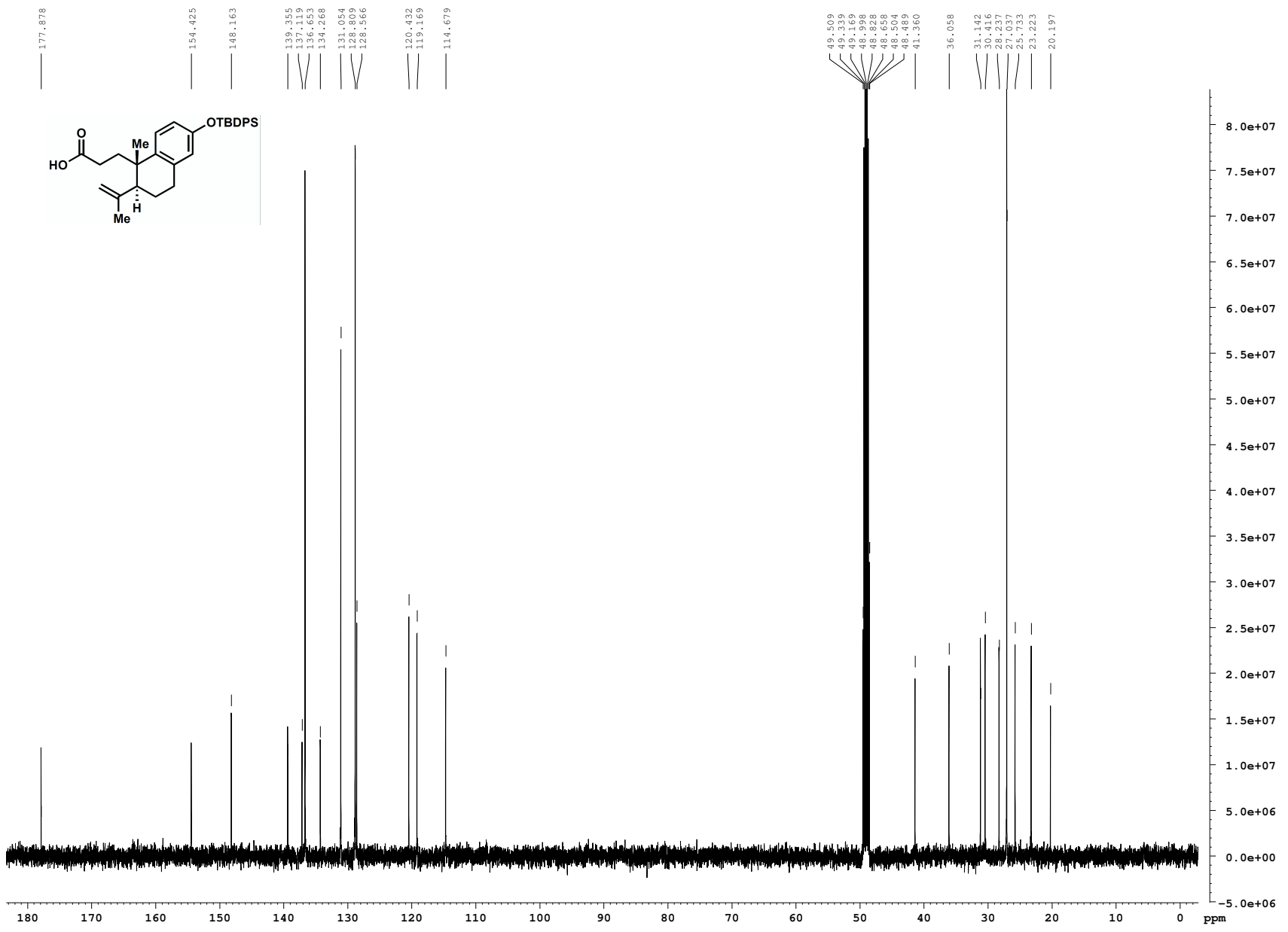
177.878
154.425
148.163
139.355
137.119
136.653
134.268
131.054
128.809
128.566
120.432
119.169
114.679
49.509
49.339
49.169
48.998
48.828
48.658
48.504
48.489
41.360
36.058
31.142
30.416
28.237
27.037
25.733
23.223
20.197
OTBDPS
O
HO
Me
H
Me
8.0e+07
7.5e+07
7.0e+07
6.5e+07
6.0e+07
5.5e+07
5.0e+07
4.5e+07
4.0e+07
3.5e+07
3.0e+07
2.5e+07
2.0e+07
1.5e+07
1.0e+07
5.0e+06
0.0e+00
-5.0e+06
180
170
160
150
140
130
120
110
100
90
80
70
60
50
40
30
20
10
0
ppm

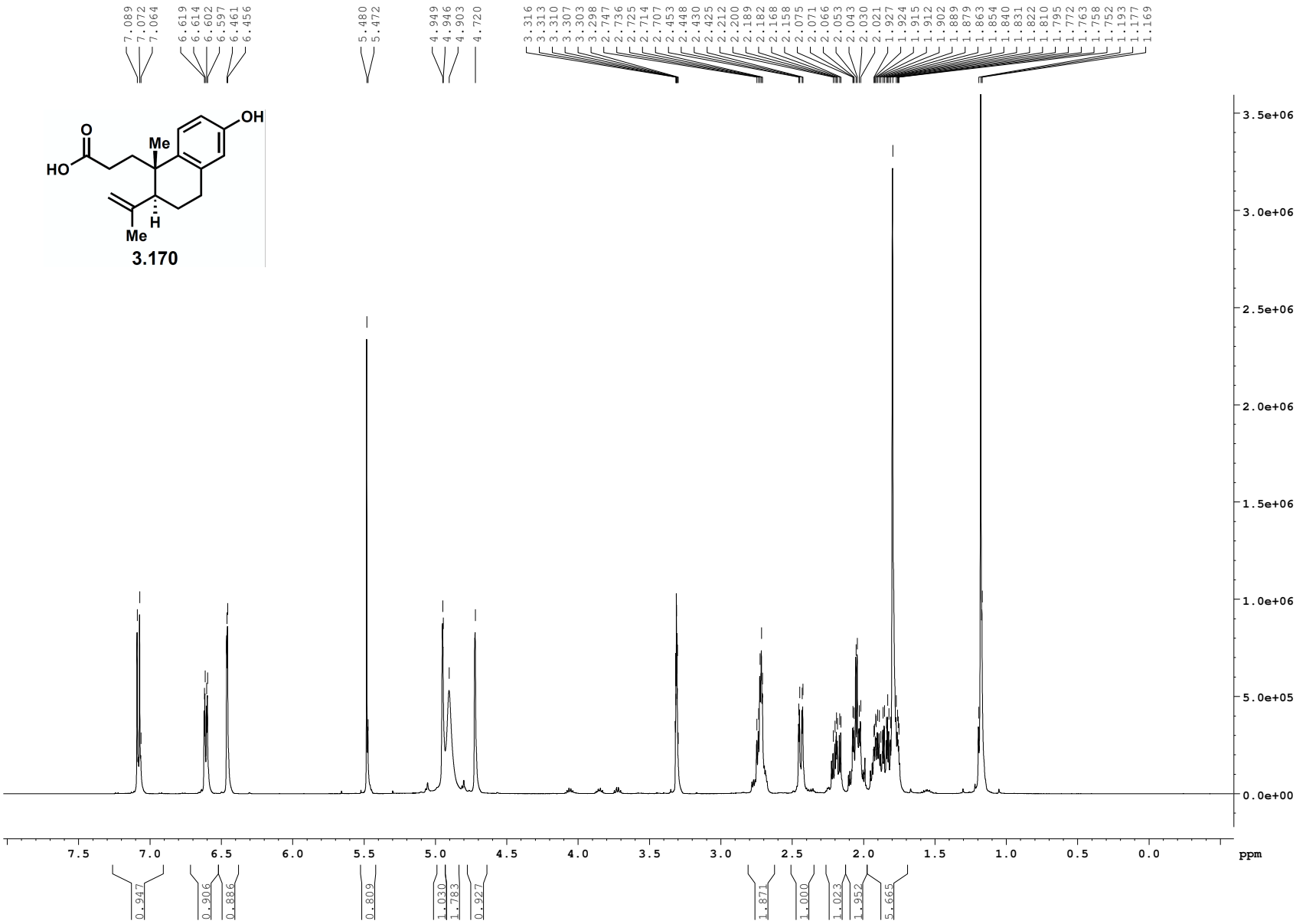
7.089
7.072
7.064
6.619
6.614
6.602
6.597
6.461
6.456
5.480
5.472
4.949
4.946
4.903
4.720
3.316
3.313
3.310
3.307
3.303
3.298
2.747
2.736
2.725
2.714
2.707
2.453
2.448
2.430
2.425
2.212
2.200
2.189
2.182
2.168
2.158
2.075
2.071
2.066
2.053
2.043
2.030
2.021
1.927
1.924
1.915
1.912
1.902
1.889
1.879
1.863
1.854
1.840
1.831
1.822
1.810
1.795
1.772
1.763
1.758
1.752
1.193
1.177
1.169
O
HO
Me
OH
H
Me
3.170
3.5e+06
3.0e+06
2.5e+06
2.0e+06
1.5e+06
1.0e+06
5.0e+05
0.0e+00
7.5
7.0
6.5
6.0
5.5
5.0
4.5
4.0
3.5
3.0
2.5
2.0
1.5
1.0
0.5
0.0
ppm
0.947
0.906
0.886
0.809
1.030
1.783
0.927
1.871
1.000
1.023
1.952
5.665

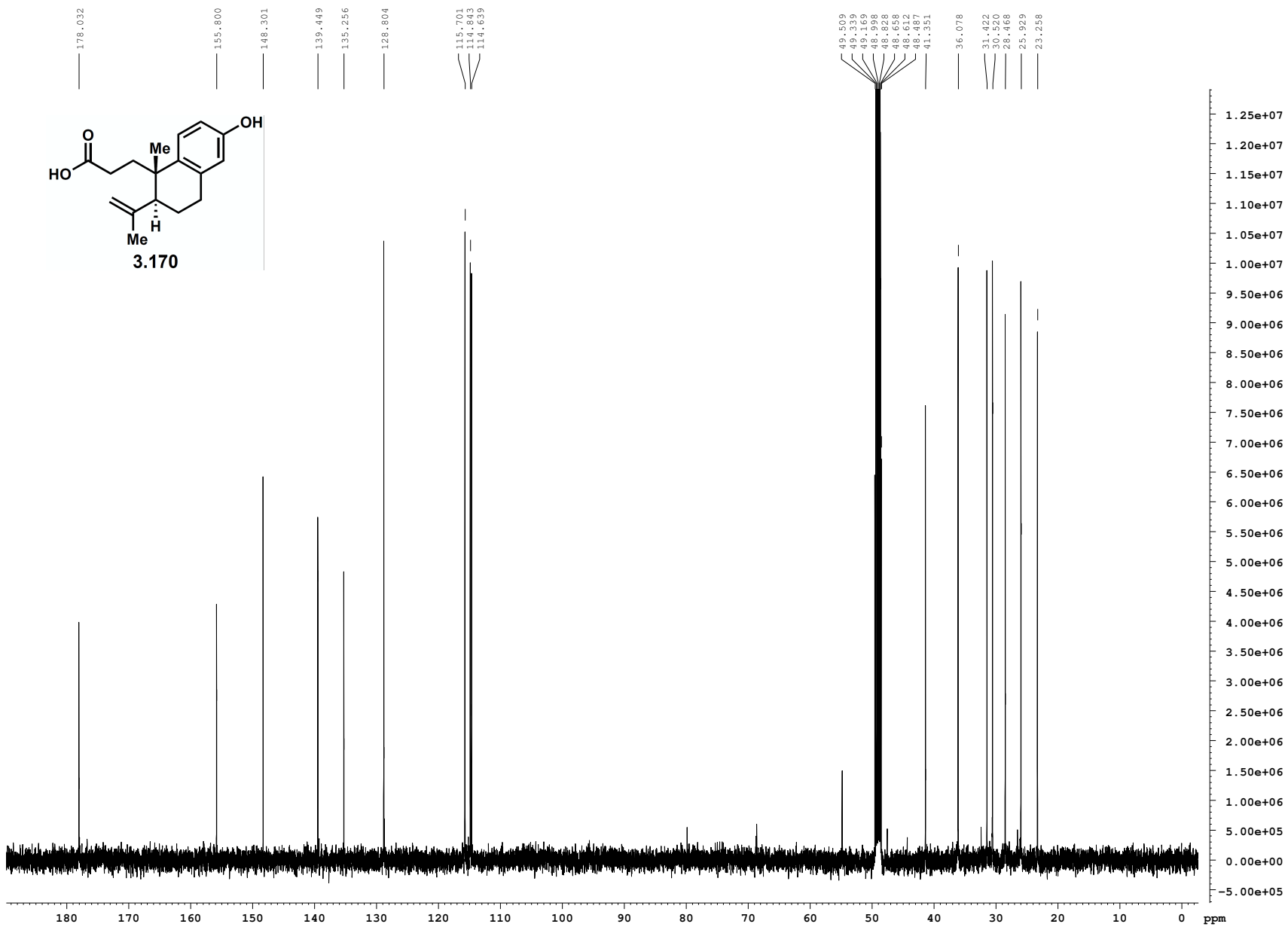
178.032
155.800
148.301
139.449
135.256
128.804
115.701
114.843
114.639
49.509
49.339
49.169
48.998
48.828
48.658
48.612
48.487
41.351
36.078
31.422
30.520
28.468
25.929
23.258
O
HO
Me
OH
H
Me
3.170
1.25e+07
1.20e+07
1.15e+07
1.10e+07
1.05e+07
1.00e+07
9.50e+06
9.00e+06
8.50e+06
8.00e+06
7.50e+06
7.00e+06
6.50e+06
6.00e+06
5.50e+06
5.00e+06
4.50e+06
4.00e+06
3.50e+06
3.00e+06
2.50e+06
2.00e+06
1.50e+06
1.00e+06
5.00e+05
0.00e+00
-5.00e+05
180
170
160
150
140
130
120
110
100
90
80
70
60
50
40
30
20
10
0
ppm

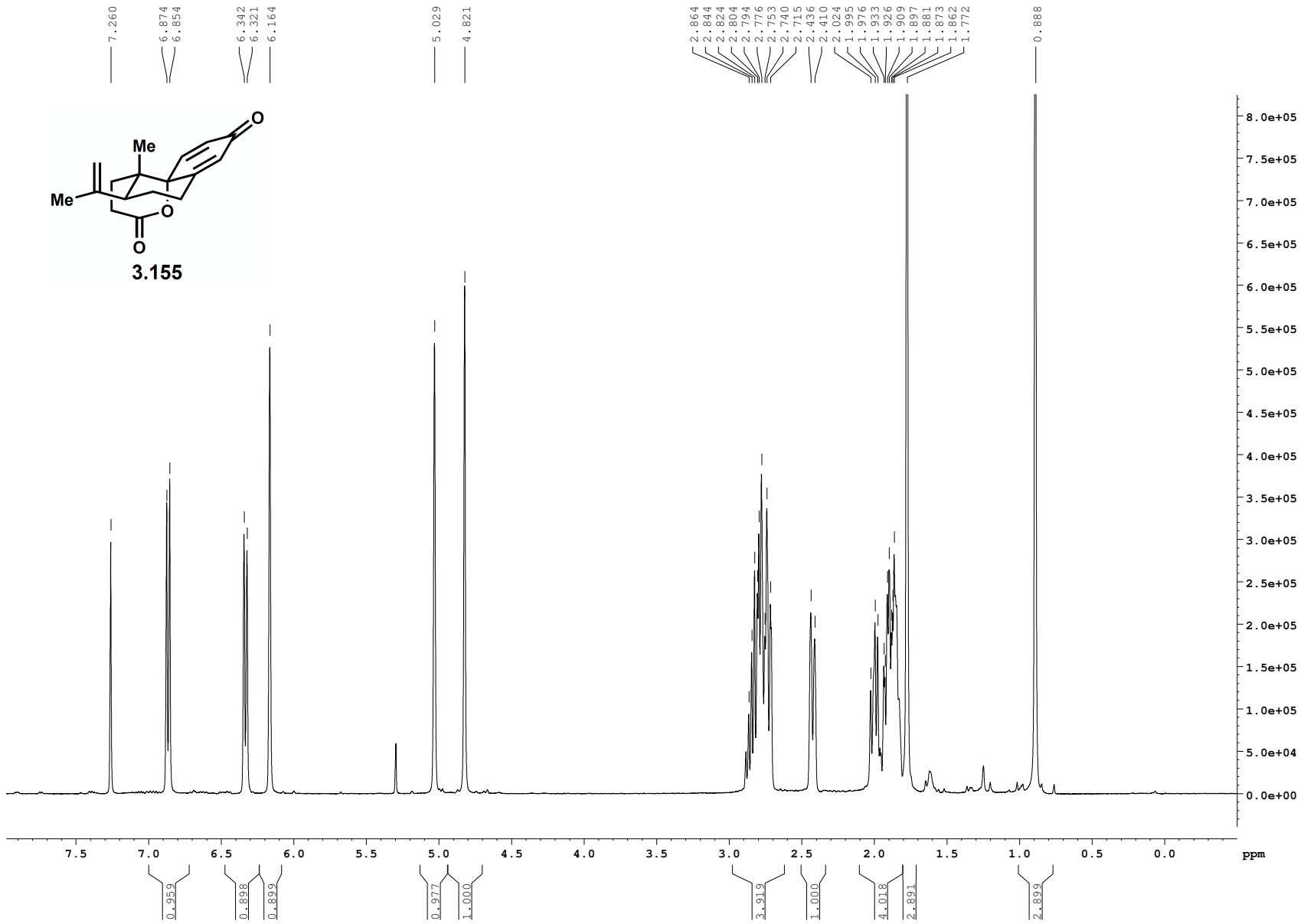
7.260
6.874
6.854
6.342
6.321
6.164
5.029
4.821
2.864
2.844
2.824
2.804
2.794
2.776
2.753
2.740
2.715
2.436
2.410
2.024
1.995
1.976
1.933
1.926
1.909
1.897
1.881
1.873
1.862
1.772
0.888
Me
Me
O
O
O
3.155
8.0e+05
7.5e+05
7.0e+05
6.5e+05
6.0e+05
5.5e+05
5.0e+05
4.5e+05
4.0e+05
3.5e+05
3.0e+05
2.5e+05
2.0e+05
1.5e+05
1.0e+05
5.0e+04
0.0e+00
7.5
7.0
6.5
6.0
5.5
5.0
4.5
4.0
3.5
3.0
2.5
2.0
1.5
1.0
0.5
0.0
ppm
0.959
0.898
0.899
0.977
1.000
3.919
1.000
4.018
2.891
2.899

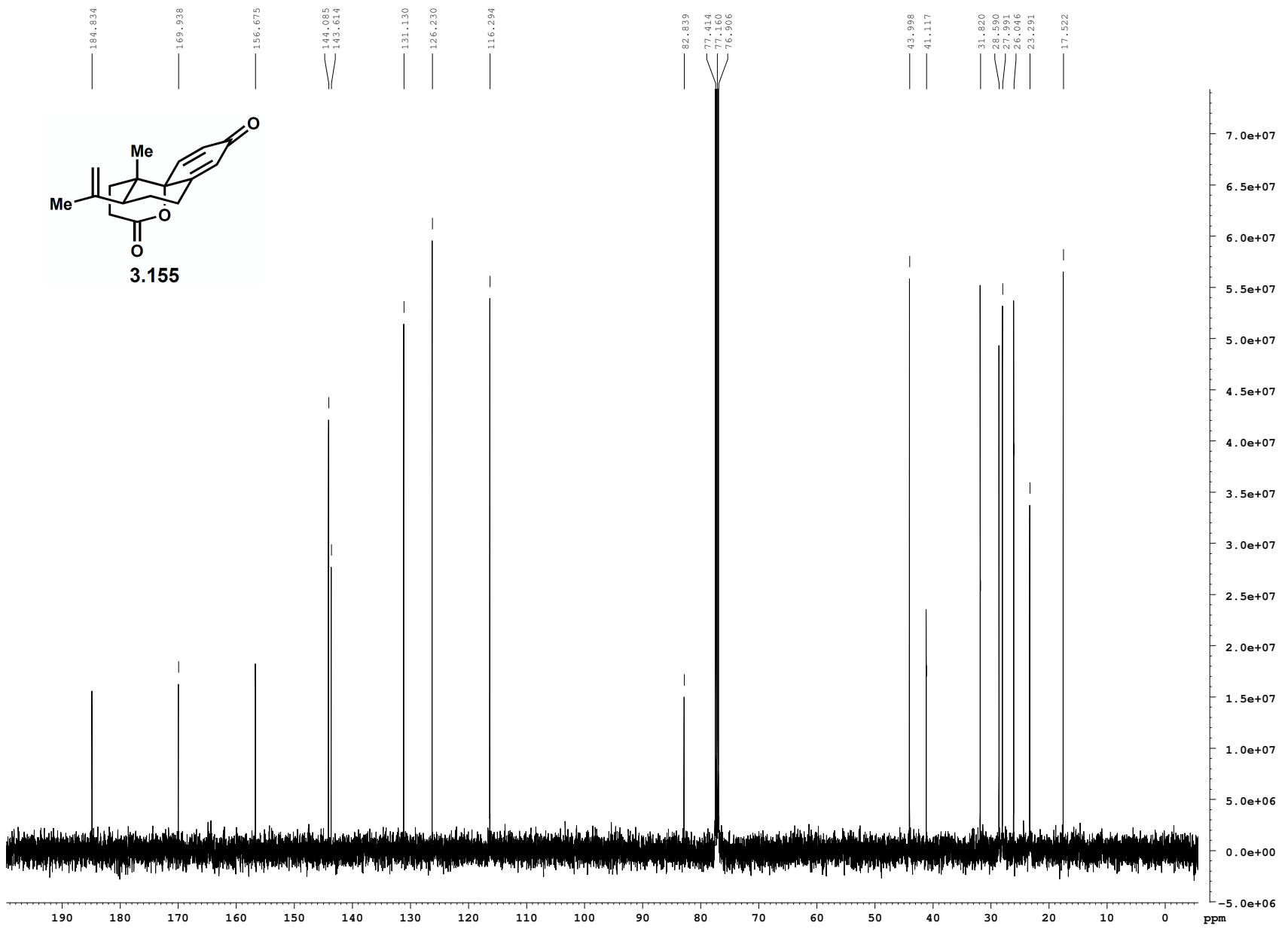
184.834
169.938
156.675
144.085
143.614
131.130
126.230
116.294
82.839
77.414
77.160
76.906
43.998
41.117
31.820
28.590
27.991
26.046
23.291
17.522
Me
Me
O
O
O
3.155
7.0e+07
6.5e+07
6.0e+07
5.5e+07
5.0e+07
4.5e+07
4.0e+07
3.5e+07
3.0e+07
2.5e+07
2.0e+07
1.5e+07
1.0e+07
5.0e+06
0.0e+00
-5.0e+06
190
180
170
160
150
140
130
120
110
100
90
80
70
60
50
40
30
20
10
0
ppm

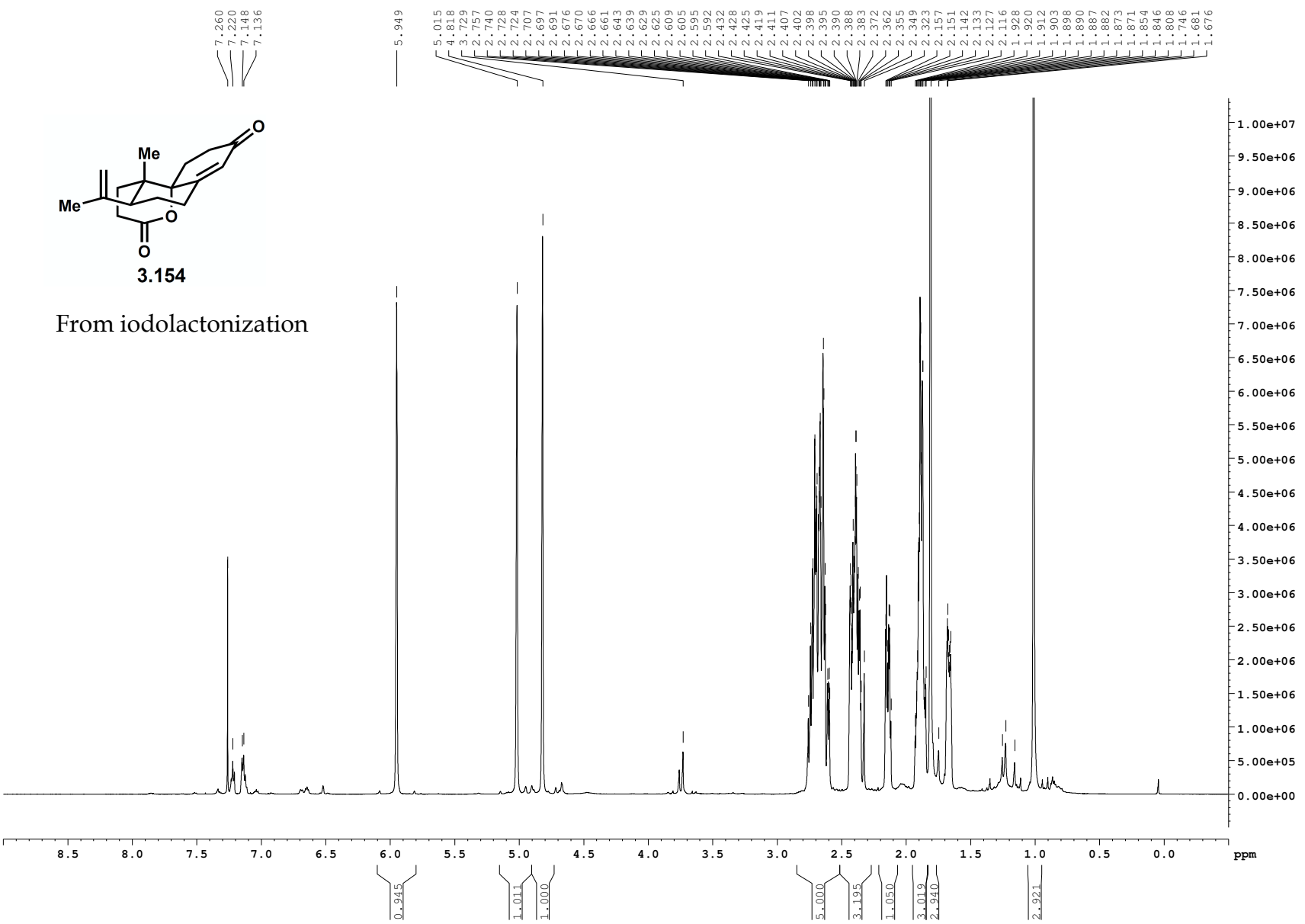
7.260
7.220
7.148
7.136
5.949
5.015
4.818
3.729
2.757
2.740
2.728
2.724
2.707
2.697
2.691
2.676
2.670
2.666
2.661
2.643
2.639
2.629
2.625
2.609
2.605
2.595
2.592
2.432
2.428
2.425
2.419
2.411
2.407
2.402
2.398
2.395
2.390
2.388
2.383
2.372
2.362
2.355
2.349
2.323
2.157
2.151
2.142
2.133
2.127
2.116
1.928
1.920
1.912
1.903
1.898
1.890
1.887
1.882
1.873
1.871
1.854
1.846
1.808
1.746
1.681
1.676
Me
Me
O
O
O
3.154
From iodolactonization
1.00e+07
9.50e+06
9.00e+06
8.50e+06
8.00e+06
7.50e+06
7.00e+06
6.50e+06
6.00e+06
5.50e+06
5.00e+06
4.50e+06
4.00e+06
3.50e+06
3.00e+06
2.50e+06
2.00e+06
1.50e+06
1.00e+06
5.00e+05
0.00e+00
8.5
8.0
7.5
7.0
6.5
6.0
5.5
5.0
4.5
4.0
3.5
3.0
2.5
2.0
1.5
1.0
0.5
0.0
ppm
0.945
1.011
1.000
5.000
3.195
1.050
3.019
2.940
2.921

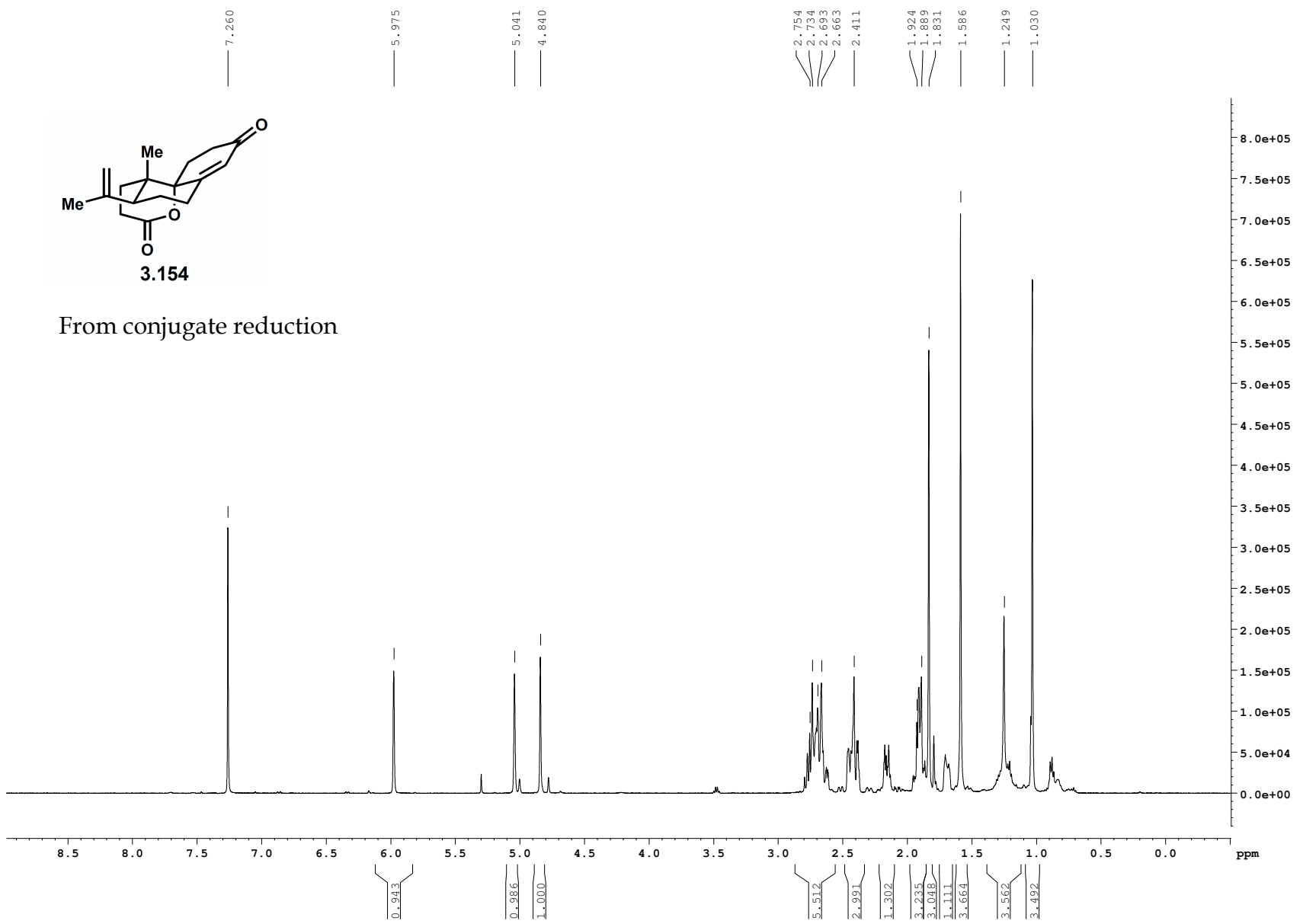

From conjugate reduction

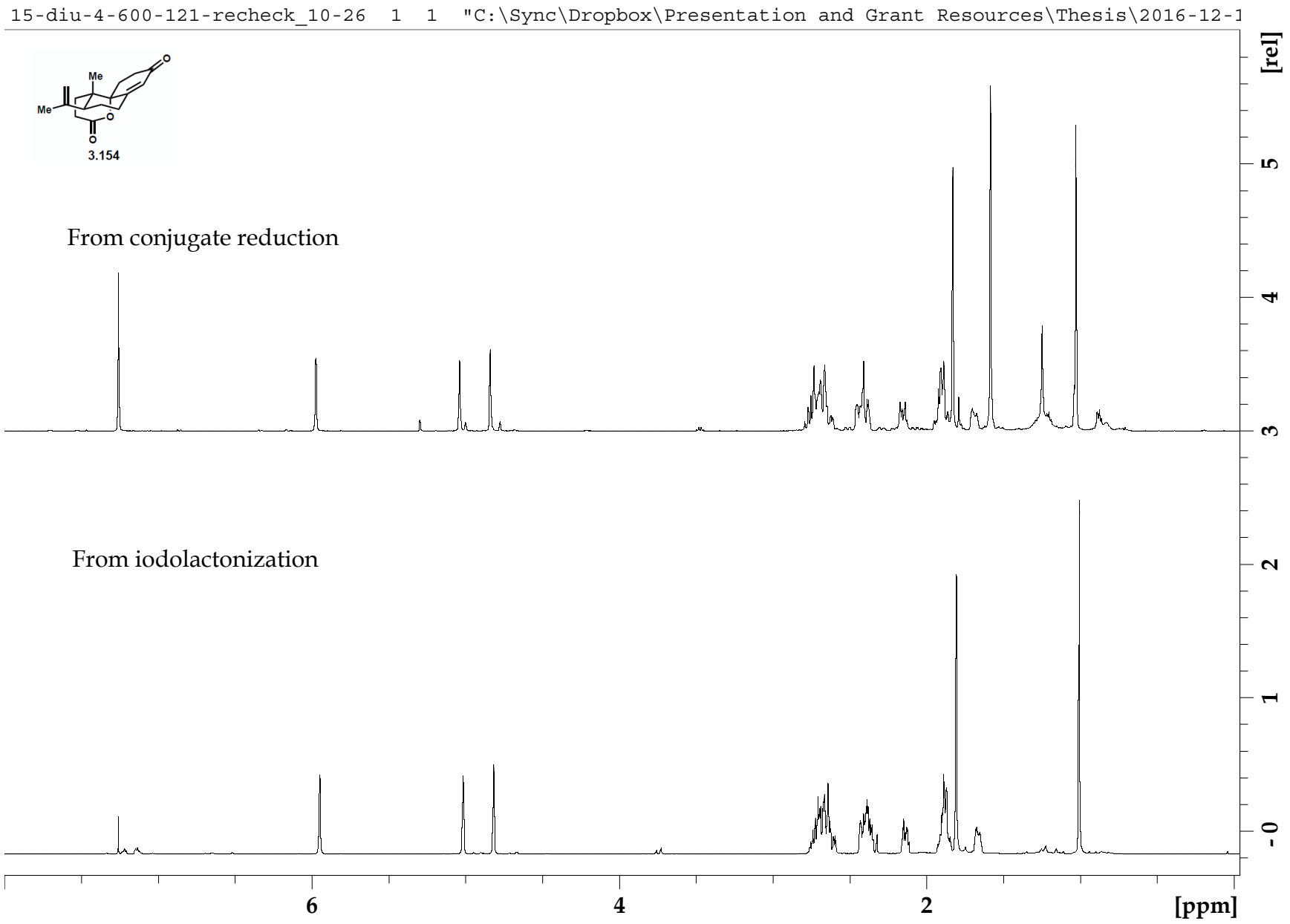
15-diu-4-600-121-recheck_10-26 1 1 "C:\Sync\Dropbox\Presentation and Grant Resources\Thesis\2016-12-1
Me
Me
O
O
O
3.154
From conjugate reduction
From iodolactonization
[rel]
5
4
3
2
1
-0
6
4
2
[ppm]

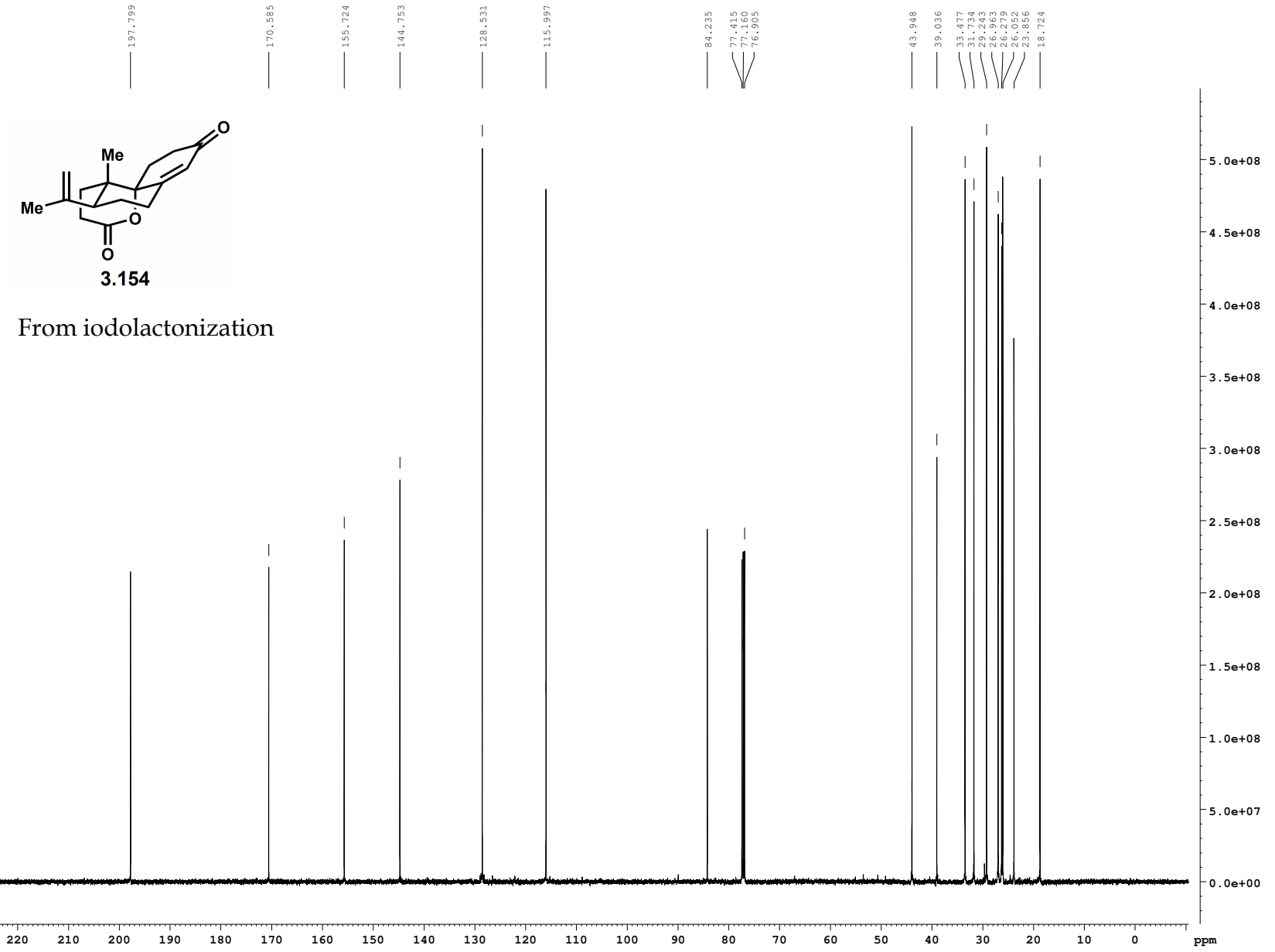

3.154

From iodolactonization

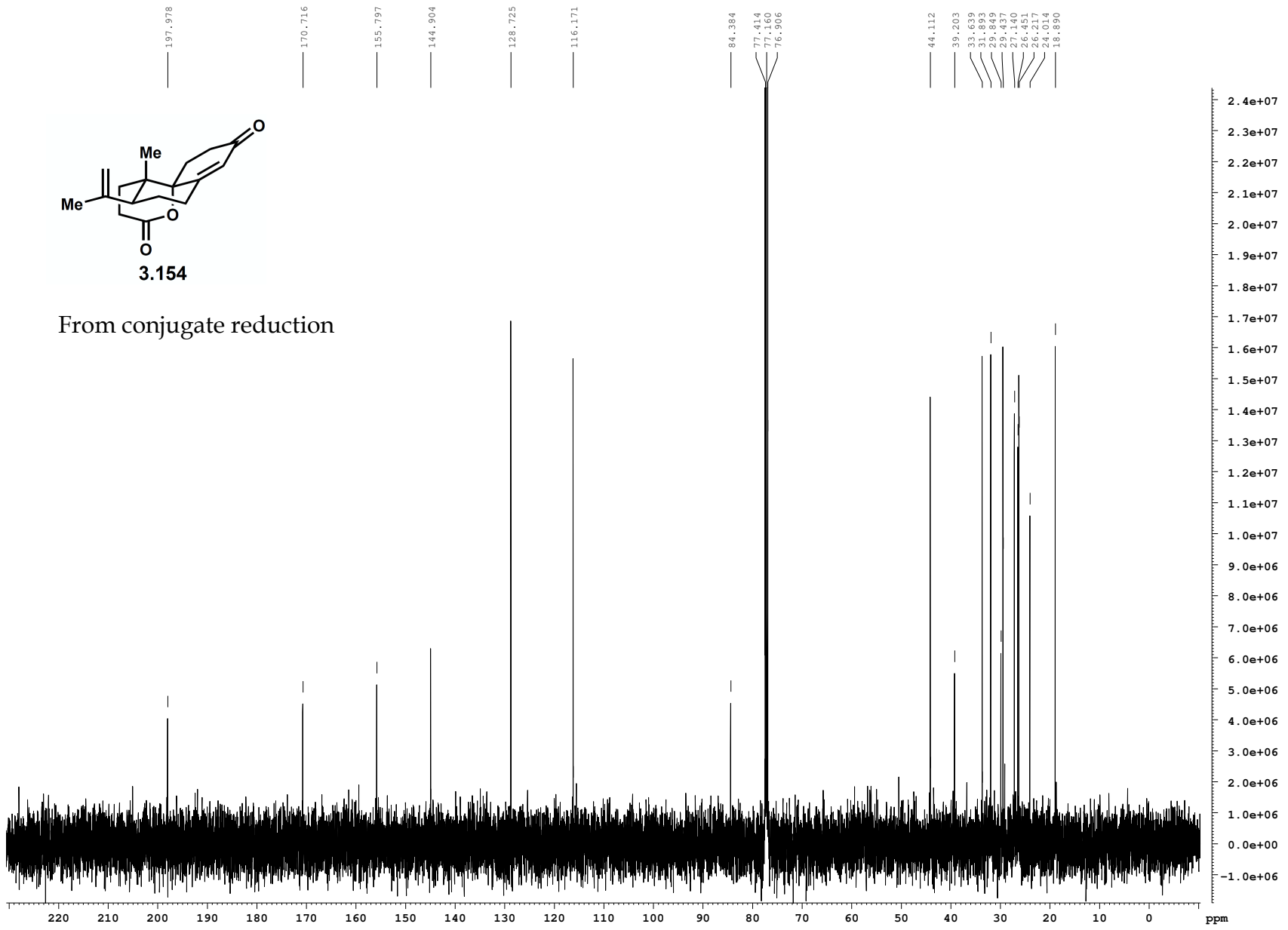
197.978
170.716
155.797
144.904
128.725
116.171
84.384
77.414
77.160
76.906
44.112
39.203
33.639
31.893
29.849
29.437
27.140
26.451
26.217
24.014
18.890
Me
Me
O
O
O
3.154
From conjugate reduction
2.4e+07
2.3e+07
2.2e+07
2.1e+07
2.0e+07
1.9e+07
1.8e+07
1.7e+07
1.6e+07
1.5e+07
1.4e+07
1.3e+07
1.2e+07
1.1e+07
1.0e+07
9.0e+06
8.0e+06
7.0e+06
6.0e+06
5.0e+06
4.0e+06
3.0e+06
2.0e+06
1.0e+06
0.0e+00
-1.0e+06
220 210 200 190 180 170 160 150 140 130 120 110 100 90 80 70 60 50 40 30 20 10 0
ppm

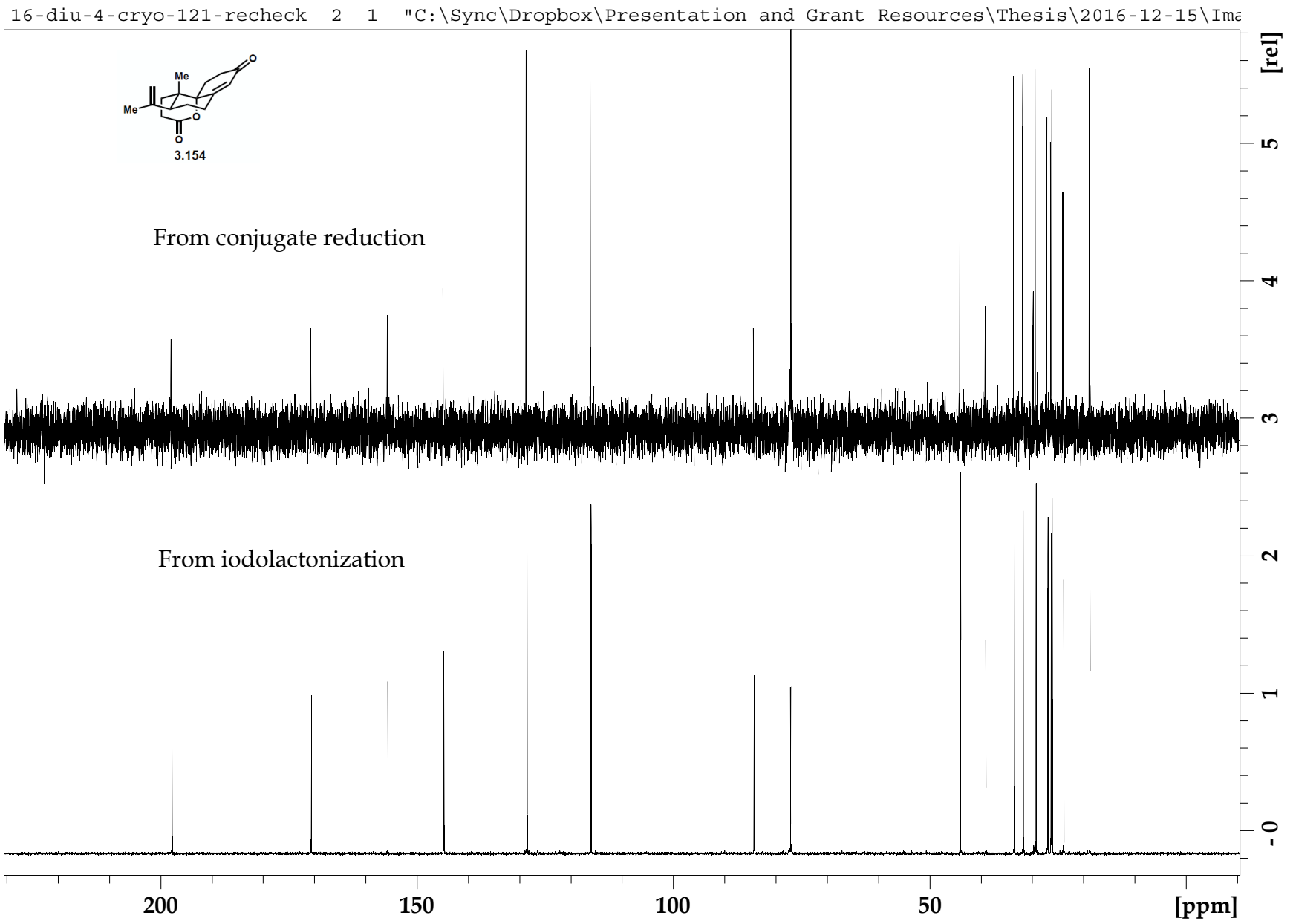
16-diu-4-cryo-121-recheck 2 1 "C:\Sync\Dropbox\Presentation and Grant Resources\Thesis\2016-12-15\Ima
Me
Me
3.154
From conjugate reduction
From iodolactonization
[rel]
5
4
3
2
1
-0
200
150
100
50
[ppm]

5.903
5.886
5.874
5.862
5.857
5.199
5.196
5.182
5.179
5.151
5.150
5.123
5.121
4.957
4.739
2.637
2.621
2.604
2.588
2.545
2.543
2.530
2.528
2.513
2.510
2.498
2.496
2.444
2.439
2.423
2.417
2.228
2.216
2.137
2.105
2.101
2.098
2.087
2.082
2.075
2.067
2.060
2.053
1.859
1.843
1.835
1.827
1.819
1.803
1.796
1.780
1.773
1.758
1.751
1.744
1.728
1.718
1.695
1.681
1.674
1.670
1.658
1.652
1.647
1.541
1.528
1.523
1.517
1.512
1.505
1.494
1.489
1.483
1.477
1.462
1.455
1.437
1.428
1.402
1.397
1.390
1.380
1.375
1.329
1.323
1.318
1.306
1.301
1.295
1.263
1.255
1.147
1.134
1.049
0.974
Me
Me
O
O
O
3.176
4.0e+06
3.5e+06
3.0e+06
2.5e+06
2.0e+06
1.5e+06
1.0e+06
5.0e+05
0.0e+00
8.5
8.0
7.5
7.0
6.5
6.0
5.5
5.0
4.5
4.0
3.5
3.0
2.5
2.0
1.5
1.0
0.5
0.0
ppm
1.145
1.076
1.083
1.054
1.000
1.080
1.100
1.078
2.284
0.824
2.141
9.945
11.074
3.130

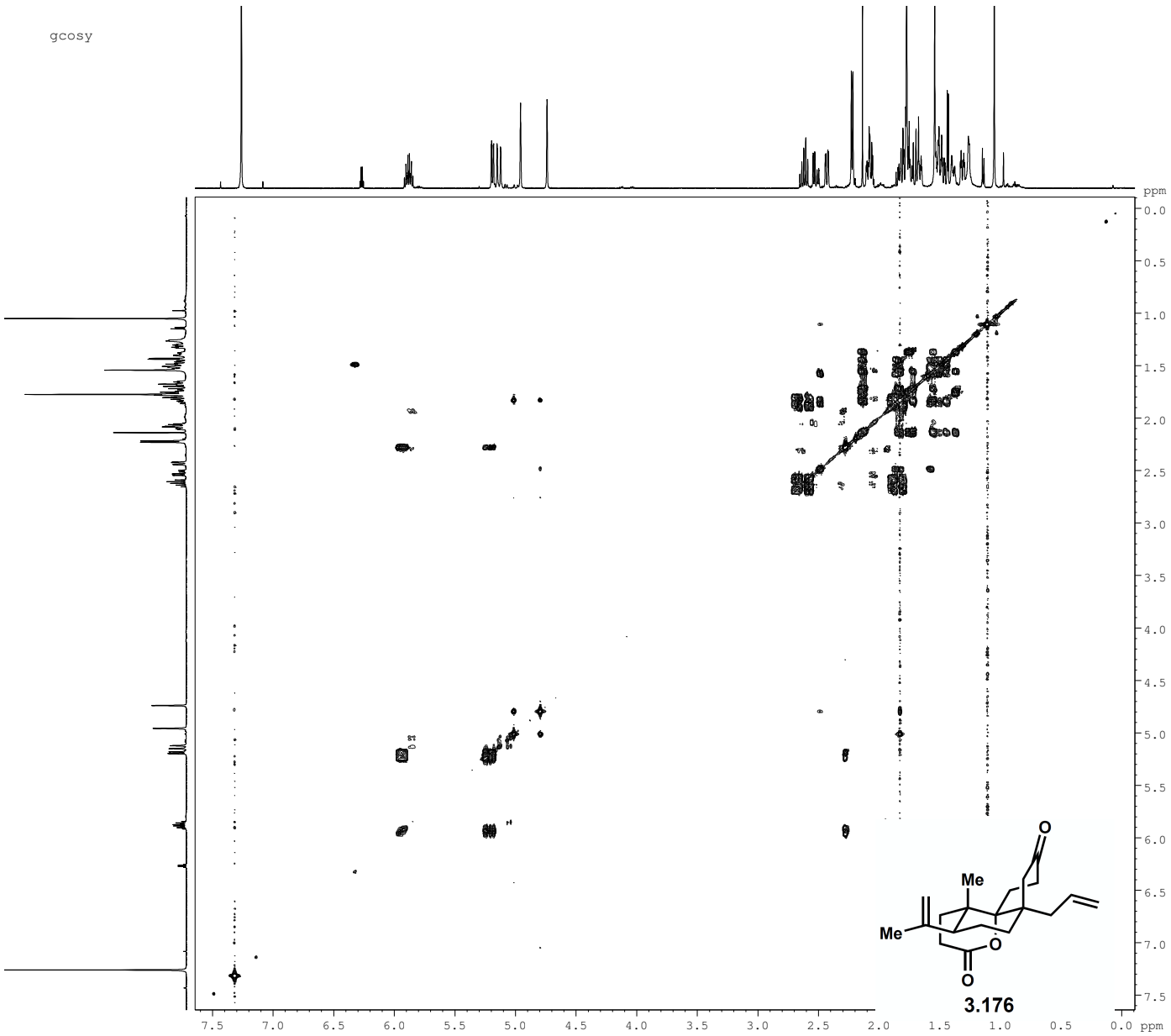
gcosy
ppm
0.0
0.5
1.0
1.5
2.0
2.5
3.0
3.5
4.0
4.5
5.0
5.5
6.0
6.5
7.0
7.5
7.5 7.0 6.5 6.0 5.5 5.0 4.5 4.0 3.5 3.0 2.5 2.0 1.5 1.0 0.5 0.0 ppm
Me
Me
O
O
O
3.176

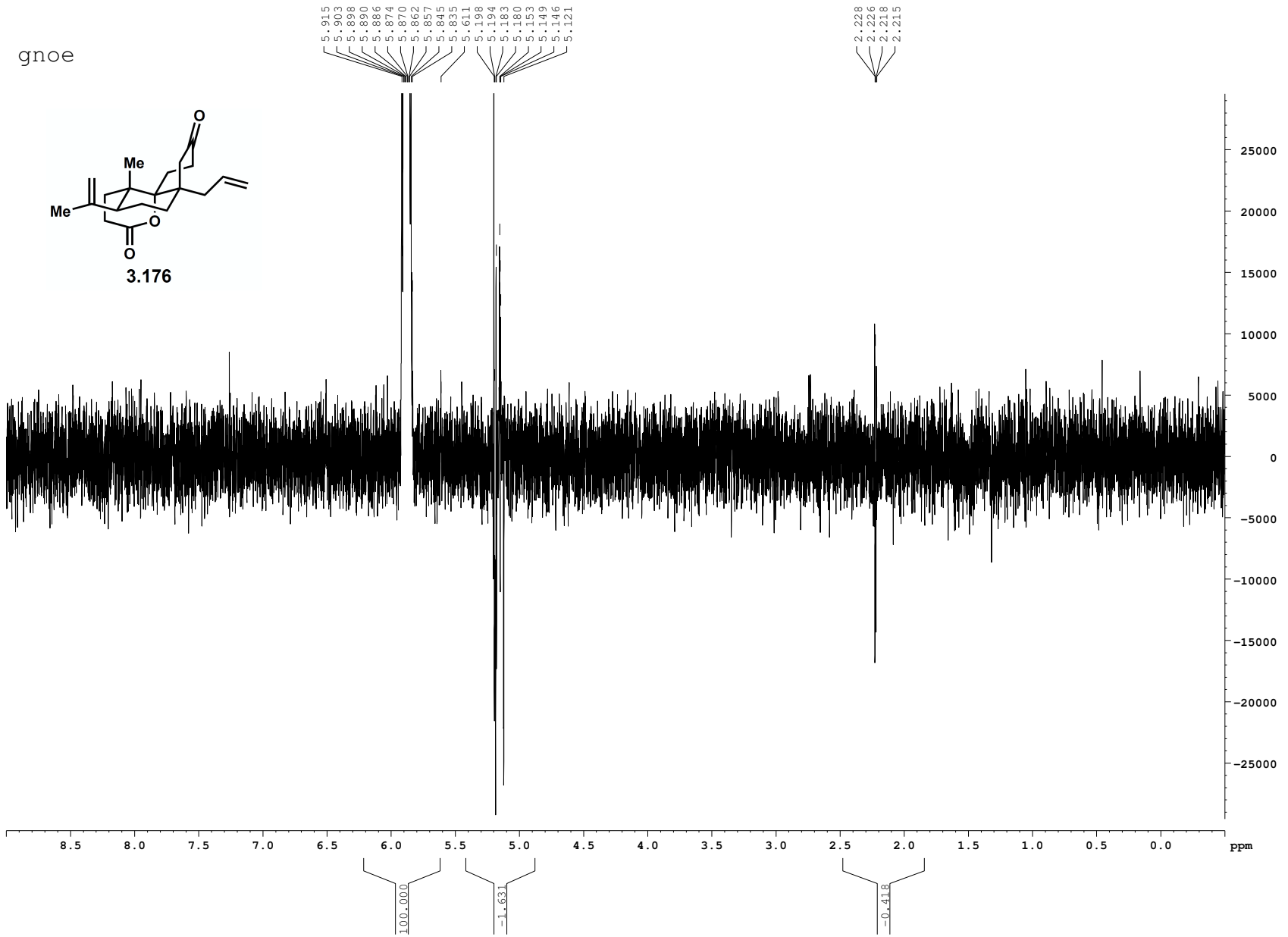
gnoe
5.915
5.903
5.898
5.890
5.886
5.874
5.870
5.862
5.857
5.845
5.835
5.611
5.198
5.194
5.183
5.180
5.153
5.149
5.146
5.121
2.228
2.226
2.218
2.215
Me
Me
O
O
O
3.176
25000
20000
15000
10000
5000
0
-5000
-10000
-15000
-20000
-25000
8.5
8.0
7.5
7.0
6.5
6.0
5.5
5.0
4.5
4.0
3.5
3.0
2.5
2.0
1.5
1.0
0.5
0.0
ppm
100.000
-1.631
-0.418

gnoe

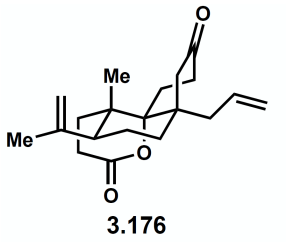
Me
Me
O
O
O

3.176

4.738
2.082
1.773
1.049
8e+04
7e+04
6e+04
5e+04
4e+04
3e+04
2e+04
1e+04
0e+00
-1e+04
-2e+04
-3e+04
-4e+04
-5e+04
-6e+04
-7e+04
-8e+04
8.5
8.0
7.5
7.0
6.5
6.0
5.5
5.0
4.5
4.0
3.5
3.0
2.5
2.0
1.5
1.0
0.5
0.0
ppm
1.019
0.995
1.022
37.564

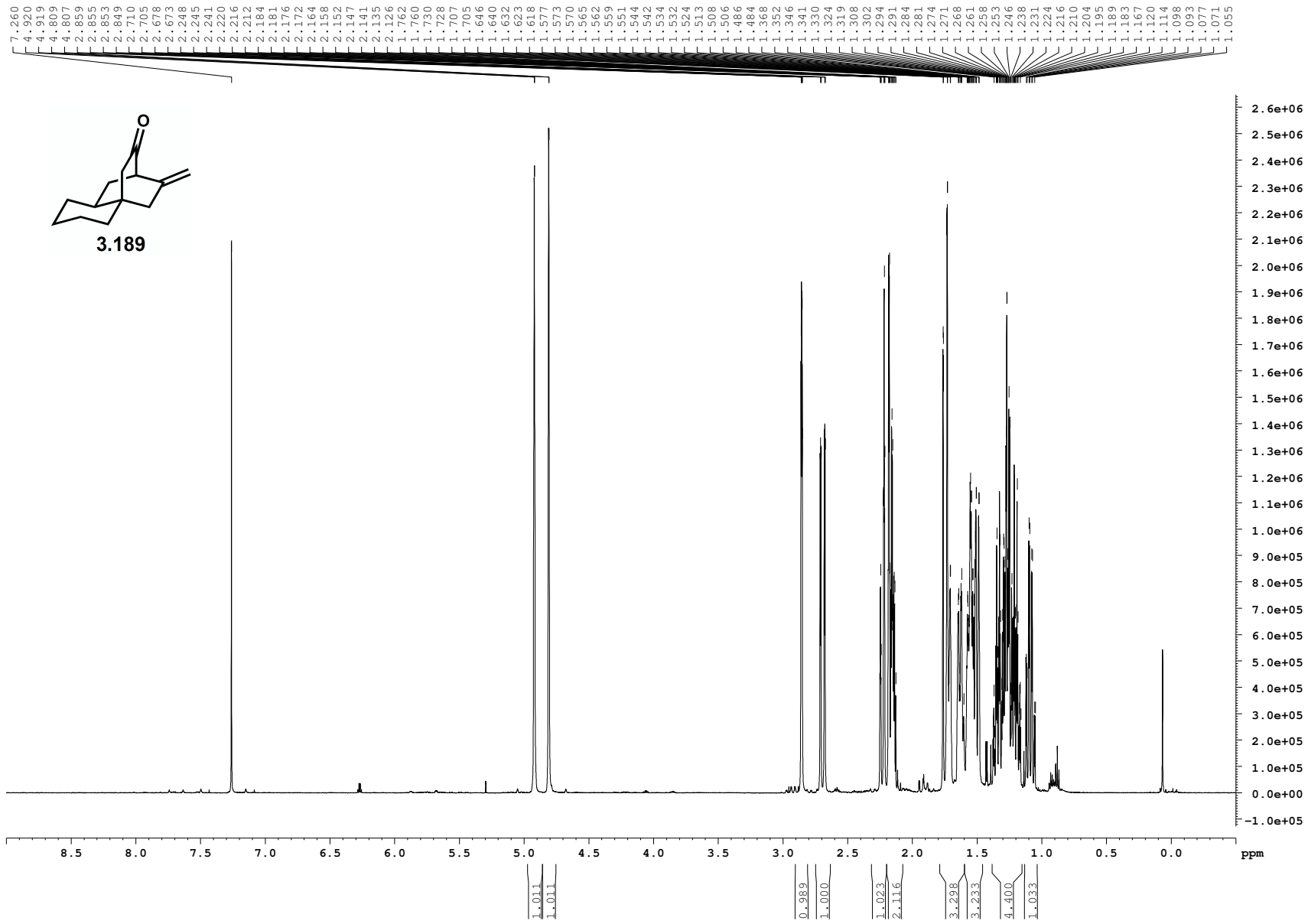
7.260
4.920
4.919
4.809
4.807
2.859
2.855
2.853
2.849
2.710
2.705
2.678
2.673
2.248
2.245
2.241
2.220
2.216
2.212
2.184
2.181
2.176
2.172
2.164
2.158
2.152
2.147
2.141
2.135
2.126
1.762
1.760
1.730
1.728
1.707
1.705
1.646
1.640
1.632
1.623
1.618
1.577
1.573
1.570
1.565
1.562
1.559
1.551
1.544
1.542
1.534
1.532
1.524
1.513
1.508
1.506
1.486
1.484
1.368
1.352
1.346
1.341
1.330
1.324
1.319
1.308
1.302
1.294
1.291
1.284
1.281
1.274
1.271
1.268
1.261
1.258
1.253
1.246
1.238
1.231
1.224
1.216
1.210
1.204
1.195
1.189
1.183
1.167
1.120
1.114
1.098
1.093
1.077
1.071
1.055
O
3.189
2.6e+06
2.5e+06
2.4e+06
2.3e+06
2.2e+06
2.1e+06
2.0e+06
1.9e+06
1.8e+06
1.7e+06
1.6e+06
1.5e+06
1.4e+06
1.3e+06
1.2e+06
1.1e+06
1.0e+06
9.0e+05
8.0e+05
7.0e+05
6.0e+05
5.0e+05
4.0e+05
3.0e+05
2.0e+05
1.0e+05
0.0e+00
-1.0e+05
8.5
8.0
7.5
7.0
6.5
6.0
5.5
5.0
4.5
4.0
3.5
3.0
2.5
2.0
1.5
1.0
0.5
0.0
ppm
1.011
1.011
0.989
1.000
1.023
2.116
3.298
3.233
4.400
1.033

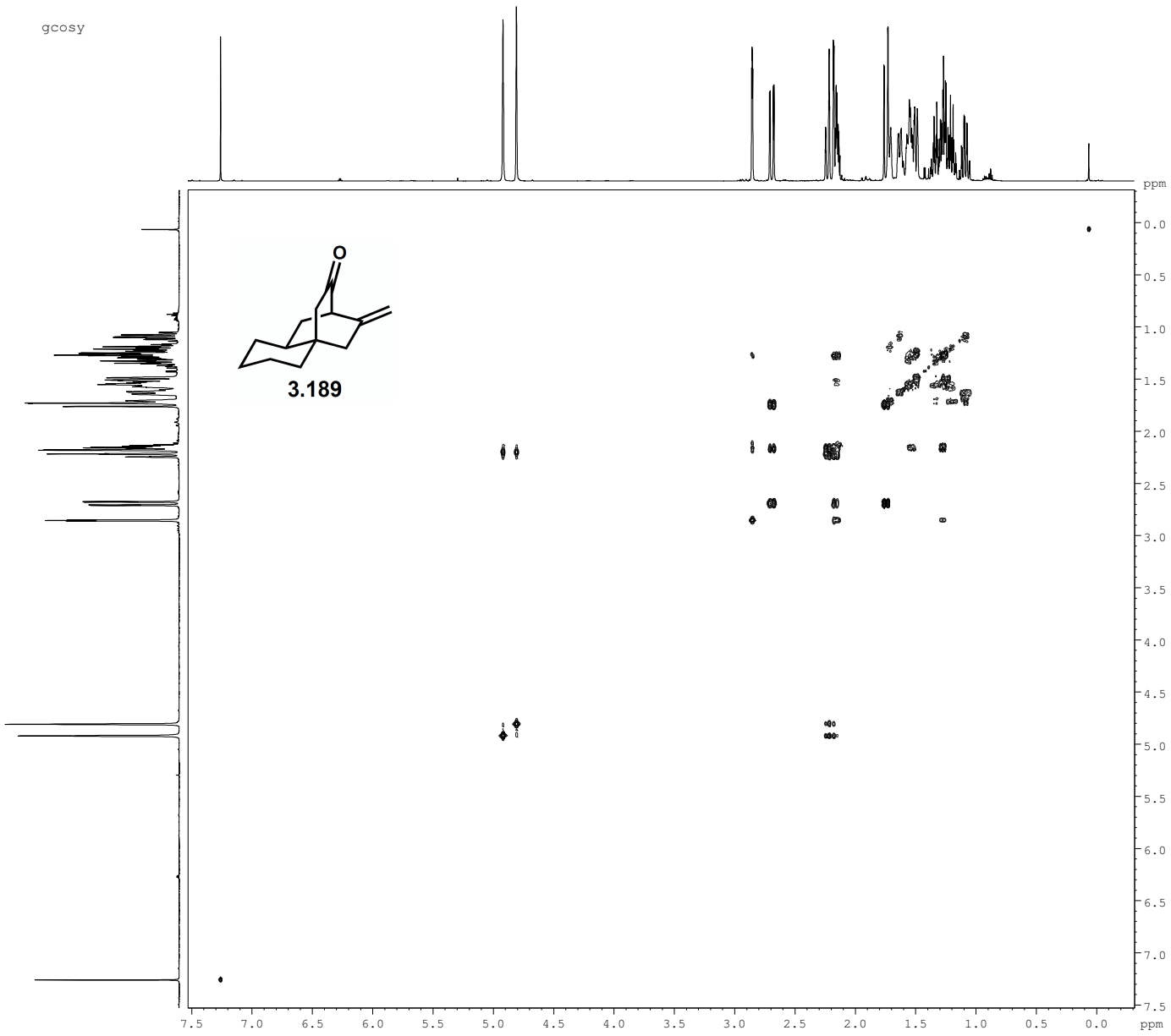
gcosy
O
3.189
ppm
0.0
0.5
1.0
1.5
2.0
2.5
3.0
3.5
4.0
4.5
5.0
5.5
6.0
6.5
7.0
7.5
7.5 7.0 6.5 6.0 5.5 5.0 4.5 4.0 3.5 3.0 2.5 2.0 1.5 1.0 0.5 0.0 ppm

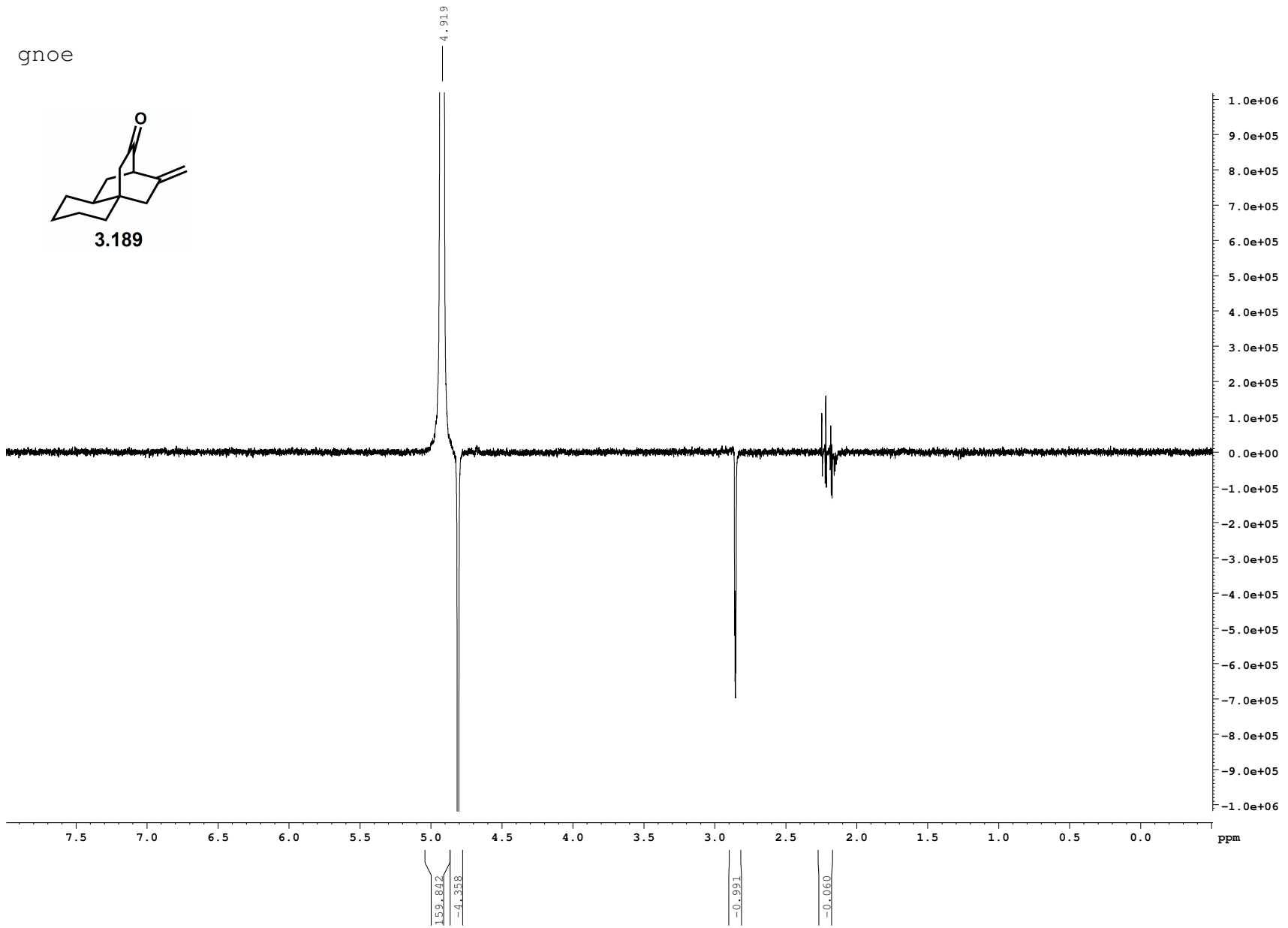
gnoe
4.919
3.189
159.842
-4.358
-0.991
-0.060
ppm

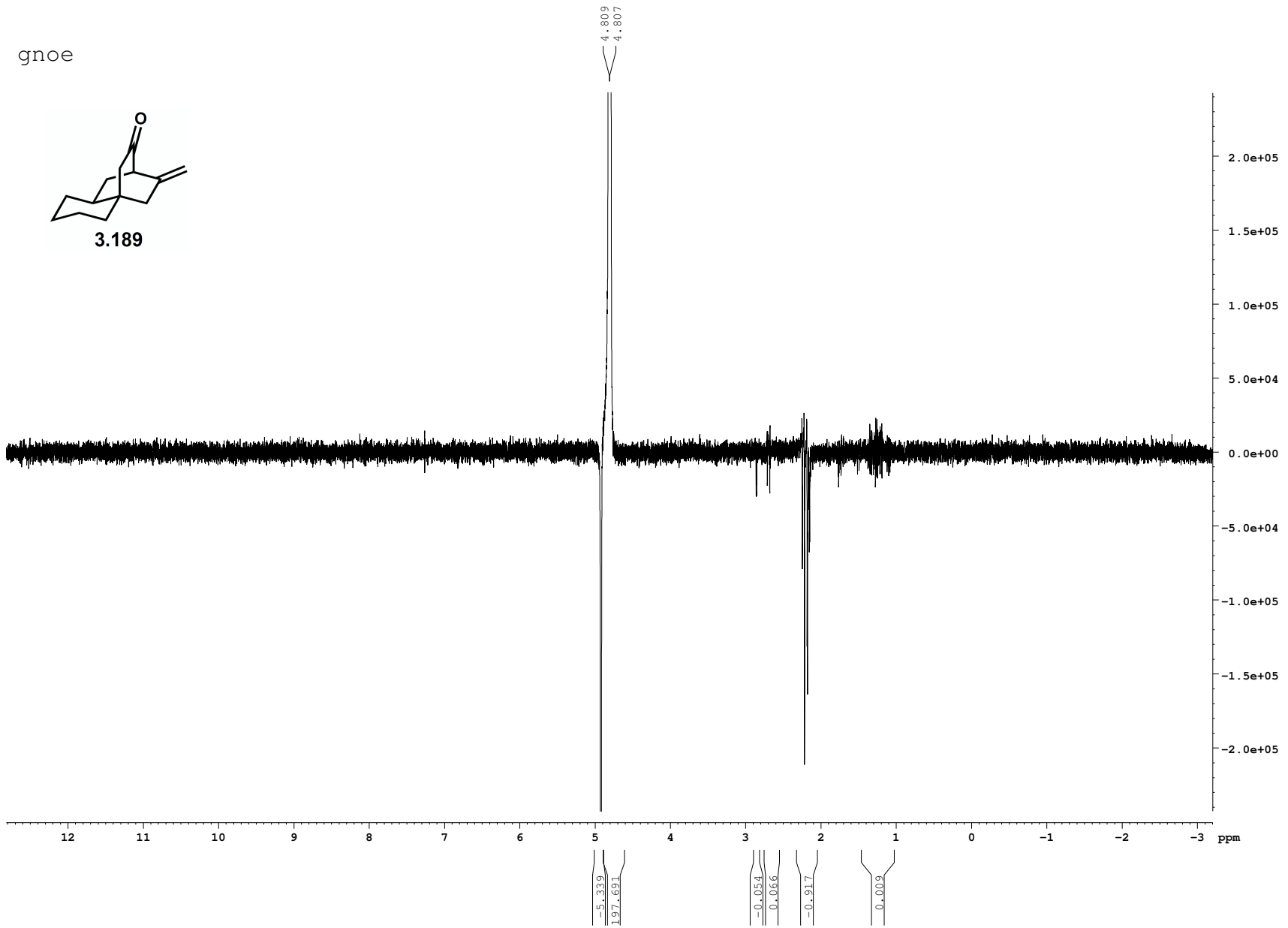
gnoe
O
3.189
4.809
4.807
2.0e+05
1.5e+05
1.0e+05
5.0e+04
0.0e+00
-5.0e+04
-1.0e+05
-1.5e+05
-2.0e+05
12
11
10
9
8
7
6
5
4
3
2
1
0
-1
-2
-3
ppm
-5.339
197.691
-0.054
0.066
-0.917
0.009

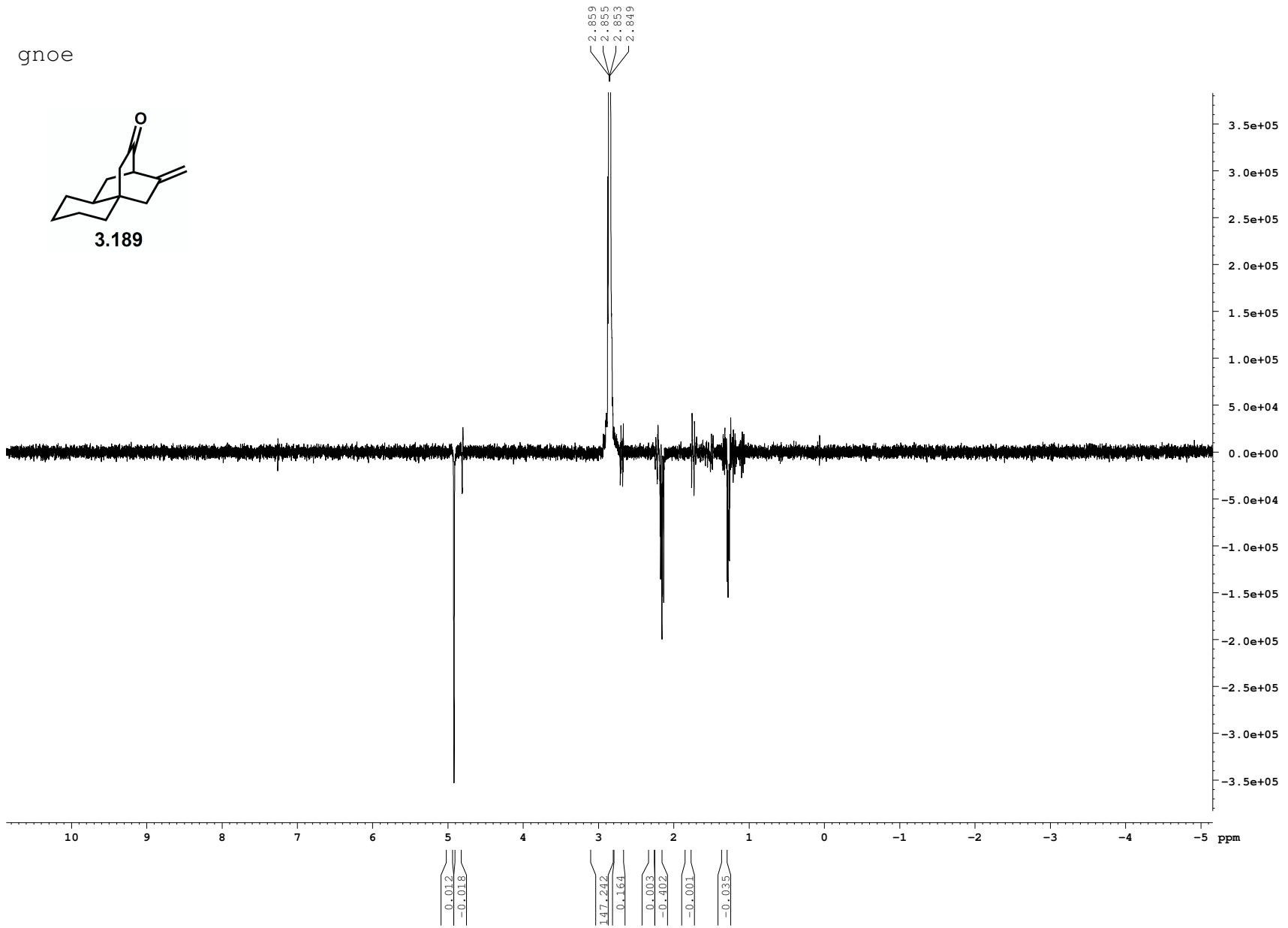
gnoe
O
3.189
2.859
2.855
2.853
2.849
3.5e+05
3.0e+05
2.5e+05
2.0e+05
1.5e+05
1.0e+05
5.0e+04
0.0e+00
-5.0e+04
-1.0e+05
-1.5e+05
-2.0e+05
-2.5e+05
-3.0e+05
-3.5e+05
10
9
8
7
6
5
4
3
2
1
0
-1
-2
-3
-4
-5
ppm
0.012
-0.018
147.242
0.164
0.003
-0.402
-0.001
-0.035

gnoe

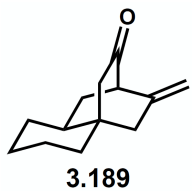
O

3.189

2.710
2.705
2.678
2.673
2.0e+06
1.5e+06
1.0e+06
5.0e+05
0.0e+00
-5.0e+05
-1.0e+06
-1.5e+06
-2.0e+06
8.5
8.0
7.5
7.0
6.5
6.0
5.5
5.0
4.5
4.0
3.5
3.0
2.5
2.0
1.5
1.0
0.5
0.0
ppm
28.048
-0.037
-0.318
-0.056
-0.271
-0.224

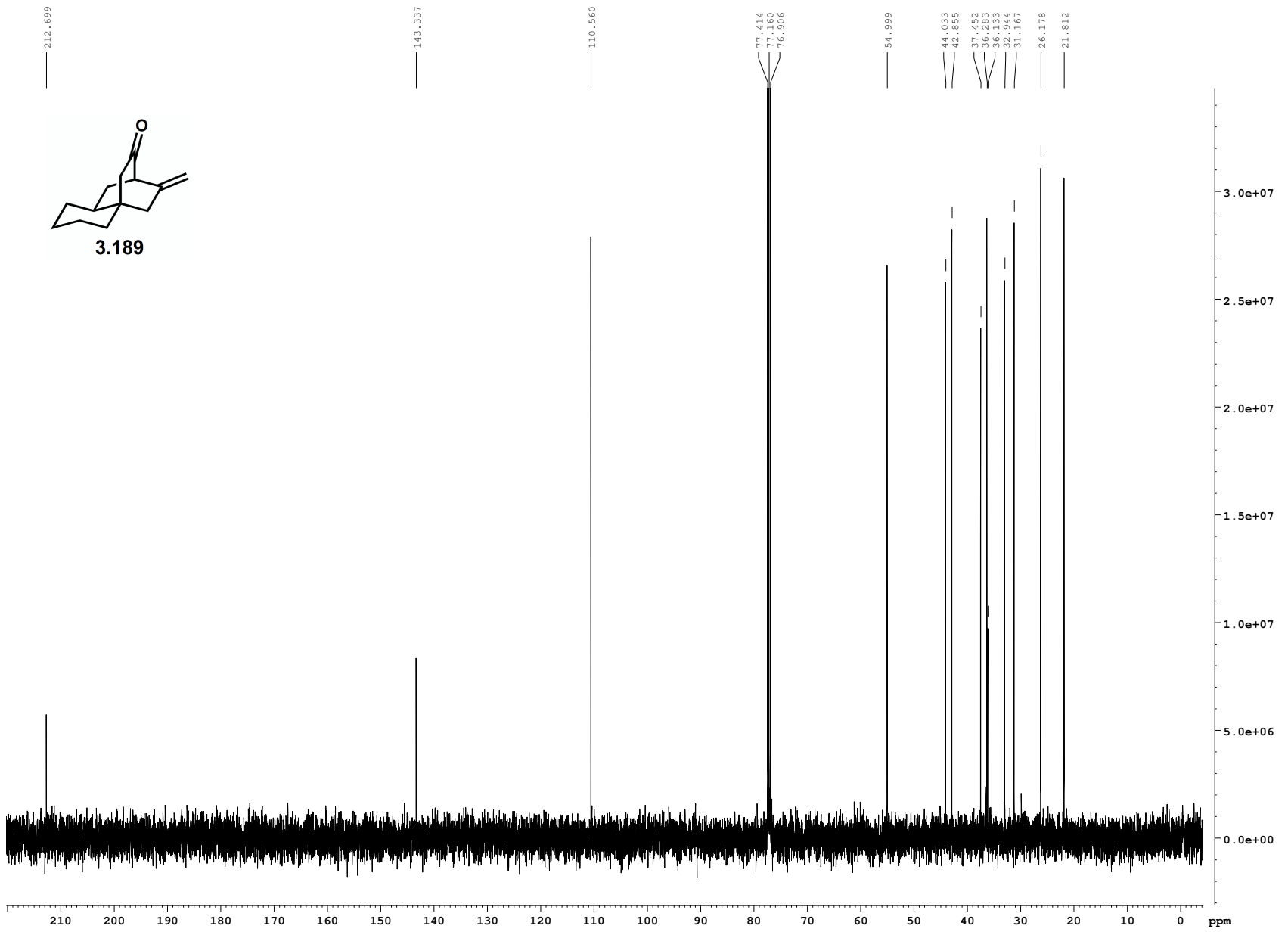
212.699
143.337
110.560
77.414
77.160
76.906
54.999
44.033
42.855
37.452
36.283
36.133
32.944
31.167
26.178
21.812
O
3.189
3.0e+07
2.5e+07
2.0e+07
1.5e+07
1.0e+07
5.0e+06
0.0e+00
210
200
190
180
170
160
150
140
130
120
110
100
90
80
70
60
50
40
30
20
10
0
ppm

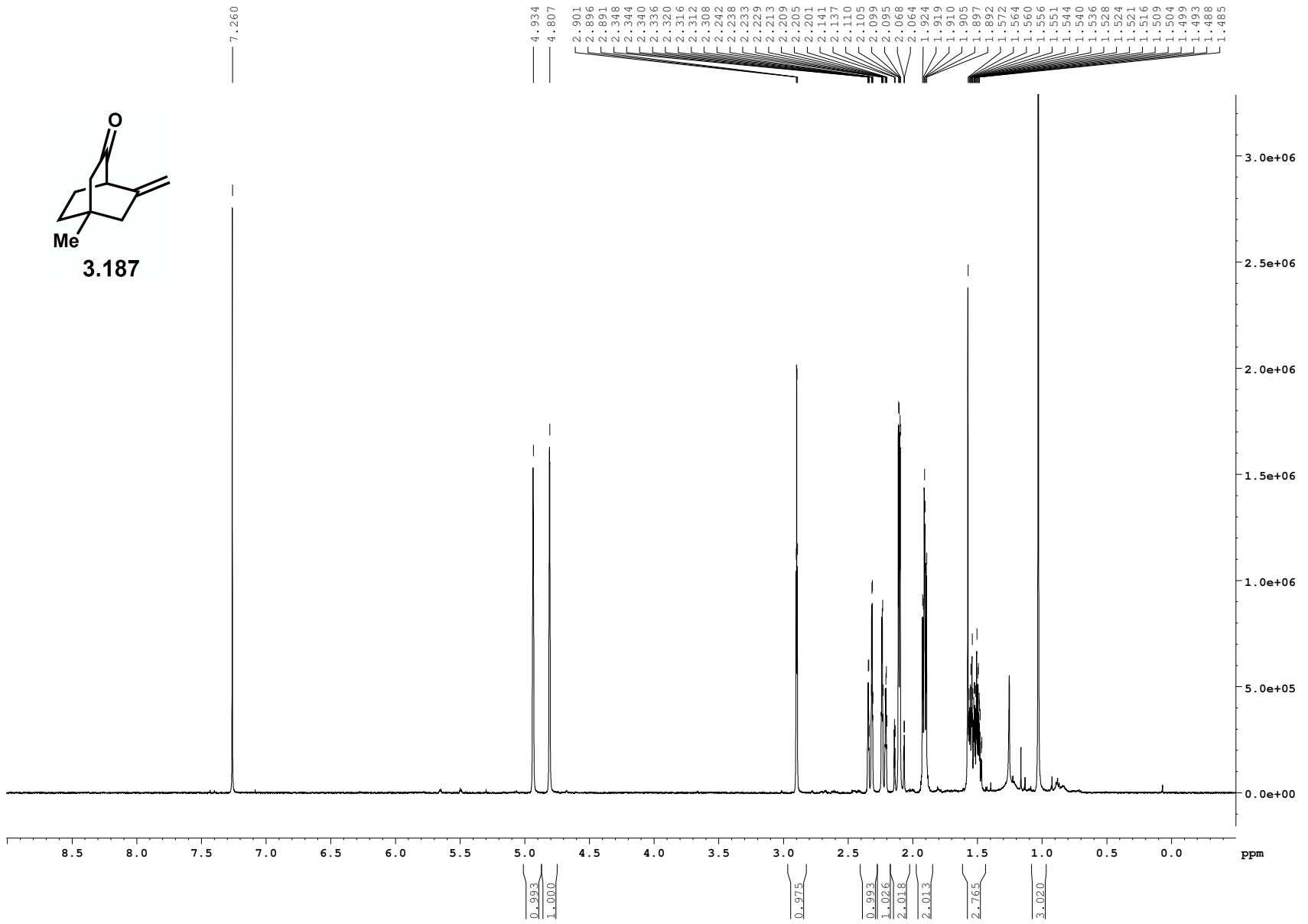
7.260
4.934
4.807
2.901
2.896
2.891
2.348
2.344
2.340
2.336
2.320
2.316
2.312
2.308
2.242
2.238
2.233
2.229
2.213
2.209
2.205
2.201
2.141
2.137
2.110
2.105
2.099
2.095
2.068
2.064
1.924
1.919
1.910
1.905
1.897
1.892
1.572
1.564
1.560
1.556
1.551
1.544
1.540
1.536
1.528
1.524
1.521
1.516
1.509
1.504
1.499
1.493
1.488
1.485
O
Me
3.187
3.0e+06
2.5e+06
2.0e+06
1.5e+06
1.0e+06
5.0e+05
0.0e+00
8.5
8.0
7.5
7.0
6.5
6.0
5.5
5.0
4.5
4.0
3.5
3.0
2.5
2.0
1.5
1.0
0.5
0.0
ppm
0.993
1.000
0.975
0.993
1.026
2.018
2.013
2.765
3.020

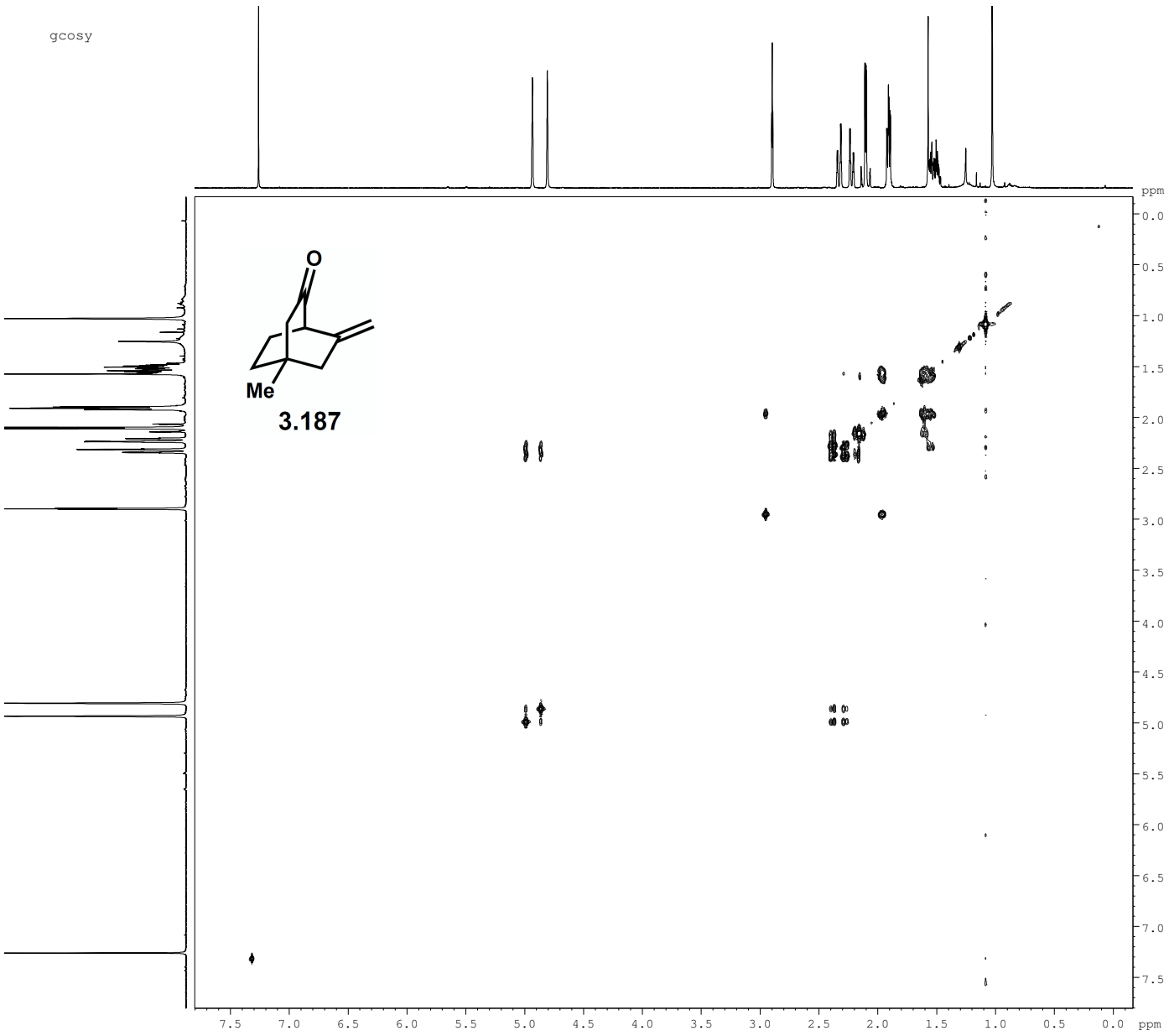
gcosy
O
Me
3.187
ppm
0.0
0.5
1.0
1.5
2.0
2.5
3.0
3.5
4.0
4.5
5.0
5.5
6.0
6.5
7.0
7.5
7.5
7.0
6.5
6.0
5.5
5.0
4.5
4.0
3.5
3.0
2.5
2.0
1.5
1.0
0.5
0.0
ppm

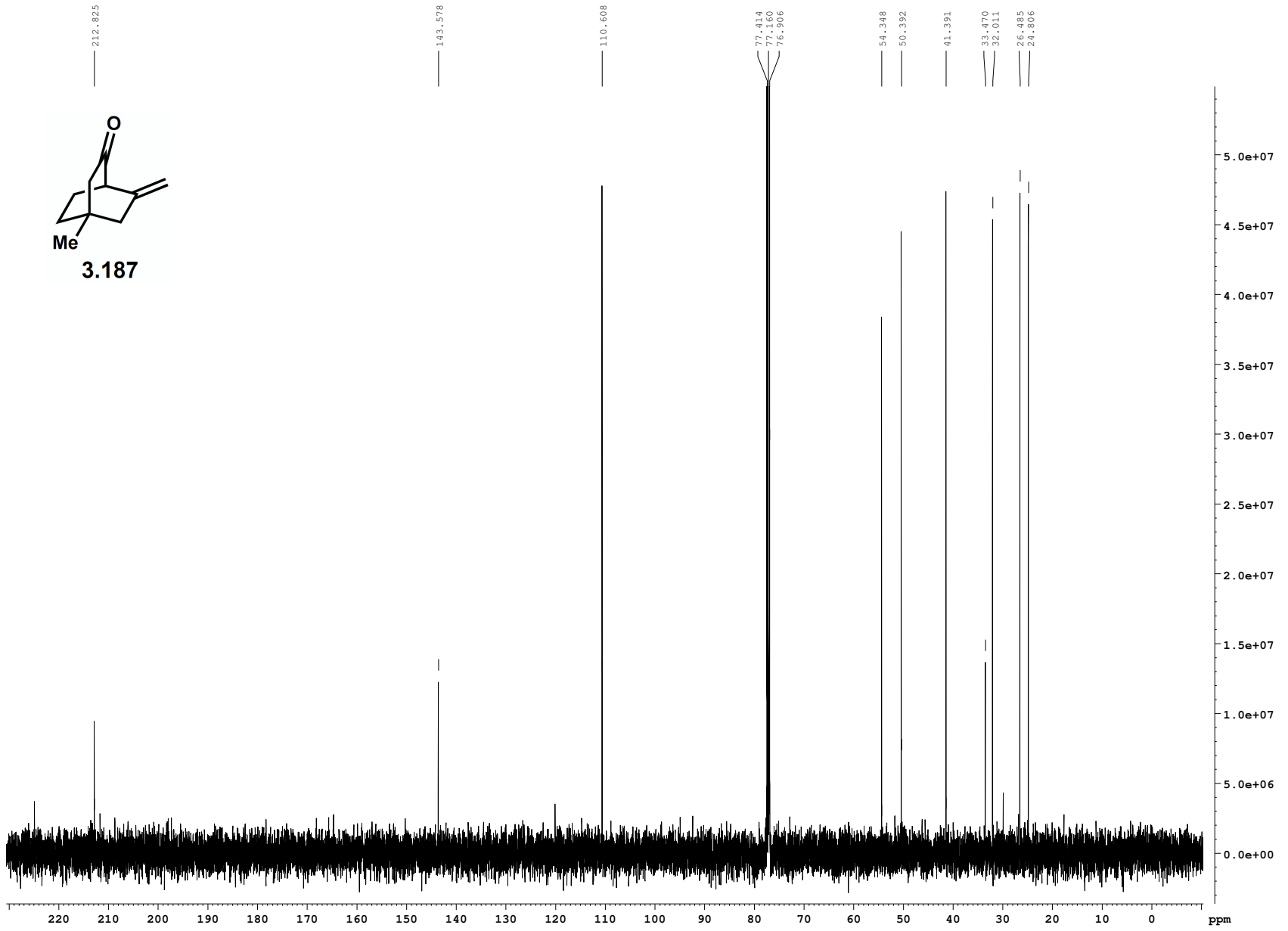
212.825
143.578
110.608
77.414
77.160
76.906
54.348
50.392
41.391
33.470
32.011
26.485
24.806
O
Me
3.187
5.0e+07
4.5e+07
4.0e+07
3.5e+07
3.0e+07
2.5e+07
2.0e+07
1.5e+07
1.0e+07
5.0e+06
0.0e+00
220 210 200 190 180 170 160 150 140 130 120 110 100 90 80 70 60 50 40 30 20 10 0
ppm

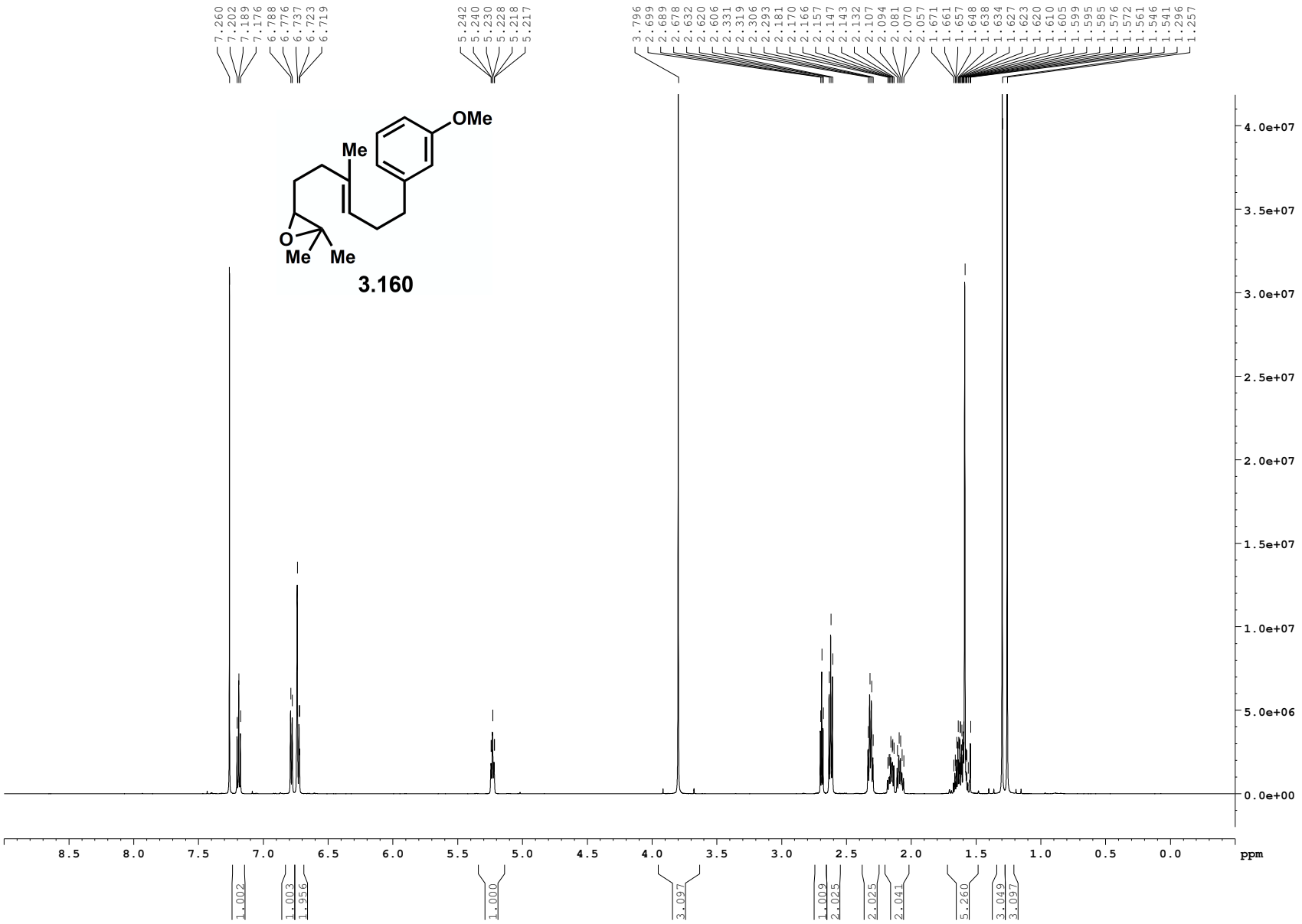
7.260
7.202
7.189
7.176
6.788
6.776
6.737
6.723
6.719
5.242
5.240
5.230
5.228
5.218
5.217
3.796
2.699
2.689
2.678
2.632
2.620
2.606
2.331
2.319
2.306
2.293
2.181
2.170
2.166
2.157
2.147
2.143
2.132
2.107
2.094
2.081
2.070
2.057
1.671
1.661
1.657
1.648
1.638
1.634
1.627
1.623
1.620
1.610
1.605
1.599
1.595
1.585
1.576
1.572
1.561
1.546
1.541
1.296
1.257
OMe
Me
O
Me
Me
3.160
4.0e+07
3.5e+07
3.0e+07
2.5e+07
2.0e+07
1.5e+07
1.0e+07
5.0e+06
0.0e+00
8.5
8.0
7.5
7.0
6.5
6.0
5.5
5.0
4.5
4.0
3.5
3.0
2.5
2.0
1.5
1.0
0.5
0.0
ppm
1.002
1.003
1.956
1.000
3.097
1.009
2.025
2.025
2.041
5.260
3.049
3.097

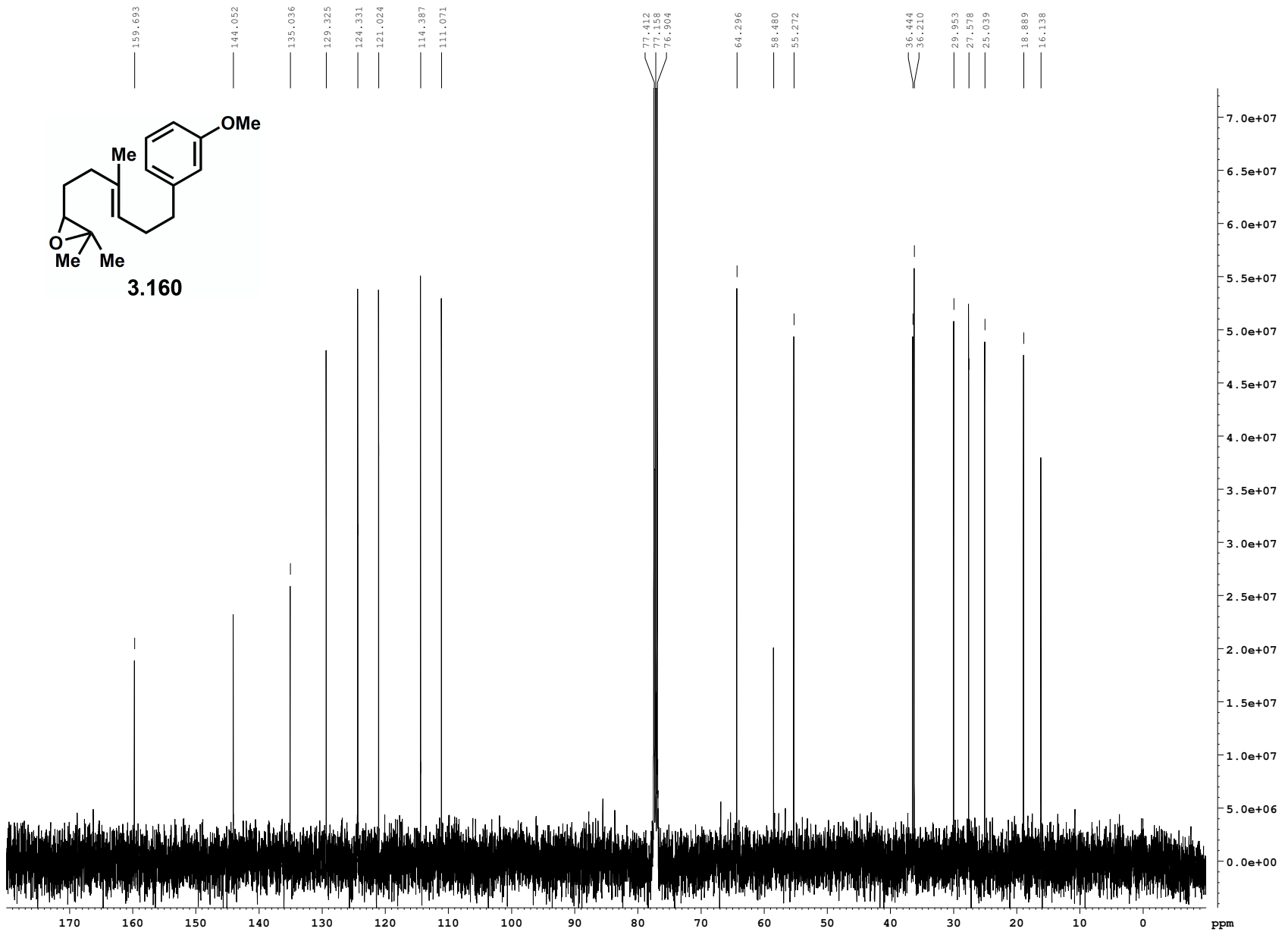
159.693
144.052
135.036
129.325
124.331
121.024
114.387
111.071
77.412
77.158
76.904
64.296
58.480
55.272
36.444
36.210
29.953
27.578
25.039
18.889
16.138
OMe
Me
O
Me
Me
3.160
7.0e+07
6.5e+07
6.0e+07
5.5e+07
5.0e+07
4.5e+07
4.0e+07
3.5e+07
3.0e+07
2.5e+07
2.0e+07
1.5e+07
1.0e+07
5.0e+06
0.0e+00
170
160
150
140
130
120
110
100
90
80
70
60
50
40
30
20
10
0
ppm

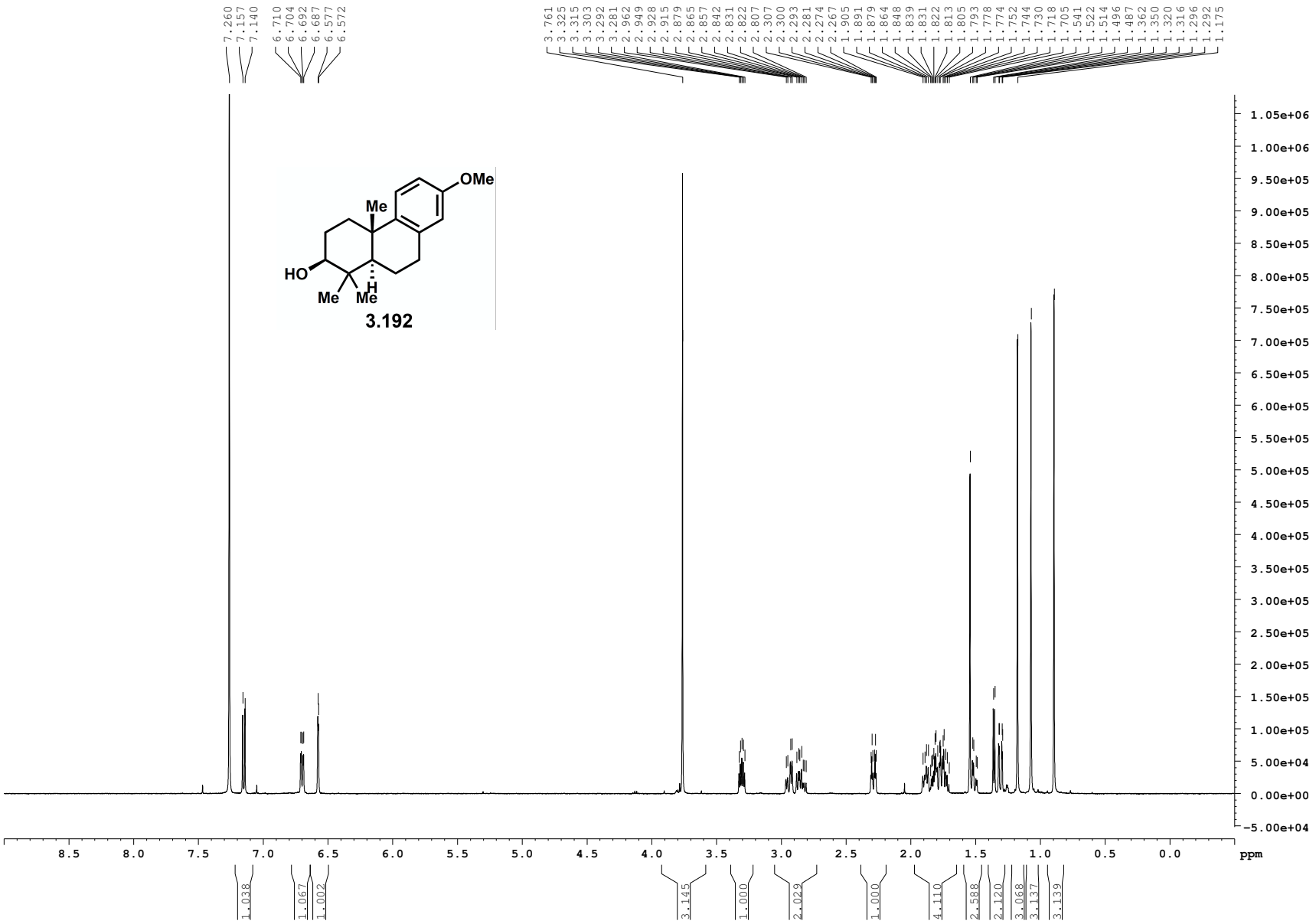
7.260
7.157
7.140
6.710
6.704
6.692
6.687
6.577
6.572
3.761
3.325
3.315
3.303
3.292
3.281
2.962
2.949
2.928
2.915
2.879
2.865
2.857
2.842
2.831
2.822
2.807
2.307
2.300
2.293
2.281
2.274
2.267
1.905
1.891
1.879
1.864
1.848
1.839
1.831
1.822
1.813
1.805
1.793
1.778
1.774
1.752
1.744
1.730
1.718
1.705
1.541
1.522
1.514
1.496
1.487
1.362
1.350
1.320
1.316
1.296
1.292
1.175
OMe
Me
HO
Me
Me
H
3.192
1.05e+06
1.00e+06
9.50e+05
9.00e+05
8.50e+05
8.00e+05
7.50e+05
7.00e+05
6.50e+05
6.00e+05
5.50e+05
5.00e+05
4.50e+05
4.00e+05
3.50e+05
3.00e+05
2.50e+05
2.00e+05
1.50e+05
1.00e+05
5.00e+04
0.00e+00
-5.00e+04
8.5
8.0
7.5
7.0
6.5
6.0
5.5
5.0
4.5
4.0
3.5
3.0
2.5
2.0
1.5
1.0
0.5
0.0
ppm
1.038
1.067
1.002
3.145
1.000
2.029
1.000
4.110
2.588
2.120
3.068
3.137
3.139

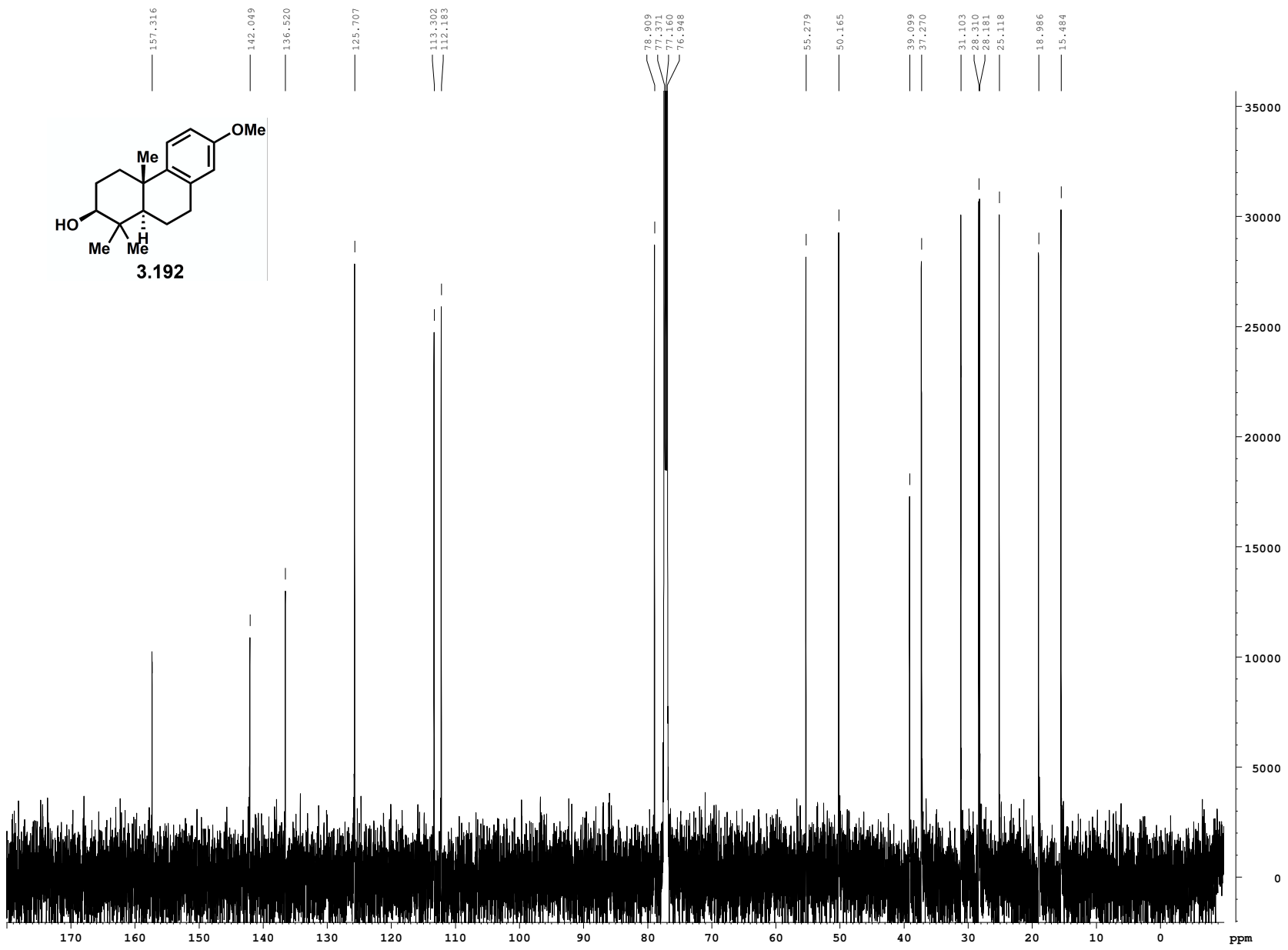
157.316
142.049
136.520
125.707
113.302
112.183
78.909
77.371
77.160
76.948
55.279
50.165
39.099
37.270
31.103
28.310
28.181
25.118
18.986
15.484
OMe
Me
HO
Me
Me
H
3.192
35000
30000
25000
20000
15000
10000
5000
0
170
160
150
140
130
120
110
100
90
80
70
60
50
40
30
20
10
0
ppm

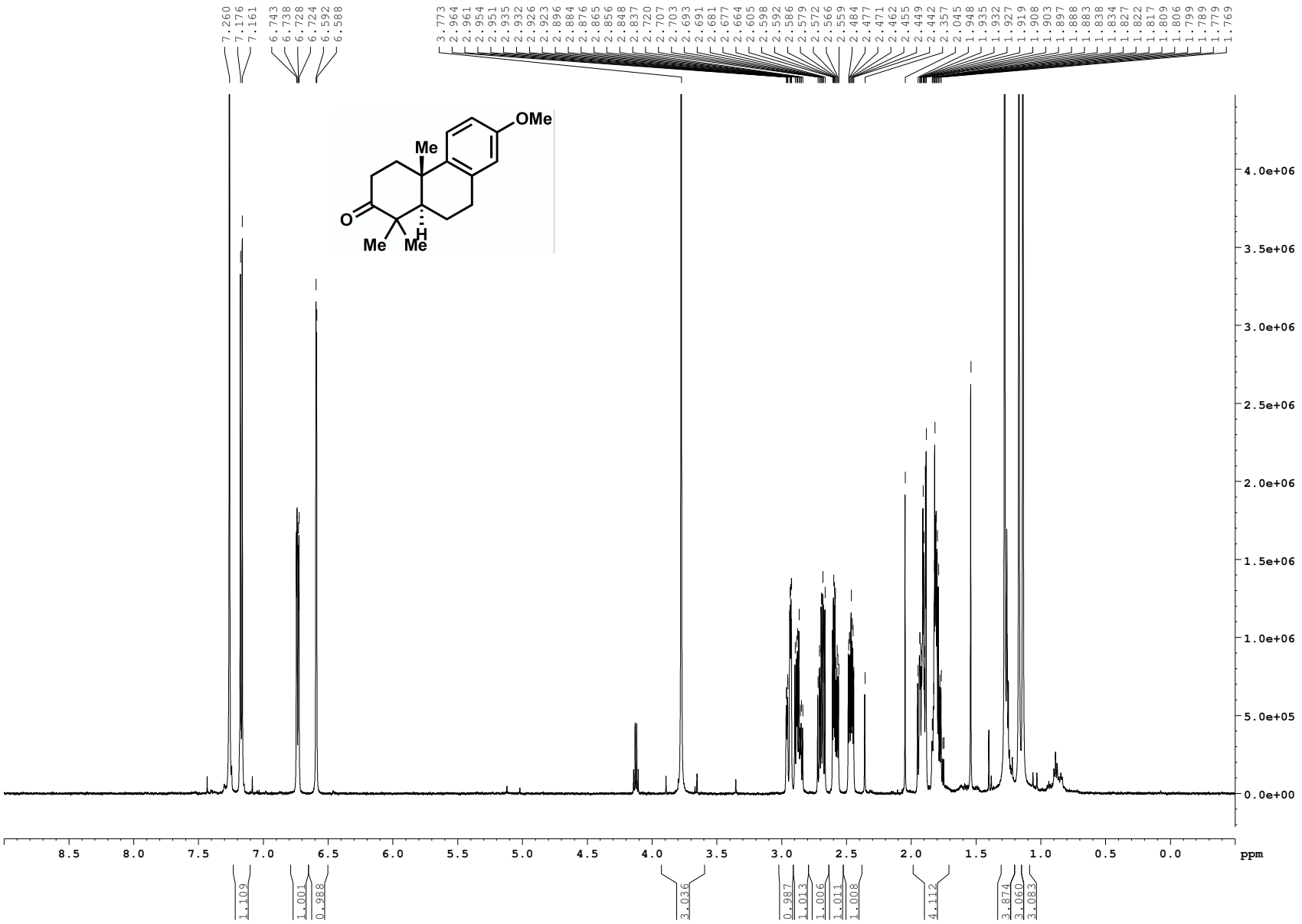
7.260
7.176
7.161
6.743
6.738
6.728
6.724
6.592
6.588
3.773
2.964
2.961
2.954
2.951
2.935
2.932
2.926
2.923
2.896
2.884
2.876
2.865
2.856
2.848
2.837
2.720
2.707
2.703
2.693
2.691
2.681
2.677
2.664
2.605
2.598
2.592
2.586
2.579
2.572
2.566
2.559
2.484
2.477
2.471
2.462
2.455
2.449
2.442
2.357
2.045
1.948
1.935
1.932
1.927
1.919
1.908
1.903
1.897
1.888
1.883
1.838
1.834
1.827
1.822
1.817
1.809
1.806
1.799
1.789
1.779
1.769
OMe
Me
O
Me
Me
H
4.0e+06
3.5e+06
3.0e+06
2.5e+06
2.0e+06
1.5e+06
1.0e+06
5.0e+05
0.0e+00
8.5
8.0
7.5
7.0
6.5
6.0
5.5
5.0
4.5
4.0
3.5
3.0
2.5
2.0
1.5
1.0
0.5
0.0
ppm
1.109
1.001
0.988
3.036
0.987
1.013
1.006
1.011
1.008
4.112
3.874
3.060
3.083

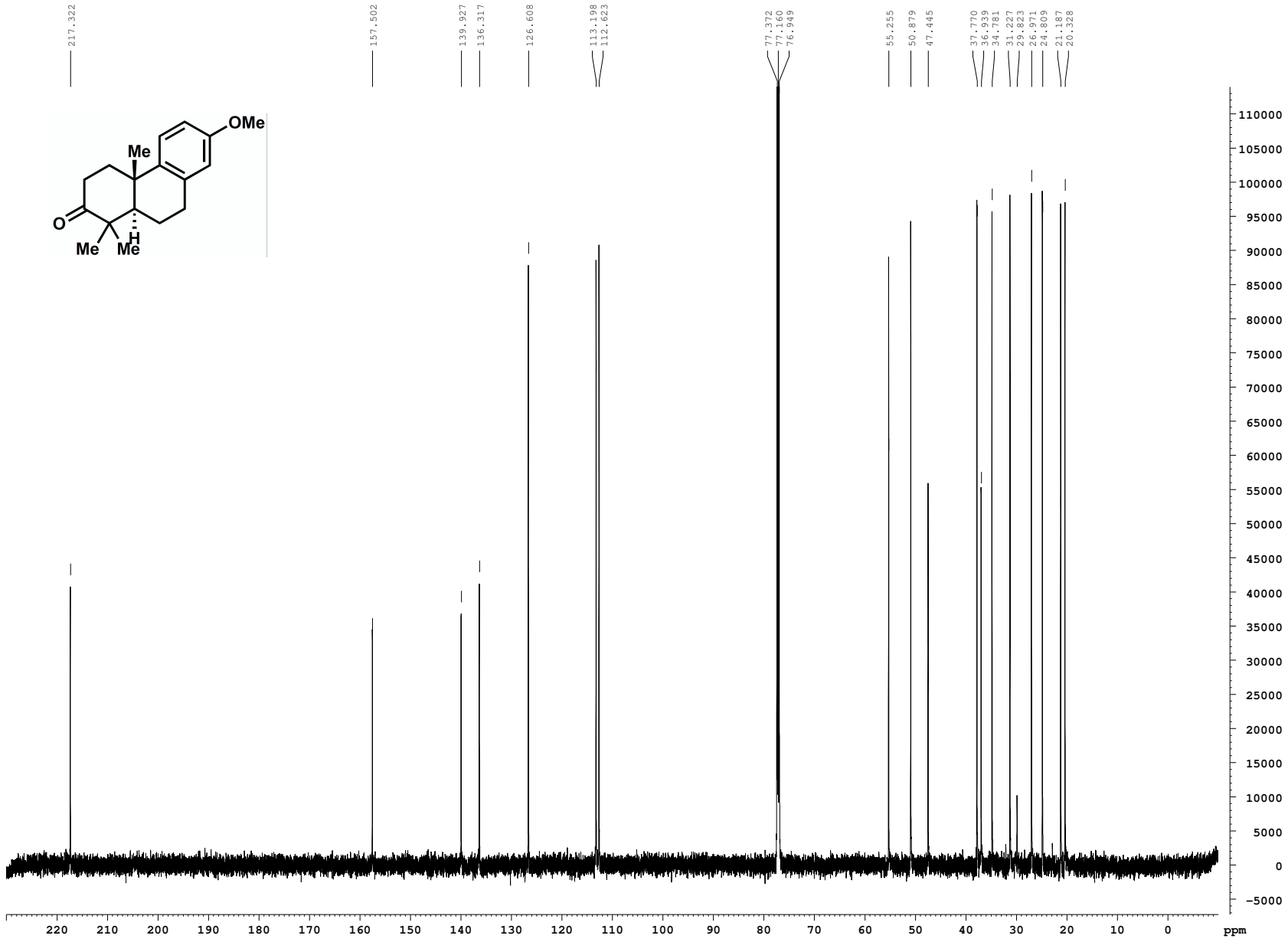
217.322
157.502
139.927
136.317
126.608
113.198
112.623
77.372
77.160
76.949
55.255
50.879
47.445
37.770
36.939
34.781
31.227
29.823
26.971
24.809
21.187
20.328
OMe
Me
O
Me
Me
H
ppm

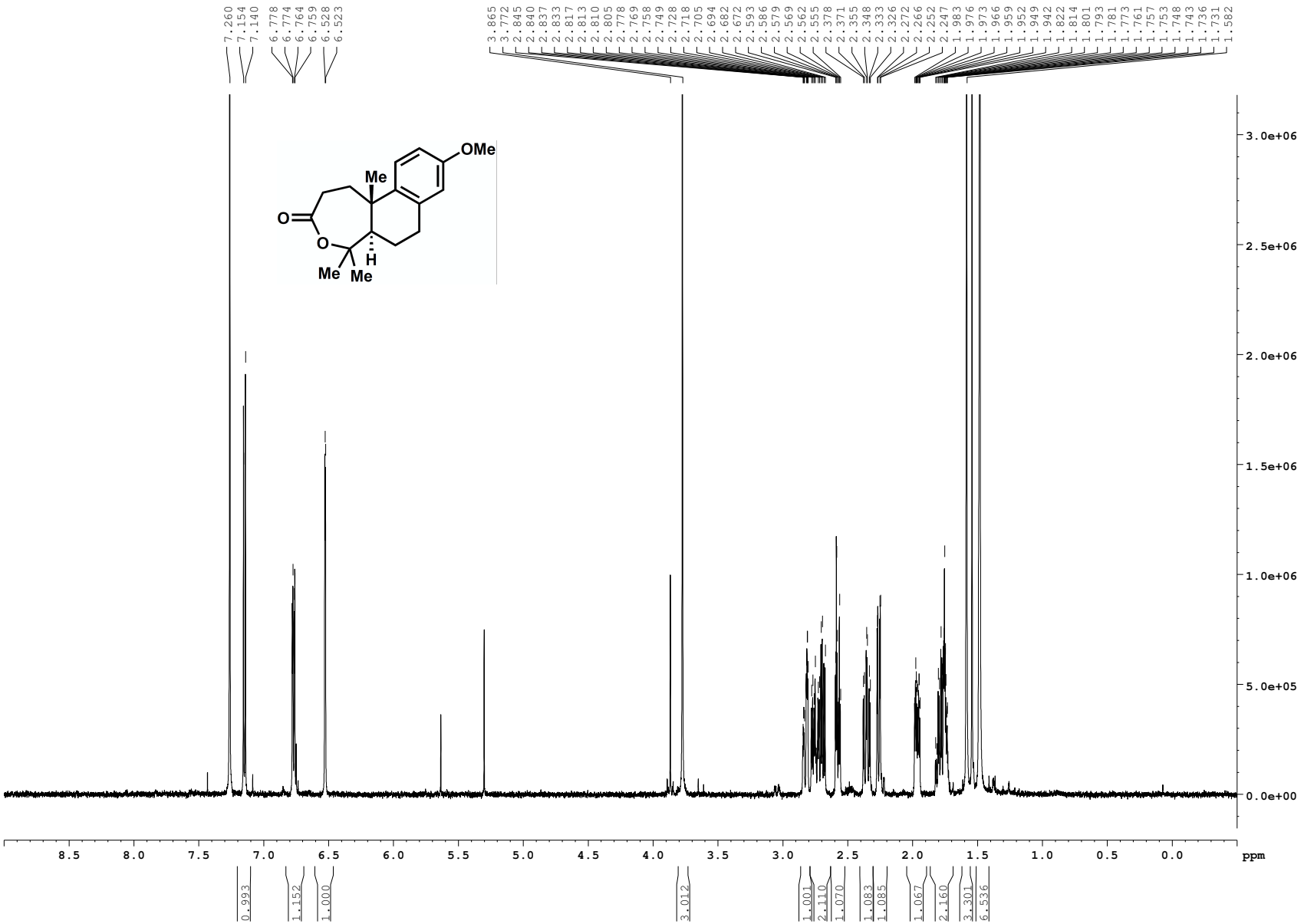
7.260
7.154
7.140
6.778
6.774
6.764
6.759
6.528
6.523
3.865
3.772
2.845
2.840
2.837
2.833
2.817
2.813
2.810
2.805
2.778
2.769
2.758
2.749
2.728
2.718
2.705
2.694
2.682
2.672
2.593
2.586
2.579
2.569
2.562
2.555
2.378
2.371
2.355
2.348
2.333
2.326
2.272
2.266
2.252
2.247
1.983
1.976
1.973
1.966
1.959
1.952
1.949
1.942
1.822
1.814
1.801
1.793
1.781
1.773
1.761
1.757
1.753
1.748
1.743
1.736
1.731
1.582
OMe
Me
O
O
Me
Me
H
3.0e+06
2.5e+06
2.0e+06
1.5e+06
1.0e+06
5.0e+05
0.0e+00
8.5
8.0
7.5
7.0
6.5
6.0
5.5
5.0
4.5
4.0
3.5
3.0
2.5
2.0
1.5
1.0
0.5
0.0
ppm
0.993
1.152
1.000
3.012
1.001
2.110
1.070
1.083
1.085
1.067
2.160
3.301
6.536

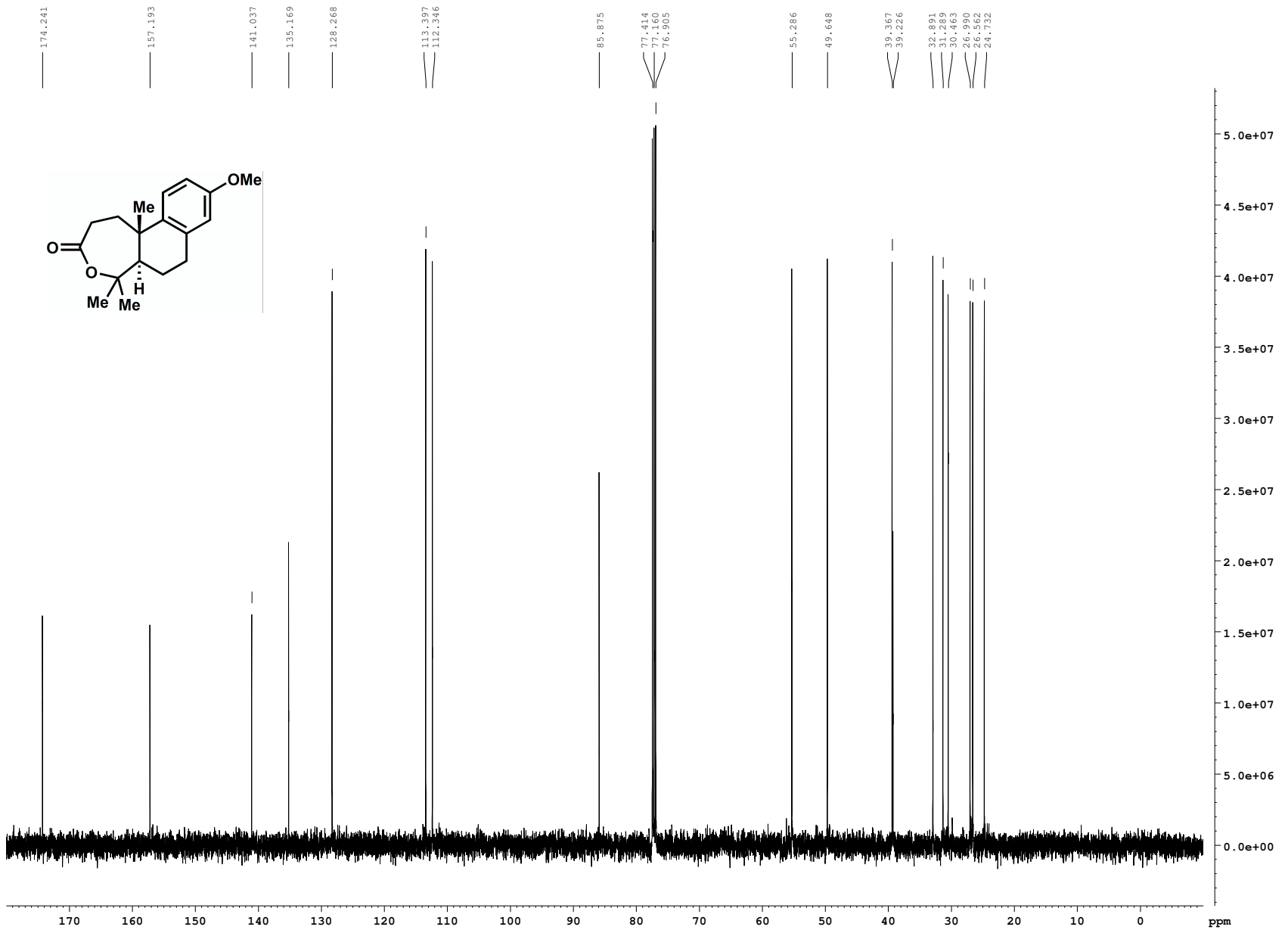
174.241
157.193
141.037
135.169
128.268
113.397
112.346
85.875
77.414
77.160
76.905
55.286
49.648
39.367
39.226
32.891
31.289
30.463
26.990
26.562
24.732
OMe
Me
O
O
H
Me
Me
5.0e+07
4.5e+07
4.0e+07
3.5e+07
3.0e+07
2.5e+07
2.0e+07
1.5e+07
1.0e+07
5.0e+06
0.0e+00
170
160
150
140
130
120
110
100
90
80
70
60
50
40
30
20
10
0
ppm

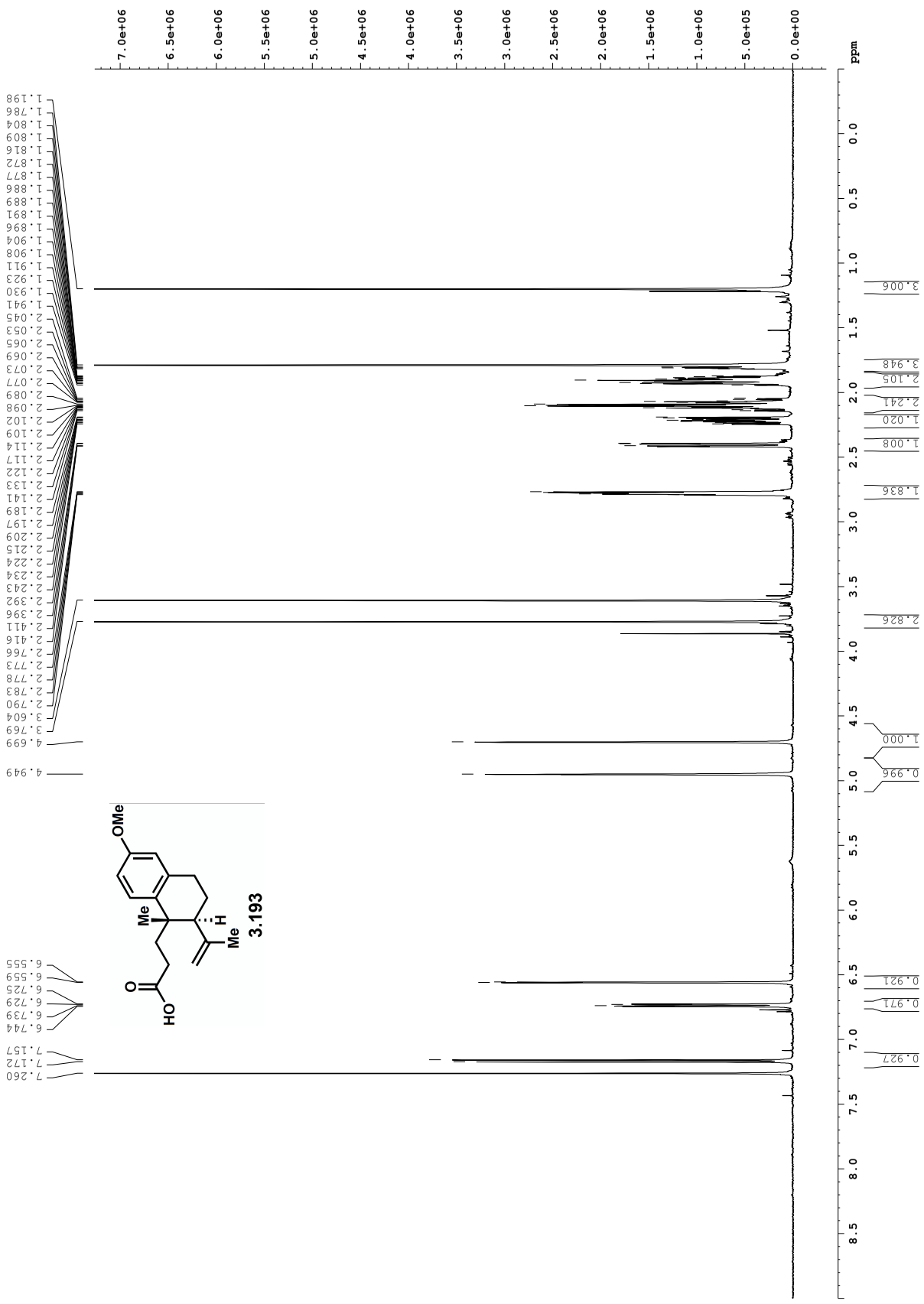
OMe
Me
H
Me
O
HO
3.193

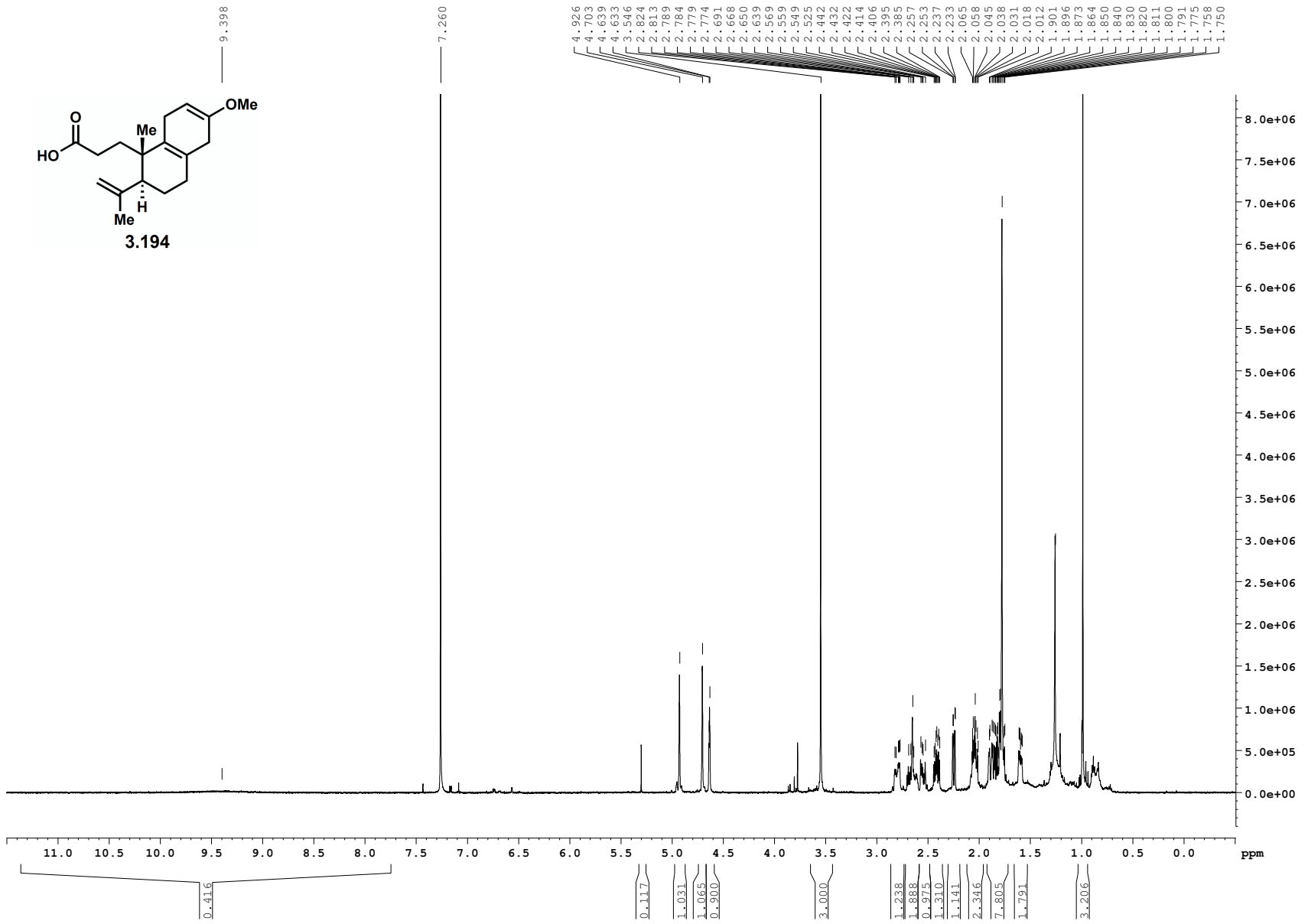
9.398
7.260
4.926
4.703
4.639
4.633
3.546
2.824
2.813
2.789
2.784
2.779
2.774
2.691
2.668
2.650
2.639
2.569
2.559
2.549
2.525
2.442
2.432
2.422
2.414
2.406
2.395
2.385
2.257
2.253
2.237
2.233
2.065
2.058
2.045
2.038
2.031
2.018
2.012
1.901
1.896
1.873
1.864
1.850
1.840
1.830
1.820
1.811
1.800
1.791
1.775
1.758
1.750
O
HO
Me
OMe
H
Me
3.194
8.0e+06
7.5e+06
7.0e+06
6.5e+06
6.0e+06
5.5e+06
5.0e+06
4.5e+06
4.0e+06
3.5e+06
3.0e+06
2.5e+06
2.0e+06
1.5e+06
1.0e+06
5.0e+05
0.0e+00
11.0
10.5
10.0
9.5
9.0
8.5
8.0
7.5
7.0
6.5
6.0
5.5
5.0
4.5
4.0
3.5
3.0
2.5
2.0
1.5
1.0
0.5
0.0
ppm
0.416
0.117
1.031
1.065
0.900
3.000
1.238
1.888
0.975
1.310
1.141
2.346
7.805
1.791
3.206

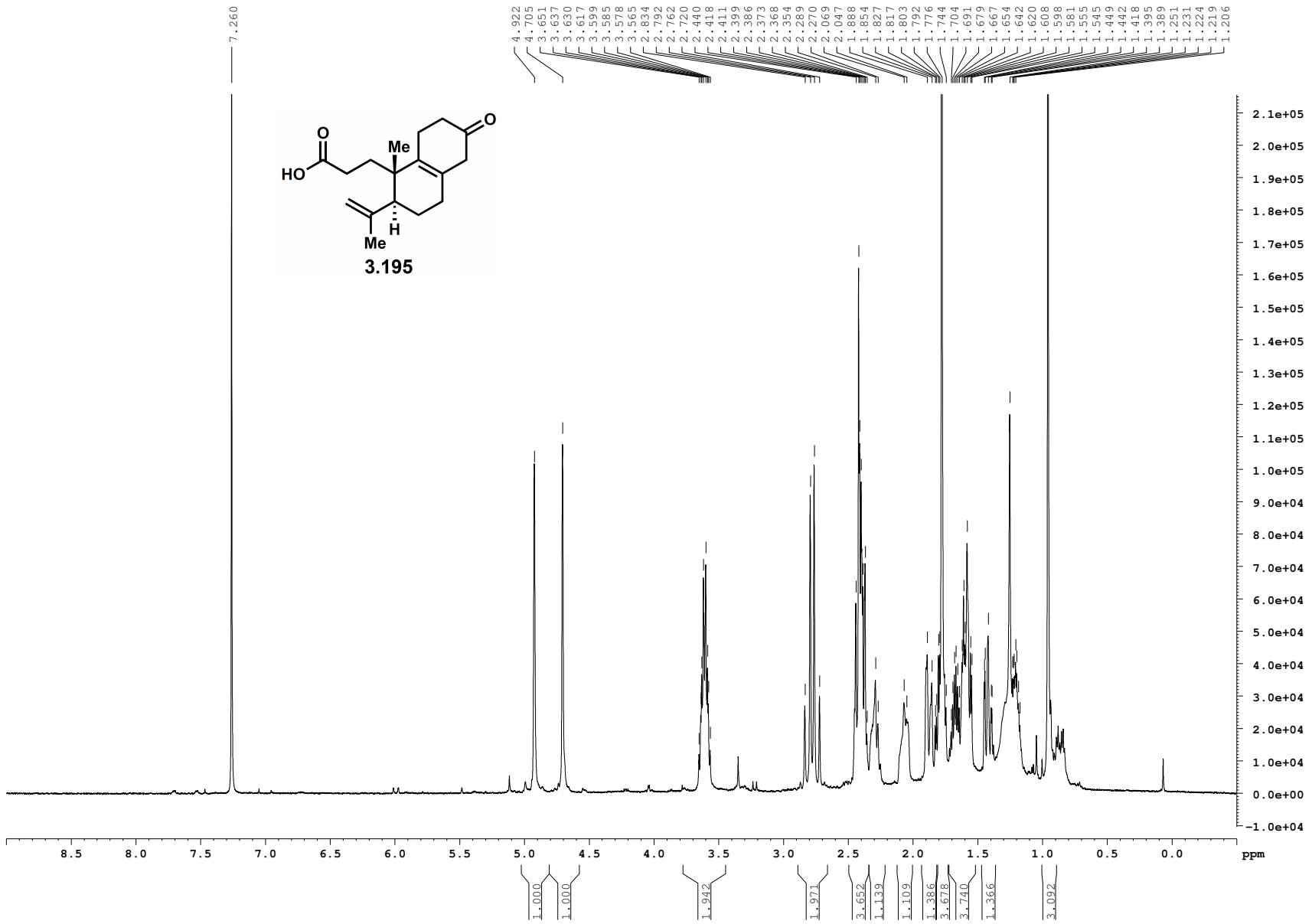
7.260
4.922
4.705
3.651
3.637
3.630
3.617
3.599
3.585
3.578
3.565
2.834
2.792
2.762
2.720
2.440
2.418
2.411
2.399
2.386
2.373
2.368
2.354
2.289
2.270
2.069
2.047
1.888
1.854
1.827
1.817
1.803
1.792
1.776
1.744
1.704
1.691
1.679
1.667
1.654
1.642
1.620
1.608
1.598
1.581
1.555
1.545
1.449
1.442
1.418
1.395
1.389
1.251
1.231
1.224
1.219
1.206
HO
O
O
Me
H
Me
3.195
2.1e+05
2.0e+05
1.9e+05
1.8e+05
1.7e+05
1.6e+05
1.5e+05
1.4e+05
1.3e+05
1.2e+05
1.1e+05
1.0e+05
9.0e+04
8.0e+04
7.0e+04
6.0e+04
5.0e+04
4.0e+04
3.0e+04
2.0e+04
1.0e+04
0.0e+00
-1.0e+04
8.5
8.0
7.5
7.0
6.5
6.0
5.5
5.0
4.5
4.0
3.5
3.0
2.5
2.0
1.5
1.0
0.5
0.0
ppm
1.000
1.000
1.942
1.971
3.652
1.139
1.109
1.386
3.678
3.740
1.366
3.092

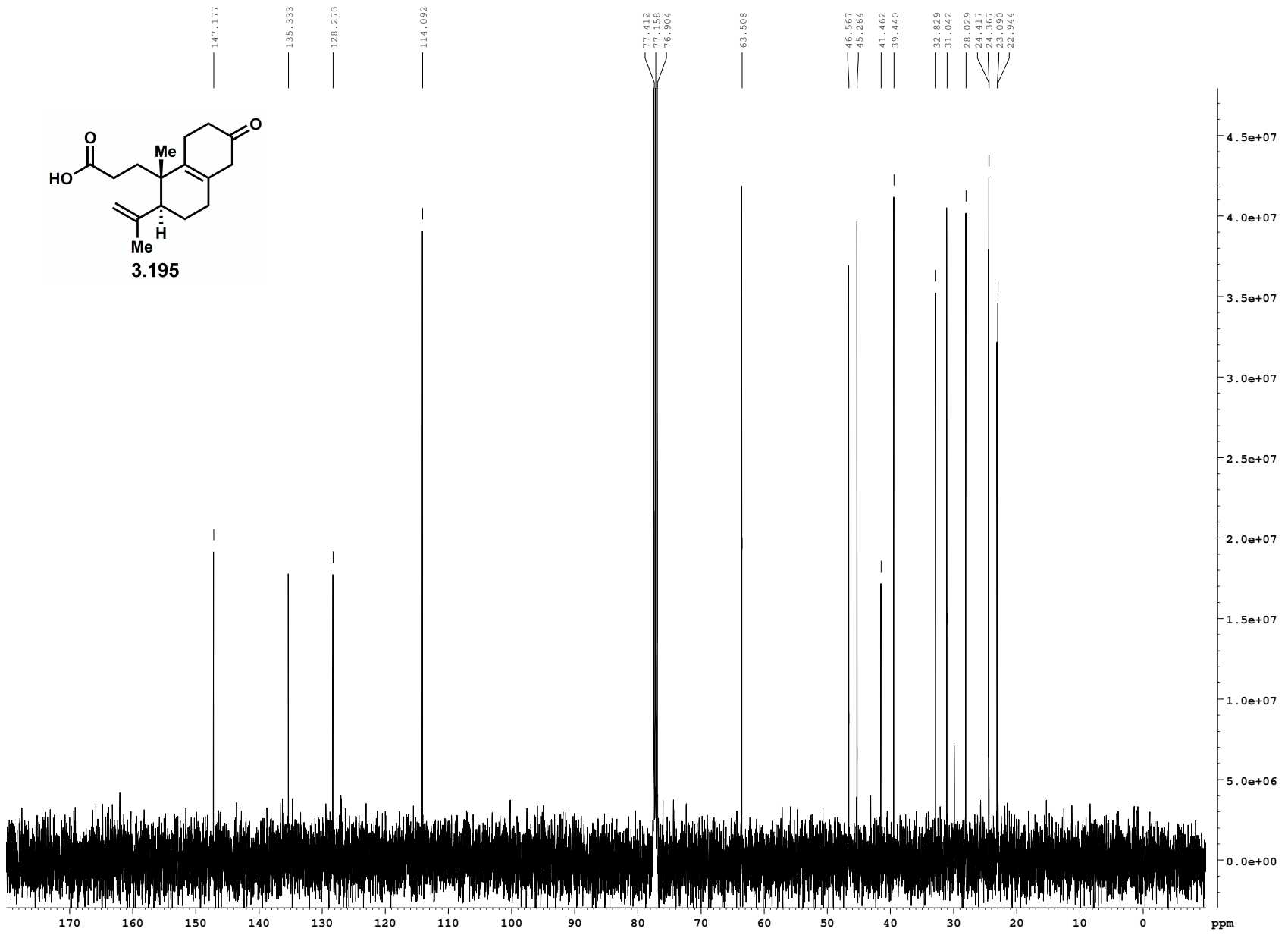
147.177
135.333
128.273
114.092
77.412
77.158
76.904
63.508
46.567
45.264
41.462
39.440
32.829
31.042
28.029
24.417
24.367
23.090
22.944
O
HO
Me
O
Me
H
3.195
4.5e+07
4.0e+07
3.5e+07
3.0e+07
2.5e+07
2.0e+07
1.5e+07
1.0e+07
5.0e+06
0.0e+00
170
160
150
140
130
120
110
100
90
80
70
60
50
40
30
20
10
0
ppm